ON THE ACCURACY OF FINITE-ELEMENT SOLUTIONS OF PROBLEMS OF BENDING OF PLATES WITH TRACTION BOUNDARY CONDITIONS

A THESIS

Presented to

The Faculty of the Division of Graduate Studies

By

HEE C. RHEE

In Partial Fulfillment

of the Requirements for Degree of

Doctor of Philosophy in the School

of Engineering Science and Mechanics

Georgia Institute of Technology

December 1976

ON THE ACCURACY OF FINITE-ELEMENT SOLUTIONS OF PROBLEMS OF BENDING OF PLATES WITH TRACTION BOUNDARY CONDITIONS

Approved:

S. N. Atluri, Chairman

D. J. McGill

C. V. Smith

M. P. Stallybrass

T. S. Wang

Date approved by Chairman 1/10/1977

ACKNOWLEDGEMENTS

The author wishes to express his sincere gratitude to Dr. S.N. Atluri for his suggestion of the topic and excellent guidance for this thesis and his considerate encouragement during the time when this thesis was prepared. The author owes a lot of things to him during that period. The author thanks very much also to Drs. C.V. Smith and J.T.S. Wang, members of reading committee, D.J. McGill and M.P. Stallybrass for their interests in this work and many valuable suggestions for the thesis. Deep thanks go to Dr. M.E. Raville, Director of the School of Engineering Science and Mechanics, for his encouragement and financial support during the study. He was kind enough to correct mistakes and give many good suggestions for the thesis. The author appreciates him for this special considerations. The author thanks to Drs. J.A. Aberson, K. Kathiresan and M. Nakagaki for helpful discussions with them on computer programming.

Finally, the author wishes to express his deep appreciation to his wife, Won and his son, Jesse, for their sacrifice and patience during the late several years of study.

During a part of the studies, the author was supported through a grant from the National Science Foundation, grant No. NSF ENG-74-21346. The author gratefully acknowledges this support.

TABLE OF CONTENTS

LIST OF ILLUSTRATIONS

LIST OF TABLES

SUMMARY

The effects of explicitly enforcing traction boundary conditions in several solid mechanics problems, on the solutions obtained in the finite-element method, are studied. The traction boundary conditions which involve higher order derivatives of displacement variables, are seen to be the "natural boundary conditions" in a variational formulation based on the principle of minimum total potential energy, whereas they are "essential boundary conditions" in the complementary energy principle. The traction boundary conditions can also be viewed as the "natural conditions" in a modified principle of complementary energy. In this thesis, the nature of implicit satisfaction of traction boundary conditions through the above mentioned variational formulations of a linear solid mechanics problem is studied for both the compatible displacement and hybrid stress finite-element models, in the Ritz-based finite-element method. Emphasis has been placed on viewing the finite-element method as a "weighted residual error" method. Systematic methods to enforce the traction boundary conditions explicitly are developed for both these finite-element models for general situations.

In the first part of the thesis, several basic topics such as, the treatment of the higher order boundary conditions in a variational formulation of a boundary-value problem; some discussions on all the existing finite element models; several new features of the finite element hybrid models concerning their suitability in using different types of

elements (with different ordered interpolation functions) in different regions of a given system; brief discussions on the methods of the explicitly enforcing traction boundary conditions in the finite element formulations for compatible displacement model and hybrid stress model, respectively, are treated. Variational formulations of the bending problem of a thin elastic plate are given for all the existing finite element models starting from their appropriate fully three-dimensional counterparts.

In the second part, several interesting problems of plate bending with various boundary conditions and curved domains are studied. The so-called "Babuska paradox" of a simply supported circular plate is studied in detail in the context of the finite element method. The nature of implicitly enforcing traction boundary conditions in compatible displacement and hybrid stress finite element models is investigated, and systematic methods to enforce traction boundary conditions explicitly for both of the above two models are discussed. Especially in the hybrid stress model with discontinuous interelement boundary tractions, it is found that through a combination of boundary collocation method and variational formulation, the traction boundary conditions of a problem can be explicitly enforced in consistent and accurate manner, even on an arbitrarily curved boundary. Some numerical examples for various circular plate bending problems based on both the compatible displacement and hybrid stress models are discussed. Finite element solution of factors of stress concentration around holes of different shapes, in thin plates are studied.

In the last part, the finite element analysis of the bending problem of a plate with a through-the-thickness crack is treated. A hybrid stress finite element model is used for this purpose. Results for bending stress intensity factors for various plate aspect ratios, and various crack length/plate length ratios are obtained. The question of the optimum size of a finite element (with built-in singularities) near the crack front is discussed. Finite size correction factors for stress intensity factors in a finite plate, as compared to the solution for an infinite domain, are obtained. Comparing the numerical results with existing analytical results for an infinite domain, it is found that explicitly enforcing traction boundary conditions is necessary to obtain reliable results for stress intensity factor in finite-sized plates.

CHAPTER I

INTRODUCTION

To improve finite element solutions of a continuum problem, the approximations involved in the process of idealization of the model should be minimized. This can be done by choosing ingenious shape functions for appropriate assumed variables, the most suitable coordinate system for a given geometry, and utilizing more accurate numerical integration techniques.

Besides this, enforcement of other constraint conditions in the formulation or during other stages of finite element solution procedures can be considered for favorable influences on obtained solutions. Among such constraints are traction boundary conditions whose satisfaction is not explicit in the formulation of Ritz-based finite element models based on assumed displacements. In the Ritz based finite element model based on assumed displacements, which is most widely used today, only geometric boundary conditions are enforced explicitly; whereas the traction boundary conditions are enforced as a consequence of the extremization of the functional in the variational formulation in an implicit manner.

In this thesis, it is found that the higher order traction boundary conditions of a solid mechanics problem are satisfied in the sense of weighted error residual in the finite element models with continuous interelement boundary displacement field such as compatible displacement

and hybrid stress models. It is also shown that the traction boundary conditions are satisfied, in approximate methods based on variational formulation, in such a manner that the sum of the integrals of weighted error residuals of the interior differential equations and traction boundary conditions is forced to vanish.

This implies the following two difficulties in obtaining accurate solutions of a problem: first, the satisfaction of boundary conditions in the sense of weighted error residual cannot guarantee the pointwise accuracy in the traction boundary conditions themselves, especially, in problems with arbitrarily curved domains. Second, due to the vanishing of the sum of both the integrals of interior differential equations error and boundary tractions error residuals, each of the equations, i.e., the interior differential equations and the traction boundary conditions, may not be accurately satisfied.

In the finite element method, the domain is discretized into a finite number of sub-domains and the unknowns in the final system of equations are directly related to actual unknown quantities at several nodal points of each sub-domain. Because of this discretization and the fact that the unknown quantities can be directly related to the quantities which are used to express any boundary conditions, the explicit enforcement of the higher order boundary conditions is more easily achieved in the finite element method than in other approximate solution techniques.

By enforcing traction boundary conditions in an explicit and accurate manner, the satisfaction of the interior differential equations can also be affected favorably, since this implies, in effect, the

vanishing of the interior and the boundary errors separately.

In this thesis, a systematic method to enforce the traction boundary conditions pointwise is developed by using the concept of boundary collocation method. Through this method, the traction boundary conditions of a problem can be enforced very accurately even for an arbitrarily curved boundary, especially for a hybrid stress model, in a consistent manner.

Several cases are reported in this thesis with improved results in finite element solutions of plate bending problems when traction boundary conditions as well as geometric boundary conditions of problems are enforced explicitly. Among them, the results on bending problems of cracked plate are prominent. Along the cracked surface of a fractured plate, stresses are zero; and the enforcement of these traction free conditions correctly has been found to be very important in obtaining accurate stress intensity factors which are related to the singular behavior of stresses near the crack tip.

The fact that the traction boundary conditions can be explicitly enforced very accurately along an arbitrarily curved boundary is very important for the above mentioned fracture problems. When the crack surfaces consist of arbitrarily curved surfaces, it is very difficults to enforce the traction free conditions on them accurately, without using the boundary collocation concept whose application to the finite element method is introduced in this thesis.

The study includes the following: first, to find the nature of implicitly enforcing traction boundary conditions in the compatible

displacement and hybrid stress models; second, to develop a systematic method to enforce traction boundary conditions in an explicit manner for both the of above methods; last, to solve the various bending problems of thin elastic plates such as circular and annular plates with various boundary conditions, stress concentration of rectangular plates with central holes of several different geometries, and fracture of plates, by using compatible displacement and hybrid stress models and the methods to explicitly enforce traction boundary conditions, which are developed in this thesis.

In the second chapter, several topics are considered, such as: the treatment of higher order boundary conditions in a variational formulation of a boundary-value problem; some discussions on all the existing finite element models; several new features of the finite element hybrid models concerning their suitability in using different types of elements (with different ordered interpolation functions) in different regions of a given system; and brief discussions on the methods of explicitly enforcing traction boundary conditions in the finite element formulations for compatible displacement, hybrid displacement and hybrid stress models, respectively.

In the third chapter, variational formulations of the bending problem of a thin elastic plate are discussed. All the finite element models are derived for plate bending problems starting from their fully three-dimensional counterparts.

In the fourth chapter, several interesting problems of plate bending with various boundary conditions and curved domains are studied.

The so-called "Babuska paradox" of a simply supported circular plate is studied in detail in the context of the finite element method. The nature of implicitly enforcing traction boundary conditions in compatible displacement and hybrid stress finite element models is investigated, and systematic methods to enforce traction boundary conditions explicitly for both of the above two models are discussed. Especially in the hybrid stress model with discontinuous interelement boundary tractions, it is found that through a combination of a boundary collocation method and variational formulation, the traction boundary conditions of a problem can be explicitly enforced in a consistent and accurate manner, even on an arbitrarily curved boundary. Some numerical examples for various circular plate bending problems based on both the compatible displacement and hybrid stress models are discussed. Finite element solution of factors of stress concentration around holes of different shapes, in thin plates are studied.

In chapter five, the finite element analysis of the bending problem of a plate with a through-the-thickness crack is treated. A hybrid stress finite element model is used for this purpose. Results for bending stress intensity factors for various plate aspect ratios, and various crack length/plate length ratios are obtained. The question of the optimum size of a finite element with built-in singularities near the crack front is discussed. Finite size correction factors for stress intensity factors in a finite plate, as compared to the solution for an infinite domain, are obtained. Comparing the numerical results with existing analytical results for an infinite domain, it is found that explicitly enforcing traction boundary conditions is necessary to obtain reliable results for stress intensity factor in finite-sized plates.

CHAPTER II

FINITE ELEMENT FORMULATIONS FOR SOLID MECHANICS PROBLEMS

In this chapter, the variational formulation of the finite element method is reviewed with emphasis on the modifications of conventional variational principles. The first section is devoted to the classical Ritz method, on which the variational formulation of the conventional finite element method is based, and to the treatment of boundary conditions of a boundary value problem in the method.

In the second section, general variational principles and their modifications are reviewed with discussions on various finite element models which are derived from these conventional and modified principles.

In the third section, several distinct advantages of modified finite element models, as compared to the conventional ones, are discussed in detail.

In the last section, the problems in solid mechanics with traction boundary conditions, which are mentioned briefly in the introduction and whose mathematical details have been given in the first section of this chapter, are reiterated. These problems will be treated in detail from the viewpoint of the finite element method, with emphasis on several practical finite element models, two of which will be used later in this thesis.

Ritz Method

For simple problems, the finite element method can be formulated directly as can be seen in the stiffness method of analysis of trusses,

frames, etc. [1]. For more complicated problems, the finite element method can be formulated by variational methods when variational principles are applicable to the problems. Otherwise, some other methods such as the weighted residual method [2,3] and the energy balance method [4,5,6] may be considered.

Most of the solid mechanics problems have variational principles in the form of several energy principles. Because of this fact, the Ritz-based finite element method is widely used in solid mechanics problems today. The Ritz method which originated from variational considerations, can be stated as: "a boundary value problem can be identified with a problem of making an appropriate functional stationary with respect to an admissible set of assumed solution functions".

The assumed solution functions, to be admissible, should satisfy essential boundary conditions, if such boundary conditions exist in the problem. The natural boundary conditions with respect to which the assumed solution functions are completely arbitrary, are satisfied as a natural consequence of the extremization of the functional. But in actual implementation, it can be seen that the sum of weighted residual errors of natural boundary conditions and interior differential equation is set to be zero when the problem has natural boundary conditions.

Consider, for example, an elliptical boundary value problem in a plane domain D, with boundary B, defined by the following differential equation and some boundary conditions.

$$\nabla^2 u = f(x, y) \qquad \text{in } D \tag{2.1}$$

$$u = h \quad \text{on } B; \text{ or } \frac{\partial u}{\partial n} = g \quad \text{on } B$$

where ∇^2 is the Laplacian operator, x, y are cartesian coordinates, n is outward normal direction to B, and f, h and g are given [Fig. 2.1]. The problem has the variational principle that the stationary condition of scalar functional I with respect to an admissible solution function u (which satisfies u=h on B, if such condition exists) yields the differential equation Eq. 2.1 and the natural boundary condition, ($\frac{\partial u}{\partial n}$ = g on B if such condition is given), where

$$I = -\int_D (\nabla u.\nabla u + 2fu)dA + 2\int_B gudS \tag{2.2}$$

The first variation of I with respect to u is

$$\delta I = -2\int_B (\frac{\partial u}{\partial n} - g)\delta u dS + 2\int_D (\nabla^2 u - f)\delta u dA \tag{2.3}$$

If the problem is of Dirichlet type, the boundary conditions are "essential" ones, such as

$$u = h \quad \text{on} \quad B \tag{2.4}$$

If it is a Neumann problem, the boundary conditions are of "natural" type, such as

$$\frac{\partial u}{\partial n} = g \quad \text{on} \quad B \tag{2.5}$$

Thus the stationary condition of I with respect to u can be written as,

$$-\int_B (\frac{\partial u}{\partial n} - g)\delta u dS + \int_D (\nabla^2 u - f)\delta u dA = 0 \tag{2.6}$$

This implies the differential equation Eq. 2.1 and the boundary condition $\frac{\partial u}{\partial n} = g$ on B, unless u satisfies the essential boundary conditions on B. If no such essential boundary conditions on u itself exist, then the condition $\frac{\partial u}{\partial n} = g$ follows as a consequence of the extremization of the functional. Thus the function u, to be admissible, has to satisfy only the essential boundary conditions.

If approximate solution is assumed as

$$u_n = \phi_o + \sum_{k=1}^{n} \phi_k a_k \quad \text{in} \quad D \tag{2.7}$$

where ϕ_o satisfies essential boundary conditions and ϕ_k are homogeneous on B, and a_k are undetermined parameters, the, Eq. 2.6 becomes

$$\int_D [\nabla^2(\phi_o + \sum_{k=1}^{n} \phi_k a_k) - f] \sum_{k=1} \phi_k \delta a_k dA$$

$$- \int_B [\frac{\partial}{\partial n} (\phi_o + \sum_{k=1}^{n} \phi_k a_k) - g] \sum_{k=1} \phi_k \delta a_k dS = 0 \tag{2.8}$$

if there are no essential boundary conditions. Since δa_k are arbitrary, Eq. 2.8 implies

$$\int_D [\nabla^2(\phi_o + \sum_{k=1}^{n} \phi_k a_k) - f]\phi_k dA$$

$$- \int_B [\frac{\partial}{\partial n} (\phi_o + \sum_{k=1}^{n} \phi_k a_k) - g]\phi_k dS = 0 \tag{2.9}$$

This means that the sum of the weighted residual errors in the interior and on the boundaries is set to be zero as the consequence of extremization of functional I. Thus, even though the mean square convergence of the solution u_n to the hypothetical exact solution u has been established

[7], the convergence of the natural boundary condition $\frac{\partial u}{\partial n} = g$ is not immediately evident.

Finite Element Method

In the finite element method, the domain of a problem is discretized into a finite number of finite elements. The approximate solution in Eq. 2.7 is assumed only locally over a finite element, and the coefficients a_k are replaced by the values of the function itself at a finite number of points or nodes in the finite element.

Because of the discretization, continuity problems of assumed solutions at interelement boundaries arise. In coventional finite element models, the interelement continuity conditions of assumed solutions should be satisfied a priori, while in modified finite element models, they are enforced a posteriori by a Lagrange multiplier method and the extremization of the appropriate functional. The latter are referred to as hybrid finite element models because of the fact that of all the assumed field variables, one or two of them are assumed within the domain and a different field variable is assumed on the boundaries. The boundary variable assumed independent of internal variables, in general, has the role of a Lagrange multiplier. These new models can be obtained by modifications of conventional variational principles.

Conventional Variational Principle

All the field equations and boundary conditions of a linear solid mechanics problem can be obtained from a general variational principle by Hu and Washizu [8, 9], and the functional can be written as,

$$\Pi_{HW}(u_i, \varepsilon_{ij}, \sigma_{ij}) = \int_V [A\ (\varepsilon_{ij}) - \sigma_{ij}(\varepsilon_{ij} - u_{(i,j)}) - \bar{F}_i u_i]dV$$

$$- \int_{S_\sigma} \bar{T}_i u_i dS - \int_{S_u} T_i (u_i - \bar{u}_i) dS \tag{2.10}$$

where V and S are, respectively, domain and its boundary of a solid continuum; S_σ and S_u are traction and displacement prescribed portions of S, respectively; ε_{ij} are strains, σ_{ij} are stresses; u_i are displacements; $\bar{F}_i$ are body forces; $\bar{T}_i$ and $\bar{u}_i$ are prescribed tractions on S_σ and prescribed displacement on S_u, respectively, and finally $A(\varepsilon_{ij})$ is strain energy density function which can be expressed in terms of the strain components as

$$A(\varepsilon_{ij}) = \frac{1}{2} C_{ijk\ell} \varepsilon_{ij} \varepsilon_{k\ell} \tag{2.11}$$

where $C_{ijk\ell} = C_{k\ell ij} = C_{k\ell ji}$ are elastic constants. The simplified notation of designating a derivative by (,) is used and $u_{(i,j)}$ is the short expression for $\frac{1}{2}(u_{i,j} + u_{j,i})$. It is understood that tractions along boundaries, whether they are prescribed or not, are related to appropriate stress components by Cauchy's formula.

The extremization of Π_{HW} with respect to its independent variables u_i, ε_{ij} and σ_{ij} gives the following Euler equations*, which are the field equations and boundary conditions for a linearized problem in elasticity.

$$\sigma_{ij,j} + \bar{F}_i = 0 \quad \text{in} \quad V \tag{2.12}$$

$$\varepsilon_{ij} = \frac{1}{2}(u_{i,j} + u_{j,i}) \quad \text{in} \quad V \tag{2.13}$$

*For convenience, all the differential equations as well as the boundary conditions that follow as a consequence of the vanishing of the first variation of a scalar functional, will be referred to as Euler equations of the variational principle in this thesis.

$$T_i = \bar{T}_i \quad \text{on } S_\sigma \tag{2.14}$$

$$u_i = \bar{u}_i \quad \text{on } S_u \tag{2.15}$$

$$\sigma_{ij} = \frac{\partial A}{\partial \varepsilon_{ij}} \quad \text{in } V \tag{2.16}$$

It is assumed that the relation given in Eq. 2.16 is invertible for ε_{ij} in terms of σ_{ij} and that the following contact transformation exists;

$$B(\sigma_{ij}) = -A(\varepsilon_{ij}) + \sigma_{ij}\varepsilon_{ij} \tag{2.17}$$

where the stress energy density function $B(\sigma_{ij})$ can be written as

$$B(\sigma_{ij}) = \frac{1}{2} d_{ijk\ell}\sigma_{ij}\sigma_{k\ell} \tag{2.18}$$

Thus, strains can be derived from stress energy density function such that

$$\varepsilon_{ij} = \frac{\partial B(\sigma_{ij})}{\partial \sigma_{ij}} \tag{2.19}$$

where $d_{ijk\ell} = d_{k\ell ij} = d_{k\ell ji}$ are elastic compliance constants.

For finite element formulation of the above principle, the domain, V, is discretized into a finite number of finite-sized non-overlapping elements, V_m. Then the functional can be expressed as the sum of its values evaluated over the individual element. Thus, Eq. 2.10 can be written as,

$$\Pi_{HW} = \sum_m \{ \int_{V_m} [A(\varepsilon_{ij}) - \sigma_{ij}(\varepsilon_{ij} - u_{(i,j)}) - \bar{F}_i u_i] dV$$

$$- \int_{S_{\sigma_m}} \bar{T}_i u_i dS - \int_{S_{u_m}} T_i (u_i - \bar{u}_i) dS \} \qquad (2.20)$$

where V_m, S_{σ_m} and S_{u_m} are individual element versions of V, S_σ and S_u, respectively. For Eq. 2.20 to be a correct sum of individual element quantities, it is implied that the displacements and tractions should be continuous along interelement boundaries.

Modified Variational Principle

The requirement of continuity in displacements and traction along interelement boundaries restricts the choice of assumed functions and, thus, severely restricts the flexibility of the finite element method in practical application. This difficulty can be resolved by relaxing the continuity conditions on the variables when they are initially assumed, and these conditions are enforced by the extremization of the functional with respect to them by a Lagrange multiplier method. This means that the continuity conditions are enforced as a posteriori conditions when the functional is extremized. The systematic work for this method has been done by Atluri [10], and it will be briefly mentioned here.

Considering a finite element, it is evident that an element can have up to three different kinds of boundaries according to its location in the system, i.e., $S_m = \rho_m + S_{\sigma_m} + S_{u_m}$ where S_m is the individual element boundary and ρ_m is an interelement boundary with neighboring elements. The integration of some quantities along interelement boundary AB of two neighboring m^{th} and $(m+1)^{th}$ elements, whose two dimensional figure is given by Figs. 2.2 and 2.3, can occur twice in opposite directions. The signs of quantities on each AB of m^{th} and $(m+1)^{th}$ elements are given conveniently.

Vanishing of the first variation of Eq. 2.20 gives

$$\sum_m \{ \int_{V_m} (\frac{\partial A}{\partial \varepsilon_{ij}} - \sigma_{ij}) \delta \varepsilon_{ij} dV - \int_{V_m} (\varepsilon_{ij} - u_{(i,j)}) \delta \sigma_{ij} dV$$

$$- \int_{V_m} (\sigma_{ij,j} + \bar{F}_i) \delta u_i dV - \int_{S_{\sigma_m}} (\bar{T}_i - T_i) \delta u_i dS$$

$$- \int_{S_{u_m}} (u_i - \bar{u}_i) \delta T_i dS + \int_{\rho_m} T_i \delta u_i d\rho \} = 0 \qquad (2.21)$$

Considering the last integral of the above equation, it can be seen that the traction continuity follows the displacement continuity at inter-element boundaries, i.e., if

$$u_i^+ = u_i^- \quad \text{on} \quad \rho_m \qquad (2.22)$$

then,

$$T_i^+ = T_i^- \quad \text{on} \quad \rho_m \qquad (2.23)$$

Thus the functional in Eq. 2.20 can be modified by introducing the displacement continuity condition at ρ_m as a constraint condition with continuous functions T_{iL} along ρ_m which have the role of Lagrange multipliers and will be identified as boundary tractions. Of course, in this case, the interelement continuity condition on u_i can be relaxed in the initial stage of assuming the field variables. The new modified functional can be written as

$$\Pi_{HWM1}(u_i, \varepsilon_{ij}, \sigma_{ij}, T_{iL}) = \sum_m \{ \int_{V_m} [A(\varepsilon_{ij}) - \sigma_{ij}(\varepsilon_{ij} - u_{(i,j)}) - \bar{F}_i u_i] dV$$

$$- \int_{S_{\sigma_m}} \bar{T}_i u_i dS - \int_{S_{u_m}} T_i (u_i - \bar{u}_i) dS - \int_{\rho_m} T_{iL} u_i d\rho \; \} \tag{2.24}$$

Using the divergence theorem, the above can equivalently be written as,

$$\Pi_{HWM1}(u_i, \epsilon_{ij}, \sigma_{ij}, T_{iL}) = \sum_m \{ \int_{V_m} [A(\epsilon_{ij}) - \sigma_{ij}\epsilon_{ij} - (\sigma_{ij,j} + \bar{F}_i)u_i] dV$$

$$+ \int_{S_{\sigma_m}} (T_i - \bar{T}_i) u_i dS + \int_{S_{u_m}} T_i \bar{u}_i dS + \int_{\rho_m} (T_i - T_{iL}) u_i d\rho \; \} \tag{2.25}$$

These functionals can be written in more condensed form by defining the Lagrange multipliers T_{iL} along S_{σ_m} and S_{u_m} as well as ρ_m of the element such that $T_{iL} = \bar{T}_i$ on S_{σ_m} and $T_{iL} = T_i$ on S_{u_m}; then, Eqs. 2.24 and 2.25 can be expressed as

$$\Pi_{HWM1}(u_i, \epsilon_{ij}, \sigma_{ij}, T_{iL}) = \sum_m \{ \int_{V_m} [A(\epsilon_{ij}) - \sigma_{ij}(\epsilon_{ij} - u_{(i,j)}) - \bar{F}_i u_i] dV$$

$$- \int_{S_m} T_{iL} u_i dS + \int_{S_{u_m}} T_{iL} \bar{u}_i dS \; \} \tag{2.26}$$

and

$$\Pi_{HWM1}(u_i, \epsilon_{ij}, \sigma_{ij}, T_{iL}) = \sum_m \{ \int_{V_m} [A(\epsilon_{ij}) - \sigma_{ij}\epsilon_{ij} - (\sigma_{ij,j} + \bar{F}_i)u_i] dV$$

$$+ \int_{S_m} (T_i - T_{iL}) u_i dS + \int_{S_{u_m}} T_{iL} \bar{u}_i dS \; \} \tag{2.27}$$

Alternatively, the modification can be done by assuming continuous displacement functions u_{iL} on ρ_m. The interelement displacement continuity conditions can be introduced into the functional, Eq. 2.20, by Lagrange multipliers, $T_{i\ell}$, which are assumed independently at ρ_m and

will later be identified as boundary tractions. Thus the functional can be written as

$$\Pi_{HWM2}(u_i, \varepsilon_{ij}, \sigma_{ij}, u_{iL}, T_{i\ell}) = \sum_m \{ \int_{V_m} [A(\varepsilon_{ij}) - \sigma_{ij}(\varepsilon_{ij} - u_{(i.j)}) - \bar{F}_i u_i] dV$$

$$- \int_{S_{\sigma_m}} \bar{T}_i u_i dS - \int_{S_{u_m}} T_i(u_i - \bar{u}_i) dS - \int_{\rho_m} T_{i\ell}(u_i - u_{iL}) d\rho \} \qquad (2.28)$$

Using the divergence theorem, the above can be written, equivalently, as

$$\Pi_{HWM2}(u_i, \varepsilon_{ij}, \sigma_{ij}, u_{iL}, T_{i\ell}) = \sum_m \{ \int_{V_m} [A(\varepsilon_{ij}) - \sigma_{ij}\varepsilon_{ij} - (\sigma_{ij,j} + \bar{F}_i) u_i] dV$$

$$+ \int_{S_{\sigma_m}} (T_i - \bar{T}_i) u_i dS + \int_{S_{u_m}} T_i \bar{u}_i dS + \int_{\rho_m} T_{i\ell} u_{iL} d\rho + \int_{\rho_m} (T_i - T_{i\ell}) u_i d\rho \} \qquad (2.29)$$

The above also can be expressed in more compact forms by defining u_{iL} and $T_{i\ell}$ on S_{u_m} and S_{σ_m} as well as on ρ_m such that $u_{iL} = \bar{u}_i$ on S_{u_m}, $u_{iL} = u_i$ on S_{σ_m} and $T_{i\ell} = T_i$ on S_m. Then, Eqs. 2.28 and 2.29 can be

$$\Pi_{HWM2}(u_i, \varepsilon_{ij}, \sigma_{ij}, u_{iL}) = \sum_m \{ \int_{V_m} [A(\varepsilon_{ij}) - \sigma_{ij}(\varepsilon_{ij} - u_{(i,j)}) - \bar{F}_i u_i] dV$$

$$- \int_{S_m} T_i(u_i - u_{iL}) dS - \int_{S_{\sigma_m}} \bar{T}_i u_{iL} dS \} \qquad (2.30)$$

and

$$\Pi_{HWM2}(u_i, \varepsilon_{ij}, \sigma_{ij}, u_{iL}) = \sum_m \{ \int_{V_m} [A(\varepsilon_{ij}) - \sigma_{ij}\varepsilon_{ij} - (\sigma_{ij,j} + \bar{F}_i) u_i] dV$$

$$+ \int_{S_m} T_i u_{iL} dS - \int_{S_{\sigma_m}} \bar{T}_i u_{iL} dS \qquad (2.31)$$

The extremizations of these functionals with respect to the relevant field variables give the continuity conditions of tractions and displacements along interelement boundaries as well as other field equations and system boundary conditions.

Finite Element Models

All the finite element models which are in practical application today can be systematically derived from above mentioned functionals in Eqs. 2.26, 2.27, 2.30 and 2.31. The differences among models arise in their respective a priori and a posteriori conditions, and their assumed variables. According to the field variables assumed, the models can be categorized into three groups, and they are displacement, stress, and mixed models, respectively.

Displacement Models If strain displacement relations, Eq. 2.13, and the constitutive relations, Eq. 2.16, are assumed a priori, the functionals in Eqs. 2.26 and 2.30 yield hybrid displacement model versions 1 and 2, respectively, and they can be written as

$$\Pi_{HD1}(u_i, T_{iL}) = \sum_m \{ \int_{V_m} [A(\epsilon_{ij}) - \bar{F}_i u_i] dV - \int_{S_m} T_{iL} u_i dS + \int_{S_{u_m}} T_{iL} \bar{u}_i dS \} \tag{2.32}$$

$$\Pi_{HD2}(u_i, T_i, u_{iL}) = \sum_m \{ \int_{V_m} [A(\epsilon_{ij}) - \bar{F}_i u_i] dV - \int_{S_m} T_i (u_i - u_{iL}) dS - \int_{S_{\sigma_m}} \bar{T}_i u_{iL} dS \} \tag{2.33}$$

where T_i are independently assumed boundary tractions. The Euler equations of these functionals are equilibrium equations, Eq. 2.12, traction and displacement boundary conditions, Eqs. 2.14 and 2.15, displacement and traction continuity conditions along interelement boundaries, Eqs. 2.22 and 2.23, respectively, and matching of T_i and boundary tractions which are derived from the interior displacements u_i.

If the interelement boundary displacement continuity conditions are satisfied a priori, the functionals in Eqs. 2.29 and 2.30 will correspond to the compatible displacement model.

$$\Pi_{CD}(u_i) = \sum_m \{ \int_{V_m} [A(\varepsilon_{ij}) - \bar{F}_i u_i] dV - \int_{S_{\sigma_m}} \bar{T}_i u_i dS - \int_{S_{u_m}} T_i (u_i - \bar{u}_i) dS \} \tag{2.34}$$

The Euler equations are the same as those of hybrid displacement models except the interelement boundary displacement continuity conditions, which are satisfied a priori. In practical implementation the last term is dropped by assuming displacement boundary conditions a priori; then the functional becomes

$$\Pi_{CD}(u_i) = \sum_m \{ \int_{V_m} [A(\varepsilon_{ij}) - \bar{F}_i u_i] dV - \int_{S_{\sigma_m}} \bar{T}_i u_i dS \} \tag{2.35}$$

which is the minimum potential energy functional.

Stress Models Assuming equilibrium equations, Eq. 2.12, and constitutive relations, Eqs. 2.17 and 2.19, a priori, the functionals in Eqs. 2.31 and 2.27 yield hybrid stress model versions 1 and 2, respectively, as follows:

$$\Pi_{HS1}(\sigma_{ij}, u_{iL}) = \sum_m \{- \int_{V_m} B(\sigma_{ij})dV + \int_{S_m} T_i u_{iL} dS - \int_{S_{\sigma_m}} \bar{T}_i u_{iL} dS \} \quad (2.36)$$

$$\Pi_{HS2}(\sigma_{ij}, T_{iL}, u_{is}) = \sum_m \{- \int_{V_m} B(\sigma_{ij})dV + \int_{S_{u_m}} T_{iL}\bar{u}_i dS + \int_{S_m} (T_i - T_{iL})u_{is} dS \} \quad (2.37)$$

where u_{is} are independently assumed boundary displacement.

The Euler equations are strain displacement relations, Eq. 2.13, traction and displacement boundary conditions, Eqs. 2.14 and 2.15, respectively, $u_i = u_{is}$ on S_{σ_m}, and interelement boundary continuity conditions of displacements and tractions, Eqs. 2.22 and 2.23, respectively.

If interelement traction continuity conditions are assumed a priori, the functionals in Eqs. 2.36 and 2.37 become an equilibrium stress model:

$$\Pi_{ES}(\sigma_{ij}, u_{is}) = \sum_m \{- \int_{V_m} B(\sigma_{ij})dV + \int_{S_{u_m}} T_i \bar{u}_i dS + \int_{S_{\sigma_m}} (T_i - \bar{T}_i)u_{is} dS \} \quad (2.38)$$

If $T_i = \bar{T}_i$ on S_{σ_m} are assumed a priori, further, then

$$\Pi_{ES}(\sigma_{ij}) = \sum_m \{- \int_{V_m} B(\sigma_{ij})dV + \int_{S_{u_m}} T_i \bar{u}_i dS \} \quad (2.39)$$

which the minimum complementary energy functional. The Euler equations of the functional are the same as those of hybrid stress models except the interelement traction continuity conditions which are assumed a priori.

Mixed Models If only constitutive relations are assumed a priori, the

functionals in Eqs. 2.26 and 2.30 will be reduced to hybrid mixed model versions 1 and 2, respectively.

$$\Pi_{HM1}(u_i, \sigma_{ij}, T_{iL}) = \sum_m \{ - \int_{V_m} [B(\sigma_{ij}) - \sigma_{ij} u_{(i,j)} + \bar{F}_i u_i] dV - \int_{S_m} T_{iL} u_i dS + \int_{S_{u_m}} T_{iL} \bar{u}_i dS \} \tag{2.40}$$

$$\Pi_{HM2}(u_i, \sigma_{ij}, u_{iL}) = \sum_m \{ - \int_{V_m} [B(\sigma_{ij}) - \sigma_{ij} u_{(i,j)} + \bar{F}_i u_i] dV - \int_{S_m} T_i (u_i - u_{iL}) dS - \int_{S_{\sigma_m}} \bar{T}_i u_{iL} dS \} \tag{2.41}$$

If interelement boundary continuity conditions on tractions and displacements are assumed a priori, the above functionals will become the finite element equivalent of Hellinger-Reissner principle.

$$\Pi_{ER}(u_i, \sigma_{ij}) = \sum_m \{ - \int_{V_m} [B(\sigma_{ij}) - \sigma_{ij} u_{(i,j)} + \bar{F}_i u_i] dV - \int_{S_{\sigma_m}} \bar{T}_i u_i dS - \int_{S_{u_m}} T_i (u_i - \bar{u}_i) dS \} \tag{2.42}$$

The resulting Euler equations are all field equations and boundary conditions, except the a priori assumed constitutive relations for hybrid models. Of course, for Π_{ER}, the interelement continuity conditions of tractions and displacements can not be the Euler equations, since they are enforced a priori.

All the models discussed above are summarized in Table 2.1.

Hybrid Models

Considerable research and numerical implementation of finite element hybrid models, which can be derived from modified variational principles mentioned earlier, have been presented by several authors such as Pian [11-22], Tong [18-24], Prager [28, 29], Atluri [25-27, 30-32], Nemat-Nasser and Lee [33,34], and Wolf [35,36]. The concept of a hybrid model of the finite element method can be briefly stated as that, by introducing an additional field variable along the boundary of a finite element, besides interior field variables, the interelement continuity condition of the latter in conventional models can be relaxed. Through the relaxation of the strict interelement continuity requirements on assumed variables, the finite element method can have more flexibility in practical applications and can handle complicated solid mechanics problems easily. Several examples of such problems are structures with singularities in displacements or stresses in their domain such as structures with free cut-outs or cracks [37-40] and problems with stress discontinuities or sharp variations of displacements due to the variations of material constants within the domain such as multilayered sandwich plates of composite materials [41, 42], etc.

Among other advantages of hybrid models over the conventional models, the following ones deserve special mention. First is the flexibility in the choice of shape functions for assumed variables. In the compatible displacement model which is based on the minimum potential energy principle and is one of the most widely used conventional models today, the assumed displacement field in each element should be such that it is continuous not only within the element but also across the interelement boundaries

in order that there is no infinite jump in strains and thus stresses along interelement boundaries, which are derived from displacements. Likewise, in the equilibrium stress model which is derived from the minimum complementary energy principle, the assumed stress field should be such that it is not only equilibrated within the element but also that the tractions which are derived from the stress field are continuous at interelement boundaries. These requirements on the continuity of displacements or tractions at the interelement boundaries may not provide sufficient flexibility in numerical solutions in some solid mechanics problems. For example, in plate or shell problems, by the Kirchhoff hypothesis, the inplane displacements are expressed by first derivatives of the transverse displacement. This implies that in order for all the displacements to be continuous along interelement boundaries, not only the transverse displacement but also its first derivatives should be continuous across interelement boundaries. This imposes a severe restriction on the choice of interpolation functions for the transverse displacement. However, in the hybrid displacement model of Eq. 2.33, for example, the interior displacements can be arbitrary in the form of polynomials with undetermined coefficients, and the boundary displacements are uniquely interpolated in terms of the respective nodal values at any boundary segments. Thus the choice of interior displacements should be easier. The detailed applications of this model for a plate problem can be found in [23].

The second advantage of the hybrid model is its applicability to problems with singularities in strains or stresses within the domains. Tong and Pian showed [43] that for problems with singularities, the

convergence rates for the finite element method are often controlled by the nature of the solution near the points of singularity. Thus unless the singularities are properly handled in the finite element formulation, the improvement of the rate of convergence cannot be guaranteed by using the regular high-accuracy element. Gallagher showed the limitation of the compatible displacement model in fracture mechanics problems [44]. If the finite element formulation used at the tip of a crack edge does not contain terms which handle singularities in strains and stresses, the size of the elements must be extremely small in order to obtain a reliable solution. If the assumed displacement field contains appropriate singular terms, it may not satisfy the interelement boundary continuity and, therefore, convergence of the solution cannot be guaranteed. But in the hybrid displacement [38, 39] and stress [40] models, the problem of including singular terms in the appropriate field variable can be handled easily by utilizing arbitrary interior and boundary variables.

The last very practical advantage to be mentioned is the suitability of the hybrid models to allow the use of two different order polynomials as assumed interior variables in a system. The use of two polynomials of different order in two adjacent elements of a system for the same assumed variable will immediately cause continuity problems in a conventional finite element model. Thus, in general, this type of formulation is impossible in models other than hybrid models.

The necessity of using several different order polynomials in a system can occur in the following cases. First, a system has some region where the variations of strains or stresses are so rapid or different from the remaining regions of the system that the lower order polynomial which

is good enough in other regions is not sufficient to approximate the variations of variables in that special region. Second, the geometry of a certain region such as some part of the system boundaries is so different from other regions that the system variables are not appropriate for the region.

The above practical advantage of hybrid models, which is believed to be pointed out for the first time in this thesis, is explored in some detail in the following. Consider two different shapes of adjoining elements in a system, for example, shown in Fig. 2.4. Assume that a linear displacement, which is the system field variable, is used in the triangular element and a cubic displacement field is used in the quadrilateral element. Thus, the interelement continuity problem between these two different order displacement fields arises along boundary AB.

If the model used for this problem is a compatible displacement model, the system field variable, $\underset{\sim}{u}^t$, can be expressed as

$$\underset{\sim}{u}^t = \underset{\sim}{A}(x,y)\underset{\sim}{q} \tag{2.43}$$

where $\underset{\sim}{A}$ is a n x r matrix of interpolating functions and $\underset{\sim}{q}$ is the nodal displacements vector. The displacements in the quadrilateral element, $\underset{\sim}{u}^q$, may be assumed as

$$\underset{\sim}{u}^q = \underset{\sim}{B}(x,y)\ \underset{\sim}{P} \tag{2.44}$$

where $\underset{\sim}{B}$ is a n x s matrix of cubic polynomial functions and $\underset{\sim}{P}$ is a vector of unknown parameters. At boundary AB, the following continuity conditions should be satisfied

$$\underset{\sim}{u}(\rho) - \underset{\sim}{u}^q(\rho) = \underset{\sim}{0} \tag{2.45}$$

where ρ is the boundary coordinate of AB and $\underset{\sim}{u}(\rho)$ is $\underset{\sim}{u}^t(x,y)$ at inter-element boundary AB which can be written as

$$\underset{\sim}{u}(\rho) = \underset{\sim}{A}(\rho)\ \underset{\sim}{q} \tag{2.46}$$

where $A(\rho)$ is a matrix of linear function of ρ. It is evident that $\underset{\sim}{u}(\rho)$ is unique along boundary AB, since it is interpolated by its values at the nodes on AB of the triangular element.

The above continuity conditions can be added to the original functional of quadrilateral element as constraint conditions through a set of Lagrange multiplier functions, $T(\rho)$, which are assumed arbitrarily along boundary AB of the quadrilateral element. Thus, the functional can be modified as

$$\Pi^* = \Pi + \sum_N \int_{\rho_N} \underset{\sim}{T}^T(\underset{\sim}{u} - \underset{\sim}{u}^q)d\rho \tag{2.47}$$

where Π is the original functional and

$$\underset{\sim}{T} = \underset{\sim}{C}\ \underset{\sim}{t} \tag{2.48}$$

where $\underset{\sim}{C}$ is a n x m matrix of arbitrary polynomials and $\underset{\sim}{t}$ is a vector of unknown parameters. The constraint term can be written as

$$\int_{\rho_n} \underset{\sim}{T}^T(\underset{\sim}{u} - \underset{\sim}{u}^q)d\rho = \int_{\rho_n} \underset{\sim}{t}^T\underset{\sim}{C}^T(\underset{\sim\sim}{A}\underset{\sim}{q} - \underset{\sim\sim}{B}\underset{\sim}{P})d\rho = \underset{\sim}{t}^T\underset{\sim\sim}{R}\underset{\sim}{q} - \underset{\sim}{t}^T\underset{\sim\sim}{Q}\underset{\sim}{P} \tag{2.49}$$

where

$$\underset{\sim\sim}{R} = \int_{\rho} \underset{\sim}{C}^T\underset{\sim\sim}{A}d\rho \tag{2.50}$$

$$Q = \int_{\rho} \underset{\sim}{C}^{T} \underset{\sim}{B} d\rho \tag{2.51}$$

From Eq. 2.49, the Euler equations obtained by extremization of the modified functional with respect to $\underset{\sim}{t}$ can be written as

$$\underset{\sim}{R}\underset{\sim}{q} - \underset{\sim}{Q}\underset{\sim}{P} = \underset{\sim}{0} \tag{2.52}$$

This is the relations between the unknown interior parameters $\underset{\sim}{P}$ and boundary displacements $\underset{\sim}{q}$ of the quadrilateral element. From Eq. 2.52 $\underset{\sim}{P}$ is solved in terms of $\underset{\sim}{q}$ and it is substituted into the functional. Thus, through a series of mathematical manipulations, the functional can be expressed only in terms of $\underset{\sim}{q}$, regardless of what kinds of different displacement functions are used in each element of the system, as

$$\Pi^{*} = \frac{1}{2} \underset{\sim}{q}^{*T} \underset{\sim}{K}^{*} \underset{\sim}{q}^{*} - \underset{\sim}{Q}^{*T} \underset{\sim}{q}^{*} \tag{2.53}$$

where $\underset{\sim}{q}^{*}$, $\underset{\sim}{K}^{*}$, and $\underset{\sim}{Q}^{*}$ are nodal displacement vector, stiffness matrix and equivalent nodal force vector of the system, respectively.

As can be seen in Eq. 2.49, the interelement continuity conditions between $\underset{\sim}{u}^{t}(x,y)$ and $\underset{\sim}{u}^{q}(x,y)$ along their common interelement boundary AB are established by the unique displacement field $\underset{\sim}{u}(\rho)$ in integral average sense through a Lagrange multiplier method. From Eqs. 2.51 and 2.52, it is obvious that the matrix $\underset{\sim}{Q}$ must be invertible, which means that m should be s.

Problems with Traction Boundary Conditions in Solid Mechanics

As mentioned earlier, Eq. 2.9 implies that in a problem with natural boundary conditions, the sum of boundary and interior errors is forced to be zero as a consequence of extremization of the functional.

Thus, if the two different kind of errors in Eq. 2.9 can be separately set to be zero, more accuracy in solutions in the interior and along boundaries can be expected. The traction boundary conditions of a solid mechanics problem can be viewed as natural boundary conditions in the variational formulation of the problem based on all the previously discussed principles except the complementary energy principle, where they are essential boundary conditions.

The finite element method has some advantages over other numerical methods that make these attempts possible, as mentioned earlier. But what is important in this process is to minimize the chance through which some additional errors arise, since in almost all operations in numerical methods, certain types of errors arise, and they can affect the entire formulation adversely.

When the structure is of arbitrary shape with curved boundaries, special care is needed because accurate interpolation of boundary conditions is very difficult along curved boundaries.

In the compatible displacement model, it is the usual procedure that the solution function is assumed arbitrarily regarding boundary conditions even for low order geometric boundary conditions. At the final solution step the geometric boundary conditions are enforced, and the higher order traction boundary conditions are completely ignored. Even in the conventional models, higher order boundary conditions can also be enforced by employing elements with higher order interpolation functions such as "Serendipity" elements [45] or those with higher order Hermitian polynomials [46]. Of course, this will imply an increase in the size of the finite element system of equations and the computation time. Thus,

economic considerations should be made.

As an alternative, consideration is also given to the use of hybrid models. First consider the hybrid displacement model in Eq. 2.33. The quantities u_i are differentiable displacements within V_m, but need not be continuous across the boundary S_m. The functions, u_{iL}, are the interelement boundary displacements which are continuous along S_m and subject to conditions $u_{iL} = \bar{u}_i$ on S_{u_m}. T_i has the role of Lagrange multipliers through which the condition $u_{iL} = u_i$ on S_m is enforced. These functions, T_i, are assumed arbitrarily and independently on the boundaries of each element and can be selected in such a way that they satisfy the traction boundary conditions a priori. For example, for problems with stress free conditions, T_i can be selected so that they are zero on the boundary as needed. Some works using this model have been reported with good results [38, 39].

Next consider the stress hybrid model given by Eq. 2.36. The variables which should be assumed in this model are boundary displacement functions, u_{jL}, on S_m which are continuous along interelement boundaries and $u_{iL} = \bar{u}_i$ on S_{u_m} and equilibrating stress functions, σ_{ij}, in V_m. The tractions, T_i, on S_m which are derived from the interior stresses σ_{ij} need not be continuous at interelement boundaries; this can give much flexibility in the choice of the σ_{ij} in V_m. In this model the enforcement of traction boundary conditions can be done in the following two ways depending on the shape of boundaries. First, when the boundary curves are so simple that enforcing the traction boundary condition $T_i = \bar{T}_i$ on S_{σ_m} does not give much restriction in the selection of σ_{ij}, the traction boundary conditions can be enforced directly in the process of selecting

σ_{ij}. However, when the curves of boundaries are complicated, the direct enforcement of traction boundary conditions in the process of selection of σ_{ij} is not, in general, possible. In this case, by introducing the boundary collocation method into the original variational formulation, the interior stress functions can be constrained explicitly to satisfy the traction boundary conditions pointwise, as discussed in detail in chapter four.

In this thesis, the methods which have been outlined in this section have been tried using two different models, i.e., the compatible displacement model and the hybrid stress model mentioned above to improve the satisfaction of traction boundary conditions.

CHAPTER III

VARIATIONAL FORMULATIONS FOR PLATE BENDING

In this chapter variational formulations of a thin plate bending problem are studied. Systematic derivations of variational principles of a plate bending problem, from the corresponding three dimensional forms discussed in the previous chapter, are given for all the finite element models and two conventional general principles. In all cases, body forces are ignored.

Approximate Theory of Plate Bending

In the theory of a thin elastic plate including the effects of transverse shear deformation, the following two assumptions can be employed: first, neglecting the transverse normal stress and second, neglecting the transverse normal strain component [47]. To simplify the theory, the displacement functions are taken in one of the simplest form of power series in the coordinate normal to the middle reference plate as:

$$\underset{\sim}{u}(x,y,z) = \underset{\sim}{U}(x,y) + z\,\underset{\sim}{U}_1(x,y)$$

where x,y are the inplane coordinates of undeformed reference plane and z is the normal coordinate to this plane.

The second assumption and the above displacement form imply that the linear filaments perpendicular to the undeformed middle reference plane remain straight and suffer no strains although they are not perpendicular to the deformed reference plane.

Under the above discussed assumptions, the displacements and strains for the bending of thin elastic plate in small displacement theory, can be written as:

$$u_\alpha = - z\phi_\alpha (x,y) \tag{3.1}$$

$$u_3 = w (x,y) \tag{3.2}$$

$$\varepsilon_{\alpha\beta} = - z\phi_{\alpha,\beta} \tag{3.3}$$

$$\varepsilon_{3\alpha} = \frac{1}{2}(w_{,\alpha} - \phi_\alpha) \tag{3.4}$$

$$\varepsilon_{33} = 0 \tag{3.5}$$

where the Greek indices vary from 1 to 2, w is the deflection of the reference plane in the z direction, and ϕ_α are the rotations of the normal to the reference plane due to deformation.

When the effects of transverse shear deformation are ignored, the rotations, ϕ_α , are identified to be the derivatives of w, by the additional assumption, i.e., $\varepsilon_{3\alpha} = 0$ [48,49].

$$\phi_\alpha = w_{,\alpha} \tag{3.6}$$

Thus, the inplane displacements and strains can be written as:

$$u_\alpha = -zw_{,x} \tag{3.7}$$

$$\varepsilon_{\alpha\beta} = -zw_{,\alpha\beta} \tag{3.8}$$

$$\varepsilon_{3i} = 0 \tag{3.9}$$

where the Latin index i varies from 1 to 3.

Sign conventions for various quantities are shown in Fig. 3.1. A_m is the area in the reference plane of the plate element with boundary C_m, A_m^u and A_m^L are respectively upper and lower surface of the plate element, $\vec{n}$ and $\vec{s}$ are respectively outward normal and tangential unit vectors to C_m with direction cosines n_α and s_α, respectively, h is the thickness of the plate, and p(x,y) is the external load applied on the plane $(0,0,\frac{h}{2})$. $M_{\alpha\beta}$ and Q_α are moments and shearing force intensities, respectively, and they are defined by:

$$M_{\alpha\beta} = \int_{-h/2}^{h/2} z\sigma_{\alpha\beta} dz \tag{3.10}$$

$$Q_\alpha = \int_{-h/2}^{h/2} \sigma_{3\alpha}\, dz \tag{3.11}$$

The following coordinate transformation relations can be established between various quantities given in the figure.

$$Q_n = n_\alpha Q_\alpha \tag{3.12}$$

$$M_n = n_\alpha n_\beta M_{\alpha\beta} \tag{3.13}$$

$$M_{ns} = n_\alpha s_\beta M_{\alpha\beta} \tag{3.14}$$

$$\phi_n = n_\alpha \phi_\alpha \text{ and } w_{,n} = n_\alpha w_{,\alpha} \tag{3.15}$$

$$\phi_s = s_\alpha \phi_\alpha \text{ and } w_{,s} = s_\alpha w_{,\alpha} \tag{3.16}$$

General Conventional Variational Principles

For variational formulation of a plate problem, based on general conventional principle, Eq. 2.20, nothing is assumed a priori, but strains

are expressed by new functions as:

$$\epsilon_{\alpha\beta} = - z\kappa_{\alpha\beta} \tag{3.17}$$

$$\epsilon_{3\alpha} = \rho_{\alpha} \tag{3.18}$$

Using Eqs. 3.1 - 3.5, 3.10 and 3.11, each term of Eq. 2.20 can be changes to have new limits of integration and variables, through integrations along z direction, as:

$$\frac{1}{2}\int_{V_m} C_{ijk\ell}\epsilon_{ij}\epsilon_{k\ell}dV$$

$$= \frac{1}{2}\int_{A_m}\int_{-h/2}^{h/2}(C_{\alpha\beta\gamma\delta}\epsilon_{\alpha\beta}\epsilon_{\gamma\delta} + 4C_{\alpha\beta3\gamma}\epsilon_{\alpha\beta}\epsilon_{3\gamma} + 4C_{3\alpha3\beta}\epsilon_{3\alpha}\epsilon_{3\beta})dzdA$$

$$= \frac{1}{2}\int_{A_m}(E_{\alpha\beta\gamma\delta}\kappa_{\alpha\beta}\kappa_{\gamma\delta} + E_{\alpha\beta}\rho_{\alpha}\rho_{\beta})dA \tag{3.19}$$

$$\int_{V_m}\sigma_{ij}(\epsilon_{ij} - u_{(i,j)})dV$$

$$= \int_{A_m}\int_{-h/2}^{h/2}[\sigma_{\alpha\beta}(\epsilon_{\alpha\beta} - u_{(\alpha,\beta)}) + \sigma_{3\alpha}(2\epsilon_{3\alpha} - u_{\alpha,3} - u_{3,\alpha})]\,dzdA$$

$$= \int_{A_m}[-M_{\alpha\beta}(\kappa_{\alpha\beta} - \phi_{\alpha,\beta}) + Q_{\alpha}(2\rho_{\alpha} - w_{,\alpha} + \phi_{\alpha})]dA \tag{3.20}$$

$$\int_{S_{\sigma_m}}\bar{T}_i u_i dS$$

$$= \int_{A_{u_m}}\bar{\sigma}_{i3}n_3 w dS + \int_{C_{\sigma_m}}\int_{-h/2}^{h/2}(\bar{\sigma}_{\alpha\beta}n_{\beta}u_{\alpha} + \bar{\sigma}_{3\alpha}n_{\alpha}w)dzdC$$

$$= \int_{A_m} pwdA - \int_{C_{\sigma_m}}(\bar{M}_{\alpha\beta}n_{\beta}\phi_{\alpha} - \bar{Q}_{\alpha}n_{\alpha}w)dC \tag{3.21}$$

$$\int_{S_{u_m}} T_i(u_i - \bar{u}_i)dS = -\int_{C_{u_m}} [M_{\alpha\beta}n_\beta(\phi_\alpha - \bar{\phi}_\alpha) - Q_\alpha(w - \bar{w})]dC \tag{3.22}$$

Substituting Eqs. 3.19 - 3.22 into Eq. 2.20 gives:

$$\begin{aligned}\Pi_{HW} = \sum_m \{ & \int_{A_m} [\tfrac{1}{2}(E_{\alpha\beta\gamma\delta}\kappa_{\alpha\beta}\kappa_{\gamma\delta} + E_{\alpha\beta}\rho_\alpha\rho_\beta) + M_{\alpha\beta}(\kappa_{\alpha\beta} - \phi_{\alpha,\beta}) \\ & - Q_\alpha(2\rho_\alpha - w_{,\alpha} + \phi_\alpha) - pw]dA \\ & + \int_{C_{\sigma_m}} (\bar{M}_{\alpha\beta}n_\beta\phi_\alpha - \bar{Q}_\alpha n_\alpha w)dC \\ & + \int_{C_{u_m}} [M_{\alpha\beta}n_\beta(\phi_\alpha - \bar{\phi}_\alpha) - Q_\alpha n_\alpha(w - \bar{w})]dC \ \}\end{aligned} \tag{3.23}$$

By coordinate transformations, Eqs. 3.12 -3.16, the boundary integrals of Eq. 3.23 can be expressed in boundary coordinates, thus:

$$\begin{aligned}\Pi_{HW} = \sum_m \{ & \int_{A_m} \frac{1}{2}(E_{\alpha\beta\gamma\delta}\kappa_{\alpha\beta}\kappa_{\gamma\delta} + E_{\alpha\beta}\rho_\alpha\rho_\beta)dA \\ & + \int_{A_m} [M_{\alpha\beta}(\kappa_{\alpha\beta} - \phi_{\alpha,\beta}) - Q_\alpha(2\rho_\alpha - w_{,\alpha} + \phi_\alpha) - pw]dA \\ & + \int_{C_{\sigma_m}} (\bar{M}_n\phi_n + \bar{M}_{ns}\phi_s - \bar{Q}_n w)dC \\ & + \int_{C_{u_m}} [M_n(\phi_n - \bar{\phi}_n) + M_{ns}(\phi_s - \bar{\phi}_s) - Q_n(w - \bar{w})]dC \ \}\end{aligned} \tag{3.24}$$

First variation of Eq. 3.24 with respect to the independent variables, $\kappa_{\alpha\beta}$, ρ_α, ϕ_α, w, $M_{\alpha\beta}$, and Q_α, can be written as:

$$\delta\Pi_{HW} = \sum_m \{ \int_{A_m} [(E_{\alpha\beta\gamma\delta}\kappa_{\alpha\beta} + M_{\gamma\delta})\ \delta\kappa_{\gamma\delta}$$

$$+ (E_{\alpha\beta}\rho_\alpha - 2Q_\beta)\delta\rho_\beta$$

$$+ (\kappa_{\alpha\beta} - \phi_{\alpha,\beta})\delta M_{\alpha\beta}$$

$$- (2\rho_\alpha - w,_\alpha + \phi_\alpha)\ \delta Q_\alpha$$

$$+ (M_{\alpha\beta,\beta} - Q_\alpha)\ \delta\phi_\alpha$$

$$- (Q_{\alpha,\alpha} + p)\ \delta w\ ]\ dA$$

$$+ \int_{C_{\sigma_m}} [(\bar{M}_n - M_n)\delta\phi_n + (\bar{M}_{n_s} - M_{n_s})\delta\phi_s - (\bar{Q}_n - Q_n)\ \delta w]\ dC$$

$$+ \int_{C_{u_m}} [(\phi_n - \bar{\phi}_n)\delta M_n + (\phi_s - \bar{\phi}_s)\delta M_{ns} - (w - \bar{w})\delta Q_n]\ dC\ \} \qquad (3.25)$$

The Euler equations are: constitutive relations, strain displacement relations, equilibrium equations, and traction and displacement boundary conditions as follows:

$$M_{\alpha\beta} = - E_{\alpha\beta\gamma\delta}\kappa_{\gamma\delta} \qquad \text{in } A_m \qquad (3.26)$$

$$Q_\alpha = \frac{1}{2} E_{\alpha\beta}\rho_\beta \qquad \text{in } A_m \qquad (3.27)$$

$$\kappa_{\alpha\beta} = \phi_{\alpha,\beta} \qquad \text{in } A_m \qquad (3.28)$$

$$\rho_\alpha = \frac{1}{2}\,(w_{,\alpha} - \phi_\alpha) \qquad \text{in } A_m \tag{3.29}$$

$$Q_\alpha = M_{\alpha\beta,\beta} \qquad \text{in } A_m \tag{3.30}$$

$$Q_{\alpha,\alpha} = -\,p \qquad \text{in } A_m \tag{3.31}$$

$$M_n = \bar{M}_n, \quad M_{ns} = \bar{M}_{ns} \quad \text{and} \quad Q_n = \bar{Q}_n \quad \text{on} \quad C_{\sigma_m} \tag{3.32}$$

$$\phi_n = \bar{\phi}_n, \quad \phi_s = \bar{\phi}_s \quad \text{and} \quad w = \bar{w} \quad \text{on} \quad C_{u_m} \tag{3.33}$$

from Eqs. 3.26, 3.30 and 3.31, the following two more equations can be obtained.

$$M_{\alpha\beta,\alpha\beta} = -\,p \tag{3.34}$$

$$(E_{\alpha\beta\gamma\delta}\kappa_{\gamma\delta})_{,\alpha\beta} = p \tag{3.35}$$

When the effects of transverse shear deformation are ignored, Eq. 3.24 can be written as:

$$\begin{aligned}\Pi_{HW} = \sum_m \{ & \int_{A_m} [\tfrac{1}{2} E_{\alpha\beta\gamma\delta}\kappa_{\alpha\beta}\kappa_{\gamma\delta} + M_{\alpha\beta}(\kappa_{\alpha\beta} - w_{,\alpha\beta}) - pw]\, dA \\ & + \int_{C_{\sigma_m}} (\bar{M}_n w_{,n} - \bar{V}_n w)\, dC + [\bar{M}_{ns} w]_{C_{\sigma_m}} \\ & + \int_{C_{u_m}} (w_{,n} - \bar{w}_{,n}) M_n - (w - \bar{w})\, V_n]\, dC + [(w - \bar{w}) M_{ns}]_{C_{u_m}} \}\end{aligned} \tag{3.36}$$

where

$$V_n = Q_n + M_{ns,s} \tag{3.37}$$

is the effective shearing force; and the terms in brackets represent the contributions of concentrated vertical forces at the corners of appropriate boundaries due to twisting moment intensities along the boundary. The changes in the form of boundary integrals of Eq. 3.36 are the consequences of applying the Kirchhoff hypothesis to the theory.

Due to the Kirchhoff hypothesis, ϕ_s is replaced by $w_{,s}$ and this is not an independent quantity any more. Thus three distinct boundary conditions on a boundary, as shown in Eqs. 3.32 and 3.33, are reduced to two by the following changes in the boundary integral.

$$\int_{C_m} (M_n w_{,n} + M_{ns} w_{,s} - Q_n w)\, dC = \int_{C_m} [M_n w_{,n} - (M_{ns,s} + Q_n)w]\, dC + [M_{ns} w]_{C_m} \tag{3.38}$$

Thus, the Euler equations of Eq. 3.36 are: constitutive equations, Eq. 3.26, strain displacement relations, Eq. 3.28, where ϕ_α should be replaced by $w_{,\alpha}$ equilibrium equations, Eq. 3.34, and the following boundary conditions on each of C_{u_m} and C_{σ_m}.

$$M_n = \bar{M}_n \quad \text{and} \quad V_n = \bar{V}_n \quad \text{on } C_{\sigma_m}. \tag{3.39}$$

$$w_{,n} = \bar{w}_{,n} \text{ and } w = \bar{w} \quad \text{on } C_{u_m} \tag{3.40}$$

$$M_{ns} = \bar{M}_{ns} \quad \text{at corners of } C_{\sigma_m} \tag{3.41}$$

M_{ns} in Eq. 3.41 represents concentrated force due to edgewise rate of change of twisting moment.

As was done in the case of modified principles in the second chapter, the divergence theorem, with the constitutive relations, can be used to change the functional in Eq. 2.20 into another form from which all the finite element stress models can be derived.

$$\Pi_{HW} = \sum_m \{- \int_{V_m} [B + (\sigma_{ij,j} + \bar{F}_i)u_i]dV + \int_{S_{\sigma_m}} (T_i - \bar{T}_i)u_i dS + \int_{S_{u_m}} T_i \bar{u}_i dS \quad (3.42)$$

The distributions of stresses along z direction can be assumed as given by Reissner's plate theory [50, 51, 52, 53].

$$\sigma_{\alpha\beta} = \frac{12M_{\alpha\beta}z}{h^3} \quad (3.43)$$

$$\sigma_{3\alpha} = \frac{3Q_\alpha}{2h} [1 - (\frac{2z}{h})^2] \quad (3.44)$$

$$\sigma_{33} = \frac{3p}{4} [\frac{2}{3} + \frac{2z}{h} - \frac{1}{3} (\frac{2a}{h})^3] \quad (3.45)$$

The two terms of the first integral of Eq. 3.42 can be expressed as follows, respectively, by integration along the thickness direction with the relations, Eq. 2.18 and Eqs. 3.43 - 3.45, when the body forces are ignored.

$$\int_{V_m} Bdv = \frac{1}{2} \int_{V_m} d_{ij\kappa\ell}\sigma_{ij}\sigma_{\kappa\ell}$$

$$= \frac{1}{2} \int_{V_m} (d_{\alpha\beta\gamma\delta}\sigma_{\alpha\beta}\sigma_{\gamma\delta} + 4d_{\alpha\beta3\gamma}\sigma_{\alpha\beta}\sigma_{3\gamma} + 2d_{\alpha\beta33}\sigma_{\alpha\beta}\sigma_{33}$$

$$+ 4d_{\alpha 333}\sigma_{\alpha 3}\sigma_{33} + 4d_{3\alpha 3\beta}\sigma_{3\alpha}\sigma_{3\beta} + d_{3333}\sigma_{33}^2)dA$$

$$= \frac{1}{2}\int_{A_m} (D_{\alpha\beta\gamma\delta}M_{\alpha\beta}M_{\gamma\delta} + D_{\alpha 3\beta 3}Q_\alpha Q_\beta + 2D_{\alpha\beta 33}pM_{\alpha\beta} + 2D_{\alpha 333}pQ_\alpha)dA \qquad (3.46)$$

$$+ \text{constant}$$

$$\int_{V_m} \sigma_{ij,j}u_i dV = \int_{A_m}\int_{-h/2}^{h/2} (\sigma_{\alpha\beta,\beta}u_\alpha + \sigma_{\alpha 3,3}u_\alpha + \sigma_{3\alpha,\alpha}u_3 + \sigma_{33,3}u_3)dzdA$$

$$= \int_{A_m} (- M_{\alpha\beta,\beta}\phi_\alpha + Q_\alpha\phi_\alpha + Q_{\alpha,\alpha}w + pw)dA \qquad (3.47)$$

Using these equations and further integrations similar to those in Eqs. 3.21 and 3.22 on boundary terms, Eq. 3.42 can be written as:

$$\Pi_{HW} = \sum_m \{ - \int_{A_m} [\frac{1}{2} (D_{\alpha\beta\gamma\delta}M_{\alpha\beta}M_{\gamma\delta} + D_{\alpha 3\beta 3}Q_\alpha Q_\beta) + D_{\alpha\beta 33}pM_{\alpha\beta} + D_{\alpha 333}pQ_\alpha]dA$$

$$- \int_{A_m} (Q_\alpha - M_{\alpha\beta,\beta})\phi_\alpha + (Q_{\alpha,\alpha} - p)w]dA$$

$$- \int_{C_{\sigma_m}} [M_{\alpha\beta} - \bar{M}_{\alpha\beta})n_\beta\phi_\alpha - (Q_\alpha - \bar{Q}_\alpha)n_\alpha w]dC$$

$$- \int_{C_{u_m}} (M_{\alpha\beta}n_\beta\bar{\phi}_\alpha - Q_\alpha n_\alpha\bar{w})dC + \text{constant} \qquad (3.48)$$

By coordinate transformation, the quantities in boundary integrals can be expressed in boundary coordinates, then:

$$\Pi_{HS} = \sum_m \{ - \int_{A_m} [\frac{1}{2} (D_{\alpha\beta\gamma\delta}M_{\alpha\beta}M_{\gamma\delta} + D_{\alpha 3\beta 3}Q_\alpha Q_\beta) + D_{\alpha\beta 33}pM_{\alpha\beta} + D_{\alpha 333}pQ_\alpha]dA$$

$$- \int_{A_m} [(Q_\alpha - M_{\alpha\beta,\beta})\phi_\alpha + (\phi_{\alpha,\beta} + p)w2\ ]dS$$

$$- \int_{C_{\sigma_m}} [(M_n - \bar{M}_n)\phi_n + (M_{ns} - \bar{M}_{ns})\phi_s - (Q_n - \bar{Q}_n)w]\ dC$$

$$- \int_{C_{u_m}} (M_n\bar{\phi}_n + M_{ns}\bar{\phi}_s - Q_n\bar{w})dC + \text{constant} \qquad (3.49)$$

The first variation of Eq. 3.49 with respect to $M_{\alpha\beta}$, Q_α, ϕ_α , and $\bar{w}$ is:

$$\delta\Pi_{HW} = \sum_m \{- \int_{A_m} (D_{\alpha\beta\gamma\delta}M_{\gamma\delta} + D_{\alpha\beta33}p + \phi_{\alpha,\beta})\delta M_{\alpha\beta}dA$$

$$- \int_{A_m} (D_{\alpha3\beta3}Q_\beta + D_{\alpha333}p - w_{,\alpha} + \phi_\alpha)\delta Q_\alpha dA$$

$$- \int_{A_m} (Q_\alpha - M_{\alpha\beta,\beta})\delta\phi_\alpha dA - \int_{A_m} (Q_{\alpha,\alpha} + p)\delta w dA$$

$$- \int_{C_{\sigma_m}} [(M_n - \bar{M}_n)\delta\phi_n + (M_{ns} - \bar{M}_{ns})\delta\phi_s - (Q_n - \bar{Q}_n)\delta w]dC$$

$$- \int_{C_{u_m}} [(\bar{\phi}_n - \phi_n)\delta M_n + (\bar{\phi}_s - \phi_s)\delta M_{ns} - (\bar{w} - w)\delta Q_n]dC \qquad (3.50)$$

The Euler equations are; strain-displacement relations from the first two-integrals, equilibrium equations from the third and fourth integrals, and boundary conditions from the last two integrals.

When the effects of transverse shear deformation are ignored, the

functional, Eq. 3.49 can be simplified as following by using the relations $\sigma_{33} = 0$ in interior and on boundaries, $\sigma_{3\alpha} = 0$ in interior, and Eq. 3.6 in appropriate integrations.

$$\Pi_{HW} = \sum_m \{ \int_{A_m} -[\frac{1}{2} D_{\alpha\beta\gamma\delta} M_{\alpha\beta} M_{\gamma\delta} + (M_{\alpha\beta,\alpha\beta} + p)\, w]\, dA$$

$$- \int_{C_{\sigma_m}} [(M_n - \bar{M}_n) w_{,n} - (V_n - \bar{V}_n) w]\, dC - [(M_{ns} - \bar{M}_{ns})\, w]_{C_{\sigma_m}}$$

$$- \int_{C_{u_m}} (M_n \bar{w}_{,n} - V_n \bar{w})\, dC - [M_{ns} \bar{w}]_{C_{u_m}} + \text{constant} \qquad (3.51)$$

The Euler equations are: strain displacement relations, Eq. 3.28 where ϕ_α should be replaced by $w_{,\alpha}$, equilibrium equations, Eq. 3.34, and boundary conditions, Eq. 3.39 - 3.41.

The work due to external load, pw, in Eq. 3.51, when transverse shearing deformation effects are not considered, is derived from the boundary integral $\int_{S_{\sigma_m}} (T_i - \bar{T}_i) u_i\, ds$ of Eq. 3.42. While, in Eq. 3.49, when transverse shearing deformation effects are considered, it is derived from $\int_{V_m} \sigma_{ij,j} u_i\, dV$ as shown in Eq. 3.47. The contribution of external load on S_{σ_m}, for the latter case, is cancelled by the existence of the contribution by σ_{33} as shown in the following:

$$\int_{S_{\sigma_m}} (T_i - \bar{T}_i)\, u_i ds = \int_{A_m^u + A_m^L} (\sigma_{i3} n_3 - \bar{\sigma}_{i3} n_3) u_3 dA + \int_{C_m} \int_{-h/2}^{h/2} (T_i - \bar{T}_i)\, dz dC \qquad (3.52)$$

$$\int_{A_m^u} \sigma_{i3} n_3\, u_3 dS = \int_{A_m^u} (\sigma_{\alpha 3} + \overset{*}{\sigma}_{33})\, w ds = \int_{A_m^u} p w dS \qquad (3.53)$$

$$\int_{A_m}^{L} \sigma_{i3} n_3 u_3 ds = - \int_{A_m}^{L} (\sigma_{\alpha 3} + \sigma_{33}) \, w dS = 0 \tag{3.54}$$

Thus the entire first term of the right hand side of Eq. 3.52 is dropped.

Displacement Models

When constitutive equations and strain displacement relations, Eqs. 3.26 - 3.29 are assumed a priori, all the displacement models whose three dimensional versions are given in Eqs. 2.32, 2.33 and 2.35 can be derived from Eq. 3.24 by the same modifications done on the general conventional principle in the second chapter. For hybrid models, the interior displacement u_i are released from the interelement continuity requirements and, for the modifications, additional boundary variables, T_{iL} for the first version, $T_{i\ell}$ and u_{iL} for the second version, are introduced.

In the hybrid displacement model version 1, Eq. 2.32, the boundary variable T_{iL} are assumed on S_m such that $T_{iL} = \bar{T}_i$ on S_{σ_m}, $T_{iL} = T_i$ on S_{u_m} and continuous at interelement boundary. Thus, in a plate element, $T_{iL} = p$ at $z = \frac{h}{2}$ and $T_{iL} = 0$ at $z = -\frac{h}{2}$.

$$\int_{S_m} T_{iL} u_i dS = \int_{A_m} pw dA + \int_{C_m} \int_{-h/2}^{h/2} T_{iL} u_i dz dC$$

$$= \int_{A_m} pw dA - \int_{C_m} (M_n^L \phi_n + M_{ns}^L \phi_s - Q_n^L s) \, dC \tag{3.55}$$

where

$$M_n^L = n_1 \int_{-h/2}^{h/2} T_{iL}\, z dz + n_2 \int_{-h/2}^{h/2} T_{2L}\, z dz \tag{3.56}$$

$$M_{ns}^L = S_1 \int_{-h/2}^{h/2} T_{iL} z dz + S_2 \int_{-h/2}^{h/2} T_{2L}\, z dz \tag{3.57}$$

$$Q_n^L = \int_{-h/2}^{h/2} T_{3L}\, dz \tag{3/58}$$

By the same way the integral on S_{u_m} can be written as:

$$\int_{S_{u_m}} T_{iL} \bar{u}_i dS = - \int_{A_m} (M_n^L \bar{\phi}_n + M_{ns}^L \bar{\phi}_s - Q_n^L \bar{w})\, dC \tag{3.59}$$

Substituting Eq. 3.19 with strain displacement relations, and Eqs. 3.55 and 3.59 into Eq. 2.32 yields

$$\begin{aligned} \Pi_{HD1} = \sum_m \{ & \int_{A_m} [\, \frac{1}{2} E_{\alpha\beta\gamma\delta} \phi_{\alpha,\beta} \phi_{\gamma,\delta} + \frac{1}{8} E_{\alpha\beta} (w_{,\alpha} - \phi_\alpha)\, (w_{,\beta} - \phi_\beta) - pw]\, dA \\ & + \int_{C_m} (M_n^L \phi_n + M_{ns}^L \phi_s - Q_n^L w)\, dC \\ & - \int_{C_{u_m}} (M_n^L \bar{\phi}_n + M_{ns}^L \bar{\phi}_s - Q_n^L \bar{w})\, dC \,\} \end{aligned} \tag{3.60}$$

When the effects of transverse shearing deformation are ignored, Eq. 3.60 can be written as:

$$\Pi_{HD1} = \sum_m \{ \int_{A_m} (\frac{1}{2} E_{\alpha\beta\gamma\delta} w_{,\alpha\beta} w_{,\gamma\delta} - pw) dA$$

$$+ \int_{C_m} (M_n^L w_{,n} - V_n^L w)dC + [M_{ns}^L w]_{C_m}$$

$$- \int_{C_{u_m}} (M_n^L \bar{w}_{,n} - V_n^L \bar{w})dC - [M_{ns}^L \bar{w}]_{C_{u_m}} \quad \} \tag{3.61}$$

where $V_n^L = Q_n^L + M_{ns,s}^L$

The first variation of the above is:

$$\delta\Pi_{HD1} = \sum_m \{ \int_{A_m} [(E_{\alpha\beta\gamma\delta} w_{,\gamma\delta})_{,\alpha\beta} - p]\delta w dA$$

$$+ \int_{C_m} [(M_n^L - M_n)\delta w_{,n} - (V_n^L - V_n)\delta w]dC + [(M_{ns}^L - M_{ns})\delta w]_{C_m}$$

$$+ \int_{C_{u_m}} [(w_{,n} - \bar{w}_{,n})\delta M_n^L - (w - \bar{w})\delta V_n^L]dC + [(w - \bar{w})\delta M_{ns}^L]_{C_{u_m}}$$

$$+ \int_{C_{\rho_m}} (w_{,n}\delta M_n^L - w\delta V_n^L)dC + [w\delta M_{ns}^L]_{C_{\rho_m}} \quad \} \tag{3.62}$$

where C_{ρ_m} are interelement boundaries. The Euler equations are: equilibrium equations from the first line, traction continuity and boundary conditions and displacement boundary conditions from the second and third lines, respectively, and interelement displacements continuity conditions from the last line.

In the hybrid displacement model version 2, a set of boundary tractions $T_{i\ell}$ and a set of boundary displacements u_{iL} are assumed such that $T_{i\ell}$ are arbitrary and u_{iL} are continuous and $u_{iL} = \bar{u}_i$ on S_{u_m} and $u_{iL} = u_i$ on S_{σ_m}. By similar mathematical manipulation as in the previous model, the Eq. 2.33 can be written as:

$$\Pi_{HD2} = \sum_m \{ \int_{A_m} [\tfrac{1}{2} E_{\alpha\beta\gamma\delta} \phi_{\alpha,\beta} \phi_{\gamma,\delta} + \tfrac{1}{8} E_{\alpha\beta} (w_{,\alpha} - \phi_\alpha)(w_{,\beta} - \phi_\beta) - pw] dA$$

$$+ \int_{C_m} [M_n^\ell (\phi_n - \phi_n^L) + M_{ns}^\ell (\phi_s - \phi_n^L) - Q_n^\ell (w - w^L)] dC$$

$$+ \int_{C_{\sigma_m}} [\bar{M}_n \phi_n^L + \bar{M}_{ns} \phi_s^L - \bar{Q}_n w^L] dC \; \} \qquad (3.63)$$

where ϕ_α^L and w^L are continuous boundary displacements and $M_{\alpha\beta}^\ell$ and Q_α^ℓ are boundary tractions.

When the effects of transverse shear deformation are ignored, Eq. 3.63 can be written as:

$$\Pi_{HD2} = \sum_m \{ \int_{A_m} (\frac{1}{2} E_{\alpha\beta\gamma\delta} w_{,\alpha\beta} w_{,\gamma\delta} - pw) \, dA$$

$$+ \int_{C_m} [M_n^\ell (w_{,n} - w_{,n}^L) - V_n^\ell (w - w^L)] \, dC + [M_{ns}^\ell (w - w^L)]_{C_m}$$

$$+ \int_{C_{\sigma_m}} (\bar{M}_n w_{,n}^L - \bar{V}_n w^L) \, dC + [\bar{M}_{ns} w^L]_{C_{\sigma_m}} \; \} \qquad (3.64)$$

where $V_n^\ell = Q_n^\ell + M_{ns,s}^\ell$

The first variation of the above equation is:

$$\delta\Pi_{HD2} = \sum_m \{ \int_{A_m} [(E_{\alpha\beta\gamma\delta} w_{,\gamma\delta})_{,\alpha\beta} - p] \, \delta w dA$$

$$+ \int_{C_m} [(w_{,n} - w_{,n}^L) \delta M_n^\ell - (w - w^L) \delta V_n^\ell] dC + [(w - w^L) \delta M_{ns}^\ell]_{C_m}$$

$$+ \int_{C_m} [(M_n^\ell - M_n) \delta w_{,n} - (V_n^\ell - V_n) \, \delta w] dC + [(M_{ns}^\ell - M_{ns}) \delta w]_{C_m}$$

$$+ \int_{C_{\sigma_m}} [(\bar{M}_n - M_n)\delta w^L_{,n} - (\bar{V}_n - V_n)\delta w^L]dC + [(\bar{M}_{ns} - M_{ns})\delta w^L]_{C_{\sigma_m}}$$

$$- \int_{C_{\rho_m}} (M^{\ell}_n \delta w^L_{,n} - V^{\ell}_n \delta w^L)dC - [M^{\ell}_{ns}\delta w^L]_{C_{\rho_m}} \} \qquad (3.65)$$

The Euler equations are: equilibrium equations from the first line, displacement continuity and displacement boundary conditions from the second line, traction boundary conditions from the fourth line, and interelement traction continuity conditions from the third and the last lines, respectively.

When the interelement continuity conditions of internal displacements and boundary displacements conditions are satisfied a priori, Eqs. 3.60 and 3.63 become a compatible displacement model whose three dimensional equation is given in Eq. 2.35, as follows:

$$\Pi_{CD} = \sum_m \{ \int_{A_m} [\frac{1}{2} E_{\alpha\beta\gamma\delta}\phi_{\alpha,\beta}\phi_{\gamma,\delta} + \frac{1}{8} E_{\alpha\beta}(w_{,\alpha} - \phi_\alpha)(w_{,\beta} - \phi_\beta) - pw]dA$$

$$+ \int_{C_{\sigma_m}} (\bar{M}_n \phi_n + \bar{M}_{ns}\phi_s - \bar{Q}_n w)dC \} \qquad (3.66)$$

Ignoring transverse shear deformation effects, Eq. 3.66 can be written as:

$$\Pi_{CD} = \sum_m \{ \int_{A_m} (\frac{1}{2} E_{\alpha\beta\gamma\delta} w_{,\alpha\beta} w_{,\gamma\delta} - pw)dA$$

$$+ \int_{C_{\sigma_m}} (\bar{M}_n w_{,n} - \bar{V}_n w)dC + [\bar{M}_{ns} w]_{C_{\sigma_m}} \} \qquad (3.67)$$

The first variation of the above equation is:

$$\delta\Pi_{CD} = \sum_m \{ \int_{A_m} [(E_{\alpha\beta\gamma\delta} w_{,\gamma\delta})_{,\alpha\beta} - p]\delta w dA$$

$$+ \int_{C_{\sigma_m}} [(\bar{M}_n - M_n)\delta w_{,n} - (\bar{V}_n - V_n)\delta w] dC + [(\bar{M}_{ns} - M_{ns})\delta w]_{C_{\sigma_m}} \} \qquad (3.68)$$

The Euler equations are equilibrium equations and traction boundary conditions.

Stress Models

By assuming equilibrium equations, a priori, all the finite element stress models can be obtained from Eq. 3.49 by the same modifications and additional boundary variables as appropriate displacement models. For hybrid stress model version 1, Eqs. 2.36, Eq. 3.46 and the same variables and similar integrals along boundary to those of hybrid displacement model version 2, Eqs. 3.63 and 3.64, may be used. Thus, hybrid stress model version 1, with and without considering transverse shear deformation effects, can be written, respectively, as follows:

$$\Pi_{HS1} = \sum_m \{ - \int_{A_m} [\frac{1}{2}(D_{\alpha\beta\gamma\delta} M_{\alpha\beta} M_{\gamma\delta} + D_{\alpha 3 \beta 3} Q_\alpha Q_\beta) + D_{\alpha\beta 33} p M_{\alpha\beta} + D_{\alpha 333} p Q_\alpha] dA$$

$$- \int_{C_m} (M_n \phi_n^L + M_{ns} \phi_s^L - Q_n w^L) dC$$

$$+ \int_{C_{\sigma_m}} (\bar{M}_n \phi_n^L + \bar{M}_{ns} \phi_s^L - \bar{Q}_n w^L) dC \} \qquad (3.69)$$

$$\Pi_{HS1} = \sum_m \{ - \int_{A_m} \frac{1}{2} D_{\alpha\beta\gamma\delta} M_{\alpha\beta} M_{\gamma\delta} \, dA$$

$$- \int_{C_m} (M_n w,_n^L - V_n w^L) dS - [M_{ns} w^L]_{C_m}$$

$$+ \int_{C_{\sigma_m}} (\bar{M}_n w,_n^L - \bar{V}_n w^L) dC + [\bar{M}_{ns} w^L]_{C_{\sigma_m}} \quad \} \tag{3.70}$$

It should be noted that the boundary tractions, T_i in the hybrid stress model version 1, are derived from interior stresses as can be seen in Eq. 2.36, while those of the hybrid displacement model version 2 are assumed along the boundary independently.

To obtain proper Euler equations, the following consideration should be given to all the finite element stress models. Extremizing the functionals, the first terms of Eqs. 2.36, 2.37 and 2.39 give the following:

$$- \int_{V_m} \frac{\partial B}{\partial \sigma_{ij}} \delta\sigma_{ij} dV = - \int_{V_m} \epsilon_{ij} \delta\sigma_{ij} dV \tag{3.71}$$

From this variation, any further information cannot be obtained, since $\delta\sigma_{ij}$ is not completely arbitrary but subject to the condition of:

$$\delta\sigma_{ij},_j = 0 \tag{3.72}$$

due to the equilibrium equation, Eq. 2.12. Thus, the constraint condition, Eq. 3.72, is augmented into Eq. 3.71 with a set of differentiable Lagrange multiplier functions, f_i.

$$- \int_{V_m} (\epsilon_{ij} \delta\sigma_{ij} + f_i \delta\sigma_{ij},_j) dV \tag{3.73}$$

By further manipulations, it can be seen that the Lagrange multipliers f_i are identified with displacements.

In the functional, Eq. 3.70, the interior stresses $M_{\alpha\beta}$ are subject to the plate equilibrium equation, Eq. 3.34, and the constraint term may be written as:

$$\int_{A_m} \delta M_{\alpha\beta,\alpha\beta} w dA = 0 \tag{3.74}$$

The first variation of Eq. 3.70 which is subject to Eq. 3.74 is:

$$\begin{aligned}\delta_{HS1} = \sum_m \{ & - \int_{A_m} (D_{\alpha\beta\gamma\delta} M_{\gamma\delta} + w_{,\alpha\beta}) \delta M_{\alpha\beta} dA \\ & - \int_{C_m} [(w^L_{,n} - w_{,n}) \delta M_n - (w^L - w) \delta V_n] dC - [(w^L - w) \delta M_{ns}]_{C_m} \\ & + \int_{C_{\sigma_m}} [(\bar{M}_n - M_n) \delta w^L_{,n} - (\bar{V}_n - V_n) \delta w^L] dC + [(\bar{M}_{ns} - M_{ns}) \delta w^L]_{C_{\sigma_m}} \\ & - \int_{C_{\rho_m}} (M_n \delta w^L_{,n} - V_n \delta w^L) dC - [M_{ns} \delta w^L]_{C_{\rho_m}} \quad \}\end{aligned} \tag{3.75}$$

The Euler equations are: strain displacement relations from the first line, displacement continuity and boundary conditions from the second line, and traction boundary and continuity conditions from the last two lines, respectively.

Referring to Eqs. 2.37 and 3.46, and by the same variables and similar integrals along the boundary to those of hybrid displacement model version 1, hybrid stress model version 2, with and without considering transverse shear deformation effects, can be written, respectively, as:

$$\Pi_{HS2} = \sum_m \{ - \int_{A_m} [\frac{1}{2} D_{\alpha\beta\gamma\delta} M_{\alpha\beta} M_{\gamma\delta} + D_{\alpha 3 \beta 3} Q_\alpha Q_\beta) + D_{\alpha\beta 33} P M_{\alpha\beta} + D_{\alpha 333} p Q_\alpha] dA$$

$$- \int_{C_m} [(M_n - M_n^L)\phi_n^\ell + (M_{ns} - M_{ns}^L)\phi_s^\ell - (Q_n - Q_n^L)w^\ell]dC$$

$$- \int_{C_{u_m}} (M_n^L \bar{\phi}_n + M_{ns}^L \bar{\phi}_s - Q_n^L \bar{w})dC \} \qquad (3.76)$$

$$\Pi_{HS2} = \sum_m \{ - \int_{A_m} \frac{1}{2} D_{\alpha\beta\gamma\delta} M_{\alpha\beta} M_{\gamma\delta} dA$$

$$- \int_{C_m} [(M_n - M_n^L)w_{,n}^\ell - (V_n - V_n^L)w^\ell]dC - [(M_{ns} - M_{ns}^L)w^\ell]_{C_m}$$

$$- \int_{C_{u_m}} (M_n^L \bar{w}_{,n} - V_n^L \bar{w})dC - [M_{ns}^L \bar{w}]_{C_{u_m}} \qquad (3.77)$$

where ϕ_α^ℓ and w^ℓ are arbitrary boundary displacement functions which correspond to interior displacements in the corresponding hybrid displacement model version 1.

By the same way as the previous model, the first variation of Eq. 3.77 can be written as:

$$\delta\Pi_{HS2} = \sum_m \{ - \int_{A_m} (D_{\alpha\beta\gamma\delta} M_{\gamma\delta} + W_{,\alpha\beta}) \delta M_{\alpha\beta} dA$$

$$- \int_{C_m} [(M_n - M_n^L)\delta w_{,n}^\ell - (V_n - V_n^L)\delta \bar{w}^\ell]dC - [(M_{ns} - M_{ns}^L)\delta w^\ell]_{C_m}$$

$$- \int_{C_m} [(w_{,n}^\ell - w_{,n})\delta M_n - (w^\ell - w)\delta V_n]dC - [(w^\ell - w)\delta M_{ns}]_{C_m}$$

$$- \int_{C_{u_m}} [(\bar{w}_{,n} - w_{,n}^\ell)\delta M_n^L - (\bar{w} - w^\ell)\delta V_n^L]dC - [(\bar{w} - w^\ell)\delta M_{ns}^L]_{C_{u_m}}$$

$$+ \int_{C_{\rho_m}} (w^{\ell}_{,n} \delta M^L_n - w^{\ell} \delta V^L_n) dC + [w^{\ell} \delta M^L_{ns}]_{C_{\rho_m}} \} \qquad (3.78)$$

The Euler equations are: strain displacement relations from the first line, traction continuity and boundary conditions from the second line, and displacements continuity and boundary conditions from the last two lines through the matching of boundary and interior displacements from the third line.

When traction continuity and boundary conditions are assumed a priori, the equilibrium stress model, with and without considering the effects of transverse shear deformation, can be derived from Eqs. 3.69 and 3.76 and Eqs. 3.70 and 3.77, respectively, as follows:

$$\Pi_{ES} = \sum_m \{ - \int_{A_m} [\frac{1}{2} (D_{\alpha\beta\gamma\delta} M_{\alpha\beta} M_{\gamma\delta} + D_{\alpha 3 \beta 3} Q_\alpha Q_\beta) + D_{\alpha\beta 33} {}^{p}M_{\alpha\beta} + D_{\alpha 333} {}^{p}Q_\alpha] dA$$

$$- \int_{C_{u_m}} (M_n \bar{\phi}_n + M_{ns} \bar{\phi}_s - Q_n \bar{w}) dC \} \qquad (3.79)$$

$$\Pi_{ES} = \sum_m \{ - \int_{A_m} \frac{1}{2} D_{\alpha\beta\gamma\delta} M_{\alpha\beta} M_{\gamma\delta} dA$$

$$- \int_{C_{u_m}} (M_n \bar{w}_{,n} - V_n \bar{w}) dC - [M_{ns} \bar{w}]_{C_{u_m}} \} \qquad (3.80)$$

The first variation of Eq. 3.80 is:

$$\delta\Pi_{ES} = \sum_m \{ - \int_{A_m} (D_{\alpha\beta\gamma\delta} M_{\gamma\delta} + w_{,\alpha\beta}) \delta M_{\alpha\beta} dA$$

$$- \int_{C_{u_m}} [\bar{w}_{,n} - w_{,n}) \delta M_n - (\bar{w} - w) \delta V_n] dC$$

$$- \left[(\tilde{w} - w)\delta M_{ns} \right]_{C_{u_m}} \Big\} \tag{3.81}$$

The Euler equations are: strain displacement relations and displacement boundary conditions.

Mixed Models

If the only a priori conditions are constitutive relations, hybrid mixed models can be obtained from Eqs. 2.40 and 2.41 by using appripriate integrals used in this chapter. They are:

$$\begin{aligned}
\Pi_{HM1} = \sum_m \Big\{ & - \int_{A_m} \left[\frac{1}{2} \left(D_{\alpha\beta\gamma\delta} M_{\alpha\beta} M_{\gamma\delta} + D_{\alpha 3 \beta 3} Q_\alpha Q_\beta \right) + D_{\alpha\beta 33} {}^{p}M_{\alpha\beta} + D_{\alpha 333} {}^{p}Q_\alpha \right] dA \\
& - \int_{A_m} \left[M_{\alpha\beta} \phi_{\alpha,\beta} + Q_\alpha (\phi_\alpha - w_{,\alpha}) + pw \right] dA \\
& + \int_{C_m} (M_n^L \phi_n + M_{ns}^L \phi_s - Q_n^L w) dC \\
& - \int_{C_{u_m}} (M_n^L \bar{\phi}_n + M_{ns}^L \bar{\phi}_s - Q_n^L \bar{w}) dC
\end{aligned} \tag{3.82}$$

$$\begin{aligned}
\Pi_{HM2} = \sum_m \Big\{ & - \int_{A_m} \left[\frac{1}{2} \left(D_{\alpha\beta\gamma\delta} M_{\alpha\beta} M_{\gamma\delta} + D_{\alpha 3 \beta 3} Q_\alpha Q_\beta \right) + D_{\alpha\beta 33} {}^{p}M_{\alpha\beta} + D_{\alpha 333} {}^{p}Q \right] dA \\
& - \int_{A_m} \left[M_{\alpha\beta} \phi_{\alpha,\beta} + Q_\alpha (\phi_\alpha - w_{,\alpha}) + pw \right] dA \\
& + \int_{C_m} \left[M_n (\phi_n - \phi_n^L) + M_{ns} (\phi_s - \phi_s^L) - Q_n (w - w^L) \right] dC \\
& + \int_{C_{\sigma_m}} (\bar{M}_n \phi_n^L + \bar{M}_{ns} \phi_s^L - \bar{Q}_n w^L) dC \Big\}
\end{aligned} \tag{3.83}$$

When the effects of transverse shear deformation are ignored, Eqs. 3.82 and 3.83 can be written as:

$$\Pi_{HM1} = \sum_m \{ - \int_{A_m} (\frac{1}{2} D_{\alpha\beta\gamma\delta} M_{\alpha\beta} M_{\gamma\delta} + M_{\alpha\beta} w_{,\alpha\beta} + pw) dA$$

$$+ \int_{C_m} (M_n^L w_{,n} - V_n^L w) dC + [M_{ns}^L w]_{C_m}$$

$$- \int_{C_{u_m}} (M_n^L \bar{w}_{,n} - V_n^L \bar{w}) dC - [M_{ns}^L w]_{C_{u_m}} \} \qquad (3.84)$$

$$\Pi_{HM2} = \sum_m \{ - \int_{A_m} (\frac{1}{2} D_{\alpha\beta\gamma\delta} M_{\alpha\beta} M_{\gamma\delta} + M_{\alpha\beta} w_{,\alpha\beta} + pw) dA$$

$$+ \int_{C_m} [M_n (w_{,n} - w_{,n}^L) - V_n (w - w^L)] dC + [M_{ns} (w - w^L)]_{C_m}$$

$$+ \int_{C_{\sigma_m}} (\bar{M}_n \phi_n^L - \bar{V}_n w^L) dC + [\bar{V}_n w^L]_{C_{\sigma_m}} \} \qquad (3.85)$$

As in hybrid stress model version 1, arbitrary boundary tractions of Eq. 3.85 need not be assumed independently, since the tractions which are derived from the interior stress field can be used. In the corresponding displacement model, Eq. 3.63, boundary tractions should be assumed independently. By the same manipulations done on the models mentioned previously, it can be seen that the Euler equations of Eqs. 3.84 and 3.85 are all the field equations, boundary conditions and traction and displacement continuity conditions except the a priori assumed constitutive relations.

When continuity conditions of displacements and tractions along

interelement boundaries are satisfied a priori, in addition, the finite element equivalent of Hellinger-Reissner principles with and without considering transverse shearing deformation effects can be obtained from Eqs. 3.82 and 3.83, and Eqs. 3.84 and 3.85, respectively, as:

$$\Pi_{ER} = \sum_m \{ - \int_{A_m} [\frac{1}{2} (D_{\alpha\beta\gamma\delta} M_{\alpha\beta} M_{\gamma\delta} + D_{\alpha 3 \beta 3} Q_\alpha Q_\beta) + D_{\alpha\beta 33} pM_{\alpha\beta} + D_{\alpha 333} pQ] dA$$

$$- \int_{A_m} [M_{\alpha\beta} \phi_{\alpha,\beta} + Q_\alpha (\phi_\alpha - w_{,\alpha}) + pw) dA$$

$$+ \int_{S_{\sigma_m}} (\bar{M}_n \phi_n + \bar{M}_{ns} \phi_s - \bar{Q}_n w) dC$$

$$+ \int_{S_{u_m}} [M_n (\phi_n - \bar{\phi}_n) + M_{ns} (\phi_s - \bar{\phi}_s) - Q_n (w - \bar{w})] dC \qquad (3.86)$$

$$\Pi_{ER} = \sum_m \{ - \int_{A_m} (\frac{1}{2} D_{\alpha\beta\gamma\delta} M_{\alpha\beta} M_{\gamma\delta} + M_{\alpha\beta} w_{,\alpha\beta} + pw) dA$$

$$+ \int_{C_{\sigma_m}} (\bar{M}_n w_{,n} - \bar{V}_n w) dC + [\bar{M}_{ns} w]_{C_{\sigma_m}}$$

$$+ \int_{C_{u_m}} [M_n (w_{,n} - \bar{w}_{,n}) - V_n (w - \bar{w})] dC + [M_{ns} (w - \bar{w})]_{C_{u_m}} \} \qquad (3.87)$$

The Euler equations of the functional are all the field equations and boundary conditions except constitutive relations.

CHAPTER IV

BENDING PROBLEMS OF THIN PLATES WITH VARIOUS BOUNDARY CONDITIONS

This chapter presents discussion of some problems associated with traction boundary conditions in the finite element method when the curved boundaries of a domain are approximated by piecewise straight segments. The so-called Babuska paradox in the solution for a simply supported circular plate whose boundary is approximated by that of a polygon is discussed.

Also, ways to explicitly enforce the higher order (natural) boundary conditions in the finite element method are explored. Circular and annular plates with various boundary conditions and rectangular plates with central holes of several different shapes are solved with and without explicitly enforcing traction boundary conditions. Applied external load is either a point load or uniformly distributed. For all cases, body forces and transverse shear deformation effects are ignored. Linear theory of a thin elastic plate is used. Following the general discussion of the approximations involved at a circular boundary, in the second and third sections, the results of compatible displacement model and hybrid stress model solutions for various circular shaped plates, respectively, are discussed. In the last section, stress concentration problems of rectangular plates with central holes are treated.

Approximations at Curved Boundaries

Three different types of approximations can be involved in the finite element method in problems with curved domains. In the first place,

the solution functions are approximated in terms of piecewise polynomials. Second, the arbitrarily curved domain may be approximated by some other more manageable form, such as piecewise straight segments. Last, the boundary conditions are also subject to approximation. The errors in the solution of a boundary-value problem which can occur due to approximations at the boundary are caused by combinations of the above features.

An interesting problem arises when an essential and a natural boundary condition are combined in a boundary-value problem with a curved domain which is to be approximated by an inscribed polygon. This is popularly known as the "Babuska paradox" [54,55], and is studied in detail in the present chapter.

Babuska Paradox

Consider the mathematical boundary value problem, in the domain shown in Fig. 2.1, defined by the following biharmonic linear differential equation.

$$\nabla^4 w = 1 \quad \text{in} \quad D \tag{4.1}$$

and homogeneous boundary conditions

$$w = w_{,nn} = 0 \quad \text{on} \quad B \tag{4.2}$$

where n is the direction of an outward normal to the curved boundary. Assume that the domain D is approximated by an inscribed N-sided polygon, D^h, with boundary B^h. Intuitively, the solution w^h of the preceding boundary value problem in the polygon D^h with the following boundary conditions

$$w^h = w^h_{,nn} = 0 \quad \text{on} \quad B^h \tag{4.3}$$

where now n is the outward normal to B^h, should be expected to converge to the solution in the true domain, D, as $N \to \infty$. The Babuska paradox consists in the fact that it does not.

It is considered that the difficulty involved in this problem is caused by the change in the higher order boundary conditions, due to the change of the boundary coordinates by which the boundary conditions are expressed in the approximated domain. The above problem can be modified by introducing new variable $V^h = \nabla w^h$ and replacing higher order boundary condition by harmonic equations as follows [56].

$$\nabla^2 w^h = V^h \qquad \text{in} \quad D^h \tag{4.4}$$

$$\nabla^2 V^h = 1 \qquad \text{in} \quad D^h \tag{4.5}$$

$$w^h = V^h = 0 \qquad \text{on} \quad B^h \tag{4.6}$$

For such a second-order system; convergence of the solution is guaranteed [56], and w^h and V^h approach to the solution of

$$\nabla^2 w = V \qquad \text{in} \quad D \tag{4.7}$$

$$\nabla^2 V = 1 \qquad \text{in} \quad D \tag{4.8}$$

$$w = V = 0 \qquad \text{on} \quad B \tag{4.9}$$

where V is the exact solution of V^h in D, as $N \to \infty$.

The boundary conditions given by Eq. 4.9 can be generalized as follows for a circular domain [Fig. 4.1]

$$w = 0$$

$$w_{,nn} + k\frac{w_{,n}}{a} = 0$$

where a is the radius of the circle, and k is an arbitrary parameter. It is observed that when k=0 the above boundary conditions are identical to those given by Eq. 4.2, and when k=1 the above are identical to those given by Eq. 4.9. Thus for the problem defined by Eq. 4.1 and the above boundary conditions with k=0, the approximate solutions obtained for a polygonal approximation of the circular domain do not converge to the exact solution; and with k=1, they do converge to the correct answer. Since k does not appear in the boundary condition for the polygonal domain, it can be seen that for any k≠1, the solutions for the polygonal domain converge to the solution for the circular domain with k=1. That is, there is a Babuska paradox for all values of k≠1.

A parallel problem in solid mechanics is that of a simply supported plate with a curved boundary and constant thickness which is treated briefly by Fix and Strang [56]. The problem is defined by the following when the domain is circular one [Fig. 4.1]

$$\nabla^4 w = p/\bar{D} \quad \text{in} \quad D \tag{4.10}$$

$$w = w_{,nn} + \nu\frac{w_{,n}}{a} = 0 \quad \text{on} \quad B \tag{4.11}$$

where p is the external load, $\bar{D}$ is the flexural rigidity of the plate, ν is Poisson's ratio, and w is the transverse displacement. If p is a constant and the Poisson ratio ν is replaced by k this problem is equivalent to the problem defined by Eq. 4.1 and the previous generalized boundary conditions. Thus, when a simply supported circular plate is solved by approximate methods with polygonal domain approximation, the

solution $\bar{w}^h = \bar{D}w^h$ will converge to that of a simply supported circular plate with Posson's ratio $\nu=1$ in the higher order boundary condition, regardless actual value of Poisson's ratio of the plate.

Rao and Rajaiah showed these difficulties numerically by summarizing results of the previous works of several different research groups, using the boundary collocation method [57]. The model is that of a simply supported N-sided regular polygonal plate whose domain is D^h with boundary B^h, which circumscribes a circle with constant radius a [Fig. 4.1]. The deflection function:

$$\bar{w} = \frac{Eh^3 w}{12(1-\nu^2)pa^4} = \frac{r^4}{64a^4} + \sum_{m=0,1,} (A_m + B_m r^2)\, r^{mN} \cos mN\theta \text{ in } D \qquad (4.12)$$

where E is Young's modulus of the plate, h is the plate thickness, and p is the uniformly applied load on the plate, satisfies the governing differential equation $\frac{Eh^3}{12(1-\nu^2)} \nabla^4 w = p$ and the N-fold cyclic symmetry in the problem.

It is to be noted that the assumed solution function satisfies none of the boundary conditions, and thus the constants A_m and B_m are determined by satisfying the boundary conditions at a finite number of points on the boundary, B^h. It is also noted that in the above assumed solution function, setting w=0 at a finite number of points at B^h does not automatically imply that $w_{,ss} = 0$ (s being the direction tangential to B^h) at B^h, and thus the condition $w_{,ss} = 0$ has to be imposed separately, as distinct from the condition w=0. Thus, Rao and Rajaiah [57] consider the boundary conditions for the polygon in the following general form:

$$w = 0 \qquad \text{on } B^h \qquad (4.13)$$

$$w_{,nn} + Kw_{,ss} = 0 \qquad \text{on} \quad B^h \tag{4.14}$$

where K is an arbitrary constant. In [57] results of a series of numerical experiments are presented for various values of K, N and M which is the total number of terms in solution function Eq. 4.12 (M=m+1), and these are plotted in Fig. 4.2. Dashed lines indicate the exact deflections of circular plates with different values of ν which are the same as the K values used in the boundary conditions for the polygonal plates.

From the results of [57], the following interesting conclusions can be drawn when it is assumed that the regular polygonal domains D^h are the approximations of the circular domain D with boundary B. First, for a polygonal plate with fixed number, however large, of sides N, the central deflection approaches to that of simply supported circular plate with the Poisson ratio ν=1 regardless of the original value of the Poisson ratio prescribed for the plate, as $M \to \infty$. Thus the solution $\bar{w}$ in Eq. 4.12 for the polygonal plate becomes independent of the Poisson ratio, however large the number of sides may be. This fact confirms the above mentioned Babuska paradox, numerically.

Second, when the boundary conditions simulate, at least approximately those of a circular plate as Eq. 4.14, the solution for the polygon converges to that of circular plate, with the same Poisson ratio, as the number of sides $N \to \infty$ with any fixed M. However, it is interesting to note that the rate of the above convergence decreases with the increase of M, and convergence appears to be very poor, when both M and $N \to \infty$.

As shown in Eq. 4.2 and Eq. A.2b of the Appendix A, the natural

boundary condition of a simply supported circular plate is

$$w_{,nn} + \nu \left(\frac{w_{,n}}{a} + w_{,ss} \right) = 0 \qquad (4.15)$$

The difference between the above equation and Eq. 4.14 (with K=ν), which is the simulated "circular plate boundary condition" along a straight edge, is inherently due to the difference in coordinate systems which are used at boundaries, B and B^h. The difference is caused by the approximation of a circular domain by a polygon and this difference can not be changed by simply making $N \to \infty$.

Thus the most significant results of the boundary collocation studies of [57], relevant to the present discussion, can thus be stated: when the boundary of a simply supported circular plate is approximated by a polygon, the solution for the polygon will converge to that of the circle for any fixed M (number of terms in series) when N (number of sides in polygon) $\to \infty$ and the constant K in the boundary condition Eq. 4.14 is taken to be ν (the Poisson ratio) for the circular plate. It should be emphasized however, that the condition $w_{,nn} + \nu w_{,ss} = 0$ is "unnatural" for a polygonal plate with straight edges, whereas the occurence of ν in the boundary conditions is natural for a circular plate with a curved boundary.

It is shown in the following that the satisfaction of the above natural boundary conditions at a curved boundary becomes much easier in the finite element method, in spite of the approximation of the curved boundary itself by piecewise straight segments.

Approximations on a Boundary in the Finite Element Method

It is first shown that in the context of the Ritz method (also hence

the Ritz-based finite element method), the previously discussed anomalies can be traced to the concept of "natural boundary conditions" of the variational principle.

The previous discussion is centered on the change of natural boundary conditions due to the approximation of boundary in a mixed boundary value problem. Because of the change in the shape of a boundary segment from an arbitrary curve to a straight line, the Poisson ratio disappears from the moment boundary conditions of a simply supported plate.

In the finite element method formulated through a variational method, the situation is slightly different from the above since natural boundary conditions are satisfied implicitly as a consequence of extremization of an appropriate functional. To investigate the effects of boundary approximation on these higher order boundary conditions, a simply supported circular plate with uniformly applied external load will be considered in the following discussion.

The functional of the minimum potential energy principle, Eq. 3.67, for an isotropic plate with no prescribed tractions at the boundary, can be written as:

$$\Pi_{CD} = \sum_{m} \int_{A_m} \{ \frac{D}{2} [w^2_{,xx} + w^2_{,yy} + 2\nu w_{,xx} w_{,yy} + 2(1-\nu) w^2_{,xy}] - pw \} dA \quad (4.16)$$

where $D = \frac{Eh^3}{12(1-\nu^2)}$ is the flexural rigidity of the plate, E is the Young's modulus, h is the thickness of the plate, and p is the applied external force on the upper surface of the plate. In order for a displacement finite element model to be valid for Eq. 4.16, w and its first derivatives must be continuous at all interelement boundaries. This implies that along any segment of the element boundary, the displacement w, and the derivative of

w in the direction normal to the boundary must be uniquely interpolated in terms of their respective values at nodes only along the particular boundary segment in question.

The first variation of the above with respect to w can be written as:

$$\delta\Pi_{CD} = \sum_m \{ \int_{A_m} (D\nabla^4 w - p)\delta w \, dA$$

$$- D \int_{C_m} [\frac{\partial}{\partial x} (\nabla^2 w) n_x + \frac{\partial}{\partial y} (\nabla^2 w) n_y] \delta w \, dC$$

$$+ D \int_{C_m} [(w_{,xx} + \nu w_{,yy}) n_x \delta w_{,x} + (w_{,yy} + \nu w_{,xx}) n_y \delta w_{,y}$$

$$+ (1-\nu) \, w_{,xy} \, (n_y \delta w_{,x} + n_x \delta w_{,y})] \, dC \} \qquad (4.17)$$

where n_α are the direction cosines of a unit vector normal to the boundary curve C_m. By using coordinate transformations, the boundary integrals can be expressed in the boundary coordinates, and thus:

$$\delta\Pi_{CD} = \sum_m \{ \int_{A_m} (D\nabla^4 w - p)\delta w dA + D I_{C_m} \} \qquad (4.18)$$

where

$$I_{C_m} = \int_{C_m} (w_{,nn} + \frac{\nu}{a} w_{,n} + \nu w_{,ss}) \delta w_{,n} dC$$

$$- \int_{C_m} [(1-\nu)(w_{,nss} - \frac{w_{,ss}}{a}) + \frac{\partial}{\partial n} (\nabla^2 w)] \delta w dC$$

$$+ [(1-\nu) \, w_{,ns} \delta w]_{C_m} \qquad (4.19)$$

for a circular boundary C_m, where s is measured along the boundary, n is normal to the boundary, and a is the radius of the plate. The last term in the square brackets represents the virtual work done by corner forces due to twisting moment along the boundary segment. If the geometrical boundary condition for a simply supported plate, namely, w=0 on C_m is satisfied a priori, as is required in the Ritz method, $\delta w=0$ on C_m; further the term $w_{,ss}$ in the first integral in Eq. 4.19 vanishes automatically, and thus for arbitrary variations in $\delta w_{,n}$ the vanishing of the boundary integral in Eq. 4.19 yields the natural boundary condition

$$w_{,nn} + \frac{\nu}{a} w_{,n} = 0 \tag{4.20}$$

If the boundary is a polygon, taking ξ to be the local coordinate along a straight boundary segment, and ζ normal to this boundary, then term I_{C_m} in Eq. 4.18 can be written as:

$$I_{C_m} = \int_{C_m^h} (w_{,\zeta\zeta} + \nu w_{,\xi\xi}) \delta w_{,\zeta} dC$$

$$- \int_{C_m^h} [(1-\nu) w_{,\zeta\xi\xi} + \frac{\partial}{\partial \zeta} (\nabla^2 w)] \delta w dC + [(1-\nu) w_{,\zeta\xi} \delta w]_{C_m^h} \tag{4.21}$$

where C_m^h is a straight boundary segment and the last term in square brackets represents the virtual work done by concentrated forces at corners due to twisting moment at the boundary segment. If the essential boundary condition of w=0 is imposed all along the straight boundary C_m^h, as if for a simply supported polygonal plate, then $\delta w=0$ on C_m^h; further, the term $w_{,\xi\xi}$ in the first integral in Eq. 4.21 vanishes automatically.

Thus for arbitrary variation $\delta w_{,\zeta}$, the vanishing of the integral in Eq. 4.21 yields the natural boundary condition

$$w_{,\zeta\zeta} = 0. \tag{4.22}$$

Therefore the natural boundary condition for a true polygonal plate is independent of the Poisson ratio ν. Thus, as seen from the previous discussion, the convergence of the polygonal plate solution to that of a circular plate, of which the polygon is a geometric approximation, cannot be guaranteed.

Thus, alternative ways to obtain the other natural boundary conditions (including the effect of the Poisson ratio) from the variational principle governing the plate problem with a polygonal approximation to a circular boundary, must be considered. To this end, first consider a finite element (triangular in the present case) ABC as in Fig. 4.3, the boundary A-B of which forms the boundary segment C_m^h of the polygon.

As mentioned earlier, for a valid compatible displacement finite element model for a plate problem, the transverse displacement and at least its first derivatives should be continuous at the element boundary A-B-C of the present element. Therefore, in the present problem, the simplest finite element would be one which has w; $w_{,\xi}$; and $w_{,\zeta}$ as degrees of freedom at each of the three nodes A, B, and C of the element. If the interpolation functions are required to satisfy the above continuity requirements, then w and its normal derivative along any boundary segment should be uniquely interpolated along the particular segment only in terms of their respective values at the nodes along the boundary. Thus it can be seen that:

$$w_{AB} = w_A\phi_1 + w,_{\zeta_A}\phi_2 + w_B\phi_3 + 2,_{\xi_B}\phi_4 \tag{4.23}$$

$$w,_{\zeta} = w,_{\zeta_A}\phi_5 + w,_{\zeta_A}\phi_6 \tag{4.24}$$

where w_A, w_B are the values of w at nodes A and B, respectively, etc., and $\phi_i(i=1,6)$ are unique interpolation functions. Introducing the coordinates s and n locally tangential and normal to the circular boundary at nodes A and B gives the following coordinate transformation:

$$\begin{Bmatrix} w,_{\zeta} \\ w,_{\xi} \end{Bmatrix} = \begin{bmatrix} \cos\Theta' & \sin\Theta' \\ -\sin\Theta' & \cos\Theta' \end{bmatrix} \begin{Bmatrix} w,_{n} \\ w,_{s} \end{Bmatrix} \tag{4.25}$$

where Θ' is the angle between the directions n and ζ. Then Eqs. 4.23 and 4.24 can be written as:

$$w_{AB} = w_A\phi_1 + (-\sin\Theta w,_{n_A} + \cos\Theta w,_{s_A})\phi_2 + w_B\phi_3 + (\sin\Theta w,_{n_B} + \cos\Theta w,_{s_B})\phi_4 \tag{4.26}$$

$$w,_{\zeta_{AB}} = (\cos\Theta w,_{n_A} + \sin\Theta w,_{s_A})\phi_5 + (\cos\Theta w,_{n_B} - \sin\Theta w,_{s_B})\phi_6 \tag{4.27}$$

where $\Theta=\Theta'$ at node A[Fig. 4.3]. From Eqs. 4.23, 4.24, 4.26 and 4.27, it can be seen, that:

$$\delta w_{AB} = \delta w_A\phi_1 + \delta w,_{\xi_A}\phi_2 + \delta w_B\phi_3 + \delta w,_{\xi_B}\phi_4 \tag{4.28}$$

$$(w,_{\xi\xi})_{AB} = {}_2A\phi_{1,\xi\xi} + w,_{\xi_A}\phi_{2,\xi\xi} + w_B\phi_{3,\xi\xi} + w,_{\xi_B}\phi_{4,\xi\xi} \tag{4.29}$$

and

$$\delta w,_{\zeta_{AB}} = \delta w,_{\zeta_A}\phi_5 + \delta w,_{\zeta_B}\phi_6 \tag{4.30}$$

or

$$\delta w_{AB} = \delta w_A \phi_1 + (-\sin\theta \delta w,_{n_A} + \cos\theta \delta w,_{s_A})\phi_2$$

$$+ \delta w_B \phi_3 + (\sin\theta \delta w,_{n_B} + \cos\theta \delta w,_{s_B})\phi_4 \tag{4.31}$$

$$(w,_{\xi\xi})_{AB} = w_A \phi_{1,\xi\xi} + (-\sin\theta w,_{n_A} + \cos\theta w,_{s_A})\phi_{2,\xi\xi}$$

$$+ w_B \phi_{3,\xi\xi} + (\sin\theta w,_{n_s} + \cos\theta w,_{s_B})\phi_{4,\xi\xi} \tag{4.32}$$

and

$$\delta w,_{\zeta_{AB}} = (\cos\theta \delta w,_{n_A} + \sin\theta \delta w,_{s_A})\phi_5$$

$$+ (\cos\theta \delta w,_{n_B} - \sin\theta \delta w,_{s_B})\phi_6 \tag{4.33}$$

The essential boundary condition for a polygonal plate, w=0 along AB would make the boundary integral in Eq. 4.21 independent of the Poisson ratio.

However, even if the curved boundary is approximated by straight segments, the finite element method makes it possible to satisfy the essential boundary conditions corresponding to the given curved boundary which in this case is w=0 along the arc A-E-B in Fig. 4.3. These essential boundary conditions on the circular boundary can be stated as $w_A = \delta w_A = w,_{s_A} = w,_{s_B} = w_B = \delta w_B = 0$. Thus, from Eqs. 4.31 - 4.33,

$$\delta w_{AB} = -\sin\theta\,(\delta w,_{n_A} \phi_2 - \delta w,_{n_B} \phi_4) \tag{4.34}$$

$$(w,_{\xi\xi})_{AB} = -\sin\theta\,(w,_{n_A} \phi_{2,\xi\xi} - w,_{n_B} \phi_{4,\xi\xi}) \tag{4.35}$$

and

$$\delta w,_{\zeta_{AB}} = \cos \delta w,_{n_{AB}} \tag{4.36}$$

where

$$\delta w,_{n_{AB}} = \delta w,_{n_A}\phi_5 + \delta w,_{n_B}\phi_6$$

Thus, the boundary integral in Eq. 4.21 can be written as:

$$\begin{aligned} I_{C_m} = & \int_{C_m^h} [w,_{\zeta\zeta} - \nu\sin\theta(w,_{n_A}\phi_{2,\xi\xi} - w,_{n_B}\phi_{4,\xi\xi}) \cos\theta\delta w,_n \\ & + \int_{C_m^h} [(1-\nu)w,_{\zeta\xi\xi} + \frac{\partial}{\partial\zeta}(\nabla^2 w)] \sin\theta(\delta w,_{n_A}\phi_2 - \delta w,_{n_B}\phi_4)dC \\ & - [(1-\nu)\, w,_{\zeta\xi}\sin\theta(\delta w,_{n_A}\phi_2 - \delta w,_{n_B}\phi_4)]_{C_m^h} \end{aligned} \tag{4.37}$$

It is clear from the above that the natural boundary conditions resulting from the vanishing of I_{C_m} are not independent of the Poisson ratio. Thus, for reasons discussed earlier, the solution for the polygonal plate might be expected to converge to that of the circular plate. However, the natural boundary conditions, from Eq. 4.37 are not simply those from the first integral of Eq. 4.37 but also are from the second integral.

A physical interpretation of these is as follows: the problem is stated as, "minimize the potential energy functional in Eq. 4.16 for a polygonal domain C_m^h, subject to the essential boundary conditions that the displacement w, and its tangential derivatives in the direction of the circular boundary curve, must vanish at the vertices of the polygon which also lie on the circular boundary." This is physically consistent with

the statement of the original problem of a circular plate, except, for reasons of convenience, the circular boundary is approximated by piecewise straight segments.

Thus by enforcing the essential boundary conditions that correspond to a curved boundary, even in the finite element mesh that approximates the curved boundary by a polygonal one, the natural boundary conditions in the variational function for the polygon are seen to have the effect of Poisson's ratio built into them. Thus, the finite element solution of the polygonal domain can still converge to the exact solution for a plate with curved boundaries for any assigned Poisson's ratio. Thus, in cases where only straight triangular elements are available to solve simply supported plate of curved boundaries, the polygonal solutions can be made to converge to that of curved domains when the essential boundary conditions at nodes of polygons are satisfied in the above way. In such a case the anomalies associated with the so-called "Babuska" or "polygon-circle" paradoxes disappear.

In the above formulation of a simply supported circular plate problem, dropping nodal quantities corresponding to slope is needed to guarantee to satisfy the essential boundary condition, $w=0$, along boundaries, since the deflection is expressed in terms of nodal values of slope as well as deflection itself as shown in Eq. 4.23. But, as shown in the above, dropping the degrees of freedom corresponding to slope causes disappearance of Poisson's ratio from the higher order natural boundary condition and thus, the difficulty in the problem.

When only the degrees of freedom corresponding to deflection at boundary nodes are dropped, even for the same type of element as the one

shown in Eq. 4.23, the effect of Poisson's ratio can be preserved in the higher order natural boundary condition. This essential boundary condition is that of a polygonal plate which is simply supported at the corners of the plate and free along each sides. Though the accuracy of solutions may not be so good as that in the previous method since more approximations are involved in enforcing essential boundary conditions in this method, the convergence of solutions can be expected, since two adjacent supporting points approach to make the entire boundary is simply supported one and the error caused by the approximation approaches zero infinitely, as the number of sides of approximating polygon increases infinitely.

In the following a detailed study of two finite element models, one based on a compatible displacement model, and the other based on a hybrid stress model are considered for bending problems of thin elastic plates with circular curved boundaries.

Compatible Displacement Model

The Basic Finite Element

The element that is used, is a high precision triangular element by Chernuka et. al. [58] and Cowper et. al. [59]. Though originally it was not developed in [58] with the same motivation as in the present work, because of its high accuracy and comparatively small approximation involved in the formulation, it is considered to be one of the best elements known for present study.

The formulation will be discussed briefly here. A typical element is shown in Fig. 4.4 where x, y and ξ, ζ are global and local rectangular cartesian coordinates respectively, a, b, and c are dimensions of the

element; d and e are the location of point P_4 in ξ, ζ system; and P_1, P_2 and P_3 are nodal points of the element. The line P_1- P_4- P_2 is the curved side, and P_4 is an arbitrary point on the curved side which is used to approximate P_1- P_4- P_2 curve by a quadratic curve, $\zeta = f(\xi)$, which will be discussed later.

The assumed shape function for the normal displacement, w, in the element is given by a quintic polynomial in ξ, ζ as:

$$\begin{aligned} w(\xi,\zeta) = {} & a_1 + a_2\xi + a_3\zeta + a_4\xi^2 + a_5\xi\zeta + a_6\zeta^2 + a_7\xi^3 + a_8\xi^2\zeta \\ & + a_9\xi\zeta^2 + a_{10}\zeta^3 + a_{11}\xi^4 + a_{12}\xi^3\zeta + a_{13}\xi^2\zeta^2 + a_{14}\xi\zeta^3 + a_{15}\zeta^4 \\ & + a_{16}\xi^5 + a_{17}\xi^3\zeta^2 + a_{18}\xi^2\zeta^3 + a_{19}\xi\zeta^4 + a_{20}\zeta^5 \end{aligned} \tag{4.38}$$

The degrees of freedom for each node are w, $w_{,\xi}$, $w_{,\zeta}$, $w_{,\xi\xi}$, $w_{,\xi\zeta}$, and $w_{,\zeta\zeta}$; thus the generalized displacement vector for an element is:

$$\underset{\sim}{W}_1^T = \lfloor w_1 w_{,\xi_1} w_{,\zeta_1} w_{,\xi\xi_1} w_{,\xi\zeta_1} w_{,\zeta\zeta_1} w_2 \cdots \quad w_3 \cdots \rfloor \tag{4.39}$$

From Eq. 4.38 and 4.39, $\underset{\sim}{W}_1$ can be expressed in terms of a_i as:

$$\underset{\sim}{W}_1 = \underset{\sim}{T}_1 \underset{\sim}{A} \tag{4.40}$$

where

$$\underset{\sim}{A}^T = \lfloor a_1 \; a^2 \; \ldots\ldots \quad a_{20} \rfloor \tag{4.41}$$

and $\underset{\sim}{T}_1$ is an 18 x 20 matrix.

First consider the case when side P_1-P_2 is a straight line, then the absence of the term $\xi^4\zeta$ in Eq. 4.38 guarantees that the normal slope along P_1-P_2 will be a cubic function of ξ, which guarantees normal slope

continuity between adjacent elements. Two additional equations may be found from the conditions that normal slopes be cubic functions along sides P_1-P_2 and P_2-P_3, as follows:

$$5b^4ca_{16} + (3b^2c^3 - 2b^4c)a_{17} + (2bc^4 - 3b^3c^2)a_{18} + (c^5 - 4b^2c^3)a_{19} - 5bc^4a_{20} = 0$$

$$5a^4ca_{16} + (3a^2c^3 - 2a^4c)a_{17} + (-2ac^4 + a^3c^2)a_{18} + (c^5 - 4a^2c^3)a_{19} + 5a\,c^4a_{20} = 0$$

When the relations in Eq. 4.40 are augmented by the above equations, a set of twenty equations for the coefficients a_i is obtained. It can be shown that these equations may be inverted to give:

$$\underset{\sim}{A} = \underset{\sim}{T}^{-1}\,\underset{\sim 1}{W}^{1} \tag{4.42}$$

where $\underset{\sim}{T}$ is a 20 x 20 matrix given in Table 4.1 and

$$\underset{\sim}{W}^{1} = \begin{Bmatrix} \underset{\sim 1}{W} \\ 0 \\ 0 \end{Bmatrix} \tag{4.43}$$

Substituting Eq. 4.38 into the strain energy expression of Eq. 4.16 will give the following strain energy for an element in terms of A, by appropriate integrations, as:

$$U_e = \frac{1}{2}\,\underset{\sim}{A}^T\underset{\sim 1}{K}\underset{\sim}{A} = \frac{1}{2}\,\underset{\sim 1}{W}^{1T}\underset{\sim}{T}^{-1T}\underset{\sim 1}{K}\underset{\sim}{T}^{-1}\underset{\sim 1}{W}^{1} \tag{4.44}$$

where $\underset{\sim 1}{K}$ is a 20 x 20 matrix.

The generalized displacements in x, y system can be related to those of ξ, ζ system as:

$$\underset{\sim}{W}_1 = \underset{\sim}{R}\,\underset{\sim}{W} \tag{4.45}$$

where

$$\underset{\sim}{W}^T = [w_1 w_{,x_1} w_{,y_1} w_{,xx_1} w_{,xy_1} w_{,yy_1} w_2 \ldots\ldots\ w_3 \ldots\ldots\ldots] \tag{4.46}$$

and $\underset{\sim}{R}$ is coordinate transformation tensor as shown in Table 4.2. Thus, the element strain energy, Eq. 4.44, can be written as:

$$U_e = \frac{1}{2}\,\underset{\sim}{W}^T \underset{\sim}{K}\,\underset{\sim}{W} \tag{4.47}$$

where the element stiffness matrix is given by:

$$\underset{\sim}{K} = \underset{\sim}{R}^T \underset{\sim}{T}^{-1T} \underset{\sim}{K}_1 \underset{\sim}{T}^{-1} \underset{\sim}{R} \tag{4.48}$$

The equivalent nodal force vector can be calculated by evaluating the virtual work done by the applied load.

For the approximation of the curved side $P_1 - P_2$ by a quadratic curve, a point P^4 is selected at a convenient location between the two nodal points P_1 and P_2 on the actual boundary and a quadratic curve is assumed as:

$$\zeta = C_1 + C_2\xi + C_3\xi^2 \tag{4.99}$$

The coefficients C_1, C_2 and C_3 can be determined from the locations of P_1, P_2 and P_4 in ξ,ζ system. By this modification, the limit of area integrations in an element near a curved boundary is extended from the straight line $P_1 - P_2$ to the quadratic curve $P_1 - P_4 - P_2$. It is noted that compared with a straight line this quadratic curve is a much more

accurate approximation of an actual arbitrarily curved boundary.

This element has exact representations of rigid body motions in the shape function. The only approximation involved in its formulation is the approximation of an arbitrarily curved boundary by a piecewise quadratic curve.

Enforcing geometric boundary conditions is usually done at the time when the final system of equations is solved by substituting the prescribed boundary values for the degrees of freedom which correspond to the appropriate boundary displacements at nodes on a displacement prescribed boundary . However, in a circular plate problem described with rectangular coordinate, geometric boundary conditions are expressed by combinations of several independent displacement coordinates at the boundary, as shown in Eqs. A.3 and A.6 of the Appendix A for a simply supported plate and a clamped plate, respectively.

Two different methods can be used to solve this problem. In the first place, by coordinate transformation, the generalized displacements, Eq. 4.46, at a boundary node can be expressed in terms of those of boundary coordinates as shown in Eqs. A.1b and A.1c, and then the boundary conditions can be enforced directly by suppressing appropriate degrees of freedom.

As an alternative method, the geometric boundary conditions to be enforced can be expressed in the form of some constraint conditions between the related individual degrees of freedom. Thus, the task is to obtain a $\underset{\sim}{q}^*$ which minimizes the following potential energy functional:

$$\Pi_{CD} = \frac{1}{2}\,\underset{\sim}{q}^{*T}\underset{\sim}{K}^{*}\underset{\sim}{q} - \underset{\sim}{Q}^{*T}\underset{\sim}{q}^{*} \tag{4.50}$$

and, at the same time, satisfies the following conditions:

$$\underset{\sim}{C}^{*}\underset{\sim}{q}^{*} = 0 \tag{4.51}$$

where $\underset{\sim}{q}^{*}$ are the nodal degrees of freedom in the global cartesian system. For a simply supported circular plate, for example, the matrix $\underset{\sim}{C}^{*}$ can be obtained from coordinate transformation relations as shown in Eqs. A.3b and A.3c. This second method can be applied by defining a modified functional with Lagrange multipliers $\underset{\sim}{\Lambda}$:

$$\Pi^{*}_{CD} = \frac{1}{2}\,\underset{\sim}{q}^{*T}\underset{\sim}{K}^{*}\underset{\sim}{q}^{*} - \underset{\sim}{Q}^{*T}\underset{\sim}{q}^{*} + \underset{\sim}{\Lambda}^{T}\underset{\sim}{C}^{*}\underset{\sim}{q}^{*} \tag{4.52}$$

Extremizing Eq. 4.52 with respect to $\underset{\sim}{q}^{*}$ gives:

$$\underset{\sim}{K}^{*}\underset{\sim}{q}^{*} - \underset{\sim}{Q}^{*} + \underset{\sim}{C}^{*T}\underset{\sim}{\Lambda} = 0 \tag{4.53}$$

From Eqs. 4.51 and 4.53:

$$\underset{\sim}{q}^{*} = \underset{\sim}{K}^{*-1}\underset{\sim}{Q}^{*} - \underset{\sim}{K}^{*-1}\underset{\sim}{C}^{*T}\,(\underset{\sim}{C}^{*}\underset{\sim}{K}^{*-1}\underset{\sim}{C}^{*T})^{-1}\underset{\sim}{C}^{*}\underset{\sim}{K}^{*-1}\underset{\sim}{Q}^{*} \tag{4.54}$$

From Eq. 4.52, it is clear that the original functional, which is based on the minimum potential energy principle, is modified. Hence the principle is no longer a minimum principle, and the nature of the extremum is not known. In the present work, the first method is used.

Enforcement of Traction Boundary Conditions in an Explicit Manner in the Compatible Displacement Model

Precisely the same situations as discussed above arise in explicitly enforcing traction boundary conditions in this compatible displacement model, except the fact that the same traction boundary conditions are already enforced implicitly by extremization of the functional. However, as mentioned in the second chapter, the implicit enforcement of the higher

order boundary conditions is done in an approximate manner such that the sum of the weighted residual errors of interior differential equations and boundary conditions vanish. Thus, two advantages can be obtained by explicitly enforcing traction boundary conditions. First, the boundary error can be made to vanish separately from the error of the interior equilibrium equations. Second, the traction boundary conditions, which are satisfied in the sense of the integral of weighted error residual in the formulation wherein these conditions are implicit in the variational method, can be satisfied in a pointwise sense by a change of the definitions of the appropriate boundary quantities.

In the following, detailed discussions on the above mentioned advantages are given by using the three dimensional form of the compatible displacement model. The vanishing of the first variation of the model in Eq. 2.35 can be written as:

$$\delta\Pi_{CD} = \sum_m \{ - \int_{V_m} (\sigma_{ij,j} + \bar{F}_i)\delta u_i dV + \int_{S_{\sigma_m}} (T_i - \bar{T}_i)\delta u_i dS \} = 0 \qquad (4.55)$$

The vectors corresponding to the interior displacement $\underset{\sim}{u}$, boundary displacements $\underset{\sim}{u}^b$, boundary traction $\underset{\sim}{T}$, and $\sigma_{ij,j}$ can be written, respectively, as:

$$\underset{\sim}{u} = \underset{\sim\sim}{N}\underset{\sim}{q} \qquad (4.56)$$

$$\underset{\sim}{u}^b = \underset{\sim\sim}{L}\underset{\sim}{q} \qquad (4.57)$$

$$\underset{\sim}{T} = \underset{\sim\sim}{R}\underset{\sim}{q} \qquad (4.58)$$

and

$$\{\sigma_{ij,j}\} = \underset{\sim}{P}\underset{\sim}{q} \tag{4.59}$$

where $\underset{\sim}{N}$ is the matrix of shape functions, $\underset{\sim}{q}$ is the generalized displacement vector, $\underset{\sim}{L}$ is the interpolating function matrix which can be obtained by putting boundary coordinates into $\underset{\sim}{N}$, and $\underset{\sim}{R}$ and $\underset{\sim}{P}$ are the matrices derived from $\underset{\sim}{N}$ through constitutive relations and appropriate differentiations. Substituting Eqs. 4.56, 4.57 and 4.59 to Eq. 4.55 gives:

$$\left[- \int_{V_m} (\underset{\sim}{q}^T \underset{\sim}{p}^T + \underset{\sim}{\bar{F}}^T)\underset{\sim}{N} dV + \int_{S_{\sigma_m}} (\underset{\sim}{T}^T - \underset{\sim}{\bar{T}}^T)\underset{\sim}{L} dS \right] \delta\underset{\sim}{q} = 0 \tag{4.60}$$

The above implies that by the extremization of Eq. 2.35, the sum of the interior error and the boundary error is set to be zero since $\delta\underset{\sim}{q}$ is arbitrary. Further, it is clear that the second term of the above equation is nothing but the integral of the weighted error residual of traction boundary conditions.

To enforce these traction boundary conditions explicitly, the following methods may be considered.

When the boundary nodal value of each traction component on a traction prescribed boundary can be expressed by a single (higher order) displacement degree of freedom, these higher order conditions can also be explicitly enforced by simply substituting given boundary values for the appropriate degrees of freedom at nodes along a boundary in question, as in the case of displacement boundary conditions. However, in some problems like the present plate problem with circular domains, since boundary tractions are expressed by combinations of several independent degrees of freedom, some other approximate method should be used. Two approximate methods are available; one is a Lagrange multiplier method and the other is a least

square method. Some detailed discussions on both of the methods will be given in the following,

To enforce the traction boundary conditions explicitly by a Lagrange multiplier method, those boundary conditions can be considered as constraint conditions.

$$\underset{\sim}{T} - \bar{\underset{\sim}{T}} = 0 \qquad \text{on} \qquad S_{\sigma_m} \tag{4.61}$$

and introduced into Eq. 2.35 through a set of Lagrange multipliers. This implies precisely the same conditions as the second term of Eq. 4.60, but now the conditions are enforced pointwise at some number of points on traction prescribed boundary by changing the definitions of the related quantities as follows.

The boundary tractions, whether they are known or unknown, can be expressed in terms of their values at some number of points of the boundary by using interpolation functions as follows:

$$\underset{\sim}{T} = \underset{\sim}{\phi}_n \underset{\sim}{g}_n \tag{4.62}$$

where n is the number of interpolating points on the traction prescribed boundary of an element and which need not necessarily coincide with the original nodes on the boundary, $\underset{\sim}{\phi}_n$ is the interpolating function matrix and $\underset{\sim}{g}_n$ is the vector which consists of the generalized nodal values of tractions at n points on the boundary in question.

With this definition of the generalized nodal forces $\underset{\sim}{g}_n$, the constraint term which is to be introduced, to the original functional through Lagrange multipliers $\underset{\sim}{\lambda}$ can be written as:

$$\int_{S_{\sigma_m}} (\underset{\sim}{T}^T - \bar{\underset{\sim}{T}}^T)\underset{\sim}{\lambda} dS = (\underset{\sim}{g}_n^T - \bar{\underset{\sim}{g}}_n^T) \int_{S_m} \underset{\sim n\sim}{\phi}^T \underset{\sim}{\lambda} dS = (\underset{\sim}{g}_n^T - \bar{\underset{\sim}{g}}_n^T)\underset{\sim n}{\Lambda} \tag{4.63}$$

where $\underset{\sim n}{\Lambda} = \int_{S_{\sigma_m}} \underset{n\sim}{\phi}^T \underset{\sim}{\lambda} dS$ and $\bar{\underset{\sim}{g}}_n$ is a known vector which is constructed from the nodal values of prescribed tractions at the boundary. There exists unique relation between $\underset{\sim}{g}_n$ and $\underset{\sim}{q}$ as:

$$\underset{\sim}{g}_n = \underset{\sim n\sim}{C} \underset{\sim}{q} \tag{4.64}$$

where $\underset{\sim n}{C}$ can be obtained by substituting coordinates of appropriate points on a boundary into $\underset{\sim}{R}$ of Eq. 4.58. Thus, Eq. 4.63 can be written as:

$$\int_{S_{\sigma_m}} (\underset{\sim}{T}^T - \bar{\underset{\sim}{T}}^T)\underset{\sim}{\lambda} dS = \underset{\sim}{q}^T \underset{\sim n\sim}{C}^T \underset{\sim n}{\Lambda} - \bar{\underset{\sim}{g}}_n^T \underset{\sim n}{\Lambda} \tag{4.65}$$

By adding the first variation of the above to Eq. 4.60,

$$[- \int_{V_m} (\underset{\sim}{q}^T \underset{\sim}{P}^T + \bar{\underset{\sim}{F}}^T)\underset{\sim}{N} dV + \int_{S_{\sigma_m}} (\underset{\sim}{T}^T - \bar{\underset{\sim}{T}}^T)\underset{\sim}{L} dS + \underset{\sim n\sim}{\Lambda}^T \underset{\sim n}{C}]\delta q + (\underset{\sim}{q}^T \underset{\sim n}{C}^T - \bar{\underset{\sim}{g}}_n^T)\delta \underset{\sim n}{\Lambda} = 0 \tag{4.66}$$

The terms with $\delta \underset{\sim n}{\Lambda}$ represents the pointwise traction boundary conditions. The terms with δq represents the term $\underset{\sim n\sim}{\Lambda}^T \underset{\sim n}{C}$ which is introduced to the formulation, because of the constraint conditions, Eq. 4.61 and the original error equations in which traction boundary conditions are endorced in the sense of integral of error residual.

The other method which can be applied to explicitly enforce traction boundary conditions is a least square method. The pointwise boundary conditions in Eq. 4.66 which are expressed in system quantities, $\underset{\sim n}{C}^* \underset{\sim}{q}^* = \bar{\underset{\sim}{g}}_n^*$, can be combined with the stiffness equations obtained by

extremizing the functional in Eq, 4.50 with respect $\underset{\sim}{q}^*$ to construct a new system of equations as

$$\underset{\sim}{K}'\underset{\sim}{q} = \underset{\sim}{Q}' \tag{4.67}$$

where $\underset{\sim}{K}'^T = [\underset{\sim}{K}^{*T}\underset{\sim}{C}_n^{*T}]$ and $\underset{\sim}{Q}'^T = [\underset{\sim}{Q}^{*T}\underset{\sim}{g}_n^{*T}]$, Eq. 4.67 has more equations than the number of unknowns, but it can be solved in a least square, sense as follows:

$$\underset{\sim}{q}^* = [\underset{\sim}{K}'^T\underset{\sim}{K}']^{-1}\underset{\sim}{K}'^T\underset{\sim}{Q}' = [\underset{\sim}{K}^{*T}\underset{\sim}{K}^* + \underset{\sim}{C}_n^{*T}\underset{\sim}{C}_n]^{-1}[\underset{\sim}{K}^{*T}\underset{\sim}{Q}^* + \underset{\sim}{C}_n^{*T}\underset{\sim}{g}_n] \tag{4.68}$$

In this method, since the original minimum potential energy functional is not changed, the minimum principle of the formulation is preserved, while in the Lagrange multiplier approach, the nature of the extremum of the principle is not known, since, due to the modification of the functional, the principle is longer a minimum principle. In this sense, the least square approach is considered the better suited method to the original formulation than the Lagrange multiplier approach, though, in general, it is not easy to decide, a priori, which one of the two methods can produce more accurate results.

In problems with curved domains, where the boundary tractions should be expressed by a combination of several independent degrees of freedom, the explicit enforcement of these higher order boundary conditions may not significantly improve the solutions as compared to the case where they are implicitly satisfied in a weighted residual sense through the original variational principle. In those cases when a boundary traction can be expressed by a single degree of freedom, the traction boundary

conditions can be exactly enforced in a pointwise sense in an explicit manner, similar to the geometric boundary conditions, and hence some favourable effects on the solutions can be expected, in such a case.

However, in the problems with arbitrarily curved, traction prescribed, boundaries and when either one of the above approximate methods is used to enforce traction boundary conditions explicitly, some favourable effect on the solution can be expected in the following cases.

Since the pointwise boundary conditions in Eq. 4.65 can be obtained by simply substituting coordinates of any number of boundary points into $\underset{\sim}{R}$ of Eq. 4.58 and matching the prescribed values of tractions $\underset{\sim}{T}$ at the points, the boundary conditions can be enforced very accurately even for an arbitrarily curved boundary by the increase of the matching points on the traction prescribed boundary. This point matching method to satisfy prescribed boundary tractions can be derived from the concept of boundary collocation, and this will be discussed in detail in the next section. Thus, if a compatible displacement model is applied to a problem where a highly accurate satisfaction of traction boundary conditions is known to be critical to obtain accurate solutions, such as in fracture problems which are treated in the next chapter, the only possible method is one of these two approximate methods.

In the present thesis, the Lagrange multiplier method is used in solving several plates with circular curved boundaries. In all the cases, some favourable effects are obtained, in spite of the approximations involved, and the results are dicussed later.

In the following, some details in explicitly enforcing traction boundary conditions through the process of using all the necessary higher

order derivatives of the displacement variable, as degrees of freedom at nodes of a finite element, are discussed.

To enforce the "free" boundary conditions for a plate as in Eq. A.8b, for example, third order derivatives of normal displacement should appear as degrees of freedom at each nodal point as well as the lower order ones. This results in a considerable enlargement of the size of the final system of equations.

There are two possible ways for including all the necessary higher order derivatives as degrees of freedom for boundary nodes. First, by using a shape function assumption for each of the elements in the domain which includes all the necessary higher and lower order terms as generalized displacements on the nodes in the interior of the domain as well as on the boundary. Second, by using a shape function which has a different mode for each degree of freedom of different order. Thus, by simply including corresponding higher order modes in the shape functions of elements near the boundary, along which traction boundary conditions to be enforced exist, necessary higher order terms as well as lower order terms appear as generalized displacements at boundary nodes. By dropping higher order modes in the shape functions of interior elements, only lower order degrees of freedom appear at interior nodes, as generalized displacements.

Between these two, the second type of shape function is preferred, since the first type of shape function may increase the total number of degrees of freedom inordinately, and this can hardly be justified from the view point of computational economy. There is also a similar difficulty in the second type of shape function. For example, Hermitian polynomial can easily be considered for this type of element [60, 61].

Consider a corner element of a rectangular plate whose boundaries 1, 2 and 1, 3 are free [Fig. 4.5].

Several third derivatives of the normal displacement function, as well as lower order derivatives, are needed to enforce traction boundary conditions for the element as shown in the figure. Thus, a third order Hermitian polynomial may be used for assuming the normal displacement function to include third order derivative terms, namely, $w_{,xxx}$, $w_{,xxy}$, $w_{,xyy}$ and $w_{,yyy}$. Then, the normal displacement function is given as

$$
\begin{aligned}
w(x,y) = \sum_{i=1}^{2}\sum_{j=1}^{2}[& H_{oi}(x)H_{o}(y)\, w_{ij} + H_{1i}(x)H_{oj}(y)\, w_{,x_{ij}} \\
& + H_{oi}(x)H_{1j}(y)\, w_{,y_{ij}} + H_{2i}(x)H_{oj}(y)\, w_{,xx_{ij}} \\
& + H_{oi}(x)H_{2j}(y)\, w_{,yy_{ij}} + H_{1i}(x)H_{1j}(y)\, w_{,xy_{ij}}] \\
& + H_{31}(x)H_{01}(y)\, w_{,xxx_{11}} + H_{31}(x)H_{o2}(y)\, w_{,xxx_{12}} \\
& + H_{21}(x)H_{11}(y)\, w_{,xxy_{11}} + H_{22}(x)H_{11}(y)\, w_{,xxy_{21}} \\
& + H_{11}(x)H_{21}(y)\, w_{,xyy_{11}} + H_{11}(x)H_{22}(y)\, w_{,xyy_{12}} \\
& + H_{o1}(x)H_{31}(y)\, w_{,yyy_{11}} + H_{o2}(x)H_{31}(y)\, w_{,yyy_{21}} \qquad (4.69)
\end{aligned}
$$

where $H_{ij}^{(3)}$ are third order Hermitian polynomials which can be written, for a one dimensional element with length L in x direction, with normalized coordinate, $\xi = x/L$, as

$$H_{o1}(\xi) = 1 - 35\xi^4 + 84\xi^5 - 70\xi^6 + 20\xi^7$$

$$H_{o2}(\xi) = \quad 35\xi^4 - 84\xi^5 + 70\xi^6 - 20\xi^7$$

$$H_{11}(\xi) = (\xi - 20\xi^4 + 40\xi^5 - 36\xi^6 + 10\xi^7)L$$

$$H_{12}(\xi) = (- 15\xi^4 + 39\xi^5 - 34\xi^6 + 10\xi^7)L$$

$$H_{21}(\xi) = \frac{1}{2}(\xi^2 - 10\xi^4 + 20\xi^5 - 15\xi^6 + 4\xi^7)L^2$$

$$H_{22}(\xi) = \frac{1}{2}(\quad 5\xi^4 - 14\xi^5 + 13\xi^6 - 4\xi^7)L^2$$

$$H_{31}(\xi) = \frac{1}{6}(\xi^3 - 4\xi^4 + 6\xi^5 - 4\xi^6 + \xi^7)L^3$$

$$H_{32}(\xi) = \frac{1}{6}(\quad - \xi^4 + 3\xi^5 - 3\xi^6 + \xi^7)L^3$$

Substituting the above into Eq. 4.69, it can be seen that the resulting polynomial is not capable of representing exactly any displacement of the form [46]

$$w(x,y) = \sum_{r=0}^{7} \sum_{s=0}^{7} \alpha_{rs} x^r y^s$$

due to the absence of many terms including cubic and quartic ones which are very important elements for completeness of the polynomial. To make it complete, the other higher order derivatives such as $w_{,xxxy}$, $w_{,xxyy}$, $w_{,xxxyy}$, $w_{,xxxyyy}$, etc., should be included as nodal degrees of freedom at boundary nodes. This causes an inordinate increase in the number of degrees of freedom at some nodes. The preceding problem, for example, requires 16 degrees of freedom at boundary nodes to make the shape

function polynomial complete. Thus, unless some other ingenious shape function is developed, the attempts aimed at which were not successful in this thesis, the problem of computational economy will remain as a limiting factor for this type of element.

The presently considered element is of the first type discussed above, with up to second order derivatives as degrees of freedom at each node. Thus moment boundary conditions can be enforced explicitly without any difficulties.

In the following, numerical solutions for several examples for the previously discussed problems are discussed. All the solutions are based on the present compatible displacement finite element.

Results and Discussions

The first problem is the finite element solution of a simply supported circular plate with uniformly distributed load p. The domain is approximated by an n-sided polygon which is composed of a number of triangular finite elements and Poisson's ratio is .3. Since the domain is approximated by a polygon, the triangular element P_1, P_2, P_3 with straight sides in Fig. 4.4 are used in this problem. The number of finite elements in a finite element grid of a quarter plate is equal to N (N=n/4).

By coordinate transformation, the generalized nodal displacement of a finite element in the local coordinates ξ,ζ given in Eq. 4.39 are expressed in circular boundary coordinates n,s which are shown in Fig. 4.6, the nodal degrees of freedom at a boundary nodes are

$$\underset{\sim}{q}^T = [w \; w,_n \; w,_s \; w,_{nn} \; w,_{ns} \; w,_{ss}]$$

When the geometric boundary conditions enforced are those corresponding

to a circular plate that is, $w = w_{,s} = w_{,ss} = 0$, the central deflection $\bar{w} = Dw/pa^4$ where D is the flexural rigidity of the plate, converges to the correct answer as shown in Fig. 4.8 as the number of sides, 4N, of the polygon increases. In the same figure, the results obtained by enforcing only the conditions w=0 at boundary nodes as essential boundary conditions are plotted. It shows a converging result in solution $\bar{w}$, but the solutions are worse than those of the previous case.

The actual geometric boundary conditions of the approximate polygonal plate whose quarter part is shown in Fig. 4.6 are $w = w_{,\xi_1} = w_{,\xi_1\xi_1} = w_{,\xi_2} = w_{,\xi_2\xi_2} = 0$ where ξ_1 and ξ_2 are the local coordinates parallel to the sides of two neighbouring elements which join together at a corner. It can be seen that the above mentioned geometric boundary conditions of a polygonal plate imply the following conditions for the displacements at the nodes of the polygon, expressed in circular boundary coordinates

$$w = w_{,n} = w_{,s} = w_{,ns} = 0 \tag{4.70}$$

$$w_{,nn} \sin^2\Theta + w_{,ss} \cos^2\Theta = 0 \tag{4.71}$$

The geometric boundary condition $w_{,n} = 0$ at the node, however, implies a "clamped" condition at the respective nodes of the polygonal mesh. Thus, the numerical results of $\bar{w}$ at the center converge, as the distance between the nodes decreases, to that of a clamped circular plate as shown in Fig. 4.9.

There is a method which is erroneous but a finite element analyst might be liable to try to handle this type of problem. The degrees of freedom at nodes on the boundary, for each element, are expressed in oblique

coordinates in n,τ where n is the radial direction and τ is parallel to ξ in a finite element, by coordinate transformations from ξ,ζ rectangular coordinates to n,τ oblique coordinates. This implies that there are three coordinates n,τ_1 and τ_2 at a corner node where two adjacent elements join as whown in Fig. 4.7. Thus the generalized nodal displacement vector at a node is

$$q^T = [w \; w_{,n} \; w_{,\tau_1} \; w_{,\tau_2} \; w_{,nn} \; w_{,n\tau_1} \; w_{,n\tau_2} \; w_{,\tau_1\tau_1} \; w_{,\tau_2\tau_2}]$$

and the geometric boundary conditions to be enforced at a boundary node in this system are

$$w = w_{,\tau_1} = w_{,\tau_2} = w_{,\tau_1\tau_1} = w_{,\tau_2\tau_2} = 0$$

The results obtained by enforcing the above geometric boundary conditions are shown in Fig. 4.10. They converge to that of more flexible structure as the increase of the number of sides of the polygonal plate.

As mentioned earlier, this method is not correct. All generalized displacements except w at a node are expressed by the components along three different directions, and thus physically nonsensical condition for the given problem such as $w_{,n} \neq 0$ is resulted.

From the above results, it is concluded that, as discussed earlier, when a simply supported circular plate is approximated by a polygonal domain in the finite element solution, if the actual geometric boundary conditions corresponding to the approximate straight sides are enforced, the solutions do not converge to the correct answer with the increase in the number of the sides of the approximate polygon. Thus, even though

the circular domain is approximated by a polygonal domain, unless the geometric boundary conditions corresponding to the circular boundary are enforced at the nodes of the polygonal mesh, correct solutions cannot be obtained in the above problem.

The second set of problems are the bending of circular curved plates with and without explicitly enforcing traction boundary conditions. All the circular curved domains are approximated by quadratic curves and appropriate circular geometric boundary conditions are enforced at the nodes. A simply supported circular plate, and an annular plates whose inner radii are half of the outer radii , with simply supported and clamped outer boundaries are solved with and without explicitly enforcing moment boundary conditions where they exist in all the problems. In enforcing traction boundary conditions explicitly, the matching points are selected to coincide with the nodal points for the purpose of simplicity. As can be seen in the finite element grids in Fig. 4.11, the circular arc becomes very close to a straight line as the grids are refined; and thus two point matching is considered accurate enough in this situation. The Poisson ratio is assumed as .3, and the external load is uniformly distributed for all cases.

The results are shown graphically in Figs. 4.12 - 4.19 by percentage errors (percentage error=(finite element solution - analytical solution) x 100/ analytical solution); and in all the cases the values marked with solid symbols are the results without explicitly enforcing moment boundary condition. The analytical solutions of displacements are obtained from [62], and then strain energy and stress solutions are calculated from the displacements for all the cases.

In Figs. 4.12 and 4.13, the results of central deflection and strain energy of a simply supported circular plate are given. In both of the solutions, the results with explicitly enforcing traction boundary condition are slightly worse in coarse grids, but they converge to the exact solutions faster than those without explicitly enforced moment boundary condition. Thus in the finest grid, the numerical results with explicit enforcement of traction boundary condition are slightly better. As shown in the graphs, the displacements and strain energy solutions converge from above. This apparent contradiction to the lower bound character of compatible displacement model solutions is considered to be caused by the approximation of the circular domain by a piecewise quadratic curved domain.

In Figs. 4.14 and 4.15, central bending moment and edge tangential moment of the same problem are respectively shown. In these stress solutions explicitly enforcing the moment boundary condition gives improvement in all the cases from the coarse to the finest grids. Especially, the improvement of the edge tangential moment is considerable in magnitude. The central bending moment in Fig. 4.14, converge to the exact solution from lower values for both the results, with and without explicitly enforcing the moment boundary condition. In the case of the edge tangential moments in Fig. 4.15, the solutions without explicitly enforcing moment boundary condition converge from higher value monotonically, and those with explicitly enforced moment boundary condition start from the lower values, and then pass the exact solution around $N = 7$ where N is the number of finite elements in a quarter plate and then, converge monotonically. The - sign in Figs. 4.14 and 4.15 and elsewhere implies that the errors

are negative by the original definition of them. In Fig. 4,16 the edge radial bending moments which are obtained when the problem is solved without explicitly enforced moment boundary condition are plotted. The exact value is zero; thus the errors are compared with central bending moment as (edge radial moment x 100/ analytical solution of central bendong moment). When the problem is solved with explicitly enforcing moment boundary condition, the results are actually zero (always less than 10^{-10}).

In Fig. 4.17, the results of a uniformly loaded annular plate with simply supported outer edge are plotted. In the solutions for displacement and strain energy, there are some improvements in all the grids, though the magnitudes are trivial, by explicitly enforcing traction boundary conditions. However, the outer edge tangential moment solution is improved significantly. When N = 60 (ref. Fig. 4.11 for N) the errors in the outer edge tangential moment solution for the two cases, with and without explicitly enforcing moment boundary condition are respectively .016% and 2.3%. The solutions of all the quantities, i.e., displacement, strain energy, and stress converge monotonically from the higher values to the appropriate exact ones.

In Fig. 4.18, the results for a uniformly loaded annular plate with outer edge fixed are given. Again, in the central deflection and strain energy solutions, no noticeable improvements are obtained by explicitly enforcing the moment boundary condition. Inner edge tangential moment solutions are improved significantly as in the previous case. The percentage errors of outer edge tangential and radial moments are almost the same, thus the results are plotted by the same curves, in both of the

cases, with and without explicitly enforcing the moment boundary condition. Thus moment solutions on the outer edge are seen to be improved considerably by the explicit enforcement of moment boundary condition along the inner free edge. This implies that the improvements in solutions by explicitly enforcing traction boundary conditions are not local but have global effects for the entire system. In this problem, all the solutions converge to the appropriate exact values monotonically from the higher values.

Finally, Fig. 4.19 shows the actual numerical results for boundary radial moments obtained through finite element solutions without explicitly enforcing appropriate moment boundary conditions. Their exact values are zeros; thus they are compared with respective tangential moments at the appropriate boundaries in the same way as in the case of the simply supported circular plate. When the problems are solved with explicitly enforced moment boundary conditions, they are always actually zero (less than 10^{-9}).

In general, in these circular curved plate problems solved by compatible displacement model, the displacement and strain energy solutions are not improved very much by explicitly enforcing traction boundary conditions, but considerable improvements in stress solutions are obtained. Thus, for problems in which accurate stress solutions are required, it is recommended to apply this method.

Finally, the present element is highly sophisticated in its formulation, with very little approximations in treating problems with curved domains. The displacement of a circular plate with uniform load is fourth order in radial coordinates, and the assumed solution in Eq. 4.38 contains a complete quartic polynomial. The error in area for an element

involved by the approximation of the circular curved domain by a quadratic curved one is only about $.00823a^2N^{-4}$[58]. Further the number of generalized displacements at a node, which include up through second derivatives of transverse displacement, are six.

Thus, in finite element formulations for plate problems with only three degrees of freedom at a node (the transverse displacement and it derivatives with respect to inplane coordinates) in which the transverse displacement is interpolated by cubic shape functions, considerable improvements in solutions, especially in stresses, are expected by explicitly enforcing traction boundary conditions.

Hybrid Stress Model

The Basic Finite Element

For a plate of isotropic material, the functional for hybrid stress model version 1, Eq. 3.70, which will be called simply a hybrid stress model from now on, can be written as

$$\Pi_{HS} = \sum_m \{ -\frac{1}{2} \int_{A_m} \underset{\sim}{M}^T \underset{\sim\sim}{D} \underset{\sim}{M} dA + \int_{C_m} \underset{\sim}{T}^T \underset{\sim}{u} dC - \int_{C_{\sigma_m}} \underset{\sim}{\bar{T}}^T \underset{\sim}{u} dC \} \qquad (4.72)$$

where $\underset{\sim}{M}$, $\underset{\sim}{T}$ and $\underset{\sim}{u}$ will be defined later, $\underset{\sim}{\bar{T}}$ is prescribed boundary traction vector, and

$$\underset{\sim}{D} = \frac{12}{Eh^3} \begin{bmatrix} 1 & -\nu & 0 \\ -\nu & 1 & 0 \\ 0 & 0 & 2(1+\nu) \end{bmatrix}$$

with Young's modulus E and thickness of plate h. The necessary variables are a set of equilibrated stress functions in the interior and a set of inherently continuous boundary displacement functions. The interior stress

functions which are moments in plate problems based on Kirchhoff hypothesis, are assumed as

$$\underset{\sim}{M} = \underset{\sim\sim}{N}\underset{\sim}{\beta} + \underset{\sim p}{N} \tag{4.73}$$

where

$$\underset{\sim}{M}^T = [M_x \; M_y \; M_{xy}]$$

$$\underset{\sim}{N} = \begin{bmatrix} 1 & x & y & x^2 & xy & y^2 & 0 & 0 & 0 & 0 & 0 & 0 & 0 & 0 & 0 & 0 \\ 0 & 0 & 0 & 0 & 0 & 0 & 1 & x & y & x^2 & xy & y^2 & 0 & 0 & 0 & 0 \\ 0 & 0 & 0 & -xy & 0 & 0 & 0 & 0 & 0 & 0 & -xy & 1 & x & x^2 & y^2 \end{bmatrix}$$

$$\underset{\sim}{\beta}^T = \{\beta_1 \beta_2 \beta_3 \; \ldots\ldots \beta_{20}\}$$

and

$$\underset{\sim p}{N}^T = [px^2/2 \; 0 \; 0 \;]$$

with uniformly distributed external load p. The first part of $\underset{\sim}{M}$, Eq. 4.73, is homogeneous solution part and the second part is particular solution part of plate equilibrium equation, Eq. 3.34. Though self-equilibrated stress functions can be determined by inspection for a problem with simple geometry and coordinates such as $\underset{\sim\sim}{N}\underset{\sim}{\beta}$ of the above, they can be determined usually by static geometric analogy [26], in more complicated cases. The finite element solutions for a problem with stress functions, Eq. 4.73, will be independent of the choice the particular solution, $\underset{\sim p}{N}$, since $\underset{\sim}{N}$ is complete polynomial of the same order as $\underset{\sim p}{N}$ [20].

The shearing forces can be derived from Eq. 4.73 by using the relations Eq. 3.30, as

$$Q = \begin{Bmatrix} Q_x \\ Q_y \end{Bmatrix} = N_Q + \begin{Bmatrix} p_x \\ 0 \end{Bmatrix} \tag{4.74}$$

where

$$N_Q = \begin{bmatrix} 0 & 1 & 0 & x & y & 0 & 0 & 0 & 0 & 0 & 0 & -x & 0 & 0 & 1 & 0 & 2y \\ 0 & 0 & 0 & -y & 0 & 0 & 0 & 0 & 1 & 0 & x & y & 0 & 1 & 0 & 2x & 0 \end{bmatrix}$$

the displacement on boundary 1, 2 [Fig. 4.20], with boundary coordinate s and length ℓ_1, can be given, in normalized coordinate $\xi = \frac{s}{\ell_1}$, as

$$\underset{\sim}{u}_{12} = \underset{\sim}{L}_{12}\underset{\sim}{q}_{12} \tag{4.75}$$

where

$$\underset{\sim}{u}_{12} = \{ w_{12} \quad w,_{x_{12}} \quad w,_{y_{12}} \}$$

$$L = \begin{bmatrix} H_{o1} & -\sin\theta_1 H_{s1} & \cos\theta_1 H_{s1} & H_{o2} & -\sin\theta_1 H_{s2} & \cos\theta_1 H_{s2} \\ 0 & \cos\theta_1 H_{n1} & \sin\theta_1 H_{n1} & 0 & \cos\theta_1 H_{n2} & \sin\theta_1 H_{n2} \\ H_{o1,_s} & -\sin\theta_1 H_{s1,s} & \cos\theta_1 H_{s1,s} & 0 & -\sin\theta_2 H_{s2,s} & \cos\theta_2 H_{s2,2} \end{bmatrix} \tag{4.76}$$

with

$$H_{o1} = 1 - 3\xi^2 + 2\xi^3$$

$$H_{o2} = 3\xi^2 - 2\xi^3$$

$$H_{s1} = (- \xi + 2\xi^2 - \xi^3)\ell_1$$

$$H_{s2} = (\xi^2 - \xi^3)\ell_1$$

$$H_{n1} = 1 - \xi$$

$$H_{n2} = \xi$$

$$\underset{\sim}{q}_{12}^{T} = \lfloor w_1 \; w_{,x_1} \; w_{,y_1} \; w_2 \; w_{,x_2} \; w_{,y_2} \rfloor \tag{4.77}$$

The boundary tractions can be derived from interior moment functions, as

$$\underset{\sim}{T}_{12} = \underset{\sim}{J}_{12} \; \underset{\sim}{t} \tag{4.78}$$

where

$$\underset{\sim}{T}_{12}^{T} = \lfloor Q_{n_{12}} \; -M_{n_{12}} \; -M_{ns_{12}} \rfloor$$

$$\underset{\sim}{J}_{12} = \begin{bmatrix} n_1 & n_{12} & 0 & 0 & 0 \\ 0 & 0 & -n_1^2 & -n_2^2 & -2n_1n_2 \\ 0 & 0 & n_1n_2 & -n_1n_2 & -n_1^2+n_2^2 \end{bmatrix}$$

with direction cosines of outward normal to a boundary n_α as shown in Fig. 4.20 and

$$\underset{\sim}{t}^{T} = \lfloor Q_x \; Q_y \; M_x \; M_y \; M_{xy} \rfloor \tag{4.80}$$

Using Eqs. 4.73 and 4.74, Eq. 4.78 can be written as

$$\underset{\sim}{T}_{12} = \underset{\sim}{R}_{12}\underset{\sim}{\beta} + \underset{\sim}{R}_{p_{12}} \tag{4.81}$$

where

$$\underset{\sim}{R}_{12} = \underset{\sim}{J}_{12} \begin{bmatrix} \underset{\sim}{N}_Q \\ \underset{\sim}{N} \end{bmatrix} \tag{4.82}$$

and

$$\underset{\sim}{R}_{p_{12}} = \underset{\sim}{J}_{12}\underset{\sim}{P}_v \tag{4.83}$$

$$\underset{\sim}{P}_v^T = \lfloor\, px \quad 0 \quad \frac{px^2}{2} \quad 0 \quad 0 \,\rfloor$$

By assembling $\underset{\sim}{u}_{23}$, $\underset{\sim}{u}_{34}$ and $\underset{\sim}{u}_{41}$, and $\underset{\sim}{T}_{23}$, $\underset{\sim}{T}_{34}$ and $\underset{\sim}{T}_{41}$, which can be obtained by similar manipulations along corresponding piecewise boundary as shown in Eqs. 4.75 and 4.81, together with $\underset{\sim}{u}_{12}$ and $\underset{\sim}{T}_{12}$, respectively, complete boundary displacements and tractions for an element can be obtained, as

$$\underset{\sim}{u} = \underset{\sim\sim}{L}\underset{\sim}{q} \tag{4.84}$$

$$\underset{\sim}{T} = \underset{\sim\sim}{R}\underset{\sim}{\beta} + \underset{\sim p}{R} \tag{4.85}$$

where $\underset{\sim}{L}$ and $\underset{\sim}{q}$, and $\underset{\sim}{R}$ and $\underset{\sim p}{R}$ are given in tables 4.3 and 4.4, respectively. Substituting Eqs. 4.73, 4.84 and 4.85 into Eq. 4.72 gives

$$\Pi_{HS} = -\sum_m \{\frac{1}{2}\,\underset{\sim}{\beta}^T\underset{\sim\sim}{H}\underset{\sim}{\beta} + \underset{\sim}{\beta}^T\underset{\sim p}{H} - \underset{\sim}{\beta}^T\underset{\sim\sim}{G}\underset{\sim}{q} - \underset{\sim p\sim}{G}^T\underset{\sim}{q} + \underset{\sim}{S}^T\underset{\sim}{q}\} + \text{constant} \tag{4.86}$$

where

$$\underset{\sim}{H} = \int_{A_m} \underset{\sim}{N}^T\underset{\sim\sim}{D}\underset{\sim\sim}{N}\, dA$$

$$\underset{\sim p}{H} = \int_{A_m} \underset{\sim}{N}^T\underset{\sim\sim}{D}\underset{\sim\sim p}{N}\, dA$$

$$\underset{\sim}{G} = \int_{C_m} \underset{\sim}{R}^T\underset{\sim}{L}\, dC$$

$$\underset{\sim p}{G} = \int_{C_m} \underset{\sim p\sim}{R}^T\underset{\sim}{L}\, dC$$

$$\underset{\sim}{S} = \int_{C_{\sigma_m}} \underset{\sim}{\bar{T}}^T\underset{\sim}{L}\, dC$$

Extremization of Eq. 4.86 with respect to $\underset{\sim}{\beta}$ gives

$$\underset{\sim}{H} + \underset{\sim}{H}_p - \underset{\sim}{G}\,\underset{\sim}{q} = 0 \tag{4.87}$$

Substituting $\underset{\sim}{\beta}$ which is solved from the above equation into Eq. 4.86 gives

$$\Pi_{HS} = \Sigma\{\, \underset{\sim}{q}^T \underset{\sim\sim}{K} \underset{\sim}{q} - \underset{\sim}{Q}^T \underset{\sim}{q} \,\} \tag{4.88}$$

where

$$\underset{\sim\sim}{K} = \underset{\sim}{G}^T \underset{\sim\sim}{H}^{-1}\, \underset{\sim}{G} \tag{4.89}$$

$$\underset{\sim}{Q} = \underset{\sim p}{H}^T \underset{\sim\sim}{H}^{-1} \underset{\sim}{G} + \underset{\sim p}{G} - \underset{\sim}{S} \tag{4.90}$$

From Eq. 4.88, the following stiffness equations can be obtained.

$$\underset{\sim\sim}{K}\underset{\sim}{q} = \underset{\sim}{Q}$$

A careful consideration should be given to the relations between the number of $\underset{\sim}{\beta}$, m, and that of $\underset{\sim}{q}$, n, in choosing interior stress and boundary displacement functions, in a single element for the solvability of the problem. It can be seen that [20], from Eq. 4.87, m should be larger than or equal to the difference between n and the number of rigid body degrees of freedom of the problem, r, i.e.,

$$m \geq n-r \tag{4.91}$$

In this problem m=15, n=12 and r=3, thus the choice of interior stress and boundary displacement fields are satisfactory with respect to this criterion.

Other features which should be kept in mind in the choice of variable fields is that the boundary displacement field should include all the rigid body modes for the convergence of solutions, as well as it

should satisfy continuity requirements. The boundary displacement field which is used here can represent all the rigid body modes for a straight boundary but it cannot represent rigid body rotations exactly along a curved boundary. To show the approximations of rigid body rotations of this displacement field, the stiffness matrices of the elements in Fig. 4.21 are shown in Tables 4.5 and 4.6 with errors in equilibrium in force VE, and moment equilibrium in x and y directions, XE and YE, respectively. As shown in the tables, the stiffness matrix of a triangular element with straight sides, is equilibriated in force and moments, while in that of a quadrilateral element with one circular curved side, the error in moment equilibrium is greater than 1/15 of corresponding diagonal elements, in the worst case.

In spite of this difficulty, this displacement field will be used here, since no better functions are available for the present problems. Converging results in compatible displacement model solutions by the similar shape functions have been reported [63].

Similar formulations to the present element have been used in rectangular plate problems by hybrid stress models to obtain good results [12, 64].

Enforcement of Traction Boundary Conditions in an Explicit Manner in the Hybrid Stress Model

As mentioned in the second chapter, in this model, the boundary tractions which are derived from the interior stress field may be made to explicitly satisfy prescribed conditions. Thus, explicitly enforcing traction boundary conditions implies constraining the interior stress field, which otherwise is quite arbitrary, to satisfy the prescribed

traction boundary conditions by some method. But, since even without the explicit enforcement of traction boundary conditions, the conditions may be enforced through the extremization of the functional in an implicit manner, the purpose of the present study is to devise a systematic way to enforce traction boundary conditions more accurately without any other additional approximations.

In the present formulation with the definitions of variables given in Eqs. 4.73, 4.84 and 4.85, the generalized nodal forces can be defined as

$$\tilde{\underset{\sim}{g}}^T \underset{\sim}{q} = \int_{S_m} T_i \tilde{u}_i \, dS = \int_{S_m} \tilde{\underset{\sim}{T}}^T \underset{\sim}{L} dS \underset{\sim}{q} \tag{4.92}$$

$$\tilde{\underset{\sim}{g}} = \int_{S_m} \underset{\sim}{L}^T \underset{\sim}{T} \, dS \tag{4.93}$$

The first variation of the functional in Eq. 2.36, can be written as (ref. Eqs. 3.71 - 3.73)

$$\delta\Pi_{HS} = \sum_m \{ - \int_{V_m} (\epsilon_{ij} - f_{i,j}) \, \delta\sigma_{ij} - \int_{S_m} \delta T_i (f_i - \tilde{u}_i) \, dS + \int_{S_{\sigma_m}} (T_i - \bar{T}_i) \delta\tilde{u}_i \, dS + \int_{\rho_m} \tilde{u}_i T_i \, d\rho \} \tag{4.94}$$

The second integral of the above represents the identification of f_i to be displacements, and, hence, this in turn guarantees the compatibility of internal strain fields from the first integral. The third and the last integrals represent, respectively, traction boundary conditions and interelement traction continuity conditions.

By the same way as in Eq. 4.92, the implicit satisfaction of

traction boundary conditions, i.e., the third integral of Eq. 4.94, can be written as

$$\int_{S_{\sigma_m}} (T_i - \bar{T}_i)\delta\tilde{u}_i \, dS = \int_{S_{\sigma_m}} (\underset{\sim}{T}^T - \underset{\sim}{\bar{T}}^T)\underset{\sim}{L} \, dS\delta\underset{\sim}{q} \tag{4.95}$$

Thus, it is clear that the traction boundary conditions are enforced in the sense of a weighted error residual as in the compatible displacement model. Further, the traction boundary conditions are satisfied in such a manner that the sum of the integral of the weighted boundary error residual and other interior errors such as in compatibility vanishes.

To make the traction boundary errors vanish separately from the interior errors and to satisfy the traction boundary conditions more accurately pointwise, the change of definitions of appropriate quantities on the traction prescribed boundary, similar to those in the previous compatible displacement model, is required. For this, the functional in Eq. 2.36 is written in other equivalent from as

$$\Pi_{HS} = \sum_m - \int_{V_m} B \, dV + \int_{S_{u_m}} T_i\bar{u}_i \, dS + \int_{S_{\sigma_m}} (T_i - \bar{T}_i)u_i \, dS + \int_{\rho_m} T_i u_{iL} d\rho \tag{4.96}$$

where $\bar{u}_i$ are prescribed boundary displacements on S_{u_m} and u_i can be interpreted as general Lagrange multipliers on S_{σ_m}. On the traction prescribed boundary S_{σ_m}, the boundary tractions can be expressed in terms of their own values $\underset{\sim}{g}_n$, at an arbitrary number, n, of points on the boundary by interpolating functions as

$$\underset{\sim}{T} = \underset{\sim}{\phi}_n \underset{\sim}{g}_n \tag{4.97}$$

Thus, from Eqs. 4.85 and 4.97

$$\underset{\sim}{g}_n = \underset{\sim}{C}_n \underset{\sim}{\beta} + \underset{\sim}{C}_{p_n} \tag{4.98}$$

where $\underset{\sim}{C}_n$ and $\underset{\sim}{C}_{p_n}$ can be obtained by simply substituting coordinates of n points on the traction prescribed boundary into $\underset{\sim}{R}$ and $\underset{\sim}{R}_p$ of Eq. 4.85. Then, the generalized Lagrange multiplier on the boundary can be defined as

$$\underset{\sim}{g}_n^T \underset{\sim}{\Lambda}_n = \int_{S_{\sigma_m}} T_i u_i \, dS = \underset{\sim}{g}_n^T \int_{S_{\sigma_m}} \underset{\sim}{\phi}_n^T \underset{\sim}{u} \, dS \tag{4.99}$$

$$\underset{\sim}{\Lambda}_n = \int_{S_{\sigma_m}} \underset{\sim}{\phi}_n^T \underset{\sim}{u} \, dS \tag{4.100}$$

The first variation of Eq. 4.96 is

$$\begin{aligned}\delta\Pi_{HS} = \sum_m \{ & - \int_{V_m} (\varepsilon_{ij} - f_{i,j}) \delta\sigma_{ij} dV - \int_{S_{\sigma_m}} \delta T_i (f_i - u_i) dS \\ & - \int_{S_{\sigma_m}} (T_i - \bar{T}_i) \delta u_i \, dS - \int_{S_{u_m}} \delta T_i (f_i - \bar{u}_i) \, dS \\ & - \int_{\rho_m} \delta T_i (f_i - \bar{u}_i) \, d\rho + \int_{\rho_m} T_i \delta u_i d\rho \}\end{aligned} \tag{4.101}$$

The second and the third integrals of the above, which are respectively the matching of $f_i = u_i$ and $T_i = \bar{T}_i$ on S_m, can be written in matrix forms, respectively, as

$$\int_{S_{\sigma_m}} \delta T_i (f_i - u_i) dS = \delta \underset{\sim}{g}_n^T \int_{S_{\sigma_m}} \underset{\sim}{\phi}_n^T (\underset{\sim}{f} - \underset{\sim}{u}) \, dS = \delta \underset{\sim}{g}_n^T (\underset{\sim}{F}_n - \underset{\sim}{\Lambda}_n) \tag{4.102}$$

and

$$\int_{S_{\sigma_m}} (T_i - \bar{T}_i)\delta u_i \, dS = (\underset{\sim}{g}_n^T - \underset{\sim}{\bar{g}}_n^T)\delta \underset{\sim}{\Lambda}_n \tag{4.103}$$

where

$$\underset{\sim}{F} = \int_{S_{\sigma_m}} \underset{\sim}{\phi}_n^T \underset{\sim}{f} \, dS$$

and $\underset{\sim}{\bar{g}}_n$ is the vector which consists of prescribed boundary values at interpolating points on the traction prescribed boundary.

The advantages of explicitly enforcing traction boundary conditions by Eq. 4.103 over implicitly enforcing traction boundary conditions by Eq. 4.95 are as follows: first the traction boundary conditions are enforced pointwise by Eq. 4.103, while they are enforced in the sense of an integral of a weighted error residual by Eq. 4.95. Second, in Eq. 4.95, the errors of boundary tractions which consist of many numbers of parameters are weighted by displacement interpolating functions which consist of only a few terms corresponding to appropriate generalized displacement nodal degrees of freedom. But, in Eq. 4.103, by a simple increase of the number of interpolating points, n, on the traction prescribed boundary, the pointwise satisfaction of traction boundary conditions can be accomplished very accurately even on an arbitrarily curved boundary. Further, from Eq. 4.102 it is clear that the matching of the interior function f_i and boundary displacement function (which has the role of Lagrange multiplier) u_i on the stress prescribed boundary can be accomplished very accurately by increasing the number of interpolating points, n, on the boundary.

Though there is very close similarity to a usual Lagrange multiplier method of the variational formulation of a problem, the replacing of the

weighted integral equation in Eq. 4.95 by the pointwise equation in Eq. 4.103 can be given an alternate physical interpretation. The pointwise equations to satisfy boundary traction in Eq. 4.103 can be obtained by pointwise matching of prescribed values of boundary tractions by a boundary collocation method. Thus, the boundary equations, Eq. 4.103 can have as many number of equations as needed for the required accuracy for the satisfaction of the traction boundary conditions for a specific problem, by the simple increase of the number of matching points, n, at the traction prescribed boundary AB of an element shown in Fig. 4.22. The coefficient matrix of the pointwise expression of boundary tractions, Eq. 4.98, can be obtained by substituting coordinates of the matching points into the boundary tractions, Eq. 4.85, which are derived from the interior stress field. Then, this pointwise expression of boundary tractions can be matched with actual boundary values at corresponding matching points.

Thus, this method can be interpreted as: an equilibrated stress field is constrained to satisty traction boundary conditions by a boundary collocation method and, at the same time, the stress field is forced to satisfy interior compatibility conditions through the variational formulation. By the combination of variational method and boundary collocation method, in this model, the traction boundary conditions are explicitly enforced pointwise in a consistent manner to the original formulation and highly accurately on a traction prescribed boundary, no matter how arbitrarily it is curved. The possibility that the traction boundary conditions can be enforced very accurately for an arbitrarily curved boundary is very important to a fracture problem with a curved crack surface, since the accurate satisfaction of traction free conditions

along the crack surfaces is known to be crucial to obtain accurate stress behavior near crack tip as shown in the next chapter.

By using the variable fields defined in Eqs. 4.73, 4.85 and 4.86 with point matching of boundary traction conditions, the functional in Eq. 4.96 can be written in a matrix from, for the case of homogeneous boundary conditions, for example, as

$$\Pi_{HS} = \sum_m \{ -\frac{1}{2} \underset{\sim}{\beta}^T \underset{\sim\sim}{H} \underset{\sim}{\beta} - \underset{\sim}{\beta}^T \underset{\sim p}{H} + \underset{\sim}{\beta}^T \underset{\sim}{\bar{U}} + \underset{\sim}{\beta}^T \underset{\sim\sim}{G} \underset{\sim p}{q} + \underset{\sim p}{G} \underset{\sim}{q}$$

$$+ \underset{\sim}{\beta}^T \underset{\sim n}{C}^T \underset{\sim n}{\Lambda} + \underset{\sim p_n}{C}^T \underset{\sim n}{\Lambda} \} + \text{constant} \qquad (4.104)$$

where $\underset{\sim}{\bar{U}} = \int_{S_{u_m}} \underset{\sim}{R}^T \underset{\sim}{\bar{u}} \, dS$, $\underset{\sim}{G} = \int_{\rho_m} \underset{\sim}{R}^T \underset{\sim}{L} \, d\rho$, and $\underset{\sim p}{G} = \int_{\rho_m} \underset{\sim p}{R}^T \underset{\sim}{L} \, d\rho$

Extremizing the above with respect to $\underset{\sim}{\beta}$ and $\underset{\sim}{\Lambda}$, the following two equations can be obtained.

$$\underset{\sim\sim}{H} \underset{\sim}{\beta} + \underset{\sim p}{\bar{H}} - \underset{\sim\sim}{G} \underset{\sim}{q} - \underset{\sim n}{C}^T \underset{\sim n}{\Lambda} = 0 \qquad (4.105)$$

$$\underset{\sim n}{C} \underset{\sim}{\beta} + \underset{\sim p_n}{C} = 0 \qquad (4.106)$$

where $\underset{\sim p}{\bar{H}} = \underset{\sim p}{H} - \underset{\sim}{\bar{U}}$.

Substituting $\underset{\sim}{\beta}$ and $\underset{\sim}{\Lambda}$ which are expressed in terms of $\underset{\sim}{q}$, from the above two equations, into Eq. 4.104 gives

$$\Pi_{HS} = \sum_m \{ \frac{1}{2} \underset{\sim}{q}^T \underset{\sim\sim}{K'} \underset{\sim}{q} - \underset{\sim}{Q'}^T \underset{\sim}{q} \} + \text{constant} \qquad (4.107)$$

where the element stiffness matrix, $\underset{\sim}{K'}$ and equivalent nodal force vector, $\underset{\sim}{Q'}$ are

$$\underset{\sim}{K}' = \underset{\sim}{G}^T[\underset{\sim}{H}^{-1} - \underset{\sim}{H}^{-1}\underset{\sim}{C}^T(\underset{\sim}{C}\ \underset{\sim}{H}^{-1}\ \underset{\sim}{C}^T)^{-1}\underset{\sim}{C}\ \underset{\sim}{H}^{-1}]\underset{\sim}{G} \tag{4.108}$$

$$\underset{\sim}{Q}' = \underset{\sim}{G}^T[\underset{\sim}{H}^{-1} - \underset{\sim}{H}^{-1}\underset{\sim}{C}^T(\underset{\sim}{C}\ \underset{\sim}{H}^{-1}\underset{\sim}{C}^T)^{-1}\underset{\sim}{C}\ \underset{\sim}{H}^{-1}]\underset{\sim}{H}_p - \underset{\sim}{G}_p + \underset{\sim}{G}^T\underset{\sim}{H}^{-1}\underset{\sim}{C}^T(\underset{\sim}{C}\ \underset{\sim}{H}^{-1}\underset{\sim}{C}^T)^{-1}\underset{\sim}{C}_p \tag{4.109}$$

Remaining mathematical manipulations are identical to those of the solution procedures without explicitly enforcing traction boundary conditions. As shown in the next chapter, when the domain of a problem is simple in geometry, traction boundary conditions of the problem can be satisfied directly, by choosing the interior stress field such a way that it satisfies the traction boundary conditions along the boundary as well as the equilibrium conditions in the interior of domain. To make the interior stress field satisfy prescribed traction boundary conditions, in the case, the assumed stress field is evaluated along the traction prescribed boundary by substituting coordinates of the boundary and dropping the terms which are not consistent with actual boundary tractions by substituting zeros for corresponding β's.

In this hybrid stress model, as mentioned earlier, it is much easier to erforce traction boundary conditions explicitly than in previously discussed compatible displacement models. Utilizing the interior stress field which can be directly related to boundary tractions, any kind of traction boundary conditions can be represented and enforced explicitly without any modifications to the original assumed variable fields.

In the following, several circular curved plates are solved with and without explicitly enforced traction boundary conditions by this hybrid stress model.

Results and Discussions

The plates solved are a clamped circular plate with uniform load, simply supported circular plates with uniform load or a point load at the center, and a uniformly loaded annular plate with a simply supported outer edge. The boundary conditions which are explicitly enforced are $M_n=0$ for a simply supported boundary and $M_n=0$, and $V_n=Q_n + M_{ns,s}=0$ for a free boundary. The number of matching points to explicitly enforce traction boundary conditions are four on each segment of traction prescribed boundary of an element. They are located equidistantly and two exterior points coincide with the two nodes on the traction prescribed boundary of an element. The finite element grids are shown in Figs. 4.23 and 4.24. The problem geometry, material constants, and error definitions are the same as those in the corresponding cases of compatible displacement model solutions in the previous section.

Though the solutions, in general, are not so accurate as those of the compatible displacement model, especially in stress solutions, strain energy and displacement solutions show good variations with N which is the number of finite elements in a quarter plate as shown in the grids and are satisfactory when N=16 in all cases. Even stress solutions, though not highly accurate, are found to be acceptable, except the tangential moments. With this exception, they are all under 3% in error when N=16.

In Fig. 4.25, the results of a uniformly loaded circular plate with clamped boundary are plotted. In this problem, there are no traction boundary conditions, to be enforced.

In Fig. 4.26, the solutions of a simply supported circular plate with uniformly distributed load, are shown. Both strain energy and

displacement solutions are not improved by explicitly enforcing traction boundary conditions. But the moment solutions are improved for the both central bending and edge tangential moments.

In Fig. 4.27, the solutions of a simply supported circular plate with a point load at the center are plotted. In the problem, the error percentages of the central displacement and strain energy vary in almost the same way, thus they are expressed by the same curves. The figure shows again considerable improvements in the solution of edge tangential moment by explicitly enforcing traction boundary conditions, but the solutions of strain energy and central displacement are not improved much.

The solutions of a uniformly loaded annular plate with simply supported outer edge, are shown in Fig. 4.28. In this problem, all the solutions vary in such a way that the solution which starts with higher or lower values when N=1, passes the exact solution when N is around 4 and then converges to the exact value from the opposite direction, as N increases. The solutions in moments are again considerably improved by explicitly enforcing traction boundary conditions.

In the Figs. 4.29, and 4.30, the numerical results of edge radial moment of simply supported circular plates with uniform load, and that of a simply supported circular plate with point load and inner and outer edge radial moments of the annular plate, which are obtained through finite element solutions for the appropriate problems without explicitly enforcing traction boundary conditions are plotted, respectively. Their exact solutions are zeros, thus each of them is compared with other appropriate analytical solution in each plate. The edge radial moment of

a simply supported circular plate with uniform load is compared with the central bending moment as (finite element results of edge radial moment) x 100/(analytical results of central bending moment). The edge radial moment of a simply supported circular plate with point load and the inner and outer edge radial moments of the annular plate are compared respectively with appripriate edge tangential moments by the same way as the above. Their numerical values which are obtained through finite element solutions with explicitly enforcing traction boundary conditions are always actually zeros (less than 10^{-10}).

In all the cases, the solutions do not converge monotonically, since hybrid finite element models are not based on extremum principles, they can not belong to either lower bound or upper bound of solutions [20].

Finally, it is considered that the comparatively low accuracy in solutions is caused by the following two facts, first the approximate representations of rigid body rotations in boundary displacement field as discussed earlier; second, this finite element is not so sophisticated as that of the previous compatible displacement model.

The number of degrees of freedom at each node in this hybrid stress model is a half of that of the previous compatible displacement model. The degrees of freedom at a node are transverse displacement and the derivatives of this deflection with respect to two inplane coordinates, i.e., w, $w_{,x}$ and $w_{,y}$, which are the minimum degrees of freedom required at a node to handle a plate problem, whereas, in compatible displacement model in the previous section, they are w, $w_{,x}$, $w_{,y}$, $w_{,xx}$, $w_{,xy}$, and $w_{,yy}$. Though the accuracy in solutions obtained by this hybrid stress model may be slightly lower than in those obtained by other sophisticated elements

with many nodal degrees of freedom, considering the economy problem of computer time to solve problems with many number of unknowns, this hybrid stress model is seen to be very useful in practical situations.

Stress Concentrations around Central Holes in Rectangular Plate due to Pure Bending

The analytical solutions of these problems with infinite domains are given in [65] by Savin. The models used by Savin are infinite plate under externally applied symmetric bending moment M at infinity. Under this situation, the tangential moment distribution M_θ along the boundary of each central hole is given as

$$M_\theta = 2M$$

for a circular hole,

$$M_\theta = M \left[2 - \frac{4(1+\nu)}{3+\nu} \frac{1+2\cos(4\theta)}{5+4\cos(4\theta)}\right]$$

for a square hole, and

$$M_\theta = M \left[2 - \frac{8(1+\nu)}{3+\nu} \frac{2-3\cos(3\theta)}{13-12\cos\theta}\right]$$

for a triangular hole where θ is the angle measured from the x axis as shown Fig. 4.31 - 4.33 with finite element grids and respective results.

The finite element model which is used for these problems is the hybrid stress model. The ratio between dimensions of the central hole and plate is 1/5 in all the cases as shown in Figs. 4.31 - 4.33.

In the problem with circular hole at center, the approximation involved is the approximate rigid body rotation modes in assumed

displacements on circular boundaries of the elements along the circular hole. Though it is oscillating, tangential moment along the central hole converges to the exact value. Further, some improvements of the solution are evident when traction boundary conditions, i.e., $M_n=0$ and $V_n=0$, are enforced explicitly along the boundary of the hole.

For the plates with square and triangular holes, no approximation is involved in the formulation. But there are stress singularities at corners of the holes, and the degree of the singularity becomes stronger as the corner angle becomes smaller. Thus, the stronger stress singularities exist at the corners of triangular hole than at those of square hole. Further, mathematical singularities of moments and curvatures exist at the corners of these holes.

Consider the corner C of square hole in Fig. 4.32, for example. Along side AC $M_x \neq 0$, $M_y = 0$ and along side BC $M_x = 0$, $M_y \neq 0$, thus $M_x = M_y = 0$ and, therefore, $w_{,xx} = w_{,yy} = 0$ at the corner C. But this is not admissible on a physical basis. Both of these types of singularity problems are not considered either in the stage of selecting the assumed solution functions or during the other formulation stage.

It is considered that the relative inaccuracy in the solutions obtained for these two problems, as compared with those for the circular hole problem, is caused by the lack of considerations of these above mentioned singularities in the formulations. More severe discontinuities of stress solutions between elements near the hole are observed in the triangular hole problem which has stronger stress singularities at corners than the square hole problem. Due to the above mentioned difficulties, in these two problems, explicitly enforcing traction boundary

conditions is not attempted, The problem of accounting for stress singularities at tips of cracks, or at reentrant corners such as discussed above, is discussed in the next chapter.

CHAPTER V

BENDING OF AN ELASTIC PLATE CONTAINING A THROUGH CRACK

In this chapter, the problem of the bending of a cracked plate is treated. In the first section, previous analytical work of the problem is reviewed starting from the general three dimensional analysis of the problem to the solutions of specific problems based on existing approximate plate theories.

In the second section, by using the qualitative features of singular solution functions which are obtained in the first section, the finite element formulation based on the hybrid stress model, which embeds the known analytical solution for singular stresses, is discussed for a cracked plate under general loading conditions.

In the third and fourth sections, solutions for cracked plates with symmetric bending loads are considered, and the results are discussed, respectively.

Analytical Solution of the Problem

The nature of stresses near the tip of a through-the-thickness crack in a plate under bending loads has been studied by many authors in several different situations. Williams [66] obtained the bending stress singularity at the base of a stationary crack of a plate under bending loads by using the method of eigenfunction expansions based on Kirchhoff plate theory. He found that the stresses near the tip of a semi-infinite crack in a plate vary as the inverse square root of the radial distance from the crack front. His results were not complete in

that the magnituds of the local stresses was left undetermined. Later, Sih and Rice [67] indicated a way for finding the coefficients in the eigenfunction expansions through the application of the theory of complex variables.

However, the above results which are based on the classical fourth order plate theory have some discrepancies. In this theory, the physically distinct three boundary conditions are reduced to two appoximate boundary conditions by Kirchhoff hypothesis. Therefore, the three actual boundary conditions along the crack edge, namely the vanishing of bending moment, twisting moment, and shear stress are satisfied approximately in such a manner that only the bending moment and the sum of shear force and the rate of change of twisting moment are made to vanish. On account of this approximation, the stress distribution near the crack edge was found to be inaccurate.

To overcome this difficulty, Knowles and Wang[68] employed a sixth order Reissner's plate bending theory [51] where the above mentioned three kinds of boundary conditions can be satisfied distinctively, to handle the problem of an infinite plate containing a finite through crack under external constant bending moment at infinity. Their results, however, were good only for a vanishingly thin plate, and the effect of the plate thickness was not considered. Their work was later generalized by Sih [69] to include the effect of the plate thickness.

Later, Wang [70] solved the same plate problem as in his previous work [68], with a constant external twisting moment instead of a bending moment, and with the consideration of the effects of the plate thickness.

From the results of the above series of works, it is found that the stress distributions near the crack front caused by bending and twisting of a cracked plate are identical to those associated with the general opening, sliding, and tearing modes of crack extension.

The solutions which can be obtained by the above mentioned methods are based on some approximate theory of three dimensional equations, i.e., bending theory for an elastic plate, whether it is a fourth order classical theory or a sixth order advanced theory. In these works, nonlinear disturbances near crack edges and plate surfaces, for cracks in thick plates, are not accounted for [71]. A study of three-dimensional effects is required for these cases.

In the study of the influence of plate thickness for a cracked plate problem, Sih [72] obtained an exact qualitative feature of solutions by using a three dimensional asympototic expansion [73] of the stresses and displacements in terms of the cylindrical polar coordinates r, θ, z for small values of r, measured from the border of a semi-infinite crack in an infinite plate.

It is possible to apply the finite element solution technique to solve these problems quantitatively once the qualitative features of the solution functions are determined. The problem is that of incorporating these singular stresses in finite elements in the vicinity of the crack front. In elements far away from the crack-tip, non-singular (regular) polynomial variation in stresses can be assumed. However, the conditions of interelement traction equilibrium and interelement displacement compatibility must be satisfied at the common boundaries of the above mentioned near-tip elements and far-field elements. It can be seen from

the general discussion of the hybrid models in the second Chapter II, that the hybrid stress finite element model (version 1, Eq. 2.36) is an ideal choice in constructing the above described finite element system, with built-in-singularities in bending moments and shear in elements near the crack-tip.

In the remaining portion of this section, first the general three dimensional treatment of a cracked plate and two cases of bending of cracked plates under constant external bending and twisting moments, respectively, will be reviewed briefly based on the previous works by Sih [69, 70] and Wang [70].

Asymptotic Expansion in Three Dimension

Consider an infinite plate shown in Fig. 5.1 with a semi-infinite through crack in negative x direction. u, v, and w denote the displacement components in the radial, tangential, and vertical directions, respectively. The corresponding stress and strain components in Cylindrical polar coordinates are σ_{rr}, $\sigma_{\theta\theta}$, $\sigma_{r\theta}$ and ε_{rr}, $\varepsilon_{\theta\theta}$ $\varepsilon_{r\theta}$, respectively.

The solution for a displacement field was sought [72] in the form of a power series in r as $r^{\lambda_m - n}$ multiplied by a function depending on both θ and z, where n is an integer and λ_m(m=0,1,2...) are the eigenvalues in the crack problem. The rigouous derivation of λ_m is given by Hartranft and Sih [73]. To obtain singularities in stresses, Sih considered the displacement field with one-half powers of r[72], as:

$$2G\,[u, v, w] = r^{\frac{1}{2}}\,[f_1(\theta, z),\ g_1(\theta,z),\ h_1(\theta,z)] + r^{\frac{3}{2}}\,[f_2(\theta,z),\ g_2(\theta,z),\ h_2(\theta,z)\ ] + O(r^{\frac{5}{2}}) \qquad (5.1)$$

where G is the shear modulus of elasticity. Substituting Eq. 5.1 into the strain displacement relations gives:

$$2G\varepsilon_{rr} = r^{-\frac{1}{2}}\left(\frac{1}{2}f_1\right) + r^{\frac{1}{2}}\left(\frac{3}{2}f_2\right) + O(r^{\frac{3}{2}})$$

$$2G\varepsilon_{\theta\theta} = r^{-\frac{1}{2}}\left[f_1 + \frac{\partial g_1}{\partial\theta}\right] + r^{\frac{1}{2}}\left[f_2 + \frac{\partial g_2}{\partial\theta}\right] + O(r^{\frac{3}{2}})$$

$$2G\varepsilon_{zz} = r^{\frac{1}{2}}\left(\frac{\partial h_1}{\partial z}\right) + r^{\frac{3}{2}}\left(\frac{\partial h_2}{\partial z}\right) + O\left(r^{\frac{5}{2}}\right)$$

$$4G\varepsilon_{r\theta} = r^{-\frac{1}{2}}\left[\frac{\partial f_1}{\partial\theta} - \frac{1}{2}g_1\right] + r^{\frac{1}{2}}\left[\frac{\partial f_2}{\partial\theta} - \frac{1}{2}g_2\right] + O(r^{\frac{3}{2}})$$

$$4G\varepsilon_{\theta z} = r^{-\frac{1}{2}}\left(\frac{\partial h_1}{\partial\theta}\right) + r^{\frac{1}{2}}\left[\frac{\partial g_1}{\partial z} + \frac{\partial h_2}{\partial\theta}\right] + O(r^{\frac{3}{2}})$$

$$4G\varepsilon_{zr} = r^{-\frac{1}{2}}\left(\frac{1}{2}h_1\right) + r^{\frac{1}{2}}\left[\frac{\partial f_1}{\partial z} + \frac{3}{2}h_2\right] + O(r^{\frac{3}{2}})$$

Through the generalized Hooke's law, the following stress components can be obtained from the above strain functions.

$$(1-2\nu)\sigma_{rr} = r^{-\frac{1}{2}}\left[\nu\frac{\partial g_1}{\partial\theta} + \frac{1}{2}(1+\nu)f_1\right]$$

$$+ r^{\frac{1}{2}}\left[\frac{\partial g_2}{\partial\theta} + \frac{\partial h_1}{\partial z} + \frac{1}{2}\nu^{-1}(3-\nu)f_1\right]$$

$$(1-2\nu)\sigma_{\theta\theta} = r^{-\frac{1}{2}}\left[(1-\nu)\frac{\partial g_1}{\partial\theta} + \frac{1}{2}(2-\nu)f_1\right]$$

$$+ r^{\frac{1}{2}}\left[\nu\frac{\partial h_1}{\partial z} + (1-\nu)\frac{\partial g_2}{\partial\theta} + \frac{1}{2}(2-\nu)f_2\right]$$

$$(1-2\nu)\sigma_{zz} = r^{-\frac{1}{2}}\nu\left[\frac{\partial g_1}{\partial\theta} + \frac{3f_1}{2\nu}\right] + r^{\frac{1}{2}}\nu\left[\frac{\partial g_2}{\partial\theta} + \frac{5}{2}f_2 + \frac{1-\nu}{\nu}\frac{\partial h_1}{\partial z}\right]$$

$$2\sigma_{r\theta} = r^{-\frac{1}{2}} \left[\frac{\partial f_1}{\partial \theta} - \frac{1}{2} g_1 \right] + r^{\frac{1}{2}} \left[\frac{\partial f_2}{\partial \theta} + \frac{1}{2} g_2 \right]$$

$$2\sigma_{\theta z} = r^{-\frac{1}{2}} \left(\frac{\partial h_1}{\partial \theta} \right) + r^{\frac{1}{2}} \left[\frac{\partial g_1}{\partial z} + \frac{\partial h_2}{\partial \theta} \right]$$

$$2\sigma_{zr} = r^{-\frac{1}{2}} \left(\frac{1}{2} h_1 \right) + r^{\frac{1}{2}} \left[\frac{\partial f_1}{\partial z} + \frac{3}{2} h_2 \right]$$

where terms with order $r^{\frac{3}{2}}$ or higher are neglected. By using equilibrium equations and the stress boundary conditions along the edge of crack $\sigma_{\theta\theta} = \sigma_{r\theta} = \sigma_{\theta z} = 0$ at $\theta = \pm\Pi$, the appropriate forms of stresses and displacements corresponding to the character of each individual problem can be obtained. When the problem is symmetric in θ, i.e., symmetric about x - axis in Fig. 5.1, the asymptotic expansions of the displacements become [71]:

$$2Gu = r^{\frac{1}{2}} C(z) \left[- (5-8\nu)\cos\frac{\theta}{2} + \cos\frac{3\theta}{2} \right]$$

$$+ r^{\frac{3}{2}} E(z) \left[- (3-8\nu)\cos\frac{\theta}{2} + \cos\frac{5\theta}{2} \right] + \ldots\ldots \qquad (5.2)$$

$$2Gv = r^{\frac{1}{2}} C(z) \left[(7-8\nu)\sin\frac{\theta}{2} - \sin\frac{3\theta}{2} \right]$$

$$- r^{\frac{3}{2}} E(z) \left[(9-8\nu)\sin\frac{\theta}{2} + \sin\frac{5\theta}{2} \right] + \ldots\ldots \qquad (5.3)$$

$$2Gw = r^{\frac{3}{2}} C'(z) \left[2\cos\frac{\theta}{2} - \frac{2}{3}(7/8\nu)\cos\frac{3\theta}{2} \right] + \ldots. \qquad (5.4)$$

It is noted that they are all bounded at the crack edge with w being one order higher than the leading terms in u and v. The corresponding stress components are:

$$\sigma_{rr} = r^{-\frac{1}{2}} C(z) \left[-\frac{5}{2}\cos\frac{\theta}{2} + \frac{1}{2}\cos\frac{3\theta}{2}\right]$$

$$+ r^{\frac{1}{2}} E(z) \left[-\frac{9}{2}\cos\frac{\theta}{2} + \frac{3}{2}\cos\frac{5\theta}{2}\right] + \ldots \quad (5.5)$$

$$\sigma_{\theta\theta} = -r^{\frac{1}{2}} C(z) \left[\frac{3}{2}\cos\frac{\theta}{2} + \frac{1}{2}\cos\frac{3\theta}{2}\right]$$

$$- r^{\frac{1}{2}} E(z) \left[\frac{15}{2}\cos\frac{\theta}{2} + \frac{3}{2}\cos\frac{5\theta}{2}\right] + \ldots \quad (5.6)$$

$$\sigma_{zz} = -r^{\frac{1}{2}} C(z) \left[4\nu\cos\frac{\theta}{2}\right] - r^{\frac{1}{2}} E(z) \left[12\nu\cos\frac{\theta}{2}\right] + \ldots \quad (5.7)$$

$$\sigma_{r\theta} = -r^{-\frac{1}{2}} C(z) \left[\frac{1}{2}\sin\frac{\theta}{2} + \frac{1}{2}\sin\frac{3\theta}{2}\right]$$

$$- r^{\frac{1}{2}} E(z) \left[\frac{3}{2}\sin\frac{\theta}{2} + \frac{3}{2}\sin\frac{5\theta}{2}\right] + \ldots \quad (5.8)$$

$$\sigma_{\theta z} = r^{\frac{1}{2}} C'(z) (3-4\nu) \left[\sin\frac{\theta}{2} - \sin\frac{3\theta}{2}\right] + \ldots \quad (5.9)$$

$$\sigma_{zr} = -r^{\frac{1}{2}} C'(z) \left[(1-4\nu)\cos\frac{\theta}{2} + (3-4\nu)\cos\frac{3\theta}{2}\right] + \ldots \quad (5.10)$$

Under the most general loading conditions, the stress components have been found [72] as:

$$\sigma_{rr} = r^{-\frac{1}{2}} A_1(z) \left[\frac{1}{2}\cos\frac{3\theta}{2} - \frac{5}{2}\cos\frac{\theta}{2}\right]$$

$$+ r^{-\frac{1}{2}} A_2(z) \left[\frac{1}{2}\sin\frac{3\theta}{2} - \frac{5}{6}\sin\frac{\theta}{2}\right] \quad (5.11)$$

$$\sigma_{\theta\theta} = -r^{-\frac{1}{2}} A_1(z) \left[\frac{1}{2}\cos\frac{3\theta}{2} + \frac{3}{2}\cos\frac{\theta}{2}\right]$$

$$- r^{-\frac{1}{2}} A_2(z) \left[\frac{1}{2} \sin \frac{3\theta}{2} + \frac{1}{2} \sin \frac{\theta}{2} \right] \tag{5.12}$$

$$\sigma_{zz} = - r^{-\frac{1}{2}} 4\nu \left[A_1(z) \cos \frac{\theta}{2} + \frac{1}{3} A_2(z) \sin \frac{\theta}{2} \right. \tag{5.13}$$

$$\sigma_{r\theta} = - r^{-\frac{1}{2}} A_1(z) \left[\frac{1}{2} \sin \frac{3\theta}{2} + \frac{1}{2} \sin \frac{\theta}{2} \right]$$

$$+ r^{-\frac{1}{2}} A_2(z) \left[\frac{1}{2} \cos \frac{3\theta}{2} + \frac{1}{6} \cos \frac{\theta}{2} \right] \tag{5.14}$$

$$\sigma_{zr} = r^{-\frac{1}{2}} A_3(z) \left[\frac{1}{4} \cos \frac{\theta}{2} \right] \tag{5.15}$$

$$\sigma_{zr} = r^{-\frac{1}{2}} A_3(z) \left[\frac{1}{4} \sin \frac{\theta}{2} \right] \tag{5.16}$$

where A(z) is equal to C(z) in Eqs. 5.5 - 5.8. To be noted is that as $r \to 0$, all the stresses tend to infinity like $r^{-1/2}$ in general loading conditions while $\sigma_{\theta z}$ and σ_{zr} remain bounded when the problem is symmetric in θ.

The coefficient $A_j(z)$ (j=1,2,3) can be evaluated from the boundary conditions of the problem. On account of the complexity of three dimensional equations of elasticity, no rigorous solution of the finite thickness problem for non-trivial loading cases has been obtained. Because of this fact, considerations may be limited to some simplified approximate theories for the present time.

In the following, the results of two simple cases of cracked plate problems which are obtained based on Reissner's plate bending theory, are compared with the above general results.

Bending of a Cracked Plate Based on Approximate Theory

As shown in Fig. 5.2, the first problem is the bending of an infinite plate containing a finite crack due to constant external bending moment at infinity, M. Based on the following Reissner's plate equations:

$$\frac{\partial Q_x}{\partial x} + \frac{\partial Q_y}{\partial y} = 0 \tag{5.17}$$

$$Q_x - k^2\nabla^2 Q_x = - D \frac{\partial}{\partial x} (\nabla^2 w) \tag{5.18}$$

$$Q_y - k^2\nabla^2 Q_y = - D \frac{\partial}{\partial y} (\nabla^2 w) \tag{5.19}$$

$$M_x = - D \left(\frac{\partial^2 w}{\partial x^2} + \nu \frac{\partial 2_w}{\partial y^2}\right) + 2k^2 \frac{\partial Q_x}{\partial x} \tag{5.20}$$

$$M_y = - D \left(\frac{\partial^2 w}{\partial y^2} + \nu\frac{\partial^2 w}{\partial x} \right) + 2k^2 \frac{\partial Q_y}{\partial y} \tag{5.21}$$

$$M_{xy} = - (1-\nu) D \frac{\partial^2 w}{\partial x \partial y} + k^2 \left(\frac{\partial Q_x}{\partial y} + \frac{\partial Q_y}{\partial x} \right) \tag{5.22}$$

where $K^2 = \frac{h^2}{10}$, and with the assumption on stress distributions given in Eqs. 3.43 - 3.45, Sih [69] obtained the singular character of moments near a crack tip, through an integral equation procedure. As $r \to 0$, the moment and shear force intensities are [69,71],

$$M_x = \frac{K_1}{\sqrt{2r}} \left(\cos \frac{\Theta}{2} - \frac{1}{2} \sin\Theta \sin \frac{3\Theta}{2} \right) \tag{5.23}$$

$$M_y = \frac{K_1}{\sqrt{2r}} \left(\cos \frac{\Theta}{2} + \frac{1}{2} \sin\Theta \sin \frac{3\Theta}{2} \right) \tag{5.24}$$

$$M_{xy} = \frac{K_1}{\sqrt{2r}} \left(\frac{1}{2} \sin\Theta \cos \frac{3\Theta}{2} \right) \tag{5.25}$$

$$Q_x = Q_y = O(1) \tag{5.26}$$

It can be seen that the above results coincide with Eqs. 5.11 - 5.16, when $A_2(z) = A_3(z) = 0$, by using Eqs. 3.10 and 3.11 and appropriate coordinate transformations. The parameter K_1, which controls the intensity of the local stress field, depends on the plate thickness h and Poisson ratio ν through $\Phi(1)$ as:

$$K_1 = \Phi(1)M\sqrt{a} \tag{5.27}$$

where the semi-crack length a denotes the half length of the crack.

The next problem is the same as the first but the external loads are constant twisting moments H instead of bending moments at infinity. This problem is solved by Wang [70] and the results as $r \to 0$, are as the following:

$$M_x = \frac{K_2}{\sqrt{2r}} \left(7\sin\frac{\theta}{2} + \sin\frac{5\theta}{2}\right) \tag{5.28}$$

$$M_y = \frac{K_2}{\sqrt{2r}} \left(\sin\frac{\theta}{2} - \sin\frac{5\theta}{2}\right) \tag{5.29}$$

$$M_{xy} = -\frac{K_2}{\sqrt{2r}} \left(3\cos\frac{\theta}{2} + \cos\frac{5\theta}{2}\right) \tag{5.30}$$

$$Q_x = \frac{K_3}{\sqrt{2r}} \left(\sin\frac{\theta}{2}\right) \tag{5.31}$$

$$Q_y = -\frac{K_3}{\sqrt{2r}} \cos\frac{\theta}{2} \tag{5.32}$$

The above forms can also be identified to Eqs. 5.11 - 5.16 when $A_1(z) = 0$, $A_2(z) = \frac{3K_2}{4\sqrt{2}}$, and $A_3 = \frac{K_3}{\sqrt{2}}$ by the same way as the previous case. Both K_2 and K_3 are also functions of the plate thickness and Poisson ratio.

As mentioned earlier, from the above two results, it is noted that the stress distributions near a crack-tip caused by symmetric bending

are precisely the same as those associated with the opening mode of crack extension and the stress distributions caused by anti-symmetric twisting are identical to those associated with the sliding and tearing modes of crack extension [70]. Thus, the unknown quantities K_1, and K_2 and K_3, which control the singular stress intensities near a crack-tip for the two cases, can be called respectively bending, and twisting stress intensity factors for a plate with cracks.

Finite Element Formulation for Hybrid Stress Model

The stress distributions near a crack tip caused by bending deformations of a plate under general loading conditions can be obtained by a combination of the above two results. This fact is confirmed by the three dimensional equations for general loading conditions, Eqs. 5.11 - 5.16. Thus, the singular stress functions for the bending problem of a cracked plate under general loading conditions can be written as:

$$M_x = \frac{K_1}{\sqrt{2r}} \left(\cos\frac{\theta}{2} - \frac{1}{2}\sin\theta\sin\frac{3\theta}{2}\right) + \frac{K_2}{\sqrt{2r}}\left(7\sin\frac{\theta}{2} + \sin\frac{5\theta}{2}\right) - 2\sqrt{2r}\,K_3\sin\frac{\theta}{2} \tag{5.33}$$

$$M_y = \frac{K_1}{\sqrt{2r}} \left(\cos\frac{\theta}{2} + \frac{1}{2}\sin\theta\sin\frac{3\theta}{2}\right) + \frac{K_2}{\sqrt{2r}}\left(\sin\frac{\theta}{2} - \sin\frac{5\theta}{2}\right) \tag{5.34}$$

$$M_{xy} = \frac{K_1}{\sqrt{2r}} \left(\frac{1}{2}\sin\frac{\theta}{2}\cos\frac{3\theta}{2}\right) - \frac{K_2}{\sqrt{2r}}\left(3\cos\frac{\theta}{2} + \cos\frac{5\theta}{2}\right) - \sqrt{2r}\,K_3\cos\frac{\theta}{2} \tag{5.35}$$

$$Q_x = \frac{K_3}{\sqrt{2r}}\sin\frac{\theta}{2} \tag{5.36}$$

$$\sigma_y = -\frac{K_3}{\sqrt{2r}} \cos\frac{\theta}{2} \tag{5.37}$$

The last terms with $\sqrt{r}$ in M_x and M_{xy} are taken from the $0(\sqrt{r})$ terms of corresponding moments in the previous results with twisting deformation for the satisfaction of equilibrium of the asymptotic functions for stress. It is to be noted that, in the discussions in the second chapter, the interior stress field should satisfy the equilibrium conditions, Eq. 3.34, in the present finite element model. Thus, the singular part, Eqs. 5.33 - 5.37, as well as the regular part of stresses should be assumed to be in equilibrium, since the interior stress field in the finite element near the tip of crack consists of the both regular and singular parts.

Near the crack-tip, the displacement field as well as the stress field has some type of asymptotic behavior in the radial coordinate r. A rigorous derivation of the asymptotic displacement behavior may be possible through integrations of Eqs. 5.33 - 5.37. by using Eqs. 3.43 - 3.45, but it involves complicated manipulations and has not been attempted in the literature. Thus the boundary displacements for the singular elements have been assumed based on the consideration of the three dimensional solution forms of displacements at the crack tip and the consistency of the assumed solutions to the approximate plate theory used, as discussed in detail in the next section.

For the finite element formulation, the plate domain with crack is discretized into a number of finite elements of two different kinds. Of the first type, are regular elements whose boundaries do not contact the crack tip, the other is of singular elements around the crack tip.

The necessary variable definitions for a regular element are precisely the same as given in the previous chapter.

For the singular element, the assumed moment functions given in Eq. 4.73 should be modified to be able to represent appropriate the stress singularity as follows:

$$\underset{\sim}{M} = \underset{\sim}{N}\ \beta + \underset{\sim}{N}_s\underset{\sim}{\beta}_s + \underset{\sim}{N}_t\underset{\sim}{\beta}_t + \underset{\sim}{N}_p \tag{5.38}$$

where

$$\underset{\sim}{\beta}_s^T = \lfloor K_1 \ K_2 \rfloor \tag{5.39}$$

$$\underset{\sim}{N}_s \quad \begin{bmatrix} \frac{1}{\sqrt{2r}}\left(\cos\frac{\Theta}{2} - \frac{1}{2}\sin\Theta\sin\frac{3}{2}\right) & \frac{1}{\sqrt{2r}}\left(7\sin\frac{\Theta}{2} + \sin\frac{5\Theta}{2}\right) \\ \frac{1}{\sqrt{2r}}\left(\cos\frac{\Theta}{2} + \frac{1}{2}\sin\Theta\sin\frac{3}{2}\right) & \frac{1}{\sqrt{2r}}\left(\sin\frac{\Theta}{2} - \sin\frac{5\Theta}{2}\right) \\ \frac{1}{\sqrt{2r}}\left(\frac{1}{2}\sin\frac{\Theta}{2}\cos\frac{3\Theta}{2}\right) & -\frac{1}{2r}\left(3\cos\frac{\Theta}{2} + \cos\frac{5\Theta}{2}\right) \end{bmatrix} \tag{5.40}$$

$$\underset{\sim}{N}_t \quad \begin{Bmatrix} -2\sqrt{2r}\ \sin\frac{\Theta}{2} \\ 0 \\ -\sqrt{2r}\cos\frac{\Theta}{2} \end{Bmatrix} \tag{5.41}$$

and $\beta_t = K_3$. The shear force intensities in Eq. 4.74 are also modified as:

$$\underset{\sim}{Q} = \begin{Bmatrix} Q_x \\ Q_y \end{Bmatrix} = \underset{\sim}{N}_Q\underset{\sim}{\beta} + \underset{\sim}{N}_{Qt}\ t + \begin{Bmatrix} px \\ 0 \end{Bmatrix} \tag{5.42}$$

where

$$\underset{\sim}{N}_{Qt} = \begin{Bmatrix} \frac{1}{\sqrt{2r}} \sin\frac{\theta}{2} \\ -\frac{1}{\sqrt{2r}} \cos\frac{\theta}{2} \end{Bmatrix} \tag{5.43}$$

By the same way, the boundary traction in Eq. 4.85, can also be modified to include singular terms as:

$$\underset{\sim}{T} = \underset{\sim}{R}\,\underset{\sim}{\beta} + \underset{\sim}{R}_s\underset{\sim}{\beta}_s + \underset{\sim}{R}_t\underset{\sim}{\beta}_t + \underset{\sim}{R}_p \tag{5.44}$$

where $\underset{\sim}{r}_s$ and $\underset{\sim}{R}_t$ can be obtained by appropriate manipulations on $\underset{\sim}{M}$ and $\underset{\sim}{Q}$ along element boundaries. The detailed form of $\underset{\sim}{L}$ of boundary displacements as in Eq. 4.84, will be discussed later.

The functional of the hybrid stress model with the effects of transverse shear deformation can be written, for an isotropic plate, as:

$$\Pi_{HS} = -\sum_m \{ \frac{1}{2}\int_{A_m} \underset{\sim}{M}^T\underset{\sim}{D}\underset{\sim}{M}dA + \frac{1}{2}\int_{A_m} D_1\underset{\sim}{Q}^T\underset{\sim}{Q}dA - \frac{1}{2}\int_{A_m} D_2\underset{\sim}{M}^T\underset{\sim}{P}_M dA$$

$$- \int_{C_m} \underset{\sim}{T}^T\underset{\sim}{U}dC + \int_{C_{\sigma_m}} \bar{\underset{\sim}{T}}^T\underset{\sim}{U}dC \} \tag{5.45}$$

where

$$\underset{\sim}{D} = \frac{12}{Eh^3}\begin{bmatrix} 1 & -\nu & 0 \\ -\nu & 1 & 0 \\ 0 & 0 & 2(1+\nu) \end{bmatrix}$$

$$D_1 = \frac{12(1+\nu)}{Eh}, \qquad D_2 = \frac{12\nu}{5Eh} \qquad \text{and} \qquad \underset{\sim}{P}_m = \begin{Bmatrix} p \\ p \\ 0 \end{Bmatrix}$$

The functional expression of a regular element can be obtained by simply adding the contributions of the second and third terms of

Eq. 5.45 to the internal complementary strain energy given in Eq. 4.86,

$$\frac{1}{2}\int_{A_m} D_1 \underset{\sim}{Q}^T \underset{\sim}{Q} dA = \frac{1}{2}\underset{\sim}{\beta}^T \underset{\sim}{U}\underset{\sim}{\beta} + \underset{\sim}{\beta}^T \underset{\sim}{U}_p + \text{constant} \tag{5.46}$$

where

$$\underset{\sim}{U} = \int_{A_m} D_1 \underset{\sim}{N}_Q^T \underset{\sim}{N}_Q \, dA \tag{5.47}$$

$$\underset{\sim}{U}_p = \int_{A_m} D_1 \underset{\sim}{N}_Q^T \begin{matrix} p_x \\ 0 \end{matrix} dA \tag{5.48}$$

and

$$\frac{1}{2}\int_{A_m} D_2 \underset{\sim}{M}^T \underset{\sim}{P}_m = \underset{\sim}{\beta}^T \underset{\sim}{V} + \text{constant} \tag{5.49}$$

where

$$\underset{\sim}{V} = \frac{1}{2}\int_{A_m} \underset{\sim}{N}^T \underset{\sim}{P}_m dA$$

Adding Eqs. 5.46 and 5.49 to the element functional of Eq. 4.86 gives the following regular element functional expression of the hybrid stress model with the effects of transverse shear deformation,

$$\Pi_{HS_m} = -\left[\frac{1}{2}\underset{\sim}{\beta}^T(\underset{\sim}{H} + \underset{\sim}{U})\underset{\sim}{\beta} + \underset{\sim}{\beta}^T(\underset{\sim}{H}_p + \underset{\sim}{U}_p) - \underset{\sim}{\beta}^T \underset{\sim}{G}\underset{\sim}{q} - \underset{\sim}{G}_p^T \underset{\sim}{q} + \underset{\sim}{S}^T \underset{\sim}{q}\right] + \text{constant} \tag{5.50}$$

Substituting the variables defined in Eqs. 5.38, 5.42, 5.44 and 4.84 into the element functional expression of Eq. 5.45 gives the following singular element functional of hybrid stress model with transverse shear deformation effects.

$$\Pi^s_{HS_m} = -\left[\frac{1}{2}\underset{\sim}{\beta}^T(\underset{\sim}{H} + \underset{\sim}{U})\underset{\sim}{\beta} + \underset{\sim}{\beta}^T \underset{\sim}{H}_s \underset{\sim}{\beta}_s + \underset{\sim}{\beta}^T(\underset{\sim}{H}_t + \underset{\sim}{U}_t)\underset{\sim}{\beta}_t + \underset{\sim}{\beta}^T(\underset{\sim}{H}_p + \underset{\sim}{U}_p - \underset{\sim}{V})\right.$$

$$+ \frac{1}{2}\underset{\sim}{\beta}_s^T \underset{\sim}{H}_{ss}\underset{\sim}{\beta}_s + \underset{\sim}{\beta}_s^T \underset{\sim}{H}_{st}\beta_t + \underset{\sim}{\beta}_s^T (\underset{\sim}{H}_{sp} - \underset{\sim}{V}_s) + \frac{1}{2}(H_{tt} + U_{tt})\beta_t^2$$

$$+ (H_{tp} + U_{tp} - V_t)\beta_t - \underset{\sim}{\beta}^T \underset{\sim}{G}\underset{\sim}{q} - \underset{\sim}{\beta}_s^T \underset{\sim}{G}_s \underset{\sim}{q} - \beta_t \underset{\sim}{G}_t \underset{\sim}{q} - \underset{\sim}{G}_p^T \underset{\sim}{q} + \underset{\sim}{S}^T \underset{\sim}{q} \ ]$$

$$+ \text{constant} \qquad (5.51)$$

where

$$\underset{\sim}{H}_s = \int_{A_m} \underset{\sim}{N}^T \underset{\sim}{D} \underset{\sim}{N}_s \, dA$$

$$\underset{\sim}{H}_t = \int_{A_m} \underset{\sim}{N}^T \underset{\sim}{D} \underset{\sim}{N}_t \, dA$$

$$\underset{\sim}{H}_{ss} = \int_{A_m} \underset{\sim}{N}_s^T \underset{\sim}{D} \underset{\sim}{N}_s \, dA$$

$$\underset{\sim}{H}_{st} = \int_{A_m} \underset{\sim}{N}_s^T \underset{\sim}{D} \underset{\sim}{N}_t \, dA$$

$$\underset{\sim}{H}_{sp} = \int_{A_m} \underset{\sim}{N}_s^T \underset{\sim}{D} \underset{\sim}{N}_p \, dA$$

$$H_{tt} = \int_{A_m} \underset{\sim}{N}_t^T \underset{\sim}{D} \underset{\sim}{N}_t \, dA$$

$$H_{tp} = \int_{A_m} \underset{\sim}{N}_t^T \underset{\sim}{D} \underset{\sim}{N}_p \, dA$$

$$\underset{\sim}{U}_t = \int_{A_m} D_1 \underset{\sim}{N}_Q^T \underset{\sim}{N}_{Qt} \, dA$$

$$U_{tt} = \int_{A_m} D_1 \underset{\sim}{N}_{Qt}^T \underset{\sim}{N}_{Qt} \, dA$$

$$\underset{\sim}{U}_{tp} = \int_{A_m} D_1 \underset{\sim}{N}_{Qt}^T \begin{Bmatrix} p_x \\ 0 \end{Bmatrix} dA$$

$$\underset{\sim}{G}_s = \int_{C_m} \underset{\sim}{R}_s^T \underset{\sim}{L} dC$$

$$\underset{\sim}{G}_t = \int_{C_m} \underset{\sim}{R}_t^T \underset{\sim}{L} dC$$

$$\underset{\sim}{V}_s = \frac{1}{2} \int_{A_m} D_2 \underset{\sim}{N}_s^T \underset{\sim}{P}_m dA$$

$$V_t = \frac{1}{2} \int_{A_m} D_2 \underset{\sim}{N}_t^T \underset{\sim}{P}_m dA$$

Thus, the functional for the system can be expressed as the sum of those of elements.

$$\Pi_{HS} = \sum_{m=1}^{s} \Pi_{HS_m}^{s} + \sum_{m=s+1}^{N} \Pi_{HS_m} \tag{5.52}$$

where N is the total number of finite elements and s is the number of singular elements out of N elements.

By extremizing Π_{HS} with respect to $\underset{\sim}{\beta}$, the following Euler equations can be obtained.

$$\underset{\sim}{\bar{H}}\underset{\sim}{\beta} + \underset{\sim}{H}_s\underset{\sim}{\beta}_s + \underset{\sim}{\bar{H}}_t\underset{\sim}{\beta}_t + \underset{\sim}{\bar{U}}_p - \underset{\sim}{G}\underset{\sim}{q} = 0 \qquad \text{for} \quad m \leq s \tag{5.53}$$

$$\underset{\sim}{\bar{H}}\underset{\sim}{\beta} + \underset{\sim}{\bar{U}}_p - \underset{\sim}{G}\underset{\sim}{q} = 0 \qquad \text{for} \quad m > s \tag{5.54}$$

where

$$\underset{\sim}{\bar{H}} = \underset{\sim}{H} + \underset{\sim}{U}$$

$$\bar{H}_t = H_t + U_t$$

$$\bar{U}_p = H_p + U_p - V$$

Substituting the β's which are solved from Eqs. 5.53 and 5.54 into Π_{HS}, the following form of the functional can be obtained through a series of matrix manipulations.

$$\Pi_{HS} = \sum_{m=1}^{s} \left(\frac{1}{2} \begin{bmatrix} q^T & \beta_s^T & \beta_t \end{bmatrix} \begin{bmatrix} K_{11} & K_{12} & K_{13} \\ K_{12}^T & K_{22} & K_{23} \\ K_{13}^T & K_{23}^T & K_{33} \end{bmatrix} \begin{Bmatrix} q \\ \beta_s \\ \beta_t \end{Bmatrix} \right.$$

$$\left. - \begin{bmatrix} Q^T & Q_s^T & Q_t \end{bmatrix} \begin{Bmatrix} q \\ \beta_s \\ \beta_t \end{Bmatrix} \right) + \sum_{m=s+1}^{N} \left(\frac{1}{2} q^T K_{11} q - Q^T q \right) \qquad (5.55)$$

where

$$K_{11} = G^T \bar{H}^{-1} G$$

$$K_{12} = G_s^T - G^T \bar{H}^{-1} H_s$$

$$K_{13} = G_t^T - G^T \bar{H}^{-1} \bar{H}_t$$

$$K_{22} = H_s^T \bar{H}^{-1} H_s - H_{ss}$$

$$K_{23} = - H_{st} + H_s^T \bar{H}^{-1} \bar{H}_t$$

$$K_{33} = \bar{H}_t^T \bar{H}^{-1} \bar{H}_t - \bar{U}_{tt}$$

$$\underset{\sim}{Q} = \underset{\sim}{G}^T \bar{\underset{\sim}{H}}^{-1} \bar{\underset{\sim}{U}}_p - \underset{\sim}{G}_p + \underset{\sim}{S}$$

$$\underset{\sim}{Q}_s = \underset{\sim}{H}_{sp} - \underset{\sim}{V}_s - \underset{\sim}{H}_s^T \bar{\underset{\sim}{H}}^{-1} \bar{\underset{\sim}{V}}_p$$

$$\underset{\sim}{Q}_t = \underset{\sim}{H}_{tp} + \underset{\sim}{U}_{tp} - \underset{\sim}{V}_t - \bar{\underset{\sim}{H}}_t^T \bar{\underset{\sim}{H}}^{-1} \bar{\underset{\sim}{U}}_p$$

There can be two different solution methods to obtain the final solutions from this point. The first one is to consider $\underset{\sim}{\beta}_s$ and β_t as the same kinds of final unknowns as $\underset{\sim}{q}$ and then construct a new unknown vector $\underset{\sim}{q}'^T = [\underset{\sim}{q}^T \; \underset{\sim}{\beta}_s^T \; \beta_t]$. By solving the Euler equations which are obtained by the extremization of the functional with respect to $\underset{\sim}{q}'$, $\underset{\sim}{q}$, $\underset{\sim}{\beta}_s$ and β_t are obtained at the same time. The other method is first to eliminate $\underset{\sim}{\beta}_s$ and β_t at element level matrix manipulation by a method similar to static condensation [74] and then the actual element stiffness matrix can be constructed. Then, by following the usual solution procedures $\underset{\sim}{\beta}_s$ and β_t can be calculated from $\underset{\sim}{q}$ which are obtained first from the system stiffness equations.

For the first method, the element functionals of Eq. 5.55 are assembled into the system functional by keeping $\underset{\sim}{\beta}_s$ and β_t common to all singular elements; then

$$\Pi_{HS} = \frac{1}{2} \begin{bmatrix} \underset{\sim}{q}^{*T} & \underset{\sim}{\beta}_s^T & \beta_t \end{bmatrix} \begin{bmatrix} \underset{\sim}{K}_{11}^* & \underset{\sim}{K}_{12}^* & \underset{\sim}{K}_{12}^* \\ \underset{\sim}{K}_{12}^{*T} & \underset{\sim}{K}_{22}^{*T} & \underset{\sim}{K}_{23}^* \\ \underset{\sim}{K}_{13}^{*T} & \underset{\sim}{K}_{23}^* & \underset{\sim}{K}_{33}^* \end{bmatrix} \begin{Bmatrix} \underset{\sim}{q}^{*T} \\ \underset{\sim}{\beta}_s^T \\ \beta_t \end{Bmatrix}$$

$$- \begin{bmatrix} \underset{\sim}{Q}^{*T} & \underset{\sim}{Q}_s^{*T} & Q_t^* \end{bmatrix} \begin{Bmatrix} \underset{\sim}{q}^* \\ \underset{\sim}{\beta}_s \\ \beta_t \end{Bmatrix} \qquad (5.56)$$

where the quantities with * denote the system quantities corresponding to appropriate element quantities. Extremization of Eq. 5.56 with respect to the vector of unknown quantities $\underset{\sim}{q}'$ gives the final system of equations as:

$$\begin{bmatrix} \underset{\sim}{K}^{*}_{11} & \underset{\sim}{K}^{*}_{12} & \underset{\sim}{K}^{*}_{13} \\ \underset{\sim}{K}^{*T}_{12} & \underset{\sim}{K}^{*}_{22} & \underset{\sim}{K}^{*}_{23} \\ \underset{\sim}{K}^{*T}_{13} & \underset{\sim}{K}^{*T}_{23} & \underset{\sim}{K}^{*}_{33} \end{bmatrix} \begin{Bmatrix} \underset{\sim}{q}^{*} \\ \underset{\sim}{\beta}_{s} \\ \beta_{t} \end{Bmatrix} = \begin{Bmatrix} \underset{\sim}{Q}^{*} \\ \underset{\sim}{Q}^{*}_{s} \\ Q^{*}_{t} \end{Bmatrix} \tag{5.57}$$

This method is not desirable when the number of degrees of freedom of the system is large since the assembling of $\underset{\sim}{\beta}_{s}$ and β_{t} in the final unknown vector like in Eq. 5.57 unually causes the band width of the coefficient matrix of the final system of equations to be large. To avoid this drawback, the second method is usually employed. In this case the element stiffness matrix of a singular element is first obtained as in the following. By extremization of the functional, Eq. 5.55, with respect to $\underset{\sim}{q}'$, the system of equations for a singular element can be written as:

$$\begin{bmatrix} \underset{\sim}{K}_{11} & \underset{\sim}{K}_{12} & \underset{\sim}{K}_{13} \\ \underset{\sim}{K}^{T}_{12} & \underset{\sim}{K}_{22} & \underset{\sim}{K}_{23} \\ \underset{\sim}{K}^{T}_{13} & \underset{\sim}{K}^{T}_{23} & K_{33} \end{bmatrix} \begin{Bmatrix} \underset{\sim}{q} \\ \underset{\sim}{\beta}_{s} \\ \beta_{t} \end{Bmatrix} = \begin{Bmatrix} \underset{\sim}{Q} \\ \underset{\sim}{Q}_{s} \\ Q_{t} \end{Bmatrix} \tag{5.58}$$

Expanding Eq. 5.58, then:

$$\underset{\sim}{K}_{11}\underset{\sim}{q} + \underset{\sim}{K}_{st}\underset{\sim}{\beta}_{st} = \underset{\sim}{Q} \tag{5.59}$$

$$\underset{\sim}{K}_{st}^{T}\underset{\sim}{q} + \underset{\sim}{K}_{s}\underset{\sim}{\beta}_{st} = \underset{\sim}{Q}_{st} \tag{5.60}$$

where

$$\underset{\sim}{K}_{st} = [\underset{\sim}{K}_{12}\ \underset{\sim}{K}_{13}]$$

$$\underset{\sim}{K}_{s} = \begin{bmatrix} \underset{\sim}{K}_{22} & \underset{\sim}{K}_{23} \\ \underset{\sim}{K}_{23}^{T} & \underset{\sim}{K}_{33} \end{bmatrix}$$

$$\underset{\sim}{\beta}_{st}^{T} = [\underset{\sim}{\beta}_{s}^{T}\ \ \beta_{t}]$$

$$\underset{\sim}{Q}_{st}^{T} = [\underset{\sim}{Q}_{s}^{T}\ \ Q_{t}]$$

From Eqs. 5.59 and 5.60, the following two equations are obtained:

$$\underset{\sim}{\beta}_{st} = \underset{\sim}{K}_{s}^{-1}\,(\underset{\sim}{Q}_{st} - \underset{\sim}{K}_{st}^{T}\underset{\sim}{q}) \tag{5.61}$$

$$\underset{\sim}{K}_{11}\underset{\sim}{q} = \underset{\sim}{Q} - \underset{\sim}{K}_{st}\,\underset{\sim}{K}_{s}^{-1}\,(\underset{\sim}{Q}_{st} - \underset{\sim}{K}_{st}^{T}\underset{\sim}{q}) \tag{5.62}$$

Eq. 5.62 is nothing but the element stiffness equation of a singular element. Assembling this with those of other singular and regular elements into the system equations, the system stiffness equations can be written as:

$$\underset{\sim}{K}^{*}\underset{\sim}{q}^{*} = \underset{\sim}{Q}^{*} \tag{5.63}$$

The element nodal displacements, $\underset{\sim}{q}$, which are obtained by solving the above equations, for the system nodal displacements, $\underset{\sim}{q}^{*}$, can be substituted into Eq. 5.61 to calculate the stress intensity factors, $\underset{\sim}{\beta}_{st}$.

The finite element method based on the hybrid stress model is formulated for a plate bending problem with a through crack under general

bending loads. In the following, a numerical implementation for a cracked plate problem under symmetric bending moment is given. Results are obtained for finite plates of various aspect ratios, various crack sizes, and various plate thicknesses. These are compared with the analytical solution by Sih [69] for an infinite plate. The purposes of this work are: to investigate the possibility of using the hybrid stress model to handle the problem of a cracked plate in bending, based on a approximate plate theory; to investigate the effects of enforcing traction boundary conditions explicitly, on the solutions, in this specific problem; and to obtain the finite size correction factors to the infinite plate solutions of Sih [69].

The formulation developed is capable of handling problems with general loading conditions, but due to the computer-time limitations, only the special case of symmetric loading is treated in the present work.

Numerical Implementation

Consider the bending of the plate containing a through crack under constant bending moment around its boundary as shown in Fig. 5.3. For the finite element model only a quarter plate, which is shown in Fig. 5.4 with a simple grid scheme, is used because of symmetry of the problem. There are two singular elements A and B which contact the crack tip, denoted as node 2 in the figure.

The formulation and the assumed variables, i.e., internal stress field and boundary displacement field for regular elements are exactly the same as discussed in the previous chapter besides the fact that the contribution of transverse shear stresses to the internal complementary

strain energy is considered by adding Eq. 5.46 to the functional.

As can be seen from Fig. 5.5, the independent boundary displacements along boundary 1, 2 of a regular element are w_{12}, and $w_{n_{12}}$ which are interpolated in terms of the nodal values of w and $w_{,s}$ and $w_{,n}$, respectively, and $w_{s_{12}}$ is the derivative of w_{12} with respect to boundary coordinate s. But in the light of the Reissner's plate theory on which the formulation is based, the independent boundary displacements along the same portion of boundary of the element should be the normal deflection w_{12} and rotations about two directions, $\phi_{s_{12}}$ and $\phi_{n_{12}}$. This implies an approximation in assuming the boundary displacement field. But, considering the difference between the present formulation for a regular element and that of the hybrid stress model solution in the previous chapter which is based on the classical plate theory, it is clear that the present formulation is another version of the previous one with consideration of the contributions of transverse shear stresses to the internal complementary strain energy. Thus, it can be seen that this approximation will not affect the solutions much. Complete boundary displacements of a regular element are shown in Table 5.1.

Singular element A which is shown in Fig. 5.6 with the degrees of freedom at each node, has two singular sides which are joined together at the crack tip and two "regular" sides which do not contact the crack tip directly.

To obtain qualitative features of displacements near the crack front, considerations to the displacement solutions of a three dimensional fracture problem are given. In the case, the displacement solutions are expressed in one half power series of the radial coordinate r [71]. The

first terms of the series solutions of displacements in three direction, which dominate near the crack front, are functions of $r^{1/2}$. But in a plate bending problem, components of inplane displacements are linearly proportional to total rotations of the normal as shown in Eq. 3.1. Further the total rotations of the normal, ϕ_α, consist of the derivatives of the transverse deflection with respect to appropriate coordinate, $w_{,\alpha}$, and small perturbations, γ_α, to them, as:

$$\phi_\alpha = w_{,\alpha} + \gamma_\alpha$$

Thus, if the transverse deflection w starts with function of $r^{1/2}$, the above equation implies that ϕ_α includes terms with the $r^{-1/2}$ function which is unbounded as $r \to 0$, which is impossible physically. To avoid this difficulty, possible displacement forms which are consistent with approximate plate theory are considered from the previous argument, such as, the inplane displacements starting with functions of $r^{1/2}$ and the transverse deflection starting with a function of $r^{3/2}$. This argument is confirmed by the previously discussed three dimensional asymptotic expansion of displacements by Sih in Eqs. 5.2 - 5.4. In the present formulation, only the first terms of each displacement will be used as assumed boundary displacement functions along singular sides. Thus, along the sides 1, 2 and 2, 3 of the element A of Fig. 5.6, the boundary displacements are approximated, respectively, as:

$$w_{12} = (1-s)^{3/2} w_1 + [1-(1-s)^{3/2}]w_2 \tag{5.64}$$

$$\phi_{n_{12}} = -\sqrt{1-s}\,\phi_{y_1} - (1-\sqrt{1-s})\phi_{y_2} \tag{5.65}$$

$$\phi_{s_{12}} = \sqrt{1-s}\ \phi_{x_1} + (1-\sqrt{1-s})\phi_{x_2} \tag{5.66}$$

$$w_{23} = (1-s^{\frac{3}{2}})\ w_2 + s^{\frac{3}{2}}\ w_3 \tag{5.67}$$

$$\phi_{n_{23}} = (1-\sqrt{s})\phi_{x_2} + \sqrt{s}\phi_{x_3} \tag{5.68}$$

$$\phi_{s_{23}} = (1-\sqrt{s})\phi_{y_2} + \sqrt{s}\phi_{y_3} \tag{5.69}$$

For the remaining regular sides, the displacements are assumed identical to those of other regular elements.

As shown in Fig. 5.6, the boundary rotations ϕ_α along singular sides 1, 2 and 2, 3 of the element A are interpolated in terms of their values at the nodes 1, 2 and 3 as shown in the above equations. But along the regular sides 3, 4 and 1, 4 of the same element, the generalized displacements corresponding to ϕ_α of the singular sides are the derivative of the transverse deflection with respect to the appropriate directions, $w_{,\alpha}$. Thus the nodal quantities at nodes 1 and 3 by which $w_{,\alpha}$ along each of the regular sides 3, 4 and 1, 4 are interpolated, as in Eq. 4.75, are identical to those of ϕ_α at the nodes, but they are the nodal values of $w_{,\alpha}$ at the node 4. This implies some approximation in the formulation of boundary displacements for the regular sides of the singular element, since there are some differences between ϕ_α and $w_{,\alpha}$. Further it can be seen that the displacements in Eqs. 5.64 - 5.69 can not represent the rigid body rotations exactly. The stiffness matrix of the singular element in Fig. 5.6 is shown in Table 5.2 with the equilibrium state in vertical

force VE, and in x and y directional moments XE and YE, respectively. In spite of these difficulties, the present element is used for singular elements since the choice of shape function for boundary displacements along the singular side is limited because of the asymptotic character of the displacement field. The complete displacements for the singular elements A and B are listed in Tables 5.3 and 5.4.

The symmetric character of the problem permits only the opening mode type stress distributions of stresses; thus the interior moment intensity functions in Eq. 5.38 are assumed as:

$$\underset{\sim}{M} = \underset{\sim\sim}{M}\beta + \underset{\sim}{N}_s\beta_s \tag{5.70}$$

where $\underset{\sim}{N}_s$ is the vector which consists of the first terms of Eqs. 5.33 - 5.35, β_s corresponds to K_1, and $\underset{\sim}{N}_p$ of Eq. 5.38 is dropped since no external load is applied on the surface of the plate. The singular element functional of Eq. 5.51 can be written in the following simplified form.

$$\Pi^s_{HS_m} = -\frac{1}{2}\underset{\sim}{\beta}^T\underset{\sim\sim}{\bar{H}}\beta - \beta_s\underset{\sim}{H}_s\underset{\sim}{\beta} - \frac{1}{2}H_{ss}\beta_s + \underset{\sim}{\beta}^T\underset{\sim\sim}{G}\underset{\sim}{q} + \beta_s\underset{\sim}{G}_s\underset{\sim}{q} \tag{5.71}$$

and similarly the functional for a regular element in Eq. 5.50 can be simplified as:

$$\Pi_{HS_m} = -\frac{1}{2}\underset{\sim}{\beta}^T\underset{\sim\sim}{\bar{H}}\beta + \underset{\sim}{\beta}^T\underset{\sim\sim}{G}\underset{\sim}{q} - \underset{\sim}{S}^T\underset{\sim}{q} \tag{5.72}$$

The remaining procedures are precisely identical to those shown in the previous formulation. The method used to calculate β_s here is the first one of the two previously discussed methods. Thus, β_s is assembled as an element of the final unknown vector and is solved with $\underset{\sim}{q}$ at the same

time.

To enforce traction boundary conditions explicitly, a direct approach to the interior stress fields is used. Crack edge 0-2 in the plate, shown in Fig. 5.4, is traction free and $M_y = M_{xy} = Q_y = 0$. To satisfy these conditions for the original stress functions given in Eq. 4.73, it can be decided by inspecting $\underset{\sim}{N}$ and $\underset{\sim}{N}_Q$ of Eqs. 4.73 and 4.74, respectively, which of the β's of Eq. 4.73 should vanish, when appropriate coordinates along the boundary are substituted into them. The stress functions which are reduced in this manner will satisfy the above mentioned boundary conditions inherently. Thus, to enforce traction boundary conditions explicitly, it is necessary only to use these reduced stress functions for the elements along the crack edge instead of the original stress functions. Also for those elements with reduced stress functions, the boundary tractions of Eq. 4.85 should be modified appropriately. The reduced stress functions, and boundary traction matrix $\underset{\sim}{R}$ and $\underset{\sim}{R}_p$ of Eq. 4.85 for an element with these reduced stress functions are listed in Table 5.5.

All integrations needed in calculating an element stiffness matrix are performed by the use of Gaussian quadrature. In using this numerical integral technique for the quantity with $\frac{1}{\sqrt{r}}$ or $\sqrt{r}$, a transformation of variable is required to obtain accurate results, as followings:

$$r = z^2$$

$$dr = 2z^2 dz$$

$$\sqrt{r}\, dr = 2z^2 dz$$

$$\frac{1}{\sqrt{r}}\, dr = 2dz$$

Results and Discussions

The analytical solution for K_1 for an infinite plate can be obtained from Eq. 5.27 by solving an integral equation for $\phi(1)$ [69]. It was found that $\Phi(1)$ is a function of the plate thickness and the Poisson ratio. The finite element solutions for K_1 with various thicknesses of the plate are tabulated in Table 5.6, when Poisson's ratio, ν=.3, and the traction boundary conditions are enforced explicitly. It was found that the results depend on the plate thickness, h, and the singular element size of a finite element grid. Thus, they are expressed as functions of the ratio h/a and c/a where a is the half of the crack length and c is the side length of a singular element of a finite element grid as shown in Fig. 5.4.

It is natural that the solutions vary with the size of a singular element in a finite element grid since there should be optimum area where the singular behavior of the stresses dominates for each plate with different thicknesses. This area can be determined by numerical experimentation, and in all the finite element grids which are used in the solution procedure the elements in this area should be singular. To keep the singular elements, which are the most critical elements in the entire system for obtaining the correct solution of stress intensity factors, in best condition their shapes are always taken as square. Further, since it was found that the shape of the regular elements adjacent to those singular elements affects the results very sensibly,

the dimensions of the grids around singular elements are taken as 1.5c, as shown in the figure, to keep the consistency in the solutions of problems with various different geometries.

The results in Table 5.6 are represented graphically in Fig. 5.7. The figure shows converging results with some consistent tendency with the variations of the plate thickness. The optimum size of a singular element becomes larger with the thickness of plate. From these results the optimum size of a singular element for each thickness can be obtained and the results are given in Fig. 5.8 and Table 5.7.

In Table 5.8, the finite element solutions with and without* explicitly enforcing traction boundary conditions, K_F and K_{F1}, respectively, are listed for problems with various thicknesses and dimensions of the plate. The optimum size of singular elements for each thickness, which is obtained from Fig. 5.8, was used for the present set of solutions. The analytical solution obtained in [69] is for an infinite plate and in that case the external bending moment is applied at infinity. The finite element solutions with fixed thickness of the plates and the magnitude of external bending moment at boundaries of the plates, and with finite dimensions should vary with the variations of the ratio between the crack length and the plate dimension, 2a/L. The correction factors due to the effects of the finiteness of the plate are plotted in Fig. 5.9, as the ratio K_F/K_1 between the finite element solutions of finite plates

* This implies the traction boundary conditions are satisfied in a weighted residual sense as in Eq. 4.95.

with thickness and semi-crack length ratio h/a = ,1 has a 4% higher stress intensity factor when the crack length is 1/10 of the plate dimension and 23% higher value when the crack length is 1/2 of the plate dimension, as compare to the analytical solution for the stress intensity factor for an infinite plate. Though there are some variation, finite dimension correction factors, in general, do not vary significantly with the variations of the ratio h/a as shown in the figure.

The entire set of results in Table 5.8 are represented graphically in Fig. 5.10 - 5.14. They show the variations of the stress intensity factor solutions, with and without explicitly enforcing traction boundary conditions, with the plate thickness for each different geometry of the problem. The improvement of the solution for the stress intensity factor, which is very important in the determination of the singular behavior of stresses near a crack tip in a cracked plate problem and the onset of crack growth, is evident when traction boundary conditions are enforced explicitly. Further the magnitude of the numerical value of the improvement is significant.

In all the cases, the solutions without enforcing traction boundary conditions explicitly are around 30% less than the analytical solutions when h/a = .1. Even in the case when the finite element solution without enforcing traction boundary conditions explicitly is closest to that of analytical results of the infinite plate, i.e., when h/a = .5 and 2a/L = .5, the finite element solution is still 4.6% less that the infinite plate solution. Considering that the finite dimension correction factors should always greater than 1, the above mentioned result with the geometry 2a/L = .5, is almost equivalently bad as the results of any other

case obtained without enforcing the boundary conditions explicitly.

From the previous observations, it is concluded that the traction boundary conditions should be enforced in an explicit manner to obtain reliable solutions for stress intensity factors in a cracked plate problem, using the assumed stress hybrid finite element model. As discussed earlier, in this problem, the direct method of explicitly enforcing traction boundary conditions can be used since the geometry of the model is simple and the crack surface is straight. But in problems with arbitrarily curved crack surfaces, which are more likely in more practical situations, than the presently discussed problem, this direct method cannot be applied. In these cases, the boundary collocation method, which is discussed in chapter four in detail, should be used to enforce traction boundary conditions explicitly.

CHAPTER VI

CONCLUSIONS AND RECOMMENDATIONS

The following conclusions can be drawn based on the studies in this thesis.

1. The Suitablity of hybrid models in enabling one to use different elements (with different order interpolations of the assumed variable) in different regions of a system, and yet maintain full interelement displacement and traction continuities, is demonstrated. For example, in solving a plane stress problem, constant strain triangles (with linear displacement interpolations) can be combined with linear strain (with quadratic displacement interpolations) or quadratic strain triangles (with cubic variation of displacement). Thus the higher order elements can be used where a high accuracy is needed, with lower order elements being used elsewhere in the structure.
2. The so-called "Babuska paradox" in the solution of a simply supported circular plate has been shown to be linked to the notion of "natural boundary conditions" in the variational principle.
3. It has been shown that, in the finite element method, in approximating a curved boundary by piecewise straight segments, such as in approximating a circular plate by a polygonal one, convergence to the "correct" answer can result only if, at the nodes of the piecewise straight boundary, the essential boundary conditions

corresponding to the curved boundary are imposed.

4. The nature of implicitly enforcing the traction boundary conditions in the hybrid stress model and the compatible displacement model is clarified, and systematic methods to enforce traction boundary conditions explicitly for the above methods are developed. The methods are based on the concept of the point matching of boundary tractions as in a boundary collocation method. Thus, through a combination of the boundary point matching method and the original variational method, the satisfaction of traction boundary conditions on an arbitrarily curved boundary with a high degree of accuracy becomes possible. By this method, fracture problems with arbitrarily curved crack surfaces, in which the accurate enforcement of the stress free conditions along the crack surface is crucial in order to obtain accurate stress intensity factors at the tip of crack, can be treated easily.

5. It is found that finite element solutions can be improved by explicitly enforcing traction boundary conditions, even in regular, well defined problems such as circular curved plate bending problems, in which highly sophisticated compatible displacement model are used.

6. In the hybrid stress model, deriving stiffness properties of a plate finite element with arbitrary geometry becomes much easier as compared to the compatible displacement finite element model, since the transverse displacement and normal slope are assumed independently at the interelement boundary. However, since, in general, it is not possible to include all the rigid body modes

in these unique boundary interpolation functions, the element stiffness matrix generated in the hybrid stress model may not be accurately equilbrated, as explained in the fourth chapter with Tables 4.5 and 4.6. However, global solutions using these element matrices were found to be acceptable.

7. The hybrid stress finite element model was found to be suitable to accurately determine the stress concentration factors around holes, of different geometries, in thin elastic plates.

8. In the bending problem of a plate with a through crack, the hybrid stress model is found to be a versatile method to solve directly for the stress-intensity factors. It is also found that, in this problem, enforcing traction free conditions along crack border in an explicit manner is very important to obtain reliable results.

9. The optimum size of the singular finite element near crack front, in a finite element grid of the solution of cracked plate bending problem by the hybrid stress model with built-in singularities in assumed interior stress field, is found, as function of the plate thickness through numerical experiments.

10. Correction factors for stress intensity factors in a finite plate, as compared to the solution for an infinite domain, are obtained in problems of the bending of cracked plate.

11. It is also found that, in the bending of cracked plate problem, the ratio of the dimension of regular elements, which are adjacent to singular elements, with that of a singular element, can affect the solution of stress intensity factor. Thus, to keep the consistency in the series of solutions obtained through the change

of the geometry, careful considerations should be given to decide optimum size also of the regular elements around singular ones in a finite element grid, as discussed in the fifth chapter.

The studies which have not been throughly investigated in this thesis which are recommended for possible future investigations are indicated below:

1. Explicitly enforcing traction boundary conditions by the concept of boundary collocation method has not been tried for fracture mechanics problems with arbitrarily curved crack surfaces.
2. In the bending problem of cracked plates, arbitrarily loading conditions have not been treated. However, through the formulation for general loading conditions given in the fifth chapter, bending problems of plates can be solved under general loading and boundary conditions.
3. A similar study on the effects of explicitly enforcing traction boundary conditions is required in the case of hybrid displacement models.
4. Some studies on the edge function method [75] are recommended for handling some practical problems in which the accurate satisfaction of traction boundary conditions is necessary to obtain good solutions by approximate methods.

APPENDIX A

BOUNDARY CONDITIONS OF A CIRCULAR PLATE

Three types of boundary conditions are common in plate problems namely simply supported, clamped and free boundary conditions. Clamped boundary conditions are pure essential type, free boundary conditions are pure natural type, and simply supported boundary conditions are combination of these two, thus, a simply supported plate has both force (natural) and geometric (essential) boundary conditions. These various conditions are listed in both cartesian and curvilinear boundary coordinates of a circle [Fig. 4.1].

The boundary conditions given here are convenient forms for the finite element solution of a problem with up to second derivatives of transverse deflection as generalized displacements.

The following simplified notations, $A = \cos\theta$ and $B = \sin\theta$ where θ is the angle between x-axis and radial direction, are used for simplicity purpose and a denotes the radius of the circle and ν is Poisson's ratio.

Simply Supported Boundary

n,s Coordinates

$$w = 0 \qquad \text{A.1a}$$

$$w_{,s} = 0 \qquad \text{A.1b}$$

$$w_{,ss} = 0 \qquad \text{A.1c}$$

$$M_{nn} = 0, \text{ or} \qquad \text{A.2a}$$

$$w_{,nn} + \nu\left(\frac{w_{,n}}{a} + w_{,ss}\right) = 0 \qquad \text{A.2b}$$

x,y Coordinates

$$w = 0 \qquad \text{A.3a}$$

$$Bw_{,x} - Aw_{,y} = 0 \qquad \text{A.3b}$$

$$B^2 w_{,xx} - 2ABw_{,xy} + A^2 w_{,yy} - \frac{A}{a} w_{,x} - \frac{B}{a} w_{,y} = 0 \qquad \text{A.3c}$$

$$A^2 M_x + 2ABM_{xy} + B^2 M_y = 0, \text{ or} \qquad \text{A.4a}$$

$$(A^2 + \nu B^2) w_{,xx} + 2(1-\nu)ABw_{,xy} + (\nu A^2 + B^2) w_{,yy} = 0 \qquad \text{A.4b}$$

Clamped Boundary

n,s Coordinates

$$w = 0 \qquad \text{A.5a}$$

$$w_{,n} = 0 \qquad \text{A.5b}$$

$$w_{,s} = 0 \qquad \text{A.5c}$$

$$w_{,ns} = 0 \qquad \text{A.5d}$$

$$w_{,ss} = 0 \qquad \text{A.5e}$$

x,y Coordinates

$$w = 0 \qquad \text{A.6a}$$

$$w_{,x} = 0 \qquad \text{A.6b}$$

$$w_{,y} = 0 \qquad \text{A.6c}$$

$$AB(w_{,xx} - w_{,yy}) + (B^2 - A^2) w_{,xy} + \frac{B}{a} w_{,x} + \frac{A}{a} w_{,y} = 0 \qquad \text{A.6d}$$

$$B^2 w_{,xx} - 2ABw_{,xy} + A^2 w_{,yy} - \frac{A}{a} w_{,x} - \frac{B}{a} w_{,y} = 0 \qquad \text{A.6e}$$

Free Boundary

n,x Coordinates

$$M_{nn} = 0, \text{ or} \qquad \text{A.7a}$$

$$w,_{nn} + \nu\left(\frac{w,_n}{a} + w,_{ss}\right) = 0 \qquad \text{A.7b}$$

$$V_n = Q_n + M_{ns,s} = 0, \text{ or} \qquad \text{A.8a}$$

$$w,_{nnn} + \frac{w,_{nn}}{a} - \frac{w,_n}{a^2} + (2 - \nu)w,_{nss} - \frac{3-\nu}{a} w,_{ss} = 0 \qquad \text{A.8b}$$

x,y Coordinates

$$A^2M_x + 2ABM_{xy} + B^2M_y = 0, \text{ or} \qquad \text{A.9a}$$

$$(A^2 + \nu B^2)w,_{xx} + 2(1 - \nu)ABw,_{xy} + (\nu A^2 + B^2)w,_{yy} = 0 \qquad \text{A.9b}$$

$$AQ_x + BQ_y + \frac{A^2 - B^2}{a}(M_y - M_x) - \frac{4AB}{a} M_{xy}$$
$$+ AB^2(M_{x,x} - M_{y,x}) + A^2B(M_{y,y} - M_{x,y})$$
$$+ (A^2 - B^2)\,(AM_{xy,y} - BM_{xy,x}) = 0 \qquad \text{A10a}$$

$$A[1+(1 - \nu)B^2]\, w,_{xxx} + B[1+(1 - \nu)A^2]w,_{yyy}$$
$$+ B[1-(1 - \nu)(2A^2 - B^2)]w,_{xxy} + A[1 - (1-\nu)(A^2 - 2B^2)]w,_{xyy}$$
$$+ \frac{(1-\nu)}{a}(A^2 - B^2)(w,_{yy} - w,_{xx}) - \frac{4(1-\nu)}{a} ABw,_{xy} = 0 \qquad \text{A.10b}$$

APPENDIX B

ILLUSTRATIONS

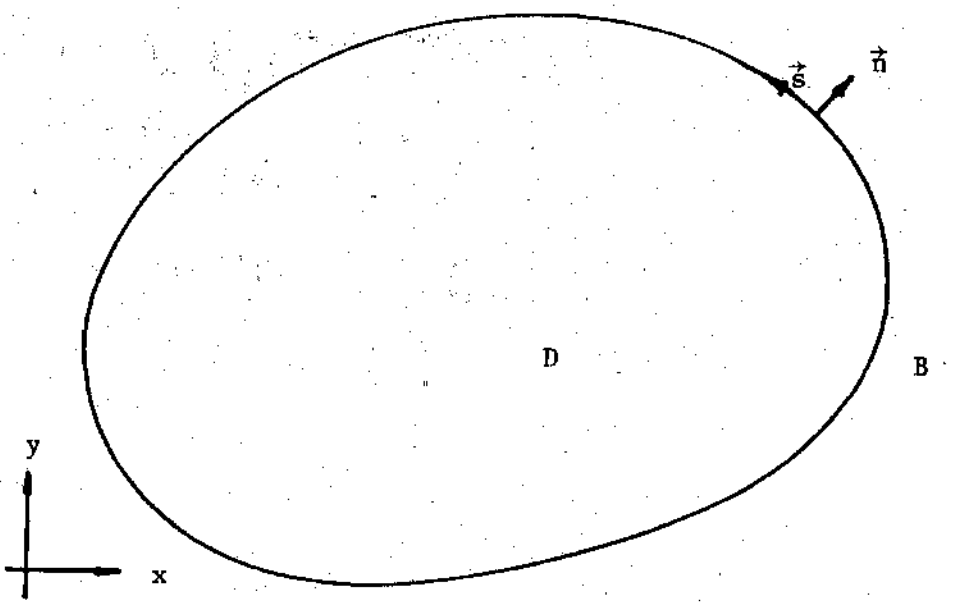

Fig. 2.1 Two Dimensional Domain of a Continuum

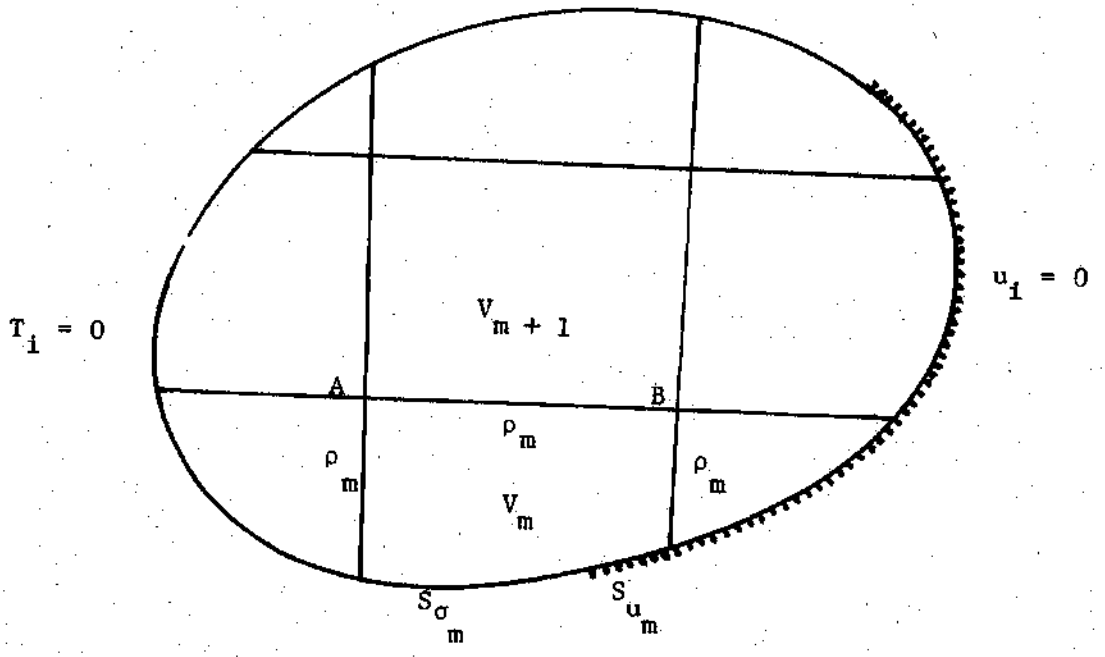

Fig. 2.2 Geometric Notations of a Finite Element Group

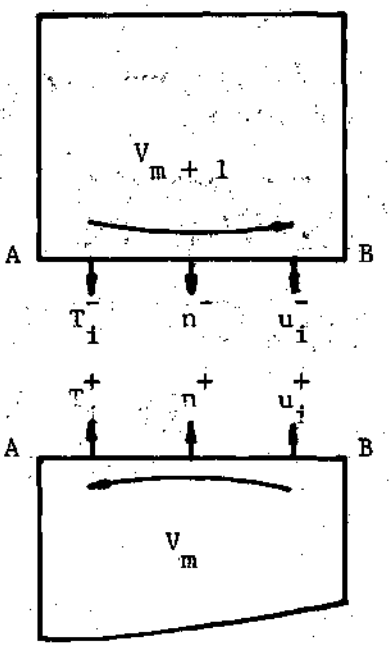

Fig. 2.3 Sign Convention for the Quantities on an Interelement Boundary between two Finite Elements

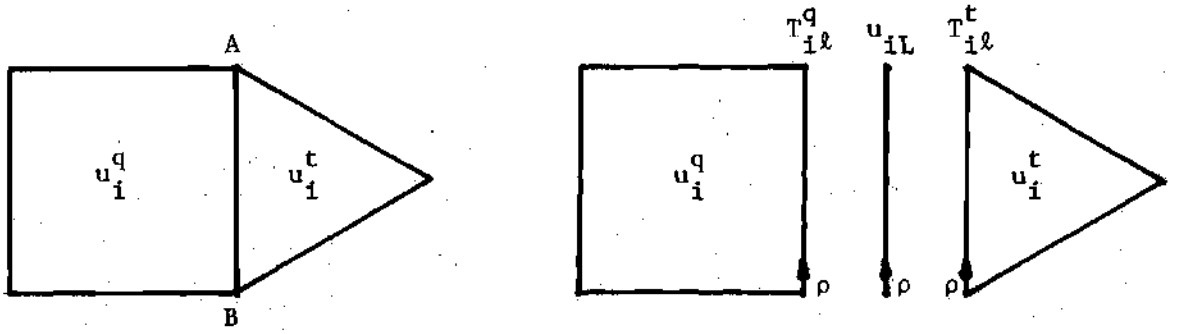

Fig. 2.4 Two Different Order Assumed Variables in a System; u_i^q are Cubic Functions and u_i^t are Linear Functions

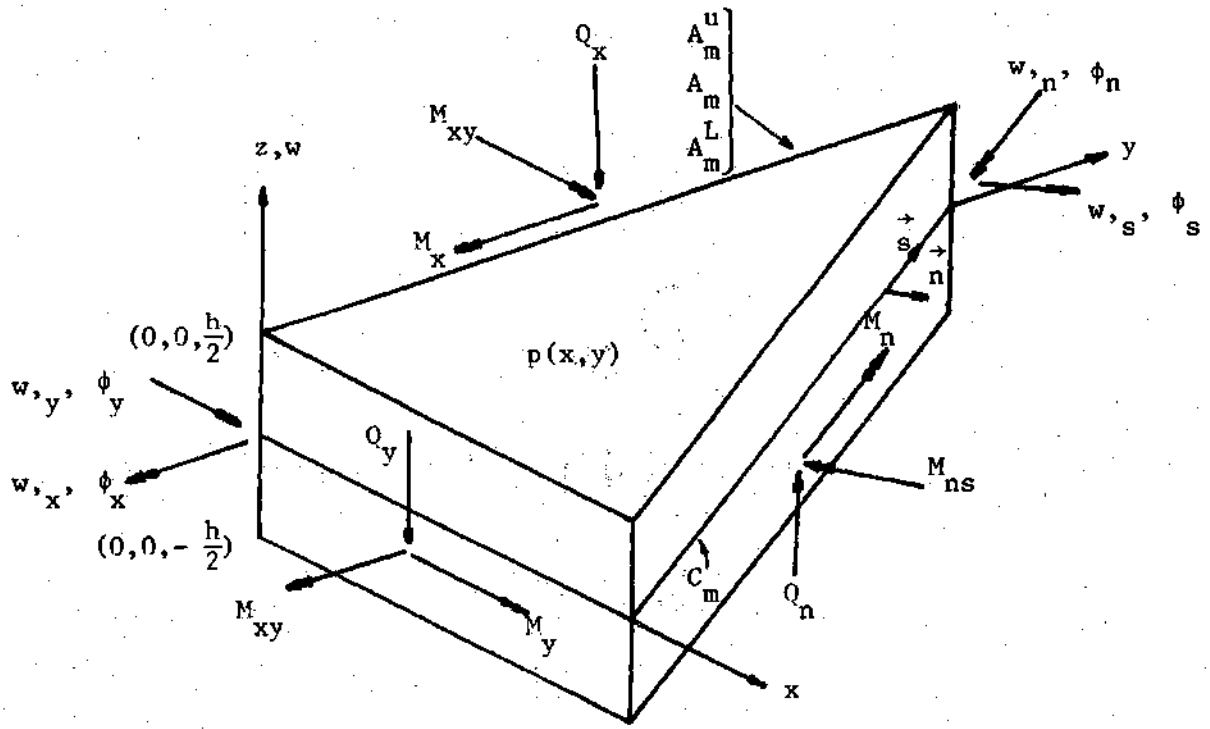

Fig. 3.1 Sign Convention for a Plate Element

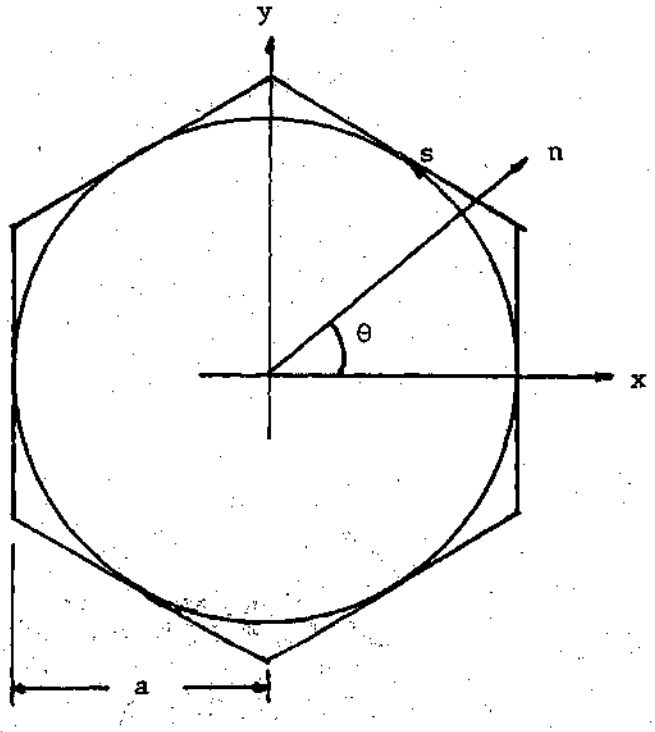

Fig. 4.1 Polygonal Approximation of a Circular Domain

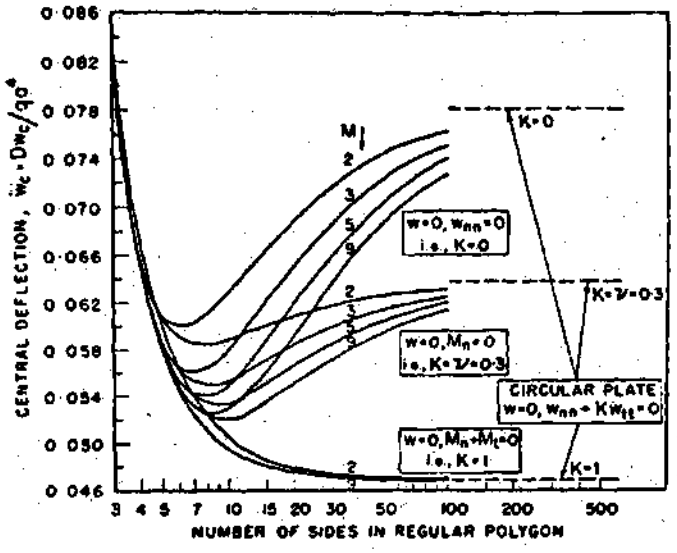

Fig. 4.2 Central Displacements of Regular Polygonal Plates with Various Boundary Conditions (from Ref. 57)

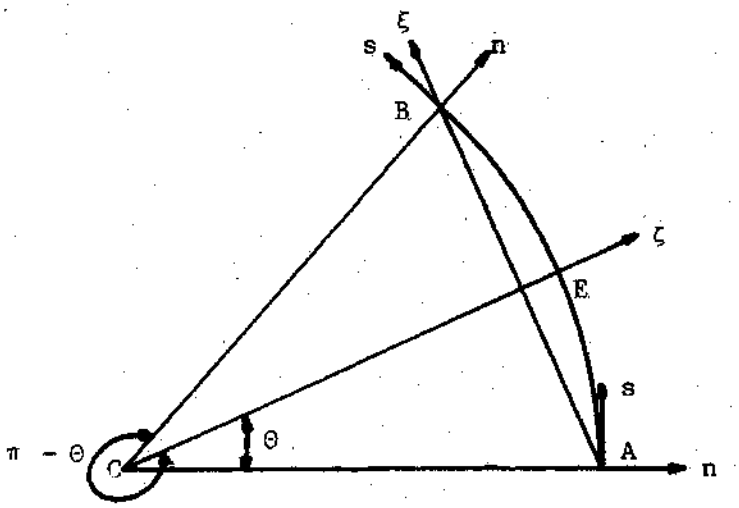

Fig. 4.3 Circular Boundary Coordinates at Boundary Nodes of a Triangular Element

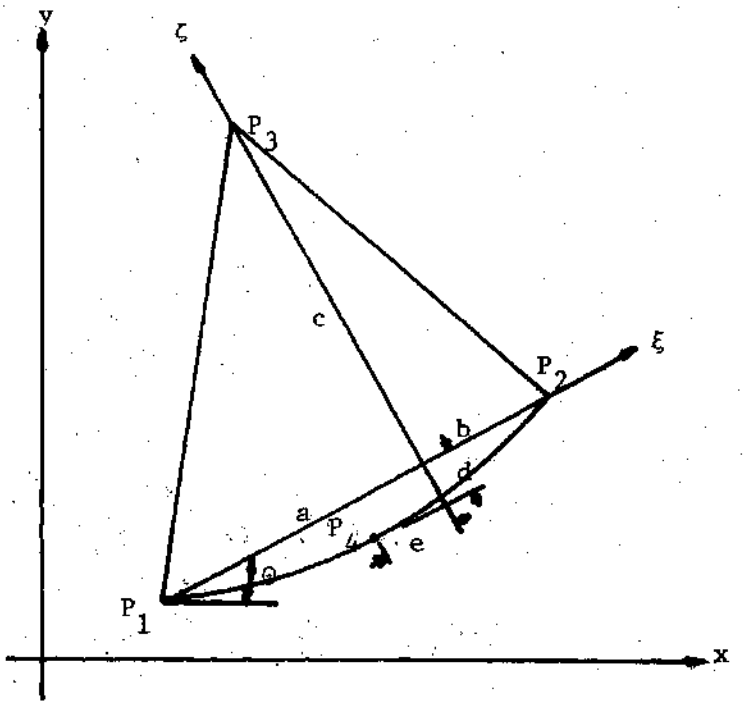

Fig. 4.4 Triangular Element with Curved Edge: Compatible Displacement Model

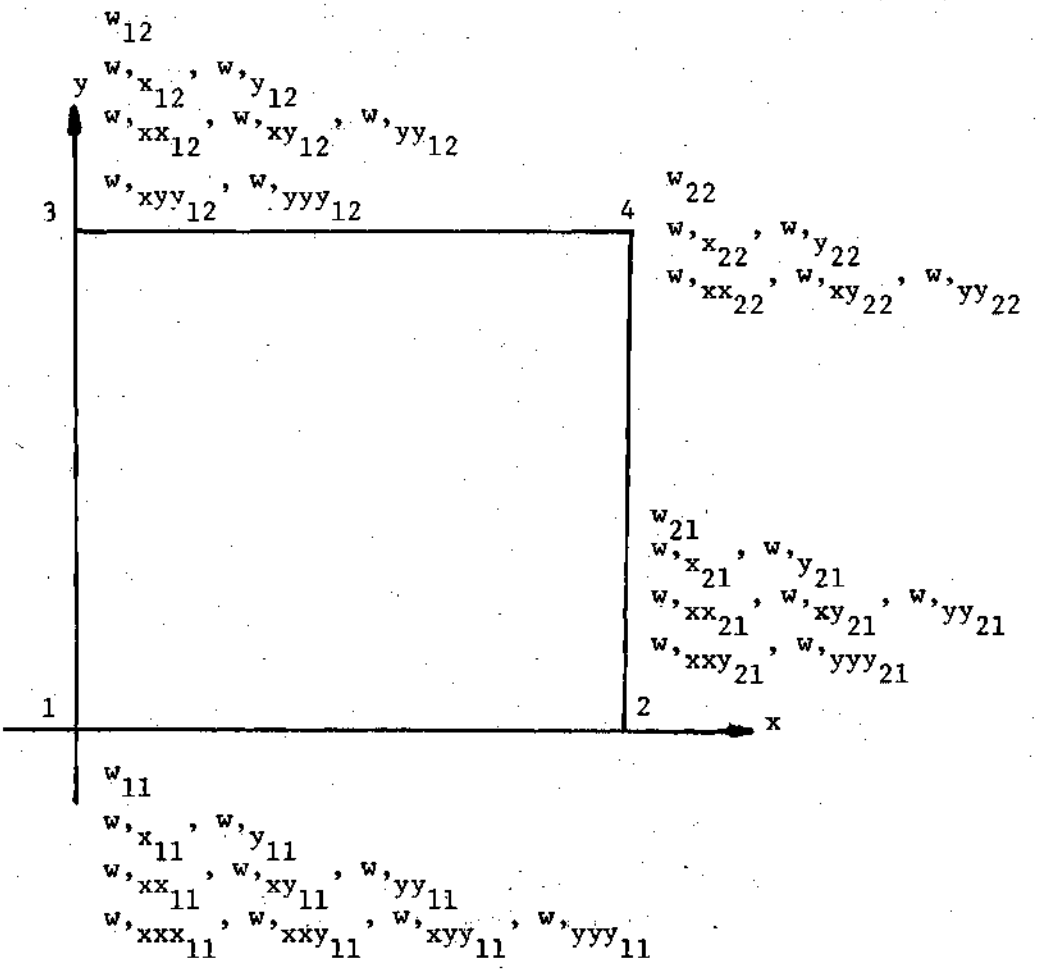

Fig. 4.5 Necessary Degrees of Freedom to enforce
$V_y = M_y = 0$ along Boundary 1-2 and
$V_x = M_x = 0$ along Boundary 1-3

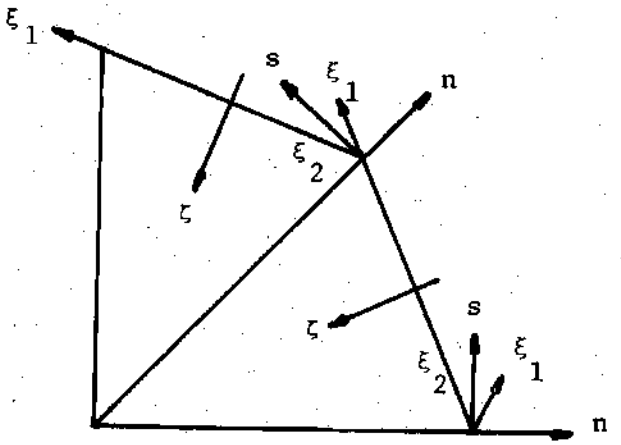

Fig. 4.6 Local Circular Boundary Coordinates at Corners of a Polygonal Plate

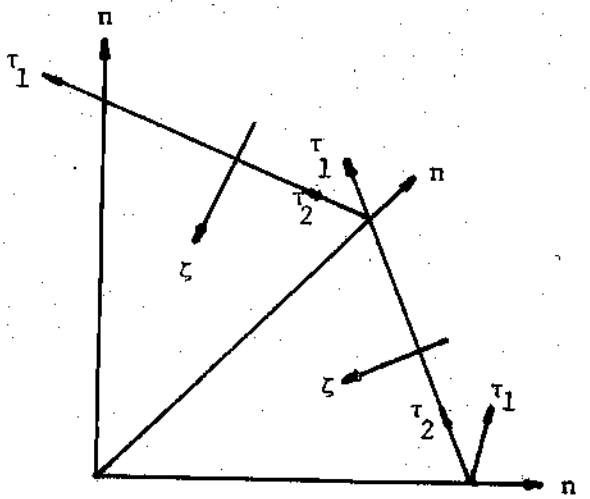

Fig. 4.7 Local Oblique Boundary Coordinates at Corners of a Polygonal Plate

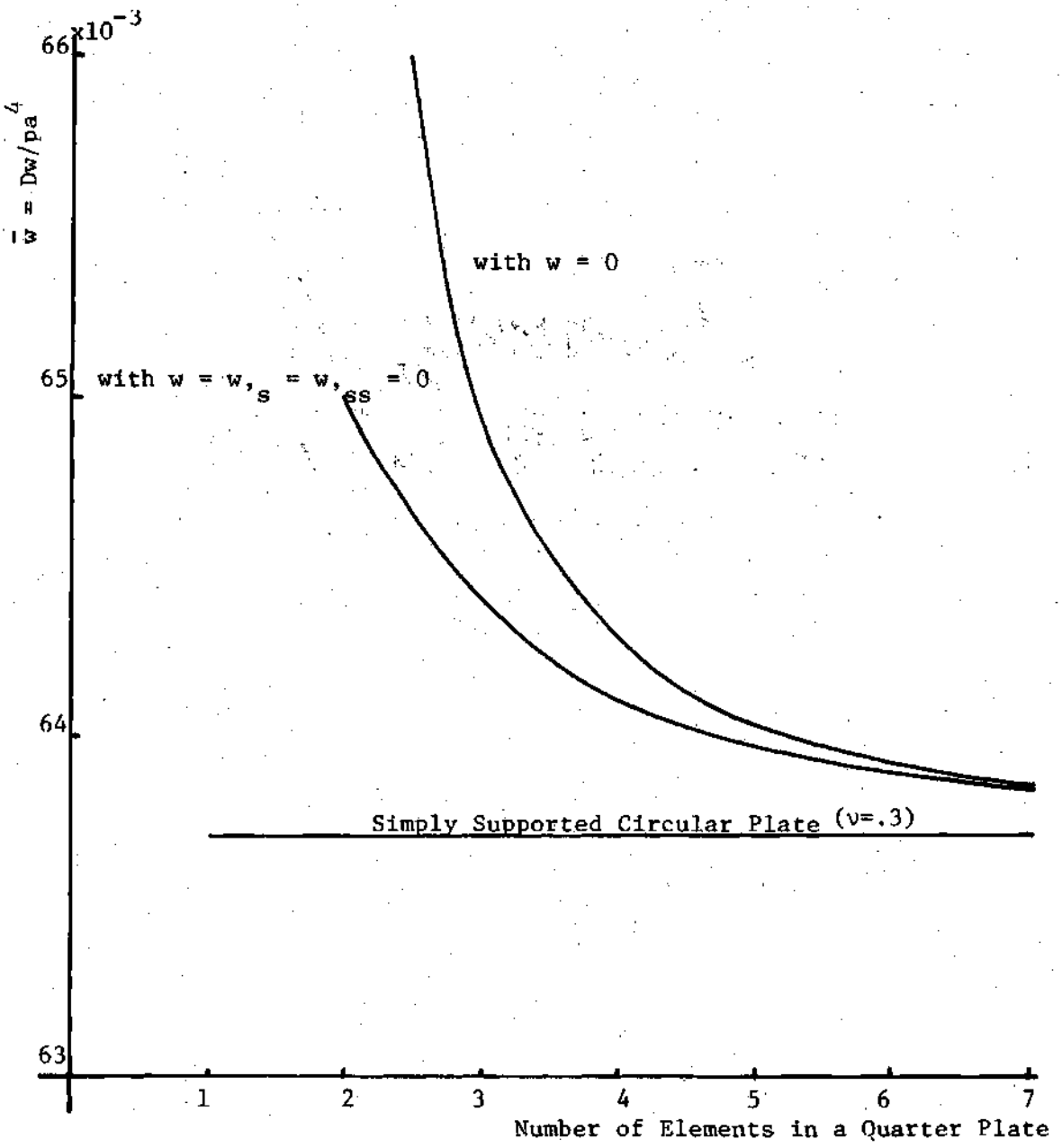

Fig. 4.8 Central Displacement of Simply Supported Circular Plate with Uniform Load p: with Two Different Geometric Boundary Conditions: Compatible Displacement Model

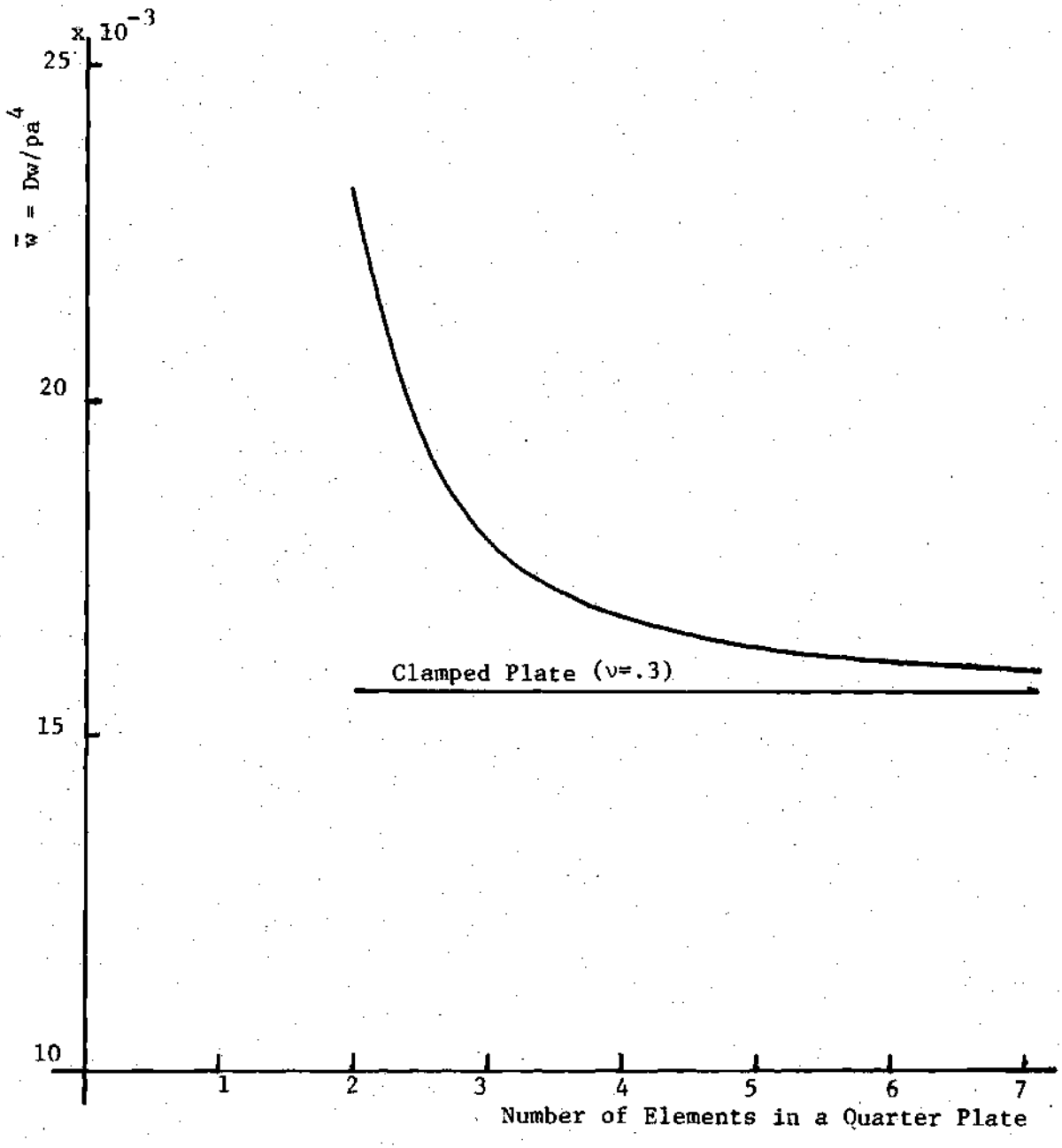

Fig. 4.9 Central Displacement of Simply Supported Circular Plate with Uniform Load p: with $w = w_{,n} = w_{,s} = w_{,ns} = 0$ and $\cos^2\theta w_{,ss} + \sin^2\theta w_{,nn} = 0$ as Geometric Boundary Conditions: Compatible Displacement Model

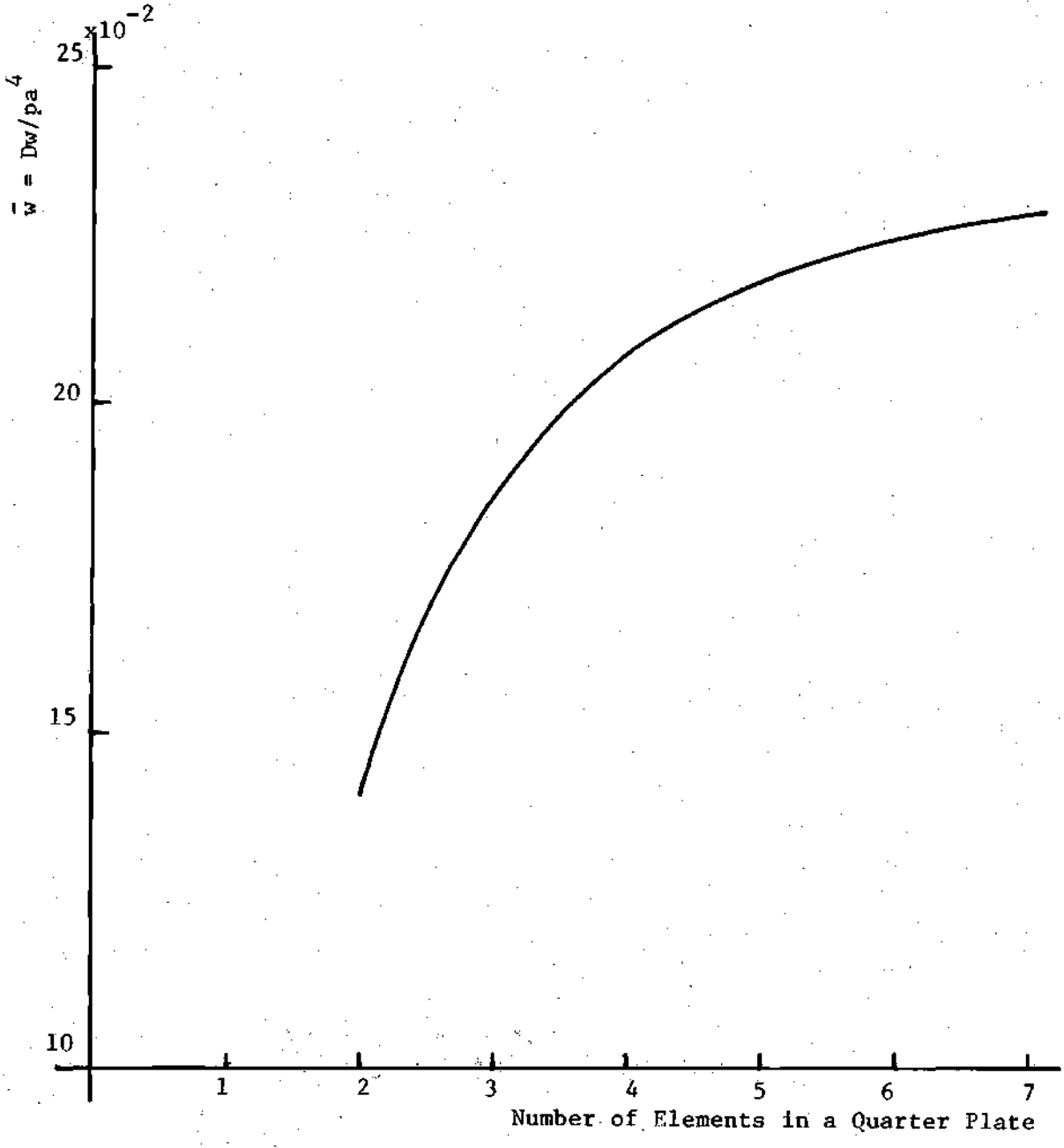

Fig. 3.10 Central Displacement of a Simply Supported Plate with Uniform Load p: with $w = w_{,\tau_1} = w_{,\tau_2} = w_{,\tau_1\tau_1} = w_{,\tau_2\tau_2} = 0$ as Geometric Boundary Conditions: Compatible Displacement Model

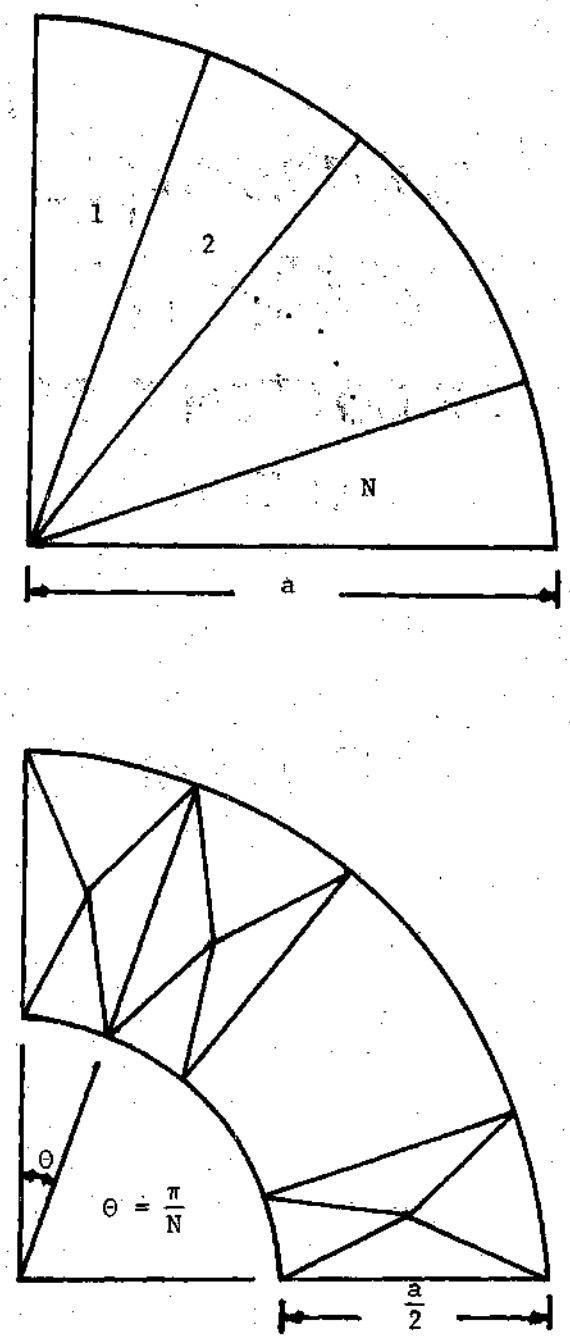

Fig. 4.11 Finite Element Grids of Circular and Annular Plates: Compatible Displacement Model

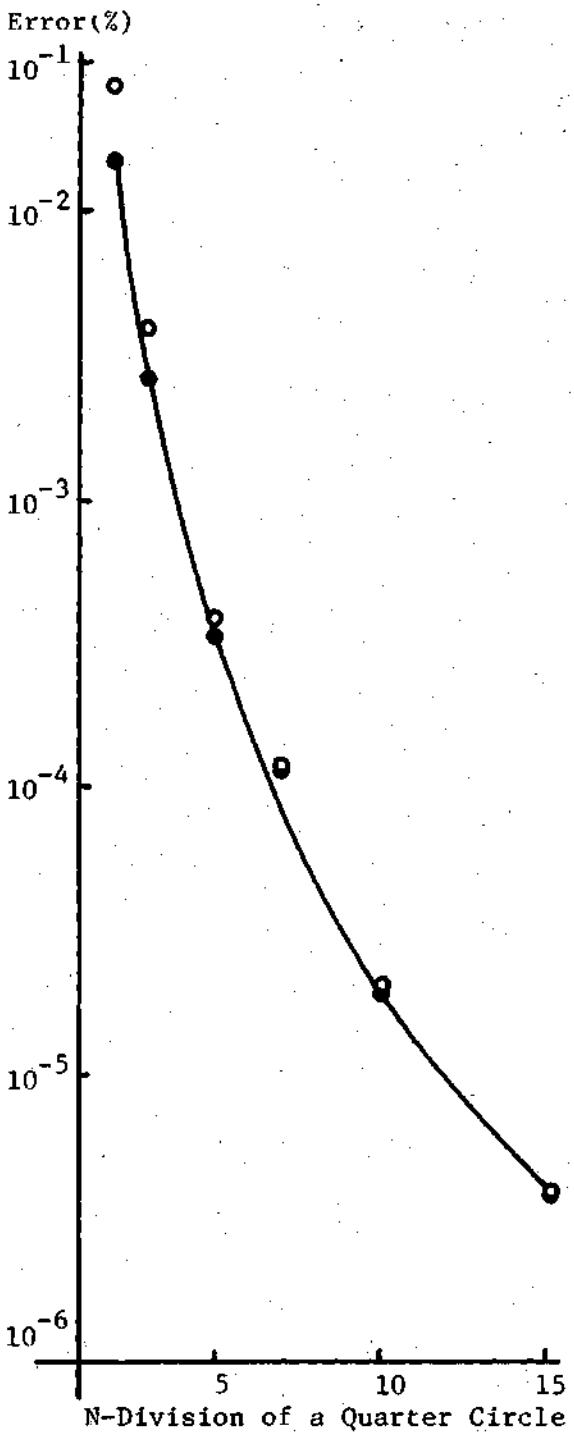

Fig. 4.12 Central Displacement

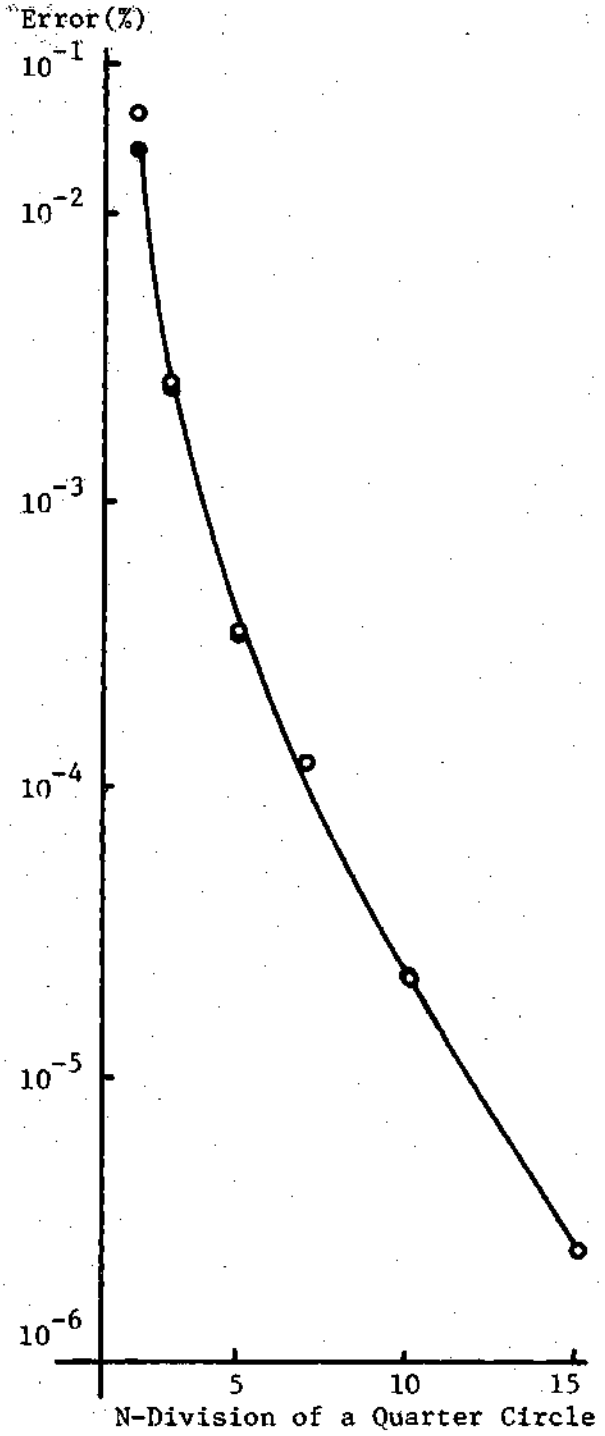

Fig. 4.13 Strain Energy

Simply Supported Circular Plate with Uniform Load:
Compatible Displacement Model

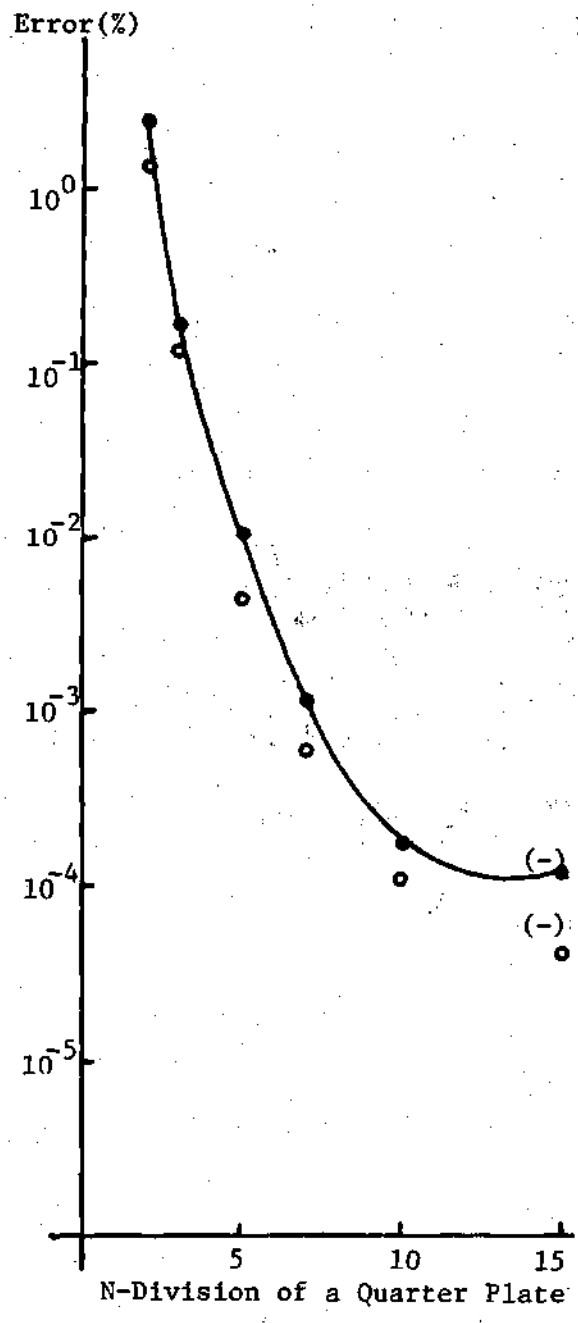

Fig. 4.14 Central Bending Moment

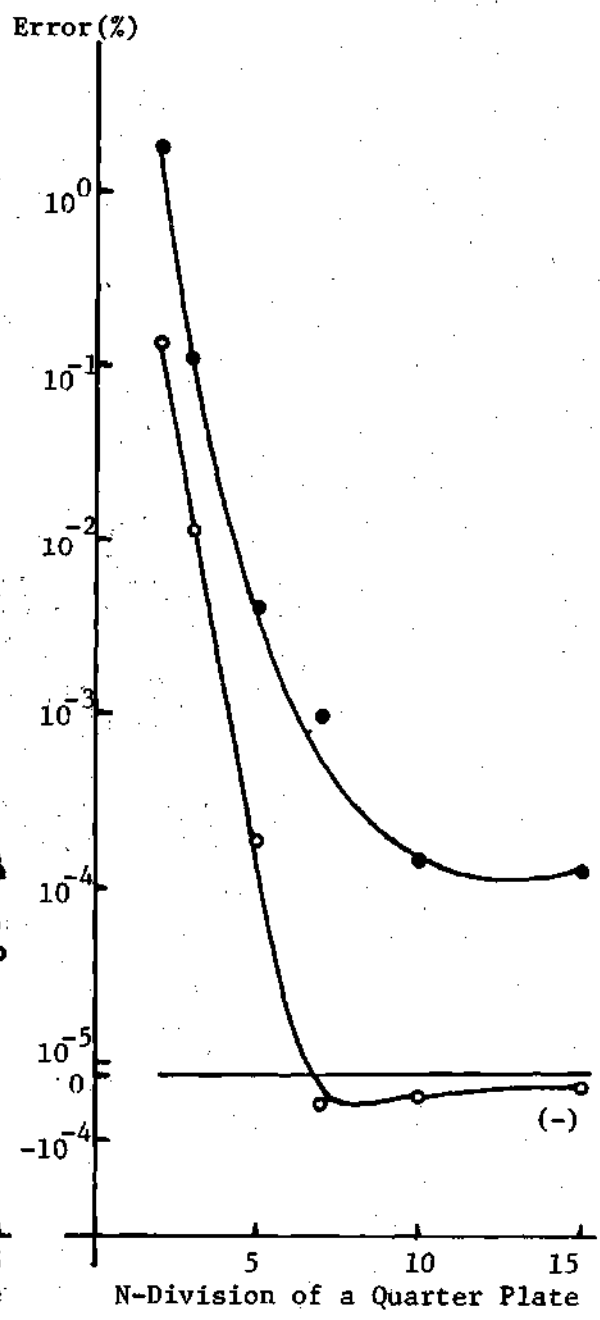

Fig. 4.15 Edge Tangential Moment

Simply Supported Circular Plate with Uniform Load: Compatible Displacement Model

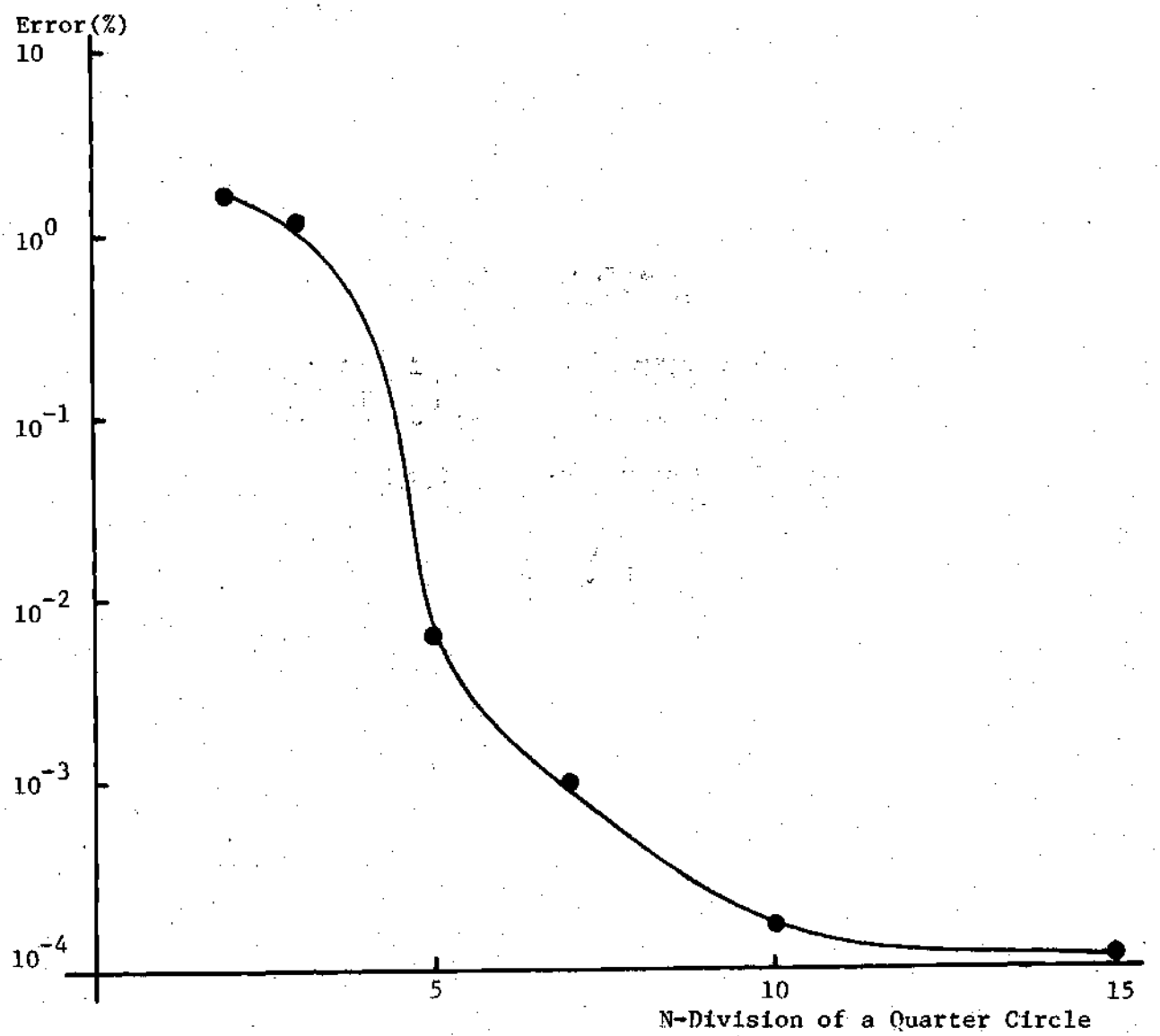

Fig. 4.16 Edge Radial Moment x 100/Exact Central Bending Moment of Simply Supported Circular Plate with Uniform Load: Compatible Displacement Model

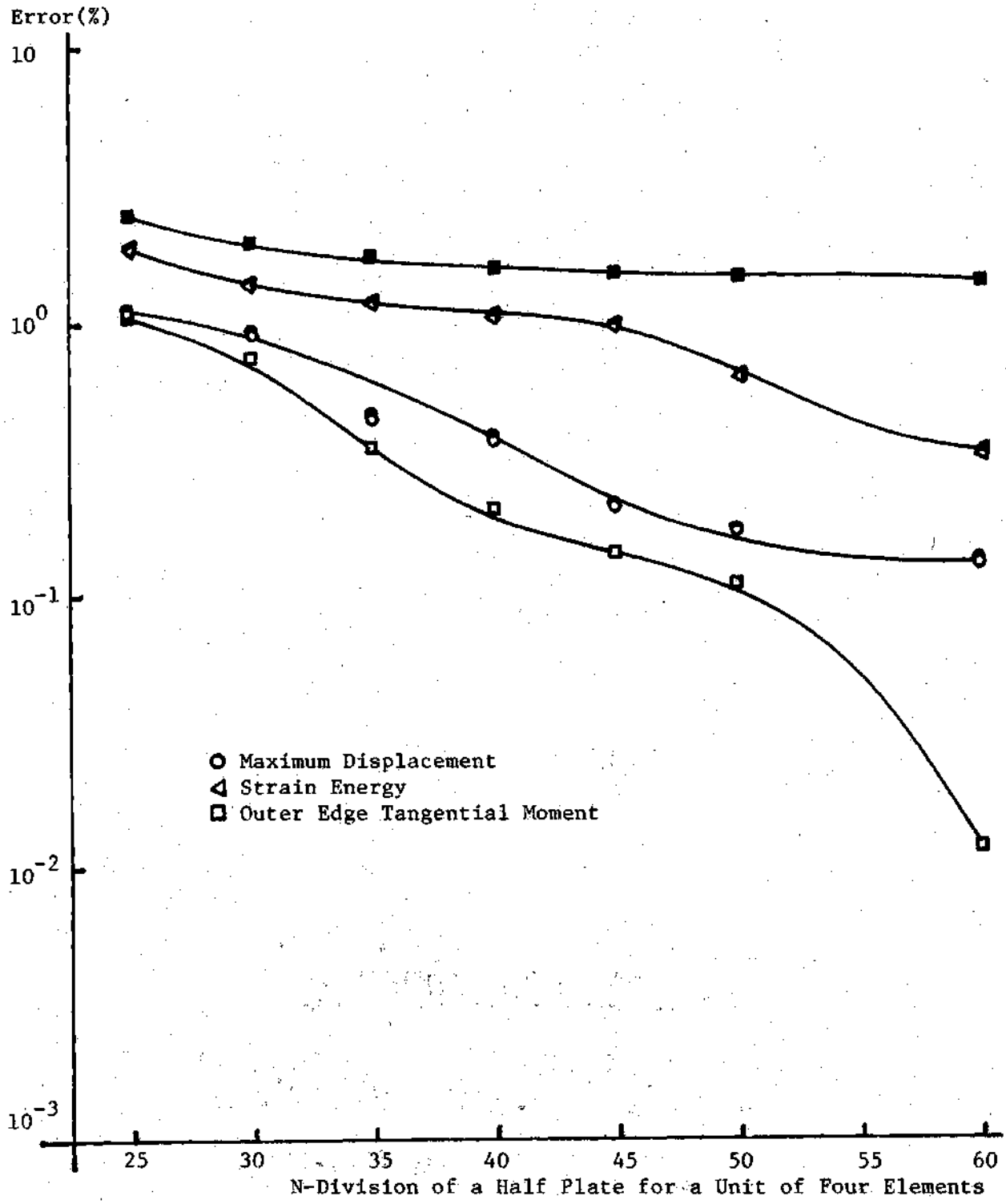

Fig. 4.17 Uniformly Loaded Annular Plate with Simply Supported Outer Edge: Compatible Displacement Model

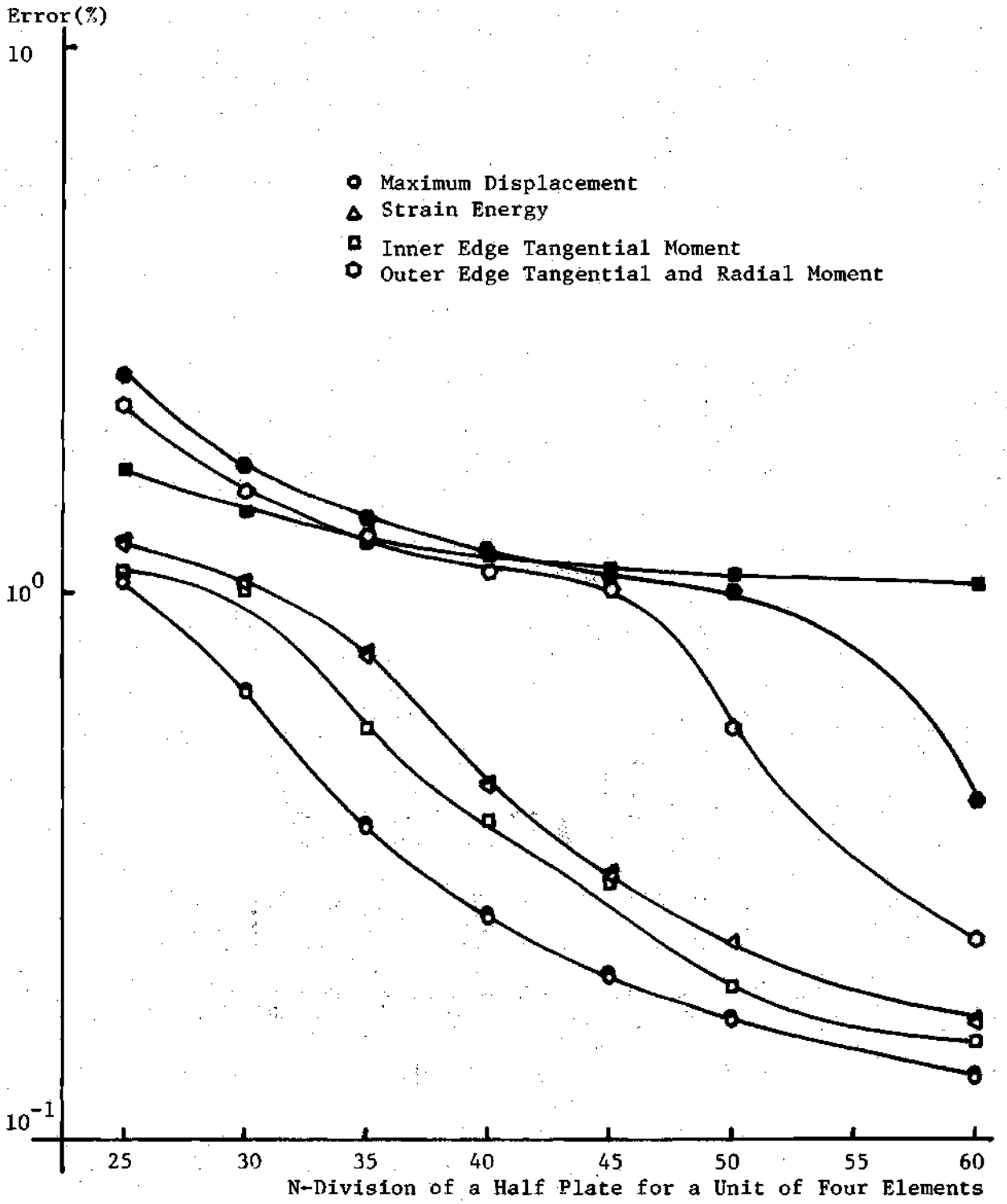

Fig. 4.18 Uniformly Loaded Annular Plate with Clamped Outer Edge: Compatible Displacement Model

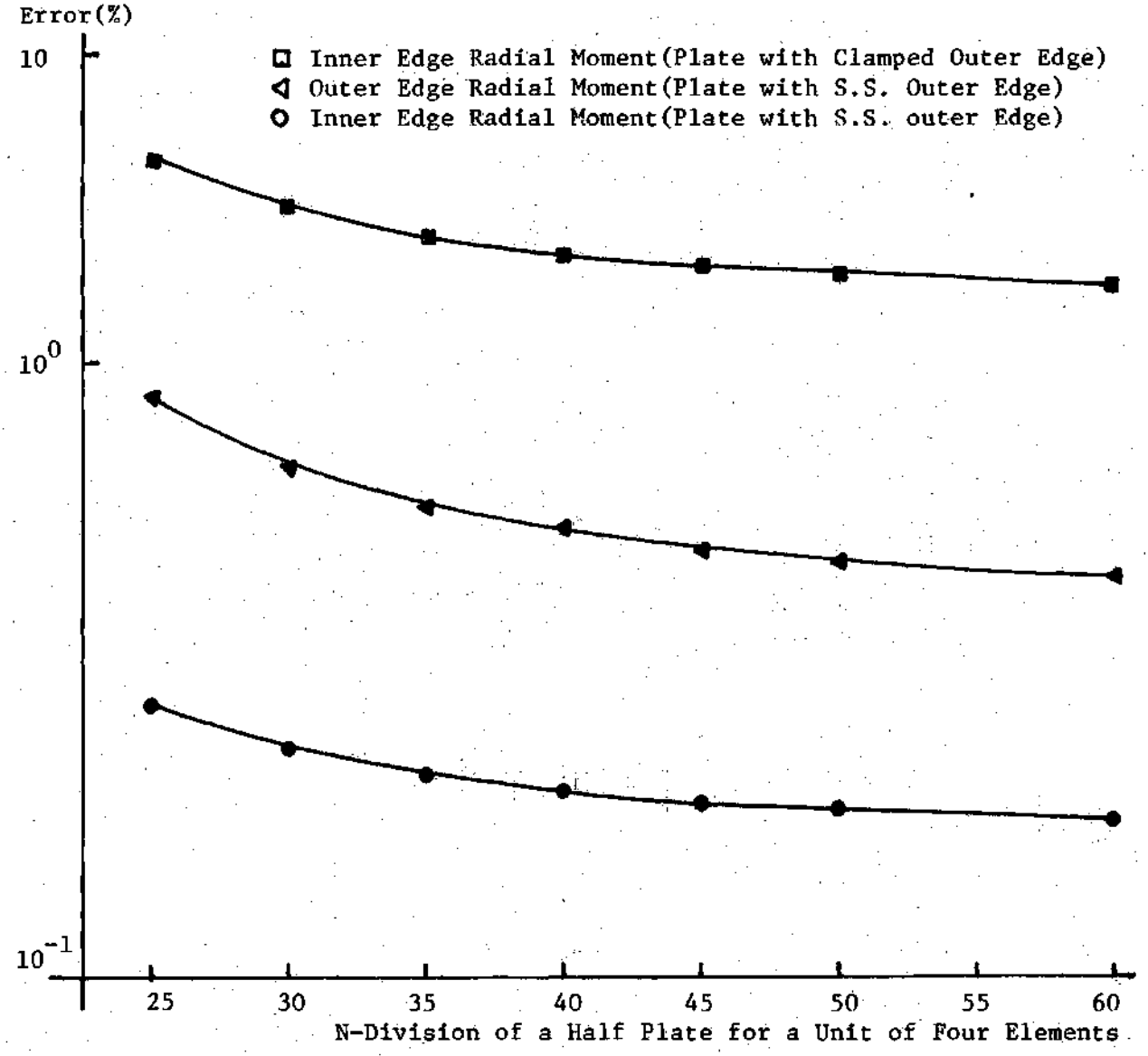

Fig. 4.19 Edge Radial Moment x 100/Exact Edge Tangential Moment of Annular Plates with Uniform Load: Compatible Displacement Model

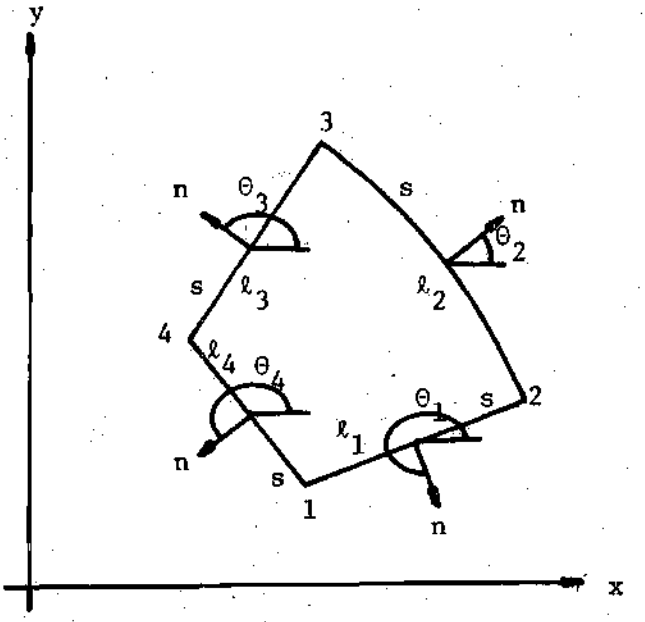

Fig. 4.20 Geometric Notations of an Element for Hybrid Stress Model

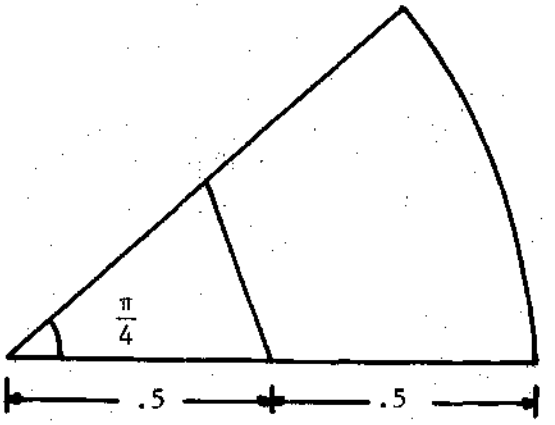

Fig. 4.21 A Triangular and a General Quadrilateral Element

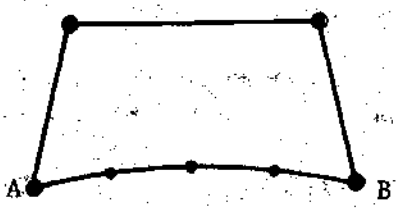

Fig. 4.22 Point Matching of Boundary Tractions along Arbitrarily Curved Boundary AB

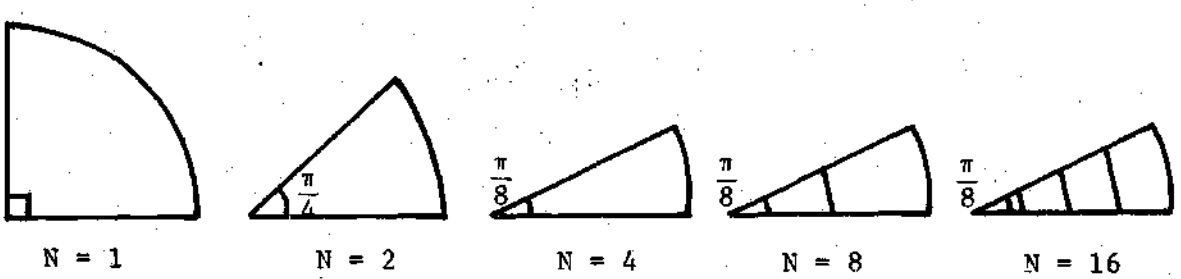

Fig. 4.23 Finte Element Grids for a Circular Plate: Hybrid Stress Model

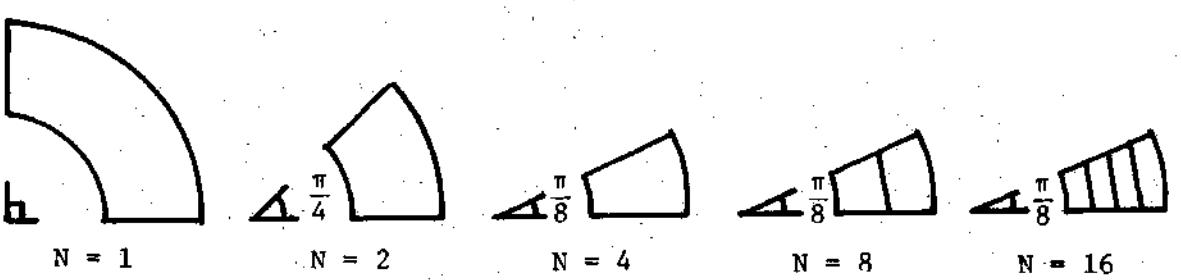

Fig. 4.24 Finite Element Grids for an Annular Plate: Hybrid Stress Model

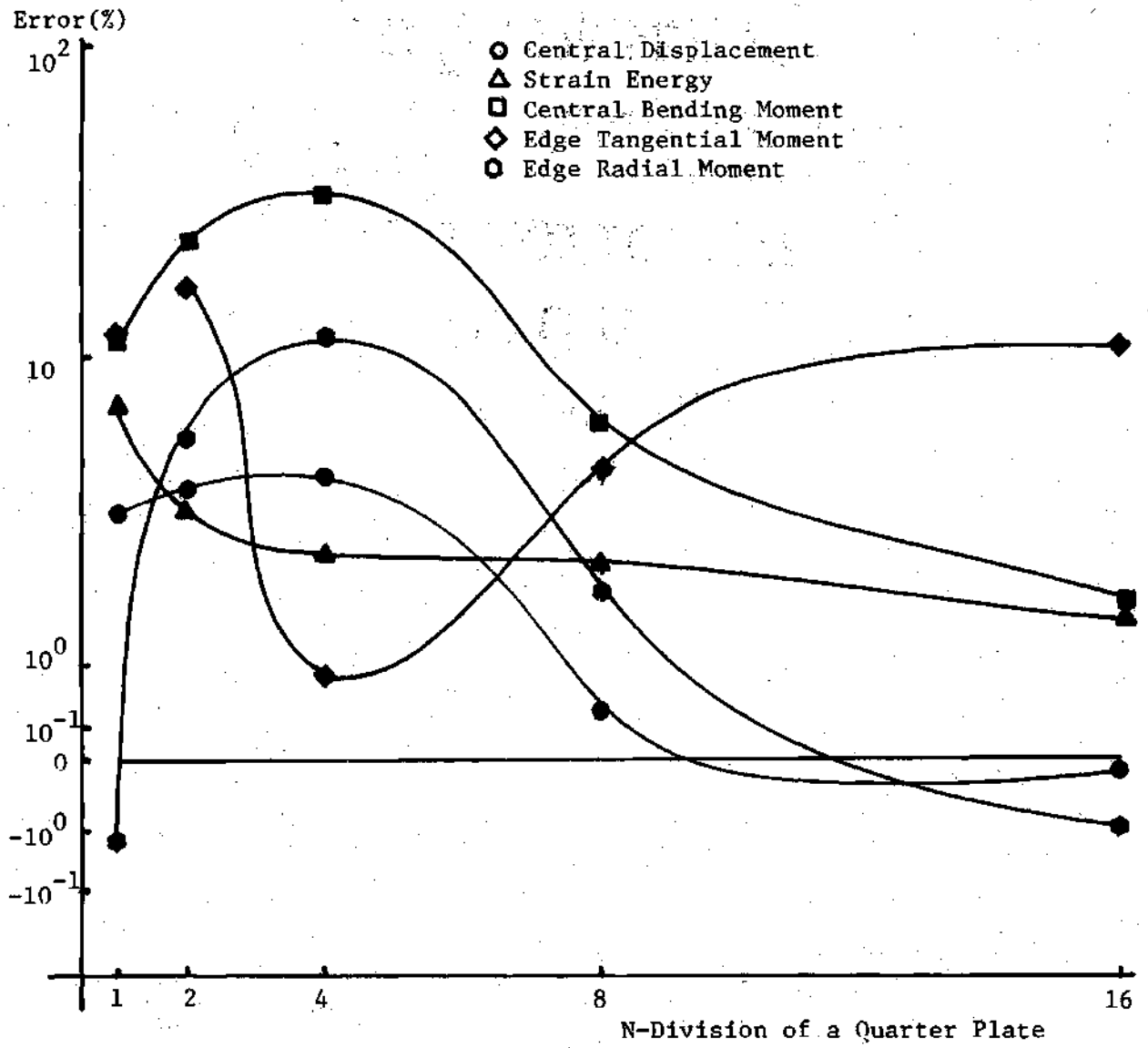

Fig. 4.25 Clamped Circular Plate with Uniform Load: Hybrid Stress Model

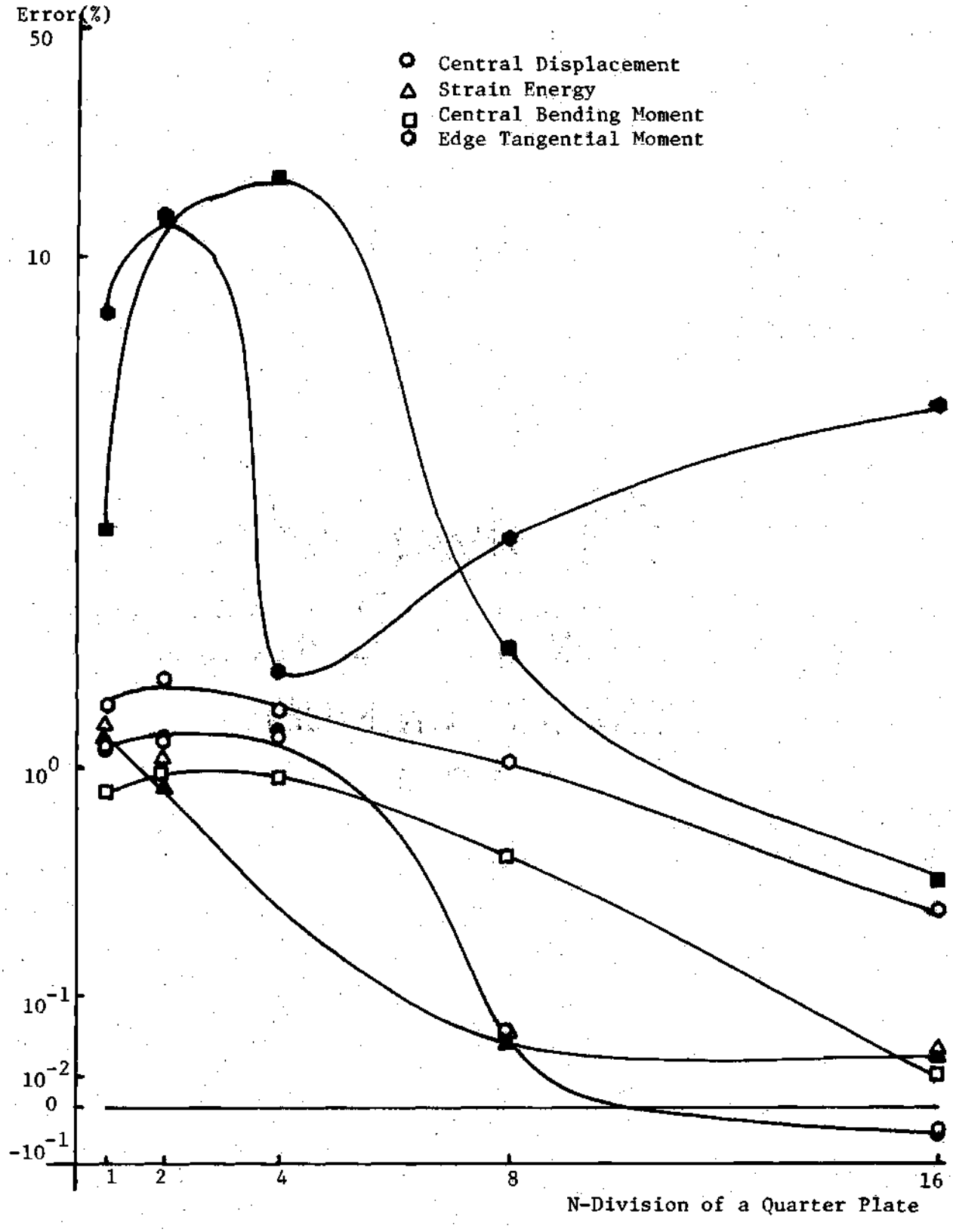

Fig. 4.26 Simply Supported Circular Plate with Uniform Load: Hybrid Stress Model

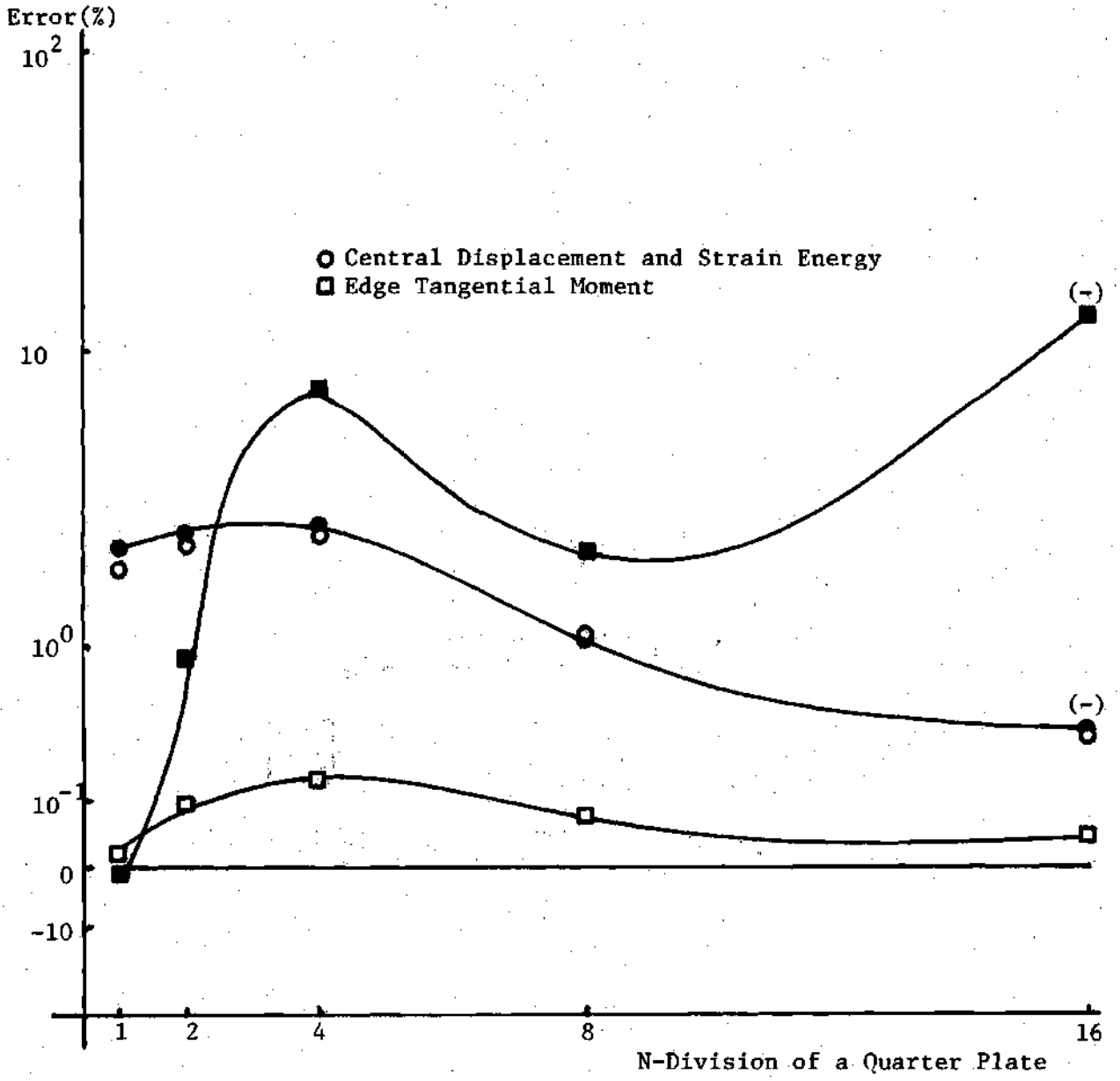

Fig. 4.27 Simply Supported Circular Plate with Point Load: Hybrid Stress Model

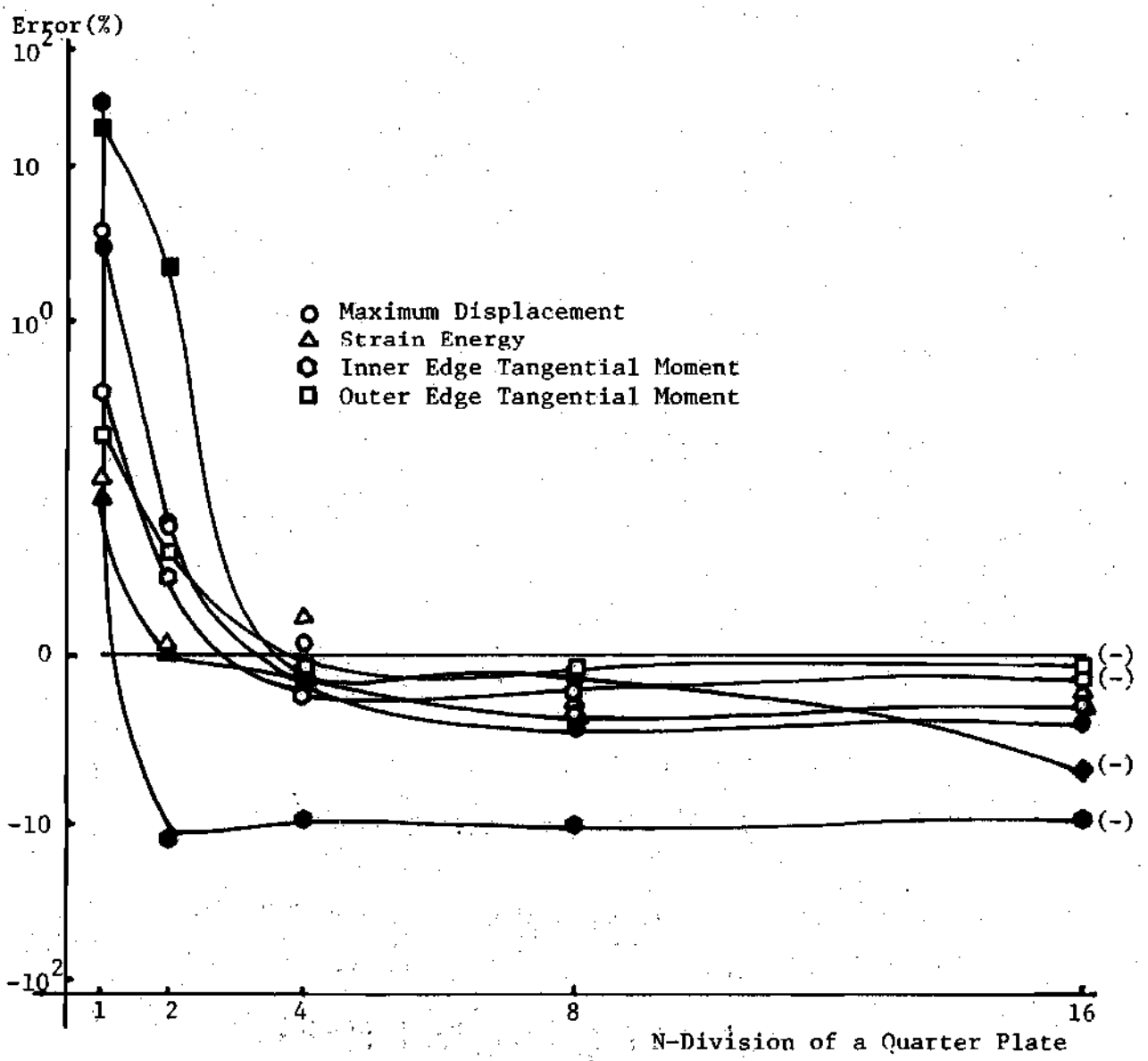

Fig. 4.28 Uniformly Loaded Annular Plate with Simply Supported Outer Edge: Hybrid Stress Model

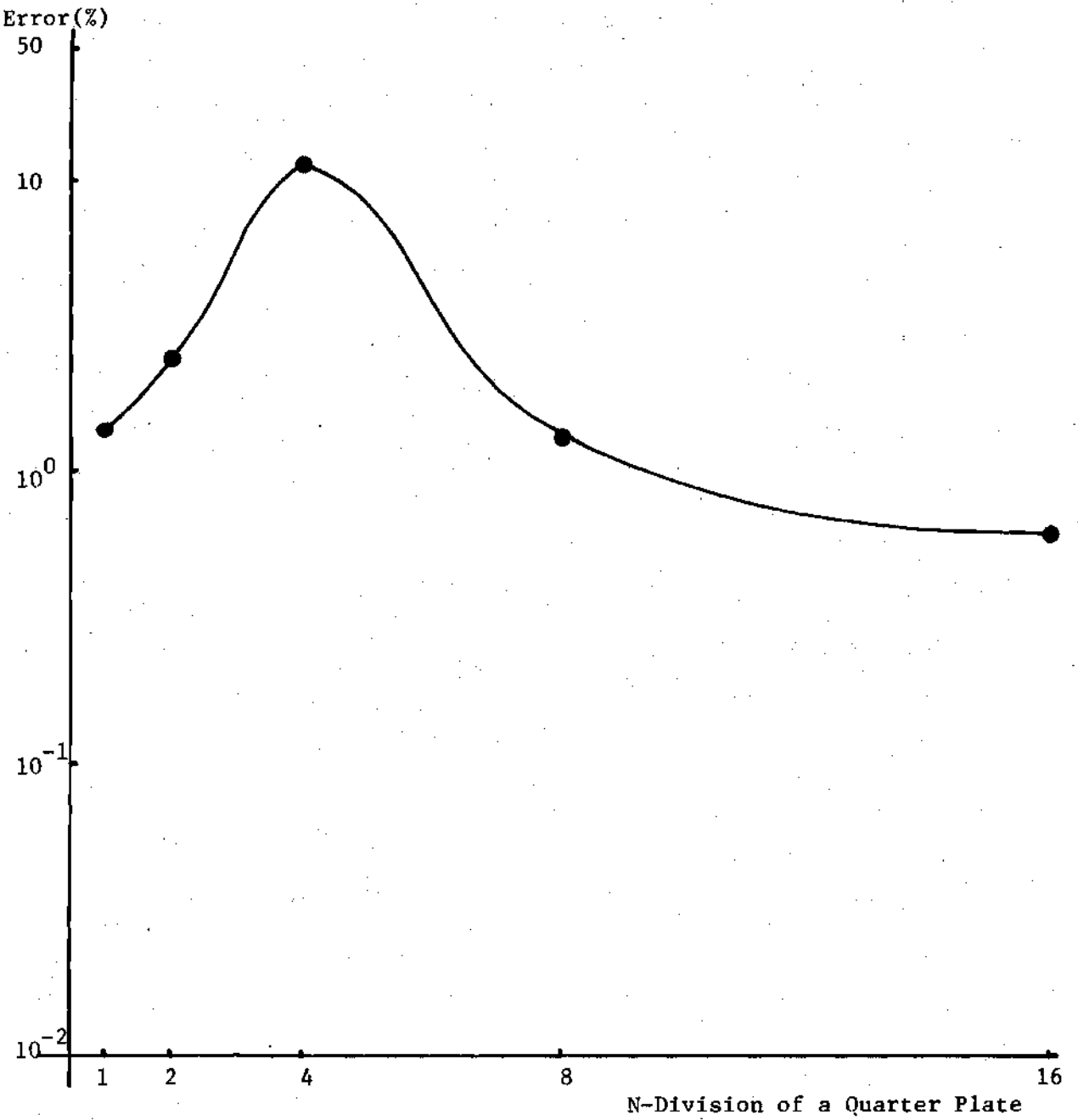

Fig. 4.29 Edge Radial Moment x 100/Exact Central Bending Moment of Simply Supported Circular Plate with Uniform Load: Hybrid Stress Model

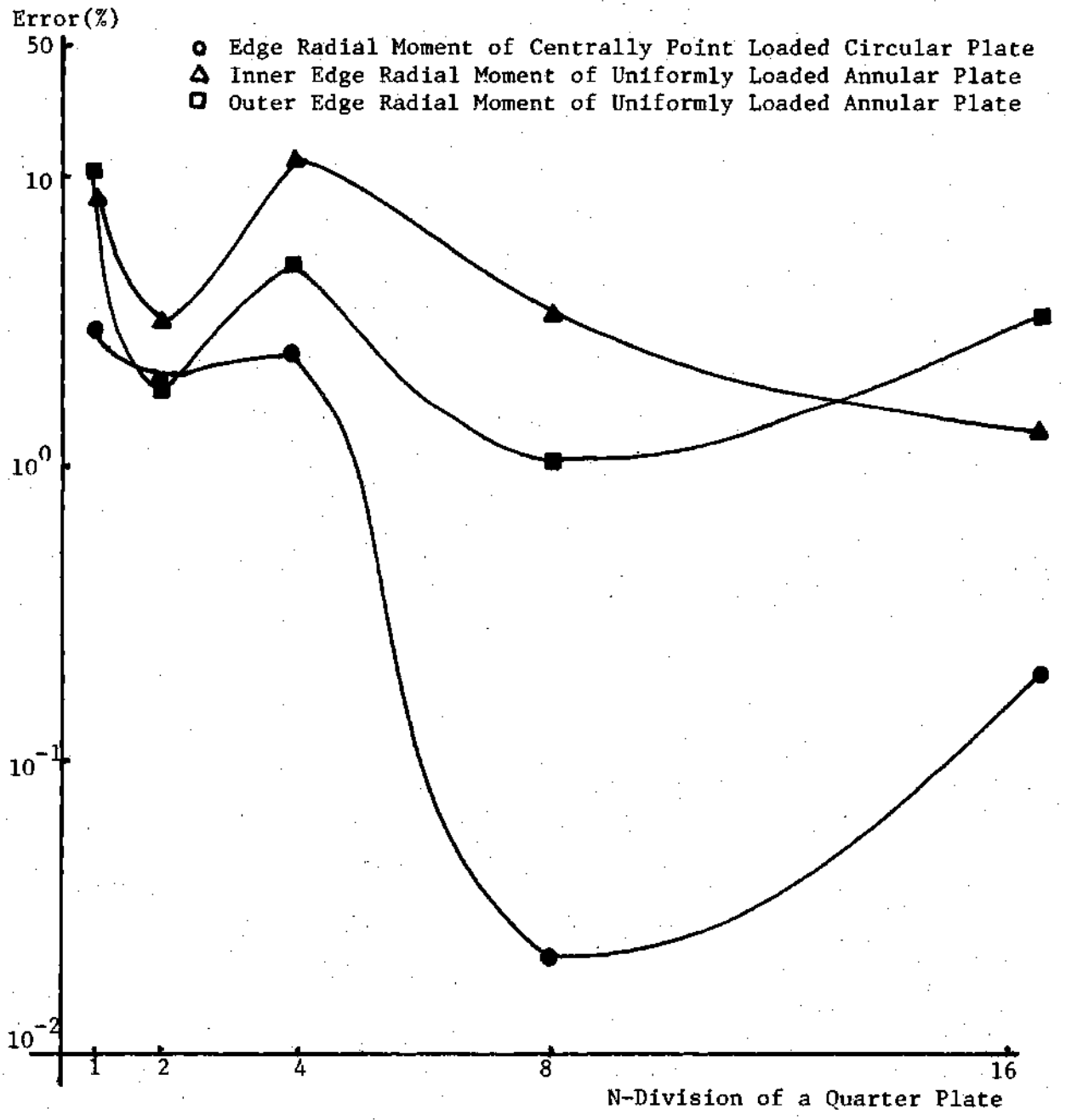

Fig. 4.30 Radial Moment x 100/Exact Edge Tangential Moment of a Circular and an Annular Plate with Simply Supported Outer Edge: Hybrid Stress Model

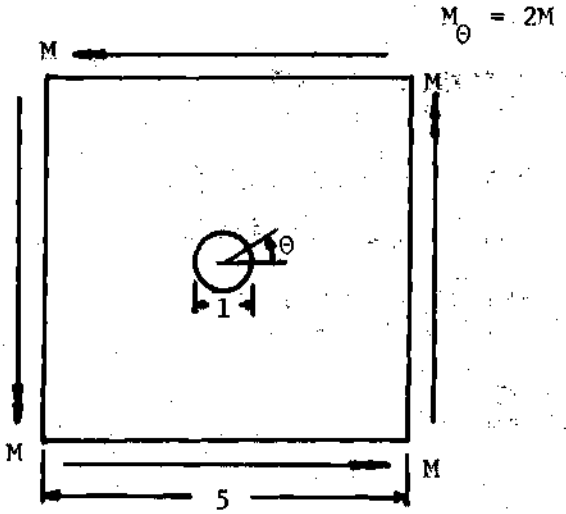

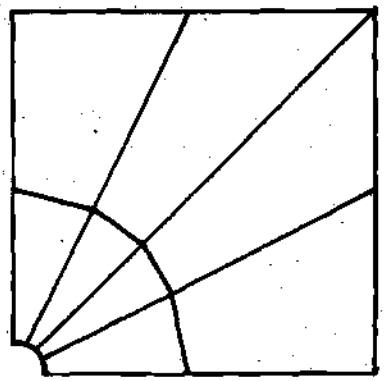

Mesh (nxm)	Number of DOF	Strain Energy (UD/M)	Max. Displ. (wD/M)	Inner Radial Moment/M	Inner Tangl. Moment/M
Exact				0	2.000
2 x 3	20	.191 (.193)	.205 (.206)	.290 (.000)	1.896 (1.502)
2 x 5	34	.191 (.191)	.204 (.204)	.145 (.000)	2.023 (1.883)
4 x 3	38	.191 (.191)	.204 (.205)	.457 (.000)	2.011 (1.758)
4 x 5	64	.191 (.191)	.205 (.205)	.106 (.000)	2.053 (2.001)
8 x 9	223	.191 (.191)	.205 (.205)	.024 (.000)	2.068 (2.061)

Numbers in ( ) are the results with explicitly enforcing $M_n = V_n = 0$ along the circular hole

Fig. 4.31 Stress Concentration around a Circular Hole

$$M_\Theta = M\left[\, 2 - \frac{4(1+\nu)\{1 + 2\cos(4\Theta)\}}{(3+\nu)\{5 + 4\cos(4\Theta)\}} \,\right]$$

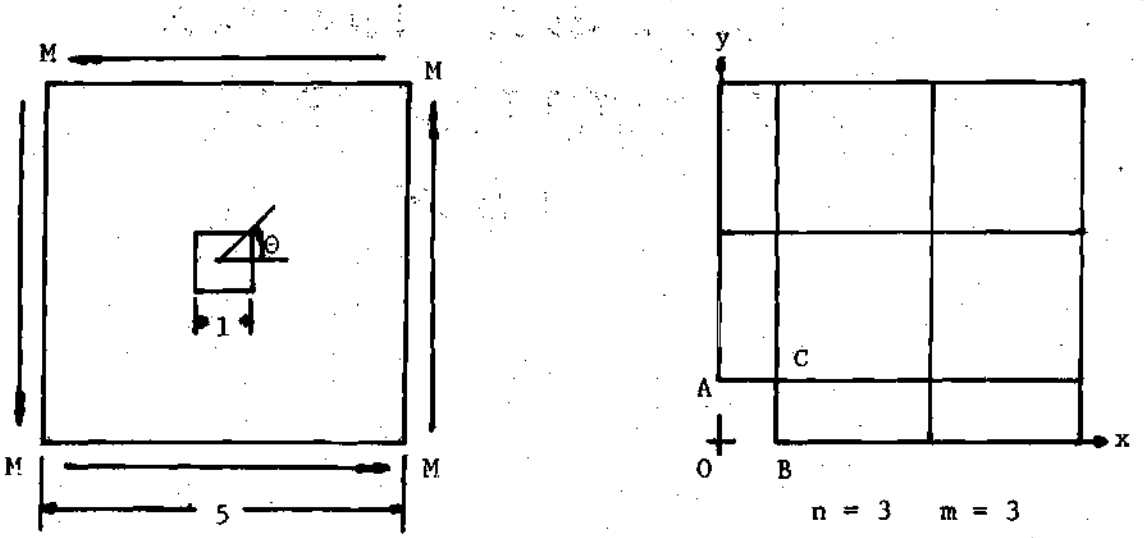

Mesh (nxm)	Number of DOF	Strain Energy (UD/M)	Displ. at A (wD/M)	Inner Tangl. Moment/M (Θ = 0)	Inner Tangl. Moment/M (Θ = π/4)
Exact				1.475	3.576
2 x 2	19	.191	.204	1.492	1.889
3 x 3	38	.194	.209	1.568	2.219
5 x 5	94	.195	.213	1.545	2.596
10 x 10	332	.197	.215	1.636	3.119

Fig. 4.32 Stress Concentration around a Rectangular Hole

$$M_\Theta = M\left[\ 2 - \frac{8(1+\nu)\{2 - 3\cos(3\theta)\}}{(3+\nu)\{13 - 12\cos(3\theta)\}}\ \right]$$

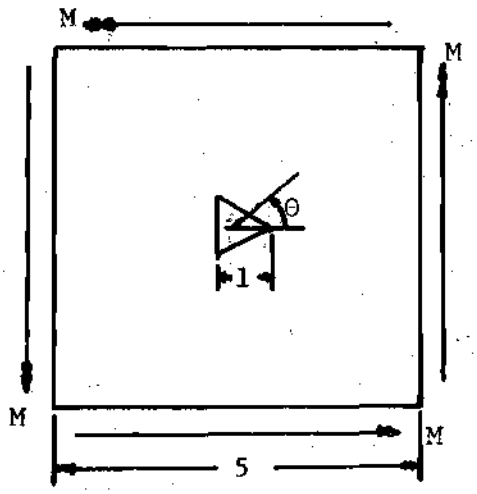

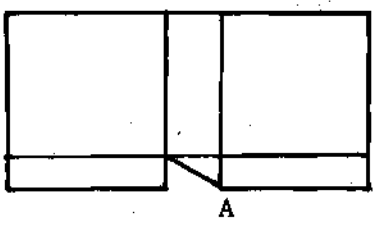

n = 3 m = 2

Mesh (nxm)	Number of DOF	Strain Energy (UD/M)	Displ. at A (wD/M)	Inner Tangl. Moment/M (θ = 0)	Inner Tangl. Moment/M (θ = π)
Exact				5.152	1.370
3 x 2	30	.175	.176	5.477	.957
5 x 3	64	.176	.177	5.288	1.039
9 x 5	166	.176	.180	5.204	1.137

Fig. 4.33 Stress Cocentration around a Triangular Hole

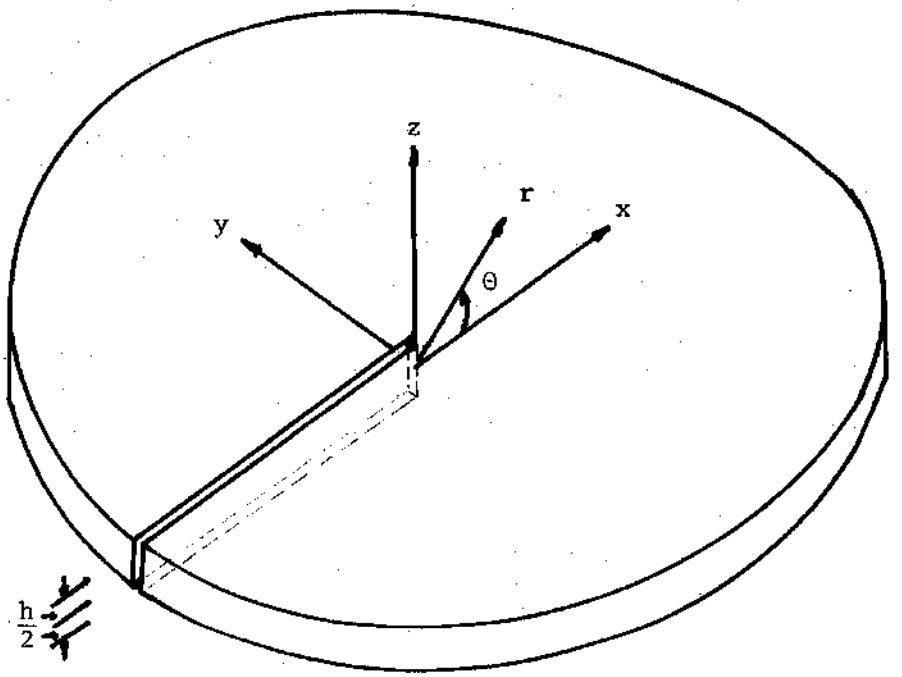

Fig. 5.1 An Infinite Plate with a Through-the-Thickness Semi-Infinite Crack

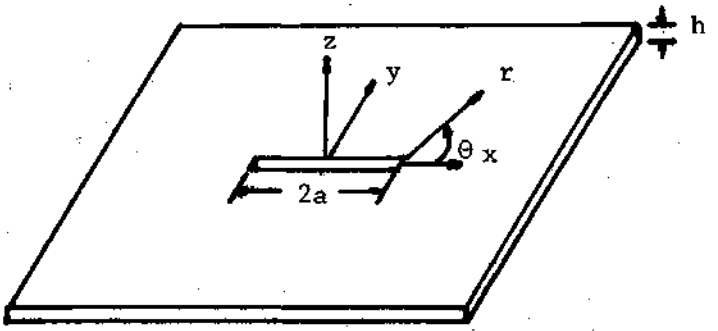

Fig. 5.2 A Flate Plate with a Through-the -Thickness Finite Crack

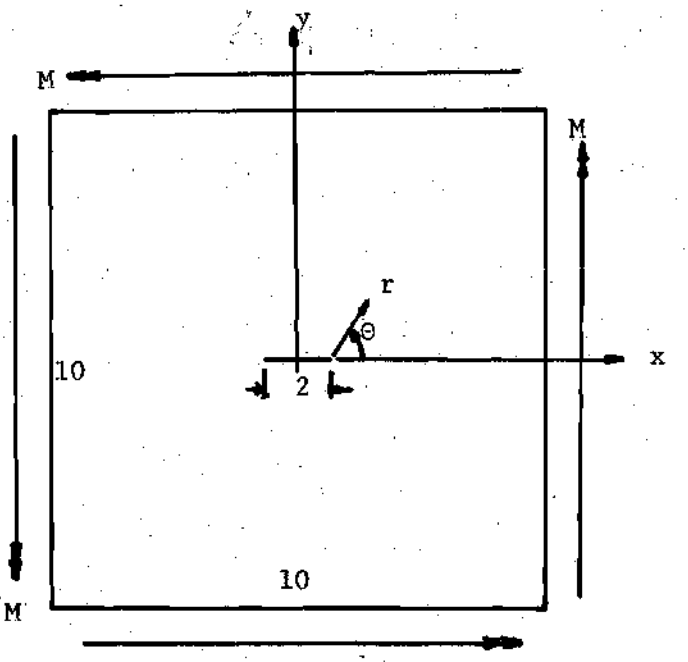

Fig. 5.3 A Plate with Through-the-Thickness Crack under Symmetric Bending Moments

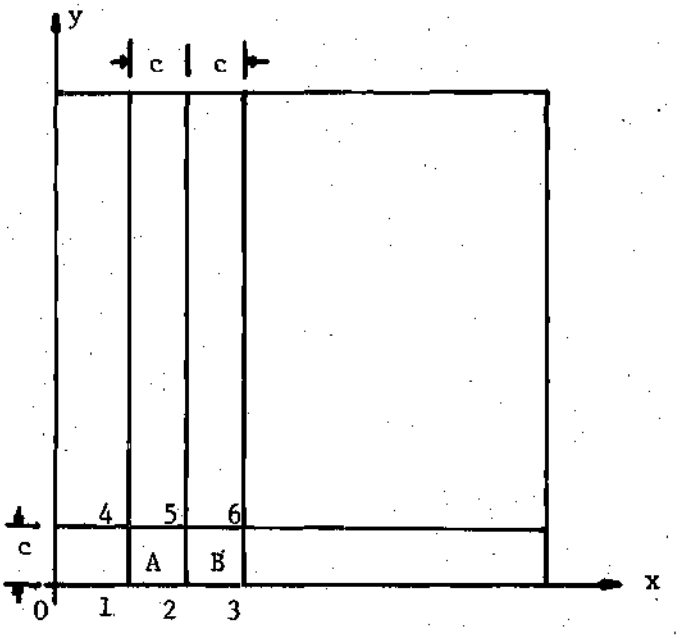

Fig. 5.4 A Finite Element Grid of a Quarter Plate

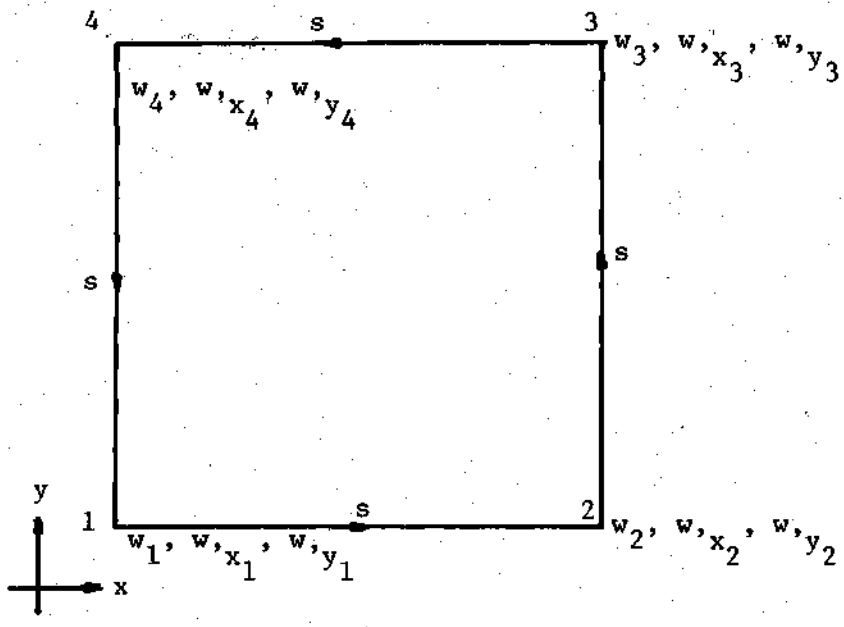

Fig. 5.5 A Regular Finite Element

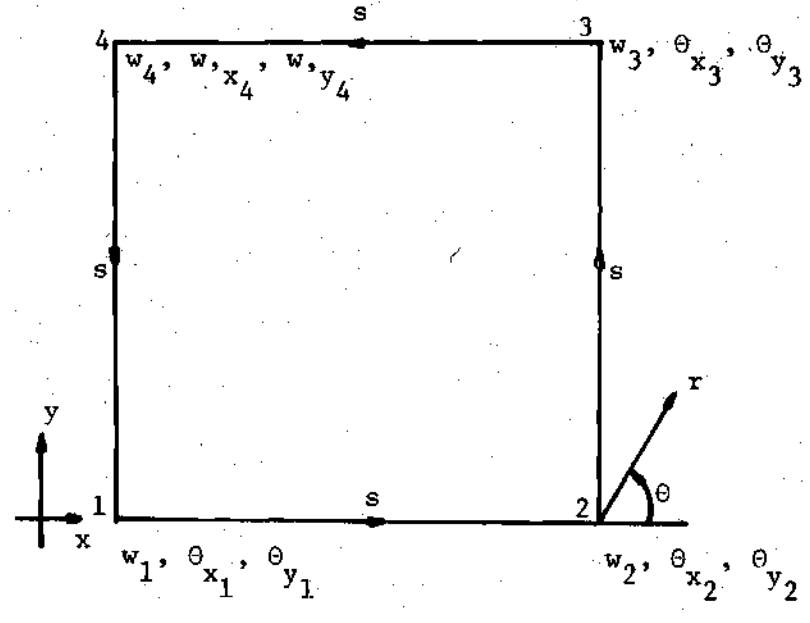

Fig. 5.6 A Singular Element: Type "A"

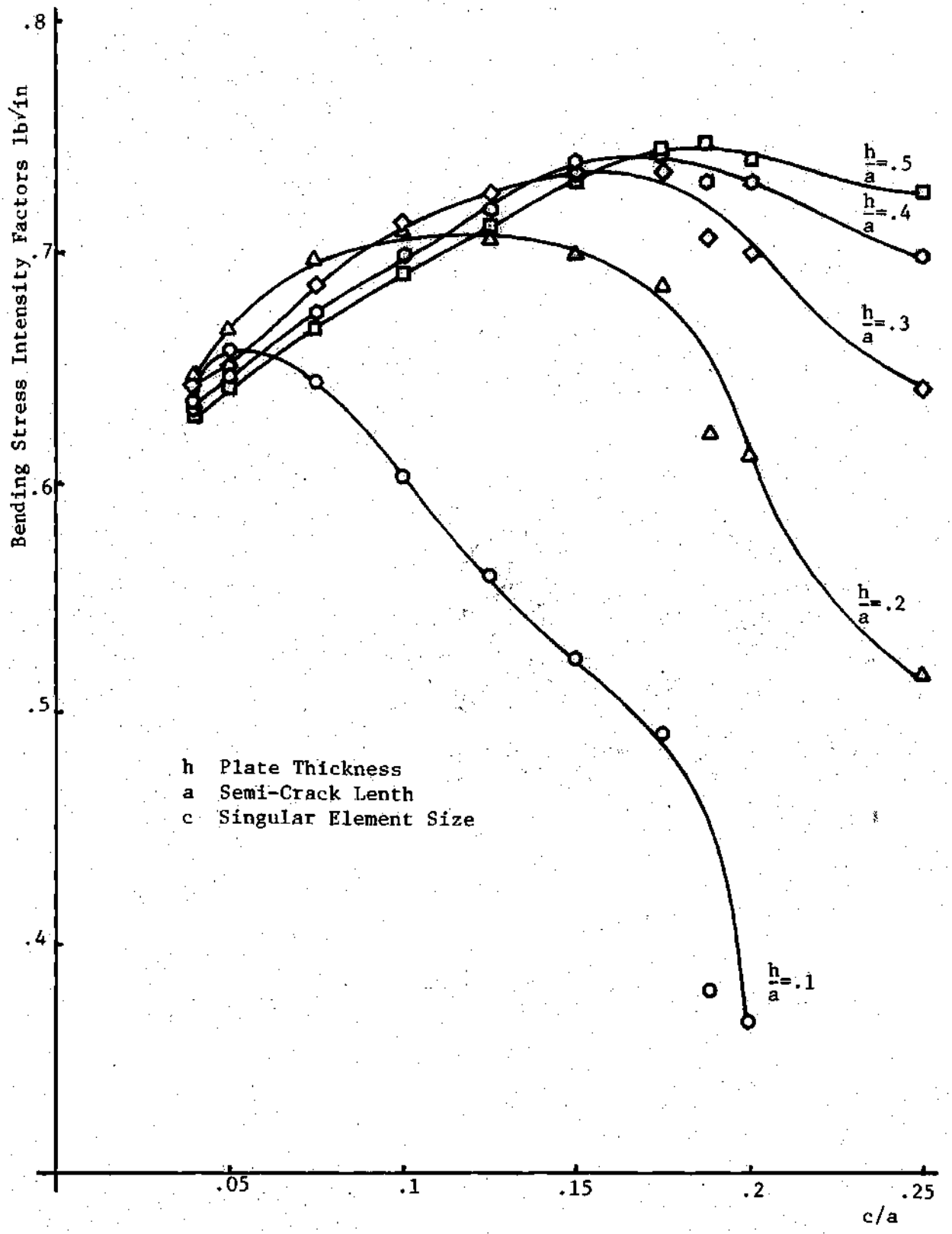

Fig. 5.7 Stress Intensity Factors with Variations of Thickness and Singular Element Size

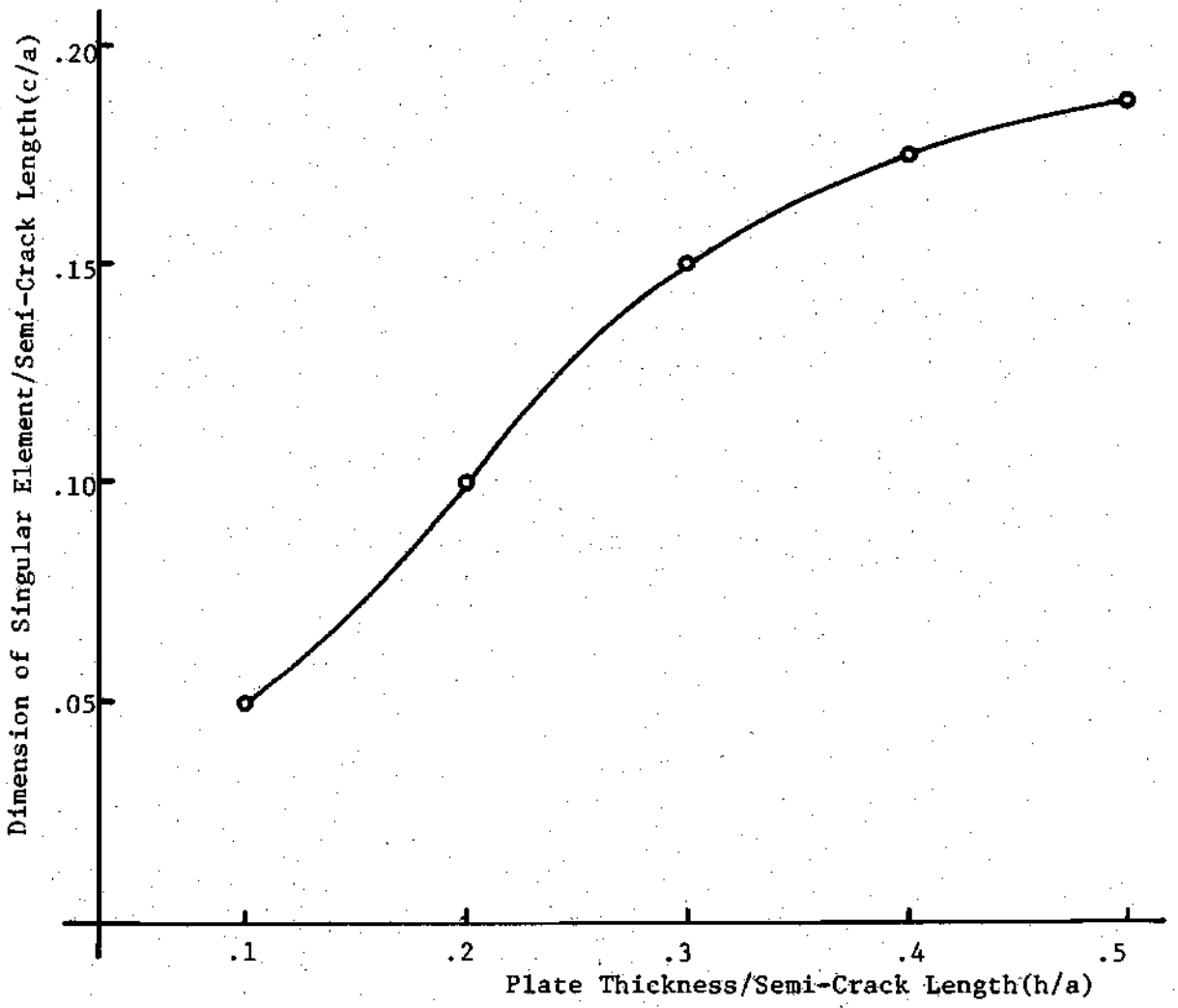

Fig. 5.8 Optimun Size of a Singular Element for Various Thickness of the Plate

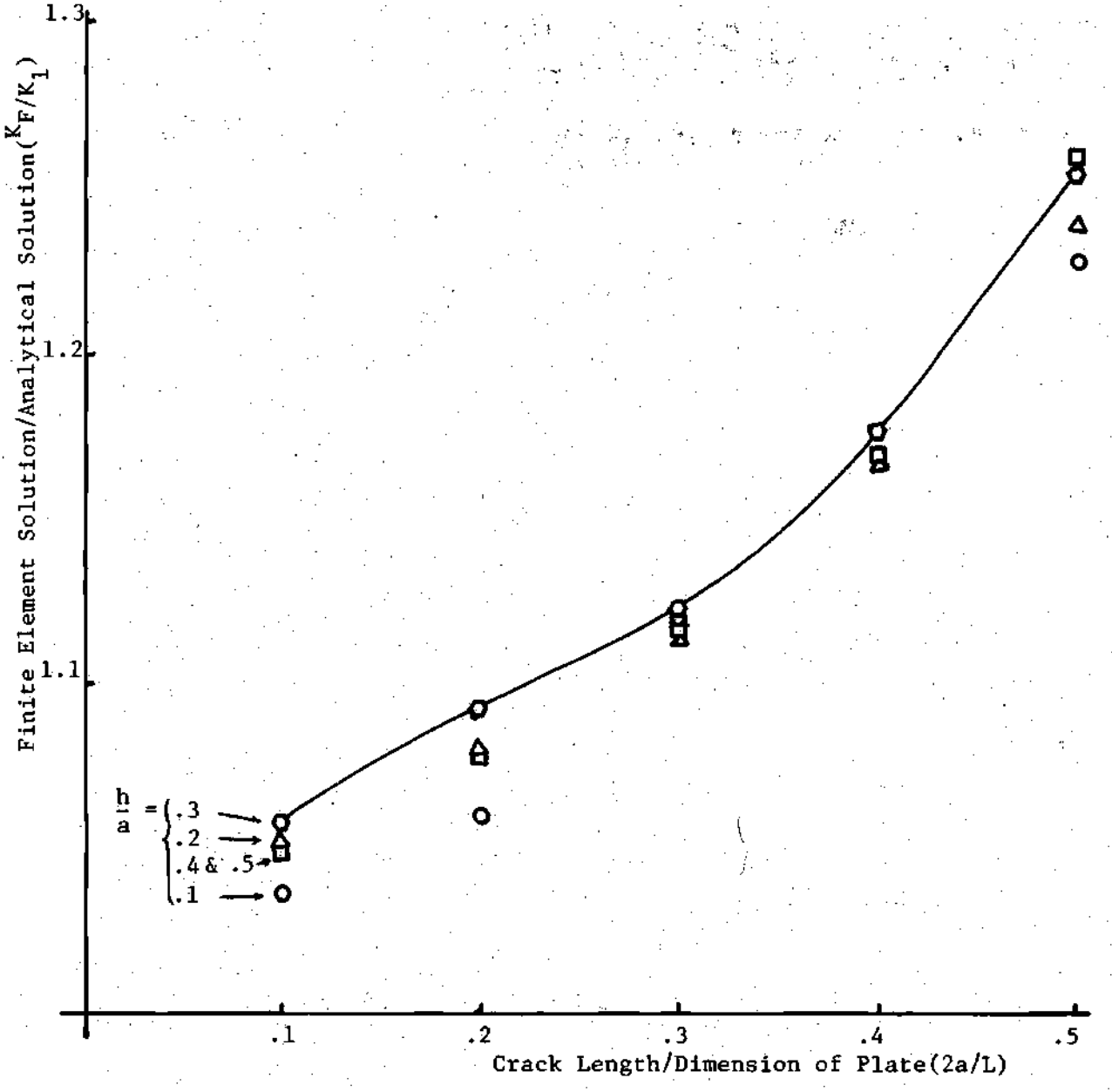

Fig. 5.9 Finite Dimension Correction Factors

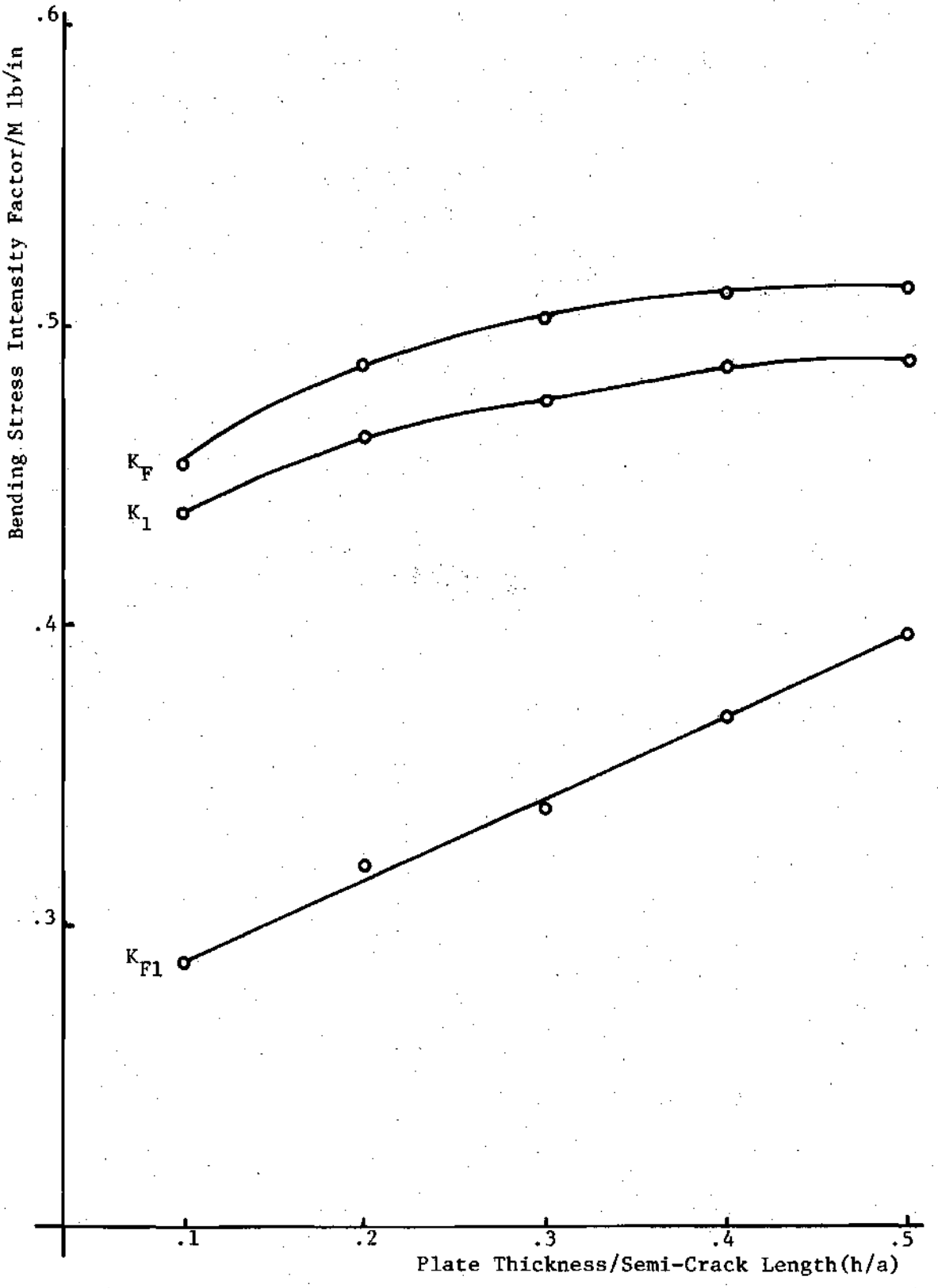

Fig. 5.10 Variation of Stress Intensity Factor with the Thickness of Plate: 2a/L = .1

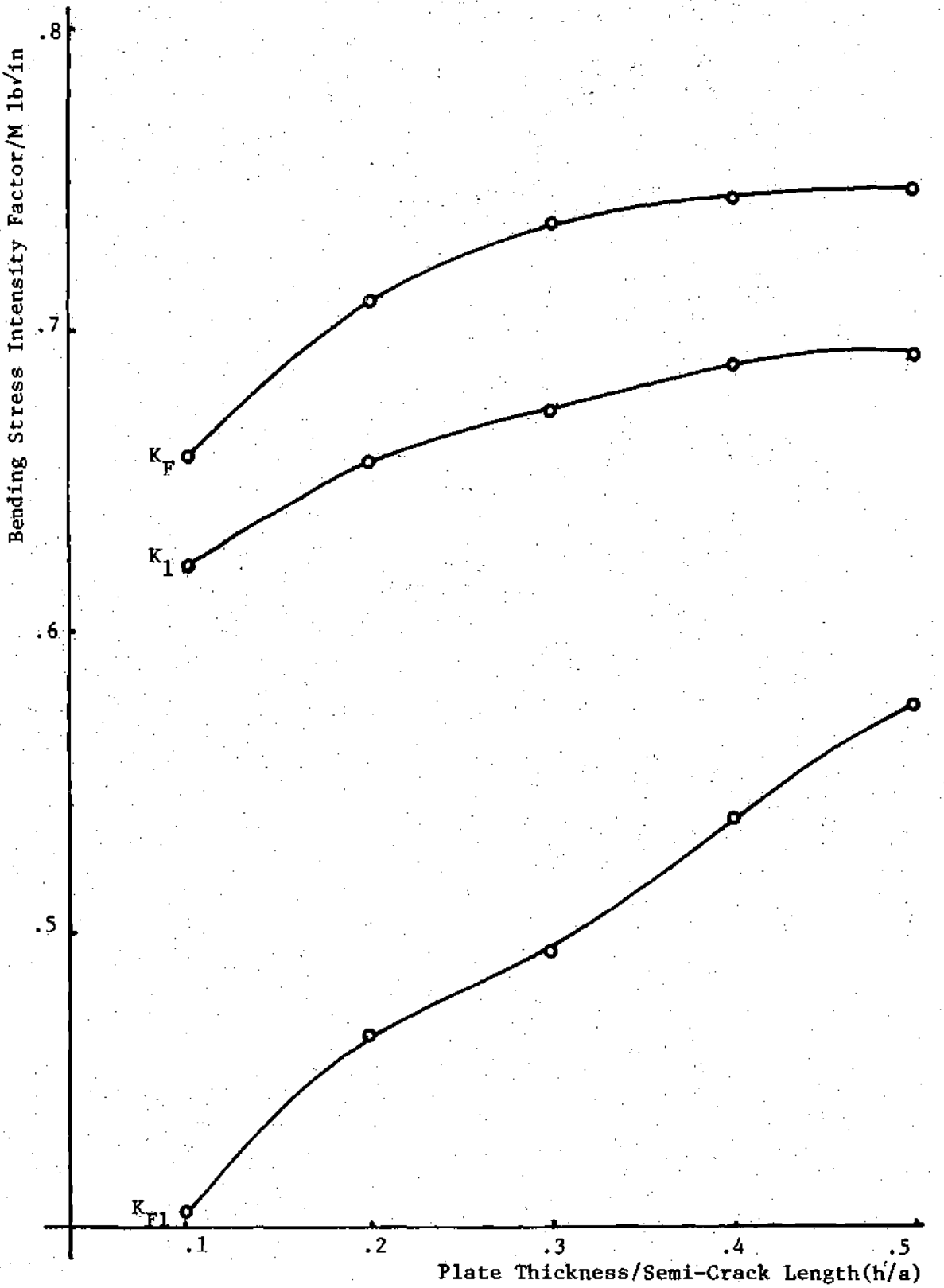

Fig. 5.11 Variation of Stress Intensity Factor with the Thickness of Plate: 2a/L = .2

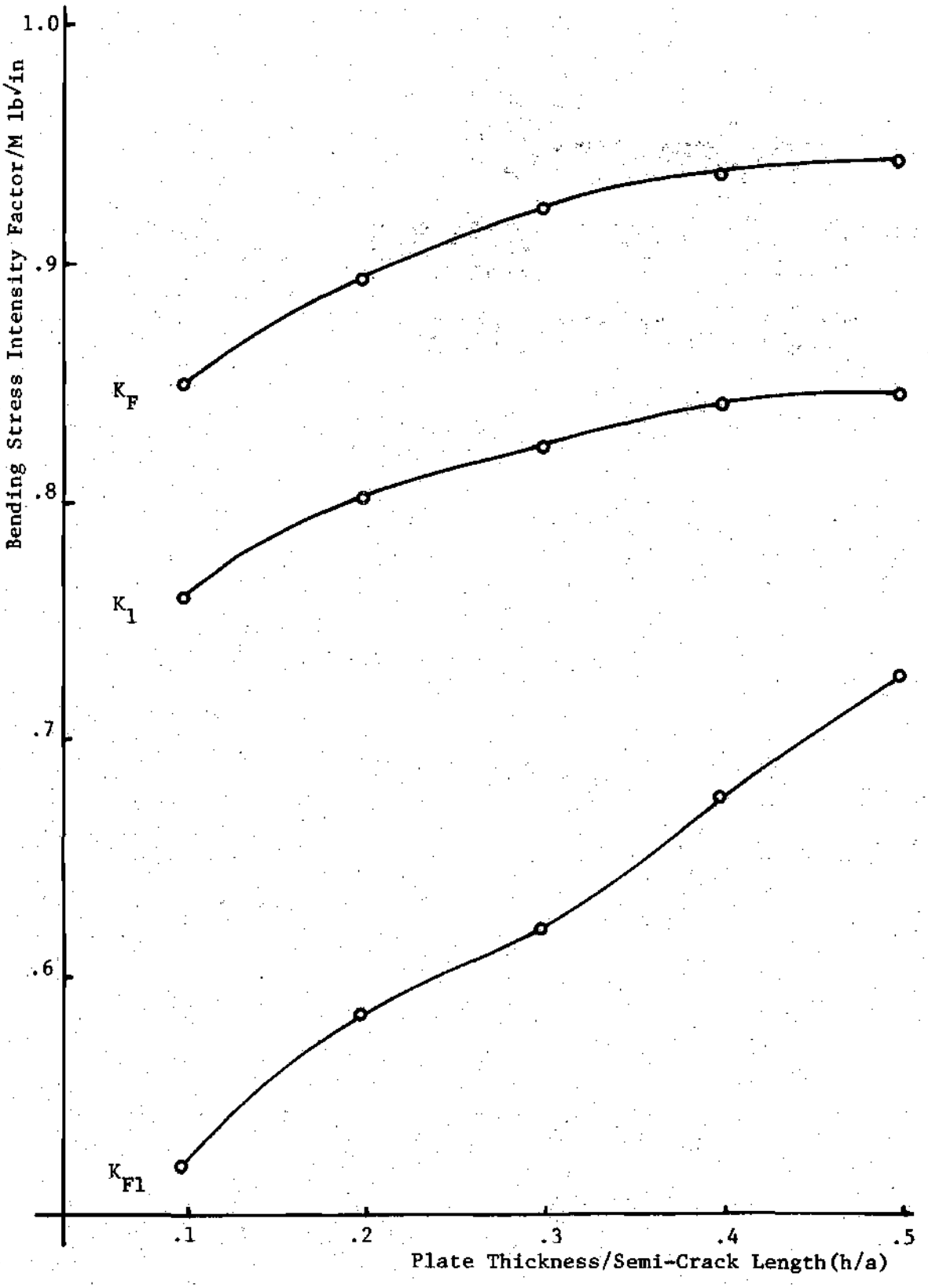

Fig. 5.12 Variation of Stress Intensit Factor with the Thickness of Plate: 2a/L = .3

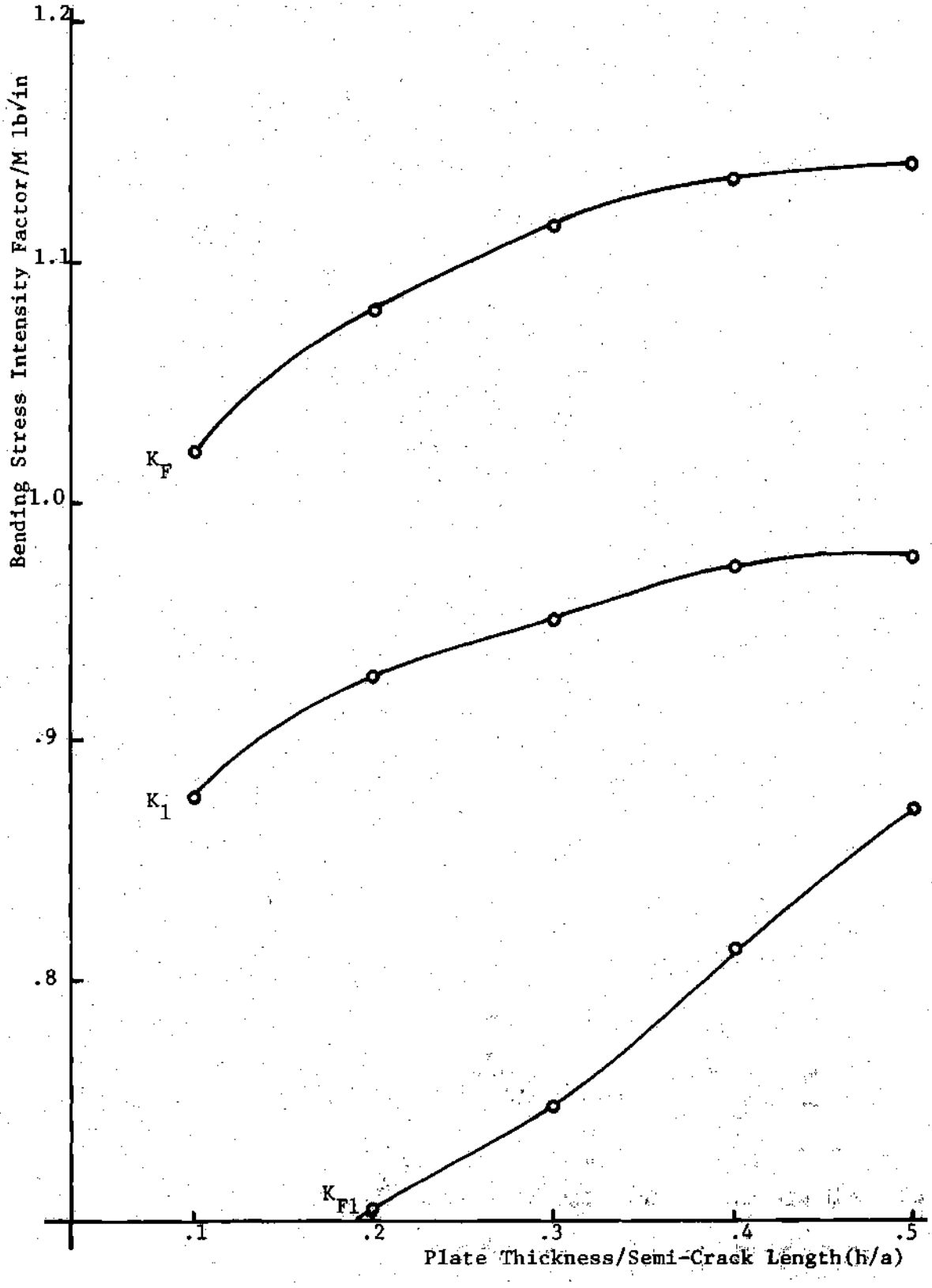

Fig. 5.13 Variation of Stress Intensity Factor with the Thickness of Plate: 2a/L = .4

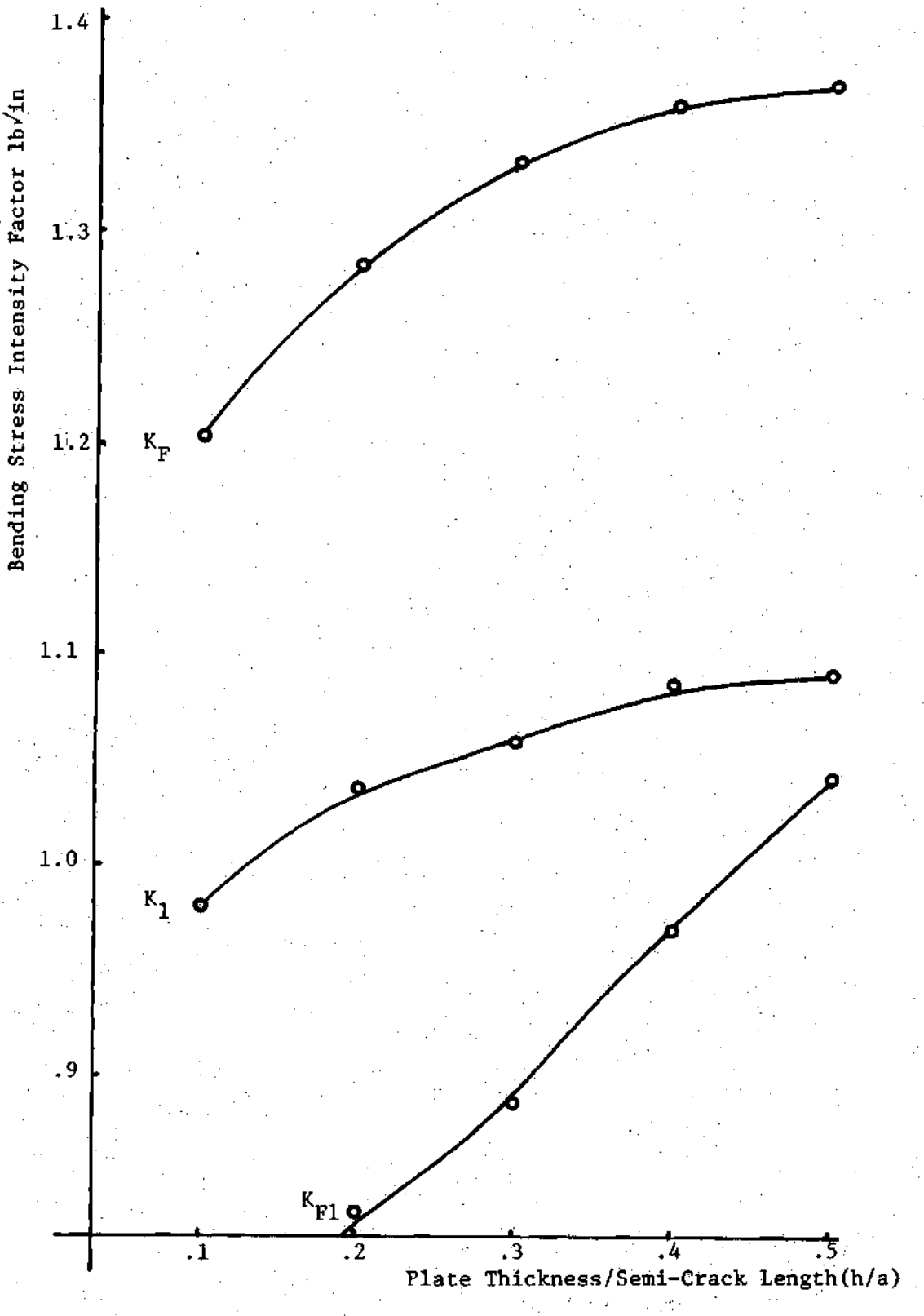

Fig. 5.14 Variation of Stress Intensity Factor with the Thickness of Plate: 2a/L = .5

APPENDIX C

TABLES

A Priori Conditions					Independent Variables							Models
Interior			Interelement Boundary		Interior			Boundary				
$\sigma_{ij,j}+\bar{F}_i=0$	$\varepsilon_{ij}=u_{(i,j)}$	$\sigma_{ij}=\frac{\partial A}{\partial \varepsilon_{ij}}$	$u_i^+=u_i^-$	$T_i^+=T_i^-$	u_i	ε_{ij}	σ_{ij}	u_{iL}	u_i	T_{iL}	$T_{i\ell}$	
					x	x	x			x		Eqs. 2.26 and 2.27
					x	x	x	x			x	Eqs. 2.30 and 2.31
	x	x			x					x		Eq. 2.32
	x	x	x		x							Eqs. 2.34 and 2.35
	x	x			x			x			x	Eq. 2.33
x		x					x	x				Eq. 2.36
x		x					x		x	x		Eq. 2.37
x		x		x			x					Eq. 2.39
		x			x		x			x		Eq. 2.40
		x			x		x	x			x	Eq. 2.41
		x	x	x	x		x					Eq. 2.42

Table 2.1 Finite Element Models

1	$-b$	0	b^2	0	0	$-b^3$	0	0	0	b^4	0	0	0	0	$-b^5$	0	0	0	0
0	1	0	$-2b$	0	0	$3b^2$	0	0	0	$-4b^3$	0	0	0	0	$5b^4$	0	0	0	0
0	0	1	0	$-b$	0	0	b^2	0	0	0	$-b^3$	0	0	0	0	0	0	0	0
0	0	0	2	0	0	$-6b$	0	0	0	$12b^2$	0	0	0	0	$-20b^3$	0	0	0	0
0	0	0	0	1	0	0	$-2b$	0	0	0	$3b^2$	0	0	0	0	0	0	0	0
0	0	0	0	0	2	0	0	$-2b$	0	0	0	$2b^2$	0	0	0	$-2b^3$	0	0	0
1	a	0	a^2	0	0	a^3	0	0	0	a^4	0	0	0	0	a^5	0	0	0	0
0	1	0	2a	0	0	$3a^2$	0	0	0	$4a^3$	0	0	0	0	$5a^4$	0	0	0	0
0	0	1	0	a	0	0	a^2	0	0	0	a^3	0	0	0	0	0	0	0	0
0	0	0	2	0	0	6a	0	0	0	$12a^2$	0	0	0	0	$20a^3$	0	0	0	0
0	0	0	0	1	0	0	2a	0	0	0	$3a^2$	0	0	0	0	0	0	0	0
0	0	0	0	0	2	0	0	2a	0	0	0	$2a^2$	0	0	0	$2a^3$	0	0	0
1	0	c	0	0	c^2	0	0	0	c^3	0	0	0	0	c^4	0	0	0	0	c^5
0	1	0	0	c	0	0	0	c^2	0	0	0	0	c^3	0	0	0	0	c^4	0
0	0	1	0	0	2c	0	0	0	$3c^2$	0	0	0	0	$4c^3$	0	0	0	0	$5c^4$
0	0	0	2	0	0	0	2c	0	0	0	0	$2c^2$	0	0	0	0	$2c^3$	0	0
0	0	0	0	1	0	0	0	2c	0	0	0	0	$3c^2$	0	0	0	0	$4c^3$	0
0	0	0	0	0	2	0	0	0	6c	0	0	0	0	$12c^2$	0	0	0	0	$20c^3$
0	0	0	0	0	0	0	0	0	0	0	0	0	0	0	$5a^4c$	$3a^2c^3-2a^4c$	$-2ac^4+3a^3c^3$	$c^5-4a^2c^3$	$5ac^4$
0	0	0	0	0	0	0	0	0	0	0	0	0	0	0	$5b^4c$	$3b^2c^3-2b^4c$	$2bc^4-3b^3c^2$	$c^5-4b^2c^3$	$-5bc^4$

Table 4.1 Transformation Matrix T(from Ref. 58)

$$[R] = \begin{bmatrix} R_1 & 0 & 0 \\ 0 & R_1 & 0 \\ 0 & 0 & R_1 \end{bmatrix}$$

$$[R_1] = \begin{bmatrix} 1 & 0 & 0 & 0 & 0 & 0 \\ 0 & \cos\theta, & \sin\theta & 0 & 0 & 0 \\ 0 & -\sin\theta & \cos\theta & 0 & 0 & 0 \\ 0 & 0 & 0 & \cos^2\theta & 2\sin\theta\cos\theta & \sin^2\theta \\ 0 & 0 & 0 & -\sin\theta\cos\theta & \cos^2\theta - \sin^2\theta & \sin\theta\cos\theta \\ 0 & 0 & 0 & \sin^2\theta & -2\sin\theta\cos\theta & \cos^2\theta \end{bmatrix}$$

Table 4.2 Rotation Matrix R(from Ref. 58)

$$\underset{\sim}{u} = \underset{\sim}{L}\underset{\sim}{q} = \begin{bmatrix} \underset{\sim}{N}_{11} & \underset{\sim}{N}_{12} & 0 & 0 \\ 0 & \underset{\sim}{N}_{21} & \underset{\sim}{N}_{22} & 0 \\ 0 & 0 & \underset{\sim}{N}_{31} & \underset{\sim}{N}_{32} \\ \underset{\sim}{N}_{42} & 0 & 0 & \underset{\sim}{N}_{41} \end{bmatrix} \begin{Bmatrix} \underset{\sim}{g}_1 \\ \underset{\sim}{g}_2 \\ \underset{\sim}{g}_3 \\ \underset{\sim}{g}_4 \end{Bmatrix}$$

$$\underset{\sim}{u}^T = \lfloor w_{12}\ w,_{n_{12}}\ w,_{s_{12}}\ w_{23}\ w,_{n_{23}}\ w,_{s_{23}}\ w_{34}\ w,_{n_{34}}\ w,_{s_{34}}\ w_{41}\ w,_{n_{41}}\ w,_{s_{41}} \rfloor$$

$$\underset{\sim}{g}_i^T = \lfloor w_i\ w,_{x_i}\ w,_{y_i} \rfloor$$

$$\underset{\sim}{N}_{i1} = \begin{bmatrix} 2\xi^3-3\xi^2+1 & -\ell_i\sin\theta_i(\xi^3-2\xi^2+\xi) & \ell_i\cos\theta_i(\xi^3-2\xi^2+\xi) \\ 0 & \cos\theta_i(1-\xi) & \sin\theta_i(1-\xi) \\ \frac{6}{\ell_i}(\xi^2-\xi) & -\sin\theta_i(3\xi^2-4\xi+1)+A_1 & \cos\theta_i(3\xi^2-4\xi+1)+B_1 \end{bmatrix}$$

$$\underset{\sim}{N}_{i2} = \begin{bmatrix} -2\xi^3+3\xi^2 & -\ell_i\sin\theta_i(\xi^3-\xi^2) & \ell_i\cos\theta_i(\xi^3-\xi^2) \\ 0 & \cos\theta_i\xi & \sin\theta_i\xi \\ -\frac{6}{\ell_i}(\xi^2-\xi) & -\sin\theta_i(3\xi^2-2\xi)+A_2 & \cos\theta_i(3\xi^2-2\xi)+B_2 \end{bmatrix}$$

where $\xi = \frac{s}{\ell_i}$, $A_1 = A_2 = B_i = B_2 = 0$ for sides 1-2, 3-4 and 4-1 and $A_1 = -\theta_2\cos\theta_2(\xi^3-2\xi^2+\xi)$, $B_1 = -\theta_2\sin\theta_2(\xi^3-2\xi^2+\xi)$, $A_2 = -\theta_2\cos\theta_2(\xi^3-\xi^2)$ and $B_2 = -\theta_2\sin\theta_2(\xi^3-\xi^2)$ for side 2-3 where θ_2 varies with the boundary coordinate s.

Table 4.3 Boudary Displacement Matrix of a Hybrid Stress Element(ref. Fig. 4.20)

$$\underset{\sim}{T} = \underset{\sim}{R}\underset{\sim}{\beta} + \underset{\sim}{R}_p = \begin{bmatrix} \underset{\sim}{R}_1 \\ \underset{\sim}{R}_2 \\ \underset{\sim}{R}_3 \\ \underset{\sim}{R}_4 \end{bmatrix} \underset{\sim}{\beta} - \begin{Bmatrix} \underset{\sim}{R}_{p_1} \\ \underset{\sim}{R}_{p_2} \\ \underset{\sim}{R}_{p_3} \\ \underset{\sim}{R}_{p_4} \end{Bmatrix}$$

$$\underset{\sim}{T}^T = [Q_{n_{12}} \; -M_{n_{12}} \; -M_{ns_{12}} \; Q_{n_{23}} \; -M_{n_{23}} \; -M_{ns_{23}} \; Q_{n_{34}} \; -M_{n_{34}} \; -M_{ns_{34}} \; Q_{n_{14}} \; -M_{n_{14}} \; -M_{ns_{14}}]$$

$$\underset{\sim}{R}_{p_i}^T = [-pA_i x \;\; \frac{p}{2}B_i x^2 \;\; 0]$$

$$\underset{\sim}{R}_i = \begin{bmatrix} 0 & A_i & 0 & A_i x - B_i y & A_i y & 0 & 0 & 0 & 0 & B_i x & 0 & B_i & A_i & 2B_i x & 2A_i y \\ -A_i^2 & -A_i^2 x & -A_i^2 y & -A_i^2 x^2 + 2A_i B_i xy & -A_i^2 xy & -A_i^2 y^2 & -B_i^2 & -B_i^2 x & -B_i^2 y & -B_i^2 y^2 + 2A_i B_i xy & -2A_i B_i & -2A_i B_i x & -2A_i B_i y & -2A_i B_i x^2 & -2A_i B_i y^2 \\ A_i B_i & A_i B_i x & A_i B_i y & A_i B_i x^2 + (A_i^2 - B_i^2) xy & A_i B_i xy & A_i B_i y^2 & -A_i B_i & -A_i B_i x & -A_i B_i y & -A_i B_i y^2 + (A_i^2 - B_i^2) xy & B_i^2 - A_i^2 & (B_i^2 - A_i^2) x & (B_i^2 - A_i^2) y & (B_i^2 - A_i^2) x^2 & (B_i^2 - A_i^2) y^2 \end{bmatrix}$$

where $A_i = \cos\theta_i$ and $B_i = \sin\theta_i$

Table 4.4 Boudary Traction Matrix of a Hybrid Stress Element

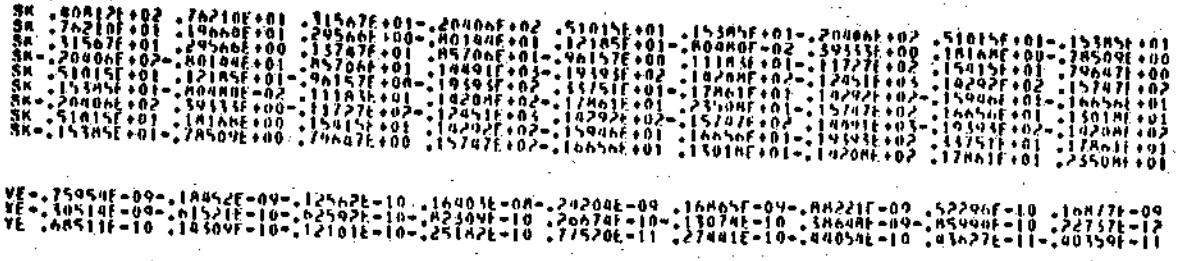

Table 4.5 Stiffness Matrix, SK = $12K/Eh^3$, of a Triangular Element with Straight Sides(Fig. 4.21)

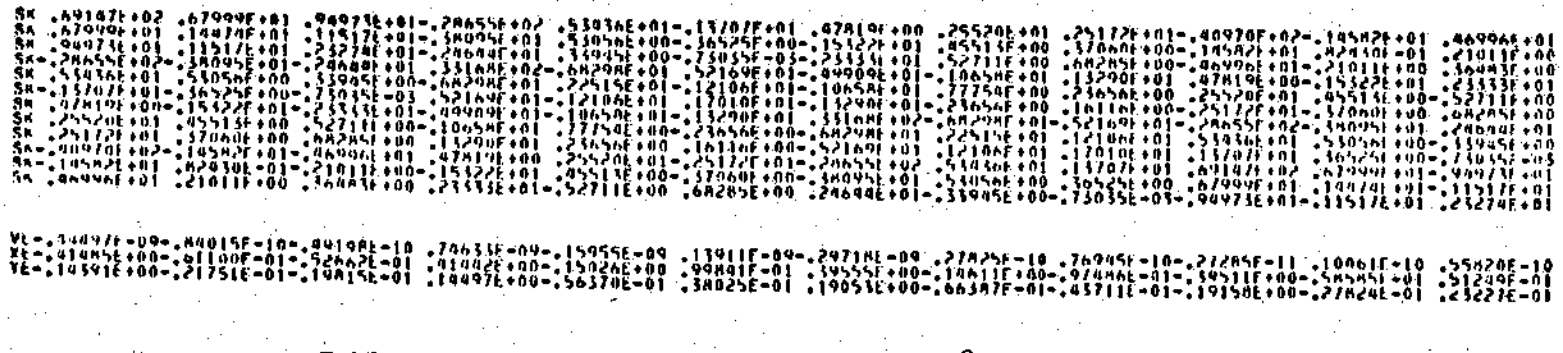

Table 4.6 Stiffness Matrix, SK = $12K/Eh^3$, of a Quadrilateral Element with One Circular Curved Side(Fig. 4.21)

$$\underset{\sim}{u} = \underset{\sim}{L}\underset{\sim}{q}$$

$$\underset{\sim}{u}^T = [w_{12}\ -w,_{y_{12}}\ w,_{x_{12}}\ w_{23}\ w,_{x_{23}}\ w,_{y_{23}}\ w_{34}\ w,_{y_{34}}\ -w,_{x_{34}}\ w_{41}\ -w,_{x_{41}}\ -w,_{y_{41}}]$$

$$\underset{\sim}{q}^T = [w_1\ w,_{x_1}\ w,_{y_1}\ w_2\ w,_{x_2}\ w,_{y_2}\ w_3\ w,_{x_3}\ w,_{y_3}\ w_4\ w,_{x_4}\ w,_{y_4}]$$

$\underset{\sim}{L}$ is as follow:

$$\begin{bmatrix}
2\xi^3-3\xi^2+1 & a(\xi^3-2\xi^2+\xi) & 0 & -3\xi^3+3\xi^2 & a(\xi^3-\xi^2) & 0 & 0 & 0 & 0 & 0 & 0 & 0 \\
0 & 0 & -(1-\xi) & 0 & 0 & -\xi & 0 & 0 & 0 & 0 & 0 & 0 \\
\frac{6}{a}(\xi^2-\xi) & 3\xi^2-4\xi+1 & 0 & -\frac{6}{a}(\xi^2-\xi) & 3\xi^2-2\xi & 0 & 0 & 0 & 0 & 0 & 0 & 0 \\
0 & 0 & 0 & 2\zeta^3-3\zeta^2+1 & 0 & b(\zeta^3-2\zeta^2+\zeta) & -\zeta^3+3\zeta^2 & 0 & b(\zeta^3-\zeta^2) & 0 & 0 & 0 \\
0 & 0 & 0 & 0 & 1-\zeta & 0 & 0 & \zeta & 0 & 0 & 0 & 0 \\
0 & 0 & 0 & \frac{6}{b}(\zeta^2-\zeta) & 0 & 3\zeta^2-4\zeta+1 & -\frac{6}{b}(\zeta^2-\zeta) & 0 & 3\zeta^2-2\zeta & 0 & 0 & 0 \\
0 & 0 & 0 & 0 & 0 & 0 & -\xi^3+3\xi^2 & -a(\xi^3-\xi^2) & 0 & 2\xi^3-3\xi^2+1 & -a(\xi^3-2\xi^2+\xi) & 0 \\
0 & 0 & 0 & 0 & 0 & 0 & 0 & 0 & \xi & 0 & 0 & 1-\xi \\
0 & 0 & 0 & 0 & 0 & 0 & -\frac{6}{a}(\xi^2-\xi) & -3\xi^2+2\xi & 0 & \frac{6}{a}(\xi^2-\xi) & -3\xi^2+4\xi-1 & 0 \\
2\zeta^3-3\zeta^2+1 & 0 & -b(\zeta^3-2\zeta^2+\zeta) & 0 & 0 & 0 & 0 & 0 & 0 & -2\zeta^3+3\zeta^2 & 0 & -b(\zeta^3-\zeta^2) \\
0 & -(1-\zeta) & 0 & 0 & 0 & 0 & 0 & 0 & 0 & 0 & -\zeta & 0 \\
\frac{6}{b}(\zeta^2-\zeta) & 0 & -3\zeta^2+4\zeta-1 & 0 & 0 & 0 & 0 & 0 & 0 & -\frac{6}{b}(\zeta^2-\zeta) & 0 & -3\zeta^2+2\zeta
\end{bmatrix}$$

where $\xi = \frac{x}{a}$ and $\zeta = \frac{y}{b}$

Table 5.1 Boundary Displacement Matrix of a Regular Element with Dimension(a x b)

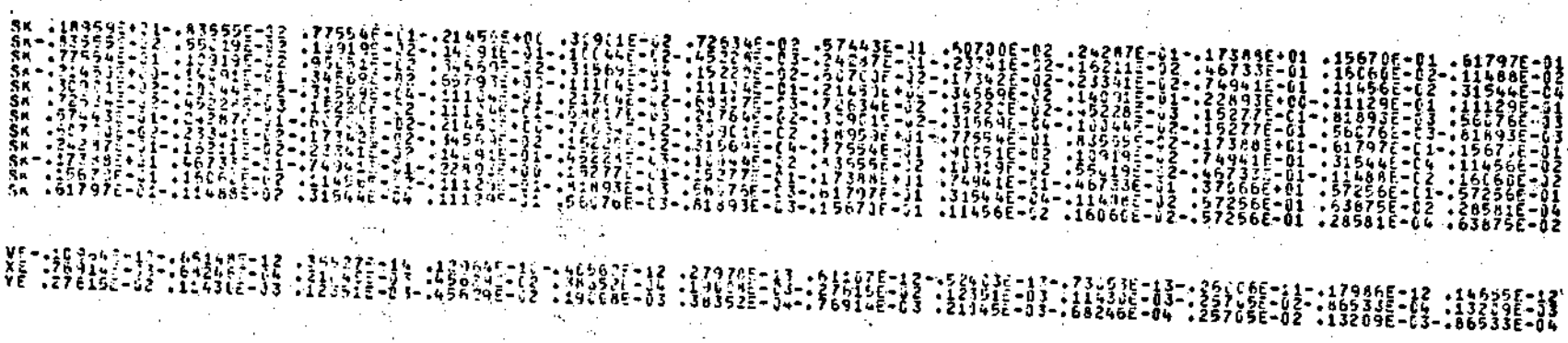

Table 5.2 Stiffness Matrix, SK = 12K/E, of "A" Type Singular Element with Dimension(.1 x .1) and Thickness .2

$$\underset{\sim}{u} = \underset{\sim}{L}\underset{\sim}{q}$$

$$\underset{\sim}{u}^T = \{w_{12}\ -\theta_{y_{12}}\ \theta_{x_{12}}\ w_{23}\ \theta_{x_{23}}\ \theta_{y_{23}}\ w_{34}\ w,_{y_{34}}\ -w,_{x_{34}}\ w_{41}\ -w,_{x_{41}}\ -w,_{y_{41}}\}$$

$$\underset{\sim}{q}^T = \{w_1\ \theta_{x_1}\ \theta_{y_1}\ w_2\ \theta_{x_2}\ \theta_{y_2}\ w_3\ w,_{x_3}\ w,_{y_3}\ w_4\ w,_{x_4}\ w,_{y_4}\}$$

$\underset{\sim}{L}$ is as follow:

$$\begin{bmatrix}
(1-\xi)^{3/2} & 0 & 0 & 1-(1-\xi)^{3/2} & 0 & 0 & 0 & 0 & 0 & 0 & 0 & 0 \\
0 & 0 & -(1-\xi)^{1/2} & 0 & 0 & -1+(1-\xi)^{1/2} & 0 & 0 & 0 & 0 & 0 & 0 \\
0 & (1-\xi)^{1/2} & 0 & 0 & 1-(1-\xi)^{1/2} & 0 & 0 & 0 & 0 & 0 & 0 & 0 \\
0 & 0 & 0 & 1-\zeta^{3/2} & 0 & 0 & \zeta^{3/2} & 0 & 0 & 0 & 0 & 0 \\
0 & 0 & 0 & 0 & 1-\zeta^{1/2} & 0 & 0 & \zeta^{1/2} & 0 & 0 & 0 & 0 \\
0 & 0 & 0 & 0 & 0 & 1-\zeta^{1/2} & 0 & 0 & \zeta^{1/2} & & 0 & 0 \\
0 & 0 & 0 & 0 & 0 & 0 & -\xi^3+3\xi^2 & -a(\xi^3-\xi^2) & 0 & 2\xi^3-3\xi^2+1 & -a(\xi^3-2\xi^2+\xi) & 0 \\
0 & 0 & 0 & 0 & 0 & 0 & 0 & 0 & \xi & 0 & 0 & 1-\xi \\
0 & 0 & 0 & 0 & 0 & 0 & -\frac{6}{a}(\xi^2-\xi) & -3\xi^2+2\xi & 0 & \frac{6}{a}(\xi^2-\xi) & -3\xi^2+4\xi-1 & 0 \\
2\zeta^3-3\zeta^2+1 & 0 & -b(\zeta^3-2\zeta^2+\zeta) & 0 & 0 & 0 & 0 & 0 & 0 & -2\zeta^3+3\zeta^2 & 0 & -b(\zeta^3-\zeta^2) \\
0 & -(1-\zeta) & 0 & 0 & 0 & 0 & 0 & 0 & 0 & 0 & -\zeta & 0 \\
\frac{6}{b}(\zeta^2-\zeta) & 0 & -3\zeta^2+4\zeta-1 & 0 & 0 & 0 & 0 & 0 & 0 & -\frac{6}{b}(\zeta^2-\zeta) & 0 & -3\zeta^2+2\zeta
\end{bmatrix}$$

where $\xi = \frac{x}{a}$ and $\zeta = \frac{y}{b}$

Table 5.3 Boundary Displacement Matrix of "A" Type Singular Element with Dimension(a x b)

$$\underset{\sim}{u} = \underset{\sim}{L}\underset{\sim}{q}$$

$$\underset{\sim}{u}^T = [w_{12} \; -\theta_{y_{12}} \; \theta_{x_{12}} \; w_{23} \; w,_{x_{23}} \; w,_{y_{23}} \; w_{34} \; w,_{y_{34}} \; -w,_{x_{34}} \; w_{41} \; -\theta_{x_{41}} \; -\theta_{y_{41}}]$$

$$\underset{\sim}{q}^T = [w_1 \; \theta_{x_1} \; \theta_{y_1} \; w_2 \; w,_{x_2} \; w,_{y_2} \; w_3 \; w,_{x_3} \; w,_{y_3} \; w_4 \; \theta_{x_4} \; \theta_{y_4}]$$

$\underset{\sim}{L}$ is as follow:

$$\begin{bmatrix}
1-\xi^{3/2} & 0 & 0 & \xi^{3/2} & 0 & 0 & 0 & 0 & 0 & 0 & 0 & 0 \\
0 & 0 & -1+\xi^{1/2} & 0 & 0 & -\xi^{1/2} & 0 & 0 & 0 & 0 & 0 & 0 \\
0 & 1-\xi^{1/2} & 0 & 0 & \xi^{1/2} & 0 & 0 & 0 & 0 & 0 & 0 & 0 \\
0 & 0 & 0 & 2\xi^3-3\xi^2+1 & 0 & b(\xi^3-2\xi^2+\xi) & -\xi^3+3\xi^2 & 0 & b(\xi^3-\xi^2) & 0 & 0 & 0 \\
0 & 0 & 0 & 0 & 1-\xi & 0 & 0 & \xi & 0 & 0 & 0 & 0 \\
0 & 0 & 0 & \frac{6}{b}(\xi^2-\xi) & 0 & 3\xi^2-4\xi+1 & -\frac{6}{b}(\xi^2-\xi) & 0 & 3\xi^2-2\xi & 0 & 0 & 0 \\
0 & 0 & 0 & 0 & 0 & 0 & -\xi^3+3\xi^2 & -a(\xi^3-\xi^2) & 0 & 2\xi^3-3\xi^2+1 & -a(\xi^3-2\xi^2+\xi) & 0 \\
0 & 0 & 0 & 0 & 0 & 0 & 0 & 0 & \xi & 0 & 0 & 1-\xi \\
0 & 0 & 0 & 0 & 0 & 0 & -\frac{6}{a}(\xi^2-\xi) & -3\xi^2+2\xi & 0 & \frac{6}{a}(\xi^2-\xi) & -3\xi^2+4\xi-1 & 0 \\
1-\zeta^{3/2} & 0 & 0 & 0 & 0 & 0 & 0 & 0 & 0 & \zeta^{3/2} & 0 & 0 \\
0 & -1+\zeta^{1/2} & 0 & 0 & 0 & 0 & 0 & 0 & 0 & 0 & -\zeta^{1/2} & 0 \\
0 & 0 & -1+\zeta^{1/2} & 0 & 0 & 0 & 0 & 0 & 0 & 0 & 0 & -\zeta^{1/2}
\end{bmatrix}$$

where $\xi = \frac{x}{a}$ and $\zeta = \frac{y}{b}$

Table 5.4 Boundary Displacement Matrix of "B" Type Singular Element with Dimension(a x b)

$$\underset{\sim}{M} = \begin{Bmatrix} M_x \\ M_y \\ M_{xy} \end{Bmatrix} = \begin{bmatrix} 1 & x & y & x^2 & xy & y^2 & 0 & 0 & 0 \\ 0 & 0 & 0 & 0 & 0 & 0 & y^2 & 0 & 0 \\ 0 & 0 & 0 & -xy & 0 & 0 & -xy & y & y^2 \end{bmatrix} \underset{\sim}{\beta} + \begin{Bmatrix} px^2/2 \\ 0 \\ 0 \end{Bmatrix}$$

$$\underset{\sim}{\beta} = \{ \beta_1 \ \beta_2 \ \cdots\cdots\cdots \ \beta_9 \}$$

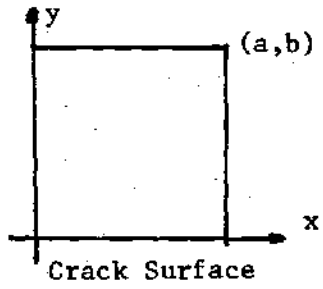

$$\underset{\sim}{T} = \underset{\sim}{R}\underset{\sim}{\beta} + \underset{\sim}{R}_p$$

$$\underset{\sim}{T}^T = \{ -Q_{y_{12}} \ -M_{y_{12}} \ M_{xy_{12}} \ Q_{x_{23}} \ -M_{x_{23}} \ -M_{xy_{23}} \ Q_{y_{34}} \ -M_{y_{34}} \ M_{xy_{34}} \ -Q_{x_{41}} \ -M_{x_{41}} \ -M_{xy_{41}} \}$$

$$\underset{\sim}{R} = \begin{bmatrix} 0 & 0 & 0 & 0 & 0 & 0 & 0 & 0 & 0 \\ 0 & 0 & 0 & 0 & 0 & 0 & 0 & 0 & 0 \\ 0 & 0 & 0 & 0 & 0 & 0 & 0 & 0 & 0 \\ 0 & 1 & 0 & a & y & 0 & -a & 1 & 2y \\ -1 & -a & -y & -a^2 & -ay & -y^2 & 0 & 0 & 0 \\ 0 & 0 & 0 & ay & 0 & 0 & ay & y & y^2 \\ 0 & 0 & 0 & -b & 0 & 0 & b & 0 & 0 \\ 0 & 0 & 0 & 0 & 0 & 0 & -b^2 & 0 & 0 \\ 0 & 0 & 0 & -bx & 0 & 0 & -bx & b & b^2 \\ 0 & -1 & 0 & 0 & -y & 0 & 0 & -1 & -2y \\ -1 & 0 & -y & 0 & 0 & -y^2 & 0 & 0 & 0 \\ 0 & 0 & 0 & 0 & 0 & 0 & 0 & -y & -y^2 \end{bmatrix} \qquad \underset{\sim}{R}_p = \begin{Bmatrix} 0 \\ 0 \\ 0 \\ ap \\ -a^2p/2 \\ 0 \\ 0 \\ 0 \\ 0 \\ 0 \\ 0 \\ 0 \end{Bmatrix}$$

Table 5.5 Reduced Regular Stress Functions and Boundary Tractions for Elements along Crack Surface

$K_{1/M}$ lb√in: h/a \ c/a	.1	.2	.3	.4	.5
	.620	.655	.670	.687	.690
.0400	.635	.646	.642	.632	.629
.0500	.657	.667	.651	.646	.641
.0750	.644	.696	.685	.673	.666
.1000	.603	.708	.709	.699	.690
.1250	.559	.706	.724	.718	.711
.1500	.523	.698	.734	.736	.730
.1750	.490	.684	.734	.742	.742
.1875	.379	.621	.703	.730	.745
.2000	.365	.610	.699	.730	.739
.2500	.258	.515	.639	.698	.726

Table 5.6 Stress Intensity Factors of Plates with Various Combinations of Thickness and Singular Element Size.

h/a	.1	.2	.3	.4	.5
c/a	.05	.1	.15	.175	.1875

Table 5.7 Optimum Size of Singular Element for Plates with Various Thickness.

2a/L	lb√in/M	h/a = .1	.2	.3	.4	.5
.1	K_1	.438	.463	.475	.486	.488
	K_F	.454	.487	.502	.510	.512
	K_{F1}	.288	.320	.339	.369	.396
.2	K_1	.620	.655	.672	.687	.690
	K_F	.657	.708	.734	.742	.745
	K_{F1}	.406	.464	.492	.536	.574
.3	K_1	.759	.802	.823	.841	.845
	K_F	.849	.893	.923	.937	.943
	K_{F1}	.521	.584	.620	.675	.726
.4	K_1	.878	.926	.950	.972	.976
	K_F	1.021	1.080	1.116	1.134	1.140
	K_{F1}	.629	.704	.747	.813	.871
.5	K_1	.980	1.036	1.063	1.086	1.091
	K_F	1.203	1.284	1.333	1.365	1.375
	K_{F1}	.731	.836	.888	.969	1.041

K_1 : Analytical Solution for an Infinite Plate

K_F : Finite Element Solution with Explicitly Enforcing Traction Boundary Conditions.

K_{F1} : Finite Element Solution with Implicitly Enforcing Traction Boundary Conditions.

Table 5.8 Stress Intensity Factors of Plates with Various Combination of thickness, Crack Length and Dimensions.

BIBLIOGRAPHY

1. Martin, H. C., Introduction to Matrix Methods of Structural Analysis, McGraw-Hill, New York, 1966.

2. Szabo, B. A. and Lee, G. C., Stiffness Matrix for Plates by Galerkin's Method, Proc. ASCE, J. Eng. Mech. Div., Vol. 95, No. EM3, June 1969, pp. 571-585.

3. Szabo, B. A. and Lee, G. C., Derivation of Stiffness Matrices for Problems on Plane Elasticity by Galerkin Method, Int. J. Numer. Methods Eng., Vol. 1, No. 3, July 1969, pp. 301-310.

4. Oden, J. T., A General Theory of Finite Elements, I: Topological Considerations, Int. J. Numer. Methods Eng., Vol. 1, No. 3, 1969, pp. 247-259.

5. Oden, J. T., A General Theory of Finite Elements, II: Applications, Int. J. Numer. Methods Eng., Vol. 1, No. 2, 1969, pp. 205-221.

6. Huebbner, K. H., The Finite Element Method for Engineers, Wily, New York, 1975.

7. Friedrichs, K. O., and Keller, J. B., A Finite Difference Scheme for Generalized Neumann Problems, in Proc. Synspade, 1965, (Bramble, Editor) Academic Press, N. Y. 1966.

8. Hu, H. C., On Some Variation Principles in the Theory of Elasticity and Plasticity, Scintia. Sinica, Vol. 4, No. 1, March 1955, pp. 33-54.

9. Washizu, K., On the Variational Principles of Elasticity and Plasticity, Aeroelastic and Structures Research Laboratory, M. I. T., TR 25-18, March 1955.

10. Atluri, S. N., On Hybrid Finite Element Models in Solid Mechanics, Advances in Computer Methods for Partial Differential Equations, AICA, (Visherevetsky, Editor), Rutgers University, June 1975, pp. 346-356.

11. Pian, T. H. H., Derivation of Element Stiffness Matrices by Assumed Stress Distributions, AIAA J., 7, July 1964, pp. 1333-1336.

12. Pian, T. H. H., Element Stiffness-Matrix for Boundary Compatibility and for Prescribed Boundary Stresses, Proceedings First Conference on Matrix Methods in Structural Mechanics, Dayton, Ohio, 1965, AFFDL-TR-66-80.

13. Pian, T. H. H., Recent Advances in Matrix Methods in Structural Analysis and Design (Gallagher et.al, Editors), University of Alabama Press, 1971, pp. 49-83.

14. Pian, T. H. H., Numerical Solution of Field Problems in Continuum Physics (Birckhoff et.al., Editors), American Math. Soc., 1972, pp. 253-271.

15. Pian T. H. H., Finite Element Formulation by Variational Principles with Relaxed Continuity Requirements, Proceedings ONR Regional Symposium on Mathematical Foundations of the Finite Element Method with Applications to Partial Differential Equations, University of Maryland, Baltimore, June 1972.

16. Pian, T. H. H., Hybrid Models, Presented at the International Symposium on Numerical and Computer Methods in Structural Mechanics, University of Illinois at Urbana, September 1971.

17. Pian, T. H. H., Variational Methods in Engineering, Proc. of Int. Conf., Dept. of Civil Engineering, Southampton University, England, 1973.

18. Pian, T. H. H. and Tong, P., Basis of Finite Element Methods for Solid Continua, Int. J. Numer. Methods, Vol. 1, No. 1, 1969, pp. 3-28.

19. Pian, T. H. H. and Tong, P., Rationalization in Deriving Element Stiffness Matrix by Assumed Stress Approach, Proceedings Second Conf. on Matrix Methods in Structural Mechanics, Dayton, Ohio, October 1968, AFFDL-TR-68-150.

20. Tong, P. and Pian, T. H. H., A Variational Principle and Convergence of a Finite Element Method Based on Assumed Stress Distribution, Int. J. Solids Structures, Vol. 5, 1969, pp. 463-472.

21. Tong, P. and Pian, T. H. H., Bounds to the Influence Coefficients by the Assumed Stress Method, Int. J. Solids Structures, Vol. 6, 1970, pp. 1429-1432.

22. Tong, P. and Pian, T. H. H., The Convergence of Finite Element Methods in Solving Linear Elastic Problems, Int. J. Solids Structures, Vol. 3, 1967, pp. 865-879.

23. Tong, P., New Displacement Hybrid Finite Element Models for Solid Continua, Int. J. Numer. Methods Eng., Vol. 2, 1970, pp. 73-83.

24. Tong, P., An Assumed Stress Hybrid Finite Element Method of an Incompressible and Near-Incompressible Material, Int. J. Solids Structures, Vol. 5, 1969, pp. 455-461.

25. Atluri, S. N. and Pian, T. H. H., Theoretical Formulation of Finite-Element Methods in Linear-Elastic Analysis of General Shells, J. Struct. Mech., 1(1), 1972, pp. 1-41.

26. Atluri, S. N. and Pian, T. H.H., Finite-Element Analysis of Shells of Revolution by Two Doubly Curved Quadrilateral Elements, J. Struct. Mech., 1(3), 1973, pp. 393-416.

27. Atluri, S. N., Static Analysis of Shells of Revolution Using Doubly Curved Quadrilateral Elements Derived from Alternative Variational Models, SAMSO-TR-69-394, Norton AFB, California, 1969.

28. Prager, W., Recent Progress in Applied Mechanics, The Folke-Odquist Vol., Almquist and Wiksell, Stockholm, 1967, pp. 463-474.

29. Prager, W., Variational Principles for Elastic Plates with Relaxed Continuity Requirements, Int. J. Solids Structures, Vol. 4, 1968, pp. 837-844.

30. Atluri, S. N., A New Assumed Stress Hybrid Finite Element Model for Solid Continua, AIAA J., 9, 1971, pp. 1647-1649.

31. Atluri, S. N., An Assumed Stress Hybrid Finite Element Model for Linear Elastodynamic Analysis, AIAA J., 11, 1973, pp. 1028-1031.

32. Atluri, S. N., On the Hybrid Stress Finite Element Model for Incremental Analysis of Large Deflection Problems, Int. J. Solids Structures. Vol. 9, 1973, pp. 1171-1191.

33. Nemat-Nasser, S. and Lee, K. N., Application of General Variational Methods with Discontinuous Fields to Bending, Buckling, and Vibration of Beams, Computer Methods in Applied Mechanics and Engineering, 2, 1973, pp. 33-41.

34. Nernat-Nasser, S. and Lee, K. N., Finite-Element Formulations for Elastic Plates by General Variational Statements with Discontinuous Fields, Developments in Mechanics, Vol. 7, Proc. of the 13th Midwestern Mechanics Conference, 1973, pp. 979-995.

35. Wolf, J. P., General Stress Models for Finite Element Analysis, Doctoral Dissertation, ETH, Zurich, 1974.

36. Wolf, J. P., Generalized Hybrid Stress Finite Element Models, AIAA J., 11, 1973, pp. 386-388.

37. Pian, T. H. H., Tong, P. and Luk, C. H., Elastic Crack Analysis by a Finite Element Hybrid Method, Proceedings of Third Conference on Matrix Methods of Structural Analysis, Wright-Patterson AFB, Ohio, 1971.

38. Atluri, S. N., Kobayahi, A. S., and Nakagaki, M., Application of an Assumed Displacement Hybrid Finite Element Procedure to Two-Dimensional Problems in Fracture Mechanics, AIAA Paper No. 74-390, Presented at 15th AIAA/ASME/SA Structures, Structural Dynamics, and Materials Meeting, Las Vegas, Nevada, April 1974.

39. Atluri, S. N., Kobayashi, A. S., and Nakagaki, M., An Assumed Displacement Hybrid Model for Linear Fracture Mechanics, Int. J. of Fracture, Vol. 11, No. 2, April 1975, pp. 257-271.

40. Luk, C., Assumed Stress Hybrid Finite-Element Method for Fracture Mechanics and Elastic-Plastic Analysis, ASRL-TR-170-1, M.I.T., Dec. 1972.

41. Pian, T. H. H. and Mau, S. T., Some Recent Studies in Assumed Stress Hybrid Model, Second Japan-U.S. Seminar on Matrix Methods of Structural Analysis, Berkeley, August 1972.

42. Mau, S. T., Tong, P. and Pian, T. H. H., Finite Element Solutions for Laminated Thick Plates, J. of Composite Materials, Vol. 6, April 1972, pp. 304-311.

43. Tong, P. and Pian, T. H. H., On the Convergence of the Finite Element Method for Problems with Singularity, Int. J. Solids Structures, Vol. 9, 1973, pp. 313-321.

44. Gallagher, R. H., Survey and Evaluation of the Finite Element Method in Fracture Mechanics Analysis, First Int. Conf. on Structural Mechanics in Reactor Technology, Berlin, September 1971.

45. Zienckiewica, O. C., Irons, B. M., et.al., Iso-parametric and Associate Elements Families for Two and Three Dimensional Analysis, Ch. 13, in Finite Element Methods in Stress Analysis, (Holand and Bell, Editors), Trondheim, Norway, 1969.

46. Bogner, F. K., Fox, R. L. and Schmit, L. A., Jr., The Generation of Inter-Element-Compatible Stiffness and Mass Matrices by the Use of Interpolation Formulas, Matrix Methods in Structural Mechanics, Proc. of AFIT Conf., October 1965, Wright-Patterson AFB, Dayton, Ohio, AFFDL-TR-66-80.

47. Washizu, K., Variational Methods in Elasticity and Plasticity, second edition, Pergamon Press, 1975.

48. Timoshenko, S. P. and Woinowsky-Krieger, S., Theory of Plates and Shells, second edition, McGraw-Hill, 1968.

49. Dym, C. L. and Shames, I. H., Solid Mechanics: A Variational Approach, McGraw-Hill, 1973.

50. Reissner, E., On the Theory of Bending of Elastic Plates, J. of Mathematics and Physics, Vol. 23, No. 4, November 1944, pp. 184-191.

51. Reissner, E., The Effect of Transverse-Shear Deformation on the Bending of Elastic Plates, J. of Applied Mechanics, Vol. 12, No. 2, June 1945, pp. 69-77.

52. Reissner, E., On Bending of Elastic Plates, Quarterly of Applied Mathematics, Vol. 5, No. 1, April 1947, pp. 55-68.

53. Reissner, E., On a Variational Theorem in Elasticity, J. of Mathematics and Physics, Vol. XXIX, No. 2, 1950, pp. 90-95.

54. Birkhoff, G., Piecewise Bicubic Interpolation and Approximation in Polygons, Approximation with Special Emphasis on Spline Functions (Schoenberg, Editor), Academic Press, New York, 1969, pp. 185-221.

55. Babuska, I., Stability of the Domain of Definition ...(in Russian), Czech. Math. J. 11(86), pp. 76-105, 165-203, 1961.

56. Strang, G. and Fix, G. J., An Analysis of the Finite Element Method, Prentice-Hall, 1973.

57. Rao, A. K. and Rajaiah, K., Polygon-Circle Paradox of Simply Supported Thin Plates under Uniform Pressure, AIAA J., 6, 1968, pp. 155-156.

58. Chernauka, M. W., Cowper, G. R., Lindberg, G. M. and Olson, M.D., Finite Element Analysis of Plates with Curved Edges, Int. J. Numer. Methods Eng., 4, 1972, pp. 49-65.

59. Cowper, G. R., Kosko, E., Lindberg, G. M. and Olson, M. D., A High Precision Triangular Plate Bending Element, NRC, NAE Aero. Report LR-514, National Research Council of Canada, December 1968.

60. Pestel, E. C., Dynamic Stiffness Matrix Formulation by Means of Hermitian Polynomials, Proceedings First Conference on Matrix Methods in Structural Mechanics, Dayton, Ohio, October 1965, AFFDL-TR-66-80.

61. Falk, S., Das Verfahren von Rayleigh-Ritz mit Hermiteschen Interpolations-ponlynomen, ZAMM, 1963, pp. 149-166.

62. Szilard, R., Theory and Analysis of Plates, Classical and Numerical Methods, Prentice-Hall, 1974.

63. Olson, M. D. and Lindberg, G. M., Annular and Circular Sector Finite Elements for Plate Bending, Int. J. Mechan. Sci., Vol. 12, 1970, pp. 17-33.

64. Severn, R. T. and Taylor, P. R., The Finite Element Method for Flexure of Slabs when Stress Distributions are Assumed, Proc. Instn. Civil Engrs., 34, 1966, pp. 153-170.

65. Savin, G. N., Stress Concentration around Holes, Translation Editor: W. Johnson, Pergamon Press, 1961.

66. Williams, M. L., The Bending Stress Distribution at the Base of a Stationary Crack, J. of Applied Mechanics, 28, 1961, pp. 78-82.

67. Sih, G. C. and Rice, J. R., The Bending of Plates of Dissimilar Materials with Cracks, J. of Applied Mechanics, 31, 1964, pp. 477-482.

68. Knowles, J. K. and Wang, N. M., On the Bending of an Elastic Plate Containing a Crack, J. of Mathematics and Physics, 39, 1960, pp. 223-236.

69. Hartranft, R. J. and Sih, G. C., Effect of Plate Thickness on the Bending Stress Distribution around Through Cracks, J. of Mathematical Physics, 47, 1968, pp. 276-291.

70. Wang, N. M., Twisting of an Elastic Plate Containing Crack, Int. J. of Fracture Mechanics, 6, 1970, pp. 367-378.

71. Sih, G. C. and Liebowitz, H., Mathematical Theories of Brittle Fracture, Fracture, an Advanced Treatise (Liebowitz, Editor), Vol. II, Academic Press, 1968, pp. 167-171.

72. Sih, G. C., A Review of the Three-Dimensional Problem for a Cracked Plate, Int. J. of Fracture Mechanics, 7, 1971, pp. 39-61.

73. Hartranft, R. J. and Sih, G. C., The Use of Eigenfunction Expansions in the General Solution of Three-Dimensional Crack Problems, J. of Mathematics and Mechanics, 19, 1969, pp. 123-138.

74. Pian, T. H. H., Derivation of Element Stiffness Matrices, AIAA J., Vol. 2, No. 3, 1964, pp. 576.

75. Quinlan, P. M., The Edge-Function Method in Elastostatics, Studies in Numerical Analysis, (Scaife, Editor), Academic Press, 1974.

VITA

Hee C. Rhee was born in Korea on January 9, 1943. He graduated from Korean Naval Academy in February, 1965 with B.S. in Naval Science and served on sea for two years since his graduation. In February, 1967, he joined the College of Engineering, Seoul National University and completed his B.E. in Architectural Engineering in February, 1970. He was enrolled the School of Civil Engineering, Georgia Institute of Technology in September, 1970 and obtained his M.S. in September, 1971 from the school. In July, 1973, he returned Georgia Tech for his Ph.D. study in the School of Engineering Science and Mechanics.

During his leaves from study between in 1970 and 1973, he served in Korean Navy as a civil engineering officer.